

Energy Efficient Vehicular Networks in a City Environment

Hamdi Idjmayyel

Submitted in accordance with the requirements for the
degree of Doctor of Philosophy

University of Leeds

School of Electronic and Electrical Engineering

September 2013

The candidate confirms that the work submitted is his/her own, except where work which has formed part of jointly authored publications has been included. The contribution of the candidate and the other authors to this work has been explicitly indicated below. The candidate confirms that appropriate credit has been given within the thesis where reference has been made to the work of others.

The work in Chapter 3 of the thesis has appeared in publications as follows:

1. Idjmayyel, H.; Qazi, B.R.; Elmirghani, J. M H, "Position Based Routing Protocol for City Environment."

2010 Fourth International Conference on Next Generation Mobile Applications, Services and Technologies (NGMAST), vol., no., pp. 174 - 179, 27-29 July 2010.

My contribution: Literature review, developed further the idea of position based routing protocol for a city environment, city model, simulation of proposed routing algorithms and performance evaluation.

Professor Elmirghani: Developed the idea of position based routing protocol for a city environment, helped with development of routing algorithms and the preparation of paper.

Dr. Qazi: Helped with development of simulators and results.

2. Idjmayyel, H.; Qazi, B.R.; Elmirghani, J. M H, "A Geographic Based Routing Scheme for VANETs."

2010 Seventh International Conference On Wireless And Optical Communications Networks (WOCN), vol., no., pp. 1-5, 6-8 Sept. 2010.

My contribution: Literature review, enhanced and extended the idea of geographic based routing scheme for VANETs, city model, simulation of proposed routing algorithms and performance evaluation.

Professor Elmirghani: Developed the idea of geographic based routing scheme for VANETs, helped with development of routing algorithms and the preparation of paper.

Dr. Qazi: Helped with development of simulators and results.

The work in Chapter 4 of the thesis has appeared in publications as follows:

1. Idjmayyel, H.; Kumar, W.; Qazi, B.R.; Elmirghani, J. M H, "Saving Energy with QoS for Vehicular Communication."

Eighth International Conference on Wireless and Optical Communications Networks (WOCN), pp. 1-5, 24-26 May 2011.

My contribution: Literature review, developed new energy efficiency improvement mechanisms in a city vehicular network, system model, energy model, simulation and performance evaluation of all schemes and scenarios.

Professor Elmirghani: Originator of the idea of energy efficiency in a city vehicular network, helped with development of routing algorithms, energy modelling, physical propagation modelling, and the preparation of paper.

Dr. Qazi: Helped with development of simulators, energy modelling and results.

Dr. Kumar: Physical propagation modelling.

2. Idjmayyel, H.; Kumar, W.; Qazi, B.R.; Elmirghani, J. M H, "Energy and QoS- a New Perspective in a City Vehicular Communication Network."

IEEE GLOBECOM Workshops (GC Wkshps), pp. 327-331, 5-9 Dec. 2011.

My contribution: Literature review, added new features and new concepts to the idea of energy efficiency in a city vehicular network, system model, energy model, simulation and performance evaluation of all schemes and scenarios.

Professor Elmirghani: Developed the idea of energy efficiency in a city vehicular network, helped with development of routing algorithms, energy modelling, physical propagation modelling, and the preparation of paper.

Dr. Qazi: Helped with development of simulators, energy modelling and results.

Dr. Kumar: Physical propagation modelling.

3. Idjmayyel, H.; Qazi, B.R.; Elmirghani, J. M H, " Energy Efficient Double Cluster Head Routing Scheme in a City Vehicular Network."

IEEE 27th International Conference on Advanced Information Networking and Applications (AINA), EASyCoSe workshop, 2013.

My contribution: Literature review, developed new routing algorithms and new energy models in a city vehicular network, system model, energy model, simulation and performance evaluation of all schemes and scenarios.

Professor Elmirghani: Developed the idea of cluster based routing schemes in a city vehicular network, helped with development of routing algorithms, energy modelling, and the preparation of paper.

Dr. Qazi: Helped with development of simulators, energy modelling and results.

This copy has been supplied on the understanding that it is copyright material and that no quotation from the thesis may be published without proper acknowledgement.

©2013 The University of Leeds and Hamdi Idjmayyel

The right of Hamdi Idjmayyel to be identified as Author of this work has been asserted by him in accordance with the Copyright, Designs and Patents Act 1988.

To:

*The bright memory of my father, Dr. Idjmayyel. May his soul rest in
peace.*

My mother, Mrs Idjmayyel.

My sisters and their families.

Miss Hala Al-Daoud.

Acknowledgements

I would like to sincerely thank my supervisor, Professor Jaafar Elmirghani, for his abundantly helpful and invaluable assistance, support, guidance, and encouragement. Professor Elmirghani has been supportive since the day I began working on my research as an undergraduate. He has offered me invaluable opportunities and continuously kept faith in me. Without his help and support, I would not have been able to achieve this.

I would also like to acknowledge Dr. Bilal Qazi and Dr. Samya Bhattacharya, Postdoctoral Research Fellows in the group, for their useful advice and fruitful discussions.

My gratitude goes to my beloved family for their understanding and tremendous support. Special thanks to my deceased father who has laid the foundations I need to achieve any success throughout my life. I am indebted to my mother for her patience, unconditional support, and encouragement. Many thanks to my sisters for their moral encouragement and special thanks to Miss Hala Al-Daoud who fully supported me and was always there during difficult times.

I would also like to offer my regards to all of those who supported and inspired me in any respect during the completion of this thesis.

Finally, I thank the students of the Communication Systems and Networks group in the School of Electronic and Electrical Engineering for their friendship and support.

Abstract

With the advent of real-time high bandwidth multimedia services, enhancing quality of service (QoS) in communication networks has been the prime focus of researchers. With environmental awareness becoming a global concern, the need to have energy efficiency in communication networks has intensified. Moreover, as the network size and the number of users increase, the introduction of energy efficient networks has become essential. Very little work has been carried out so far in vehicular communication networks for energy efficiency, even though their size and the number of users is equivalent to that of the cellular network. Provisioning multimedia services in vehicular networks is challenging due to the dynamic nature of the environment in which they operate. Analysing the performance of such systems from both QoS and energy perspectives redefines the problem. Therefore, there is a need to introduce systems which not only maintain QoS in these environments, but also save significant amounts of energy. Vehicular networks comprise intelligent vehicles fitted with an on-board unit (OBU) with wireless communication, sensing, and computing capabilities, in addition to fixed resources. Vehicular communication will play a key role in providing safety, security, and entertainment for drivers, passengers, and pedestrians in futuristic “smart cities.”

This thesis studies the performance of city vehicular communication systems in terms of QoS and energy consumption. Initially, a city vehicular mobility simulator based on a 3×3 km² Manhattan grid is developed which includes important traffic characteristics in a typical city such as vehicular flow and speed. Next, a vehicular ad hoc network (VANET) comprising three routing protocols, namely multihop (MH) routing, position based routing with most forward within radius (PRMFR), and position based routing with nearest forward progress (PRNFP), is developed in this environment. The performance of the aforementioned routing protocols is evaluated in terms of QoS. Additionally, two energy efficient routing protocols are proposed, namely single cluster-head (SCH) and double cluster-head (DCH) based routing. The performance of the SCH and DCH routing protocols from both QoS and energy perspectives is evaluated and compared with that of the MH routing, store-carry and forward (SCF) routing, and two pure vehicle-to-roadside (V2R) routing approaches. Moreover, an energy efficient content distribution network (CDN) for this environment is proposed. A mixed integer linear programming (MILP) model that optimises the number and locations of Wi-Fi enabled caching points (CPs) and cellular basestations (BSs) is developed, with the objective of minimising the total network power consumption while serving the total traffic at each hour of the day. The performance of the proposed energy efficient CDN under different scenarios and different power management mechanisms in terms of both QoS and power efficiency is evaluated. Since there is no mechanism in the MILP model to switch a CP, once installed, into low power state, an analytical

queuing model is developed for the CP, where the CP sleeps (takes vacations) during its inactivity periods to save energy while maintaining the required QoS.

Contents

Acknowledgements.....	i
Abstract.....	iii
List of Figures	xv
List of Tables	xxi
List of Abbreviations.....	xxii
List of Symbols	xxvii
1 INTRODUCTION.....	1
1.1 Research Objectives.....	7
1.2 Research Contributions	8
1.3 Thesis Outline	12
2 Vehicular Communication Networks.....	15
2.1 Introduction	15
2.2 Vehicular Networks: An Overview.....	15

2.3	Challenges of Vehicular Networks	17
2.4	Vehicular Network Applications.....	18
2.4.1	Safety related applications	19
2.4.2	Non-safety related applications.....	22
2.5	Vehicular Network Architectures.....	23
2.5.1	Vehicle-to-vehicle (V2V) networks	24
2.5.2	Vehicle-to-roadside (V2R) networks.....	26
2.5.3	Hybrid vehicular networks	28
2.6	Vehicular Networks Technologies and Standards.....	29
2.6.1	Dedicated short range communications (DSRC).....	30
2.6.2	Wireless access in vehicular environments (WAVE).....	32
2.6.3	Cellular systems.....	35
2.6.4	IEEE 802.11x.....	35
2.6.5	Infrared (IR).....	35
2.6.6	Millimetre waves (MM)	36

2.6.7	Communication air-interface long and medium (CALM).....	36
2.7	Vehicular Environments	37
2.7.1	City environment	37
2.7.2	Highway environment.....	38
2.7.3	Rural environment.....	39
2.8	Vehicular Mobility and Communication Simulators	39
2.9	Routing Protocols.....	42
2.9.1	Flooding based routing protocols	43
2.9.2	Store-carry and forward (SCF) routing protocol	45
2.9.3	Geographic based routing protocols	46
2.9.4	Ad hoc on-demand distance vector (AODV) routing protocol.....	47
2.9.5	Cluster based routing protocols.....	48
2.9.6	Auction/credit based routing protocols	50
2.10	Energy Efficiency in Wireless Networks	52
2.10.1	Energy efficiency in vehicular networks	53

2.11	Content Distribution Networks (CDNs) and Node Placement	54
2.12	Queuing Theory Based Analysis.....	57
2.13	Mixed Integer Linear Programming (MILP)	58
2.14	Summary.....	60
3	Vehicular Ad hoc Network.....	61
3.1	Introduction	61
3.2	Vehicular Ad hoc Network Simulator.....	61
3.3	Traffic Generation	63
3.4	Multihop Routing Protocol and Its Implementation.....	64
3.5	Geographic (Position)-based Routing	67
	3.5.1 Position-based routing with most forward within radius (PRMFR) protocol and its implementation.....	68
	3.5.2 Position-based routing with nearest forward progress (PRNFP) protocol and its implementation.....	70
3.6	Greedy Nodes (GNs) Integration	71
3.7	Performance Evaluation.....	72

3.7.1	Average end-to-end delay	73
3.7.2	Packet dropping probability	76
3.7.3	Total number of transmissions in the network	78
3.8	Summary.....	80
4	Energy Efficient Hybrid Vehicular Network in a City Environment.....	82
4.1	Introduction	82
4.2	The Studied City Scenario	84
4.3	Vehicle-to-Roadside (V2R) Scenarios and their Simulation Implementation	84
4.4	Hybrid Scenario, Routing Protocols and their Simulation Implementation	85
4.4.1	Store-carry and forward (SCF) routing	87
4.4.2	Single cluster-head (SCH) based routing	88
4.4.3	Double cluster-head (DCH) based routing	89
4.5	Physical Propagation Modelling	91
4.6	Energy Modelling	94

4.7	Performance Evaluation.....	97
4.7.1	Average end-to-end delay.....	98
4.7.2	Packet loss ratio.....	99
4.7.3	Total number of transmissions.....	100
4.7.4	Transmit and receive energies.....	101
4.7.5	Listening energy.....	102
4.7.6	Total network energy.....	104
4.8	Summary.....	105
5	Power Efficient Content Distribution Network for a City Vehicular Environment	107
5.1	Introduction.....	107
5.2	The Studied Scenario.....	108
5.2.1	Vehicular traffic profiles.....	109
5.2.2	Vehicular mobility simulator.....	110
5.3	Wi-Fi based CDN.....	112
5.4	Cellular Network.....	114

5.5	A Linear Programming Model for CP/BS Number and Location Optimisation.....	118
5.6	CDN/Cellular Heuristic	123
5.7	Performance Evaluation.....	125
5.7.1	Total network power consumption.....	126
5.7.2	Number of active CPs/BSs.....	130
5.7.3	Root mean square deviation between MILP model and heuristic...	134
5.8	Summary.....	136
6	Impact of Vehicular Mobility on the Performance of the City Vehicular Content Distribution Network	137
6.1	Introduction	137
6.2	The Studied Scenario	138
6.3	Vehicular Content Download Algorithm (VCDA)	138
6.4	Performance Evaluation.....	141
6.4.1	Total network power consumption.....	143
6.4.2	Number of active CPs/BSs.....	151

6.4.3 Average piece delay and average content delay.....	160
6.5 Summary.....	165
7 Sleep Enabled Wi-Fi Caching Points in a City Content Distribution	
Network.....	167
7.1 Introduction	167
7.2 The Studied Scenario	169
7.3 Analytical Modelling of CP with Multiple Random Sleep Cycles	171
7.4 Performance Evaluation.....	180
7.4.1 Energy savings.....	180
7.4.2 Average piece delay.....	182
7.4.3 Average content delay	186
7.5 Summary.....	187
8 Conclusions and Future Work	190
8.1 Conclusions and Key Findings.....	190
8.2 Future Work	198
References.....	200

Appendices	228
Appendix A: City Vehicular Simulator	228
A.1: Introduction.....	228
A.2: Overview	228
A.3 Simulator Design	233
A.3.1 Vehicle class.....	233
A.3.2 Road class	233
A.3.3 Vehicular simulator class	234
A.4 Summary	238
Appendix B: Flowcharts	239
B.1 VANET Simulator Flowchart.....	239
B.2 Traffic Generation Flowchart	240
B.3 Multihop Routing Flowchart	241
B.4 PRMFR and PRNFP Routing Flowchart.....	242
B.5 SCH Routing Flowchart.....	243

List of Figures

Figure 2.1: Traffic signal violation warning	21
Figure 2.2: Emergency electronic brake light	22
Figure 2.3: Single-hop inter-vehicle communication system	25
Figure 2.4: Multihop inter-vehicle communication system	26
Figure 2.5: Vehicle to roadside (V2R) network.....	28
Figure 2.6: Hybrid vehicular communication system	29
Figure 2.7: DSRC spectrum	31
Figure 2.8: WAVE protocol stack	33
Figure 2.9: City environment	38
Figure 2.10: Highway environment.....	39
Figure 3.1: Storing procedure of packets	64
Figure 3.2: MH routing topology	65
Figure 3.3: Packet dropping mechanism (FIFO)	66

Figure 3.4: A snapshot of MH routing.....	67
Figure 3.5: A snapshot of PRMFR and PRNFP	69
Figure 3.6: A snapshot of MH routing with GNs	72
Figure 3.7: Average E2E delay with varying vehicular load.....	75
Figure 3.8: Average E2E delay with GNs with varying vehicular load	75
Figure 3.9: PDP with varying vehicular load.....	77
Figure 3.10: PDP with GNs with varying vehicular nodes	77
Figure 3.11: Total number of transmissions in the network with varying vehicular load	79
Figure 3.12: Total number of transmissions in the network with GNs with varying vehicular load.....	80
Figure 4.1: The studied city scenario.....	83
Figure 4.2: A snapshot of the SCF routing	88
Figure 4.3: A snapshot of the SCH based routing	89
Figure 4.4: A snapshot of the double cluster-head (DCH) based routing	91
Figure 4.5: Probability of outage for a V2R system	93

Figure 4.6: Probability of outage for a V2V system	94
Figure 4.7: Average E2E delay with varying vehicular load.....	99
Figure 4.8: Packet loss ratio with varying vehicular load	100
Figure 4.9: Total number of transmissions with varying vehicular load	101
Figure 4.10: Total Tx and Rx energy with varying vehicular load	102
Figure 4.11: Total listening energy with varying vehicular load	103
Figure 4.12: Total network energy with varying vehicular load.....	105
Figure 5.1: The studied city scenario.....	108
Figure 5.2: Hourly vehicular flow and demand	110
Figure 5.3: CP block diagram.....	114
Figure 5.4: Optimised locations of the CPs through the MILP model at different hours of the day	126
Figure 5.5: Total network power consumption (Cellular vs. Wi-Fi)	128
Figure 5.6: Number of active CPs	132
Figure 5.7: Number of active BSs	133
Figure 5.8: Root mean square number deviation of active CPs or BSs	135

Figure 5.9: Root mean square location deviation of active CPs or BSs	135
Figure 6.1: Total network power consumption (Wi-Fi)	144
Figure 6.2: Total network power consumption with different power management mechanisms (Wi-Fi)	146
Figure 6.3: 1 Mb/s/user & 500 m BS range - Total network power consumption (Cellular – 30 Mb/s for vehicular content downloading).....	148
Figure 6.4: 3 Mb/s/user & 800 m BS range - Total network power consumption (Cellular – 30 Mb/s for vehicular content downloading).....	149
Figure 6.5: Power consumption with variable BS capacity for vehicular applications (Cellular- 3 Mb/s/user, 800m BS range & $W_d = 0$)	151
Figure 6.6: Number of active CPs (Wi-Fi).....	153
Figure 6.7: 1 Mb/s/user & 500 m BS range - Number of active BSs (Cellular – 30 Mb/s for vehicular content downloading)	155
Figure 6.8: 3 Mb/s/user & 800 m BS range - Number of active BSs (Cellular – 30 Mb/s for vehicular content downloading)	157
Figure 6.9: Number of BSs with variable BS capacity for vehicular applications (Cellular- 3 Mb/s/user, 800m BS range & $W_d = 0$)	159
Figure 6.10: Average piece delay (Wi-Fi)	161

Figure 6.11: Average content delay (Wi-Fi).....	163
Figure 6.12: Average piece delay (Cellular-30 Mb/s BS capacity, 3 Mb/s/user & 800 m BS range)	164
Figure 6.13: Average content delay (Cellular-30 Mb/s BS capacity, 3 Mb/s/user & 800 m BS range).....	165
Figure 7.1: The studied scenario	171
Figure 7.2: M/det-Neg/1/ ∞ queues with sleep cycles to represent CP operation	173
Figure 7.3: Energy savings.....	182
Figure 7.4 Average piece delay.....	184
Figure 7.5: Load on CPs	184
Figure 7.6: Number of simultaneous connections and queue size pdf (primary CP).....	185
Figure 7.7: Number of simultaneous connections and queue size pdf (secondary CP)	186
Figure 7.8: Average content delay	187
Figure A.1: 3x3 km ² Manhattan grid.....	231

Figure A.2: City vehicular simulator flowchart	232
Figure A.3: Assign vehicle flowchart.....	236
Figure A.4: Vehicular mobility flowchart	238
Figure B.1: VANET simulator flowchart	239
Figure B.2: Flowchart for traffic generation mechanism	240
Figure B.3: Flowchart for MH routing.....	241
Figure B.4: Flowchart for PRMFR and PRNFP protocols.....	242
Figure B.5: SCH routing flowchart.....	243

List of Tables

Table 3.1: System parameters	70
Table 4.1: System communication parameters	87
Table 5.1: Communication System Parameters and List of notations	118
Table 7.1: System parameters	172

List of Abbreviations

A-STAR	Anchor-Based Street and Traffic Aware Routing
AODV	Ad Hoc On-Demand Distance Vector
AP	Access Point
BS	Basestation
CALM	Communication Air-Interface Long and Medium
CBR	Constant Bit Rate
CDN	Content Distribution Network
CH	Cluster Head
COIN	Clustering For Open Inter-Vehicle Communication Networks
CP	Caching Point
CS	Candidate Site
CSMA/CA	Carrier Sense Multiple Access with Collision Avoidance
CuTV	Catch-up TV
DCF	Distributed Coordination Function
DCH	Double Cluster-Head

DSR	Dynamic Source Routing
DSRC	Dedicated Short Range Communication
DTN	Delay Tolerant Network
E2E	End-to-End
FCC	Federal Communication Commission
FIFO	First-In-First-Out
FS	Free Space
GN	Greedy Nodes
GPS	Global Positioning System
GSR	Geographic Source Routing
ICT	Information and Communication Technology
iid	Independent and Identically Distributed
IPTV	Internet Protocol TV
IR	Infrared
ITS	Intelligent Transportation System
IVC	Inter-Vehicle Communication
I2V	Infrastructure-to-Vehicle
LEACH	Low-Energy Adaptive Clustering Hierarchy

LP	Linear Programming
LORA_CBF	Location-Based Routing Algorithm with Cluster-Based Flooding
LOS	Line-of-Sight
LREP	Location Reply
LREQ	Location Request
LTE	Long Term Evolution
MAC	Medium Access Control
MANET	Mobile Ad Hoc Network
MFR	Most Forward within Radius
MH	Multihop
MILP	Mixed Integer Linear Programming
MIVC	Multi-hop Inter-Vehicle Communication
MM	Millimetre Wave
MPR	Market Penetration Ratio
MFR	Most Forward within Radius
OBU	On-board unit
OFDM	Orthogonal Frequency Division Multiplexing
ONU	Optical Network Unit

PCD	Push-Based Popular Content Distribution
pdf	Probability Density Function
PDP	Packet Dropping Probability
PLR	Packet Loss Ratio
POI	Point-of-Interest
PON	Passive Optical Network
PRMFR	Position based Routing with Most Forward within Radius
PRNFP	Position based Routing with Nearest Forward Progress
PS	Power Saving
QoS	Quality of Service
RMS	Root Mean Square
RREP	Route Reply
RREQ	Route Request
RERR	Route Error
RS	Relay Station
RSU	Roadside Unit
SCF	Store-Carry and Forward
SCH	Single Cluster-Head

SIVC	Single-hop Inter-Vehicle Communication
SLNC	Symbol-Level Network Coding
TP	Traffic Point
VANET	Vehicular Ad Hoc Network
VCDA	Vehicular Content Download Algorithm
VoD	Video-on-Demand
VSC	Vehicle Safety Communication
V2R	Vehicle-to-Roadside
V2V	Vehicle-to-Vehicle
WAVE	Wireless Access in Vehicular Environments
WLAN	Wireless Local Area Network
WSMP	WAVE Short Message Protocol
WWAN	Wireless Wide Area Network
ZOR	Zone of Relevance
3G	Third Generation
9BS_V2R	V2R network with 9 basestations scenario
4BS_V2R	V2R network with 4 basestations scenario

List of Symbols

A	Large number for MILP model constraint
α_c	A binary value indicating the status of a CP c
B	Wireless node capacity
$TP_j[v]$	Nearest TP j to vehicle v
$BSID$	Basestation's ID
$bSize$	Vehicular node buffer size
$BSLoc$	Basestation's location
$BSRoad$	Basestation's road
\bar{c}	Content Size (exponential distributed)
cr	V2V communication range (in meters)
\bar{D}	Average content delay
d	Distance between two entities in meters
δ	Dirac-delta function
δ_{cjt}	A binary variable that indicates if CP c is transmitting to

	TP j at time t
Δ_v	Waiting timer of vehicle v
d_i	Instantaneous data rate (General distributed)
d_r	Data rate (in Mbps)
$dRate$	Traffic generation rate (in kb/s)
d_{ref}	Reference distance in meters
E_L	Total listening energy in the network
E_{L_BS}	Total energy consumed in listening state by a BS
E_{L_Vehs}	Total energy consumed in listening state by vehicles
E_R	Total receiving energy in the network
Ψ_r	Energy consumed for reception of a bit
E_S	Energy savings
E_T	Total transmission energy in the network
Ψ_t	Energy consumed in the transmission of a bit
E_{t_BS}	Energy consumed for transmission of all packets from a BS to vehicles
E_{t_Vehs}	Energy consumed for the transmission of all packets from

	vehicles to a BS
E_{wo}	Energy overhead for each wake-up (in sleep cycle)
γ	Request generation time of piece
H	Large number for MILP model constraint
h_b	BS antenna height
h_v	Vehicle antenna height
K	Piece request
k	The sum of the original packets and the replicated packets
l	Total number of nodes in the network not in sleep mode
λ	Mean inter-arrival rate of piece requests (Poisson distributed)
λ_{cjt}	Traffic between CP c and TP j at time t
λ_{tj}	TP j demand at time t
M	Number of BSs deployed in the network
μ	Mean service rate
N	Total number of pieces per content

n	Piece number
$N_{\lambda}(t)$	Number of piece requests that arrive within $(0, t)$
N_p	Set of neighbouring TPs
N_{pc}	Set of neighbouring CPs
N_{ps}	Number of packets
N_q	Number of piece requests waiting in the queue of CP
N_s	Number of sleep cycles (sleep count)
n_{sim}	Number of nodes participating in the simulation
N_{sys}	Number of piece requests in system
\emptyset	Average content delay
ω	Instantaneous time
p	parameter which determines the degree of superposition of deterministic and negative exponential pdf in det-Neg distribution
P_a	Power amplifier power consumption
P_{BS}	Operational power consumption of BS
$P_{BS_{min_OP}}$	Total operational power consumption of a BS including all

	elements
P_C	CP circuitry power consumption
$P_{CP_{\min_OP}}$	Operational power consumption of CP
$P_{CP_{RX_{ct}}}$	Receiver power consumption of CP c at time t
$P_{CP_{TX_{cjt}}}$	Distance dependent transmitting power consumption of CP c to TP j at time t
$P_{CP_{TX_{ct}}}$	Transmitter power consumption of CP c at time t
P_{ct}	Power consumption of the transmitter circuitry of the CP
$pDelay$	Individual packet end-to-end delay
P_{HD}	Hard drive power consumption
$pktID$	The ID of a packet
$PktSize$	Packet size (in bits)
$PktSize_i$	Size of the i^{th} packet in bits
P_{lc}	Power consumed in the listening state at the receiver
$P_{MAC/ALG}$	MAC and algorithm processor unit power consumption
P_{MAX}	Maximum operational power of CP
P_{MC}	Microcontroller power consumption

P_{MIN}	Minimum operational power of CP
P_N	Total network power consumption
P_O	Operational power consumption of a V2R BS
P_{ONU}	Optical network unit power consumption
P_{out}	Outage probability
P_{rc}	Power consumed by the receiver circuitry
$P_r(d)$	Mean received power at a distance d
$P_r(d_{ref})$	Reference power at a distance d_{ref}
P_s	Piece size in MByte
P_{tc}	Power consumed by the transmitter circuitry
P_{th}	Receiver threshold power
$pTime$	Packet generation time
$P_{V_{RX}it}$	Transceiver's power consumption of vehicle i
$P_{V_{TX}it}$	Transmitter power consumption of vehicle i at time t
\bar{R}	Mean residual time
$receivedPkts$	Number of received packets
ρ	Offered load of a CP

$r(\omega)$	Residual time for the ongoing service or sleep
$R[x]$	Request for content x
\bar{S}	Mean sleep cycle duration (negative exponential distributed)
σ	Mean inter-arrival time for a piece request
S_j	j^{th} sleep time
T	Set of time points within an hour
τ	Mean inter-arrival time for a content request
<i>totalPkts</i>	Total number of generated packets
<i>totalPktsDropped</i>	Total number of dropped packets
<i>totalPktsInNetwork</i>	Total number of packets in the network (original + replicated)
<i>TOTAL_VEHICLES</i>	Total number of vehicles in the network used for simulation
<i>totDelay</i>	Total end-to-end delay for all successfully received packets
<i>TotSimTime</i>	Total simulation duration
$T_{r,k}$	Time taken for the reception of total (original + replicated)

	packets in the network
T_{r_N}	Time taken for the reception of the original packets for a BS
T_{Sim}	Total simulation time in seconds
T_{t_k}	Time taken for the transmission of total (original + replicated) packets in the network
T_{t_N}	Time taken for the transmission of the original packets for a BS
U_s	System utilization
ν	Path loss exponent
ϑ	Average piece delay
W	Mean piece delay
W_d	Waiting duration
W_q	Average waiting time for a piece at the CP
x	Content ID
\bar{X}	Mean service duration (det-Neg distributed)
X_i	i^{th} service time

$x(t)$ pdf of service duration (det-Neg distributed)

$\zeta[x]$ Request generation time of content x

1 INTRODUCTION

Nowadays, transportation systems are considered to be an essential element in our daily lives. The high demand placed on transportation systems, resulting in considerable growth in car manufacturing and ownership, has led to delays, traffic jams, and accidents. This does not only cause wastage of energy resources and a reduction in productivity, but also causes deaths [1]. The quest to achieve an efficient, secure, and safe transportation system, in addition to utilising specialised applications for drivers and passengers using existing technologies, has led to significant challenges [2-4].

The rapid development in technology, coupled with the state-of-the-art electronic devices, has enhanced the way we live and communicate, leading to intelligent transportation systems. The use of wireless communications in vehicles emerged in the 1980s [5] and was followed by technologies and applications drafted by a number of IEEE organisations and intelligent transportation system (ITS) committees [6]. These advances in electronic devices and applications, in addition to the gradual deployment of wireless technologies in vehicles that is witnessed today, contribute towards efficient and safer road networks.

A vehicular network is a wireless communication network which manages and connects intelligent vehicles (nodes) to one another and to the fixed infrastructure. An Intelligent vehicle is fitted with an on-board unit (OBU) with wireless communication and computing capabilities, in addition to a global positioning system (GPS) device, allowing the vehicle to follow its spatial and temporal trajectory [7]. Intelligent vehicles might also possess pre-stored digital maps and sensors used to report accidents. These vehicles are a key part of ITS [8], as they have two key goals: enhancing safety and reducing congestion. Vehicular networks use three main network architectures: vehicle-to-vehicle (V2V) network architectures which are infrastructure-less networks (ad-hoc), vehicle-to-roadside (V2R) network architectures which are infrastructure-based networks, and hybrid network architectures, which are a combination of V2V and V2R architectures [9]. Applications from which intelligent vehicles can benefit are categorised as either safety or non-safety related (such as infotainment).

Vehicular communication is seen as a key future technology in intelligent transportation systems. Since at present the market penetration ratio (MPR) of vehicular communications is very low compared to existing mobile communications, there is significant potential in terms of development and deployment. This allows system designers to build on existing technologies and establish new methods to support safety and non-safety related applications for vehicular networks. Due to the mobility of vehicles in such networks,

maintaining quality of service (QoS) for real time applications is challenging. Furthermore, due to the increase in the carbon footprint levels of information and communication technology (ICT) networks, energy efficiency in such networks including vehicular networks has recently attracted researchers' interest [10-13].

In V2V or inter-vehicle communication (IVC) networks, vehicles that are equipped with the appropriate OBUs and are within each other radio range can form a vehicular ad hoc network (VANET) [4,7]. Data packets can be transmitted in VANETs in a single-hop or multihop manner. In the case of the former, the packets are transmitted from the source vehicle to all its one-hop neighbours, whereas in the latter instance, data packets can be exchanged between intermediate vehicles to achieve better connectivity. Hence, routing protocols are very important in V2V networks in order to successfully deliver packets, and to maintain and enhance network connectivity.

Due to the range of possible hybrid network architectures and nodes' mobility, the design of an efficient routing protocol for VANETs is crucial. The main requirement of all routing protocols is to achieve minimal message delivery time with minimum consumption of network resources [14]. Flooding based routing or multihop routing is extremely useful in areas that lack infrastructure, as intermediate vehicles can relay packets to out-of-range vehicles/destinations. Moreover, in the case of a hybrid network architecture, extending the range of a roadside unit (RSU) or basestation (BS) can also be achieved by MH routing,

as intermediate vehicles can relay packets to/from an out of range RSU. Furthermore, geographic-based routing protocols are also utilised in vehicular networks as they take advantage of the geographic location of nodes instead of topological data connectivity. These protocols utilise information about the geographic position (coordinates) of certain nodes to establish efficient routes [15]. It is demonstrated in [15,16] that geographic-based routing protocols reduce flooding; however, this is achieved at the cost of a higher end-to-end delay.

As the focus on global warming increases, the growth in ICT networks has caused concerns due to their continuously expanding carbon footprints. The total carbon footprint of the ICT sector in 2007 was estimated to be 2% of global carbon emissions, with a predicted 6% annual increase until 2020 [17]. Energy efficiency in vehicular networks has also gained interest recently [10-13], [18-20]. Since almost 80% of the power is consumed by the BS's hardware and accessories in centralised networks [21], new approaches to energy efficiency have been developed including energy aware BS deployment strategies [22], which include installing fewer BSs efficiently, switching off as many as possible or utilising BSs with lower power consumption. However, maintaining a certain QoS level with such deployment strategies is challenging. According to [23], a third generation (3G) BS consumes 500 W and it is shown in [18] that nine BSs are needed to cover a typical city area of $3 \times 3 \text{ km}^2$, which would equate to a total of $9 \times 500 = 4.5 \text{ kW}$. Additionally, the maximum number of vehicles in the

same area is around 500 during peak hours, and each radio-enabled vehicle typically consumes around 10 W [24] for transmission. Hence, the total transmission power consumption of the vehicles is approximately 5 kW. This results in a total power consumption of 9.5 kW in a typical city. Hence, with the increased use of road networks it is very important to introduce energy efficiency in vehicular networks, both in the RSUs and in vehicular transceivers.

The implementation of an actual prototype vehicular network is very costly, in addition to the associated high complexity. Hence, researchers have developed simulation tools to evaluate these networks. Simulation tools dedicated to this purpose usually incorporate real network characteristics such as measured vehicular mobility (e.g. flow, speed, and density) and channel characteristics in different environments. Additionally, different mobility models such as the Manhattan model [25] or random way point model [26] are also available in conjunction with these simulation tools. All these models, characteristics and measurements help evaluate the performance of different communication protocols in an efficient and accurate manner in a vehicular communications environment. Furthermore, analytical models exist for network optimisation and design and can offer upper and lower bounds and independent results for verification.

Due to the current overwhelming interest in media-rich files, content distribution networks (CDNs) have also drawn considerable attention. For example, Internet protocol TV (IPTV), video-on-demand (VoD) and catch-up TV (CuTV) are

among the services offered by these CDNs [27,28]. Such services demand high bandwidth for transmission and large storage capacity for audio and video files. According to [29], more than 91% of global IP traffic is going to be in the form of video by 2014, with an annual growth of 33%. These growing figures, coupled with a desire to download media-rich content (multimedia files) in vehicles, aggravate the problem of providing the required QoS in such a dynamic environment, while saving energy. To provide energy efficient, and reliable content download services at different times and locations in a V2R network, the number of RSUs and their locations should be optimised with the objective of minimising energy consumption, while attaining certain levels of QoS. Mixed integer linear programming (MILP) is an efficient tool that can be used to optimise the number and locations of network components in a communication network.

The abovementioned reasons motivate this study, which aims to analyse vehicular networks in a city environment. In order to conduct the analysis, a city vehicular simulator has been developed which includes key traffic characteristics such as flow, speed control, and choice of direction. Furthermore, a VANET comprising three routing protocols, namely multihop routing (MH), position based routing with most forward within radius (PRMFR), and position based routing with nearest forward progress (PRNFP), has been developed [15,16]. The performance of these VANETs under different routing

protocols has been evaluated in terms of QoS for varying vehicular load. Moreover, new energy efficient routing protocols have been developed, namely single cluster-head (SCH) routing and double cluster head (DCH) routing, and utilised in a hybrid vehicular network [18,19,24]. The performance of these routing protocols in terms of QoS and energy efficiency has been evaluated and compared in a hybrid city vehicular network. The performance was also compared with two pure V2R networks considering realistic channel characteristics. Next, a power efficient Wi-Fi-based CDN for a city vehicular scenario has been proposed to study the feasibility of content distribution using these vehicular networks. The performance of the proposed CDN in terms of energy efficiency and QoS was compared to that of a traditional cellular network. MILP models which optimise the number and locations of the required caching points (CPs) and BSs in the city environment have been developed with the objective of minimising the total network power consumption while serving the total traffic throughout the day. A heuristic which mimics the behaviour of the MILP model has also been developed to validate the analytical results. Moreover an algorithm, namely vehicular content download algorithm (VCDA), has been developed to study the impact of vehicles' mobility on the performance of the network. Finally, a sleep cycle mechanism is introduced in the optimised CPs to save more energy while fulfilling the required QoS.

1.1 Research Objectives

The research objectives of this thesis were:

- To study the topology and characteristics of a realistic city vehicular communications environment so that an accurate vehicular simulator for such an environment, able to capture these dynamics, can be developed.
- To introduce and evaluate the performance of a number of routing protocols under the city vehicular communications scenario.
- To evaluate the energy efficiency of these protocols and improve the performance of the system by implementing energy efficient routing protocols.
- To investigate the feasibility of vehicular network based content distribution and minimise the power consumption of such a network.
- To introduce sleep cycles to the vehicular communications network to save energy while maintaining the required QoS.

1.2 Research Contributions

The author in this thesis has:

1. Studied vehicular traffic measurements of a typical city environment such as speed, acceleration, deceleration, and inter-vehicle spacing and developed an accurate city vehicular simulator based on a $3 \times 3 \text{ km}^2$ Manhattan grid which captures the mobility and dynamics of vehicular motion.

2. Developed two new routing protocols, namely PRMFR, and PRNFP for the vehicular ad hoc network. Analysed the performance of the aforementioned routing protocols in terms of QoS for varying vehicular load in a city environment. Studied the impact of greedy nodes on the system which helps evaluate the performance of these protocols.
3. Presented mathematical models for wireless channel and energy efficiency for centralised and hybrid city communication scenarios. Developed two energy efficient routing protocols, namely SCH and DCH routing. Compared the performance of two pure V2R communication scenarios with a hybrid communication scenario under SCH, DCH, MH, and store-carry and forward (SCF) routing protocols in terms of QoS and energy efficiency.
4. Studied the performance of a CDN in a city vehicular environment in terms of energy efficiency and QoS. This involved:
 - a. Studying vehicular mobility in a typical city based on vehicular measurements conducted in the city of Saskatoon in Canada by the transportation branch of the infrastructure services department [30] and scaled it to a maximum of 500 vehicles in an hour which was a reasonable quantity to evaluate the performance of such a network. As a result developed a vehicular simulator that generates traffic at different locations in the city at each hour of the day based on the statistical analysis carried out on the real vehicular data mentioned above.

- b. Developing a MILP model to optimise the number and location of CPs in a Wi-Fi based CDN with the objective of minimising the total network power consumption while serving the total traffic generated by vehicles. The traffic generated by vehicles in the simulator is used as an input to the MILP models.
- c. Developing a MILP model for the cellular network under two conditions (highly dense and lightly dense) that optimises the number and locations of BSs with the objective of minimising the total network power consumption.
- d. Validating the developed MILP models through simulations and by developing independent heuristics that mimic the behaviour of the models in switching the optimum CPs/BSs ON.
- e. Studying the impact of vehicular mobility on content downloading by developing an algorithm for content download in vehicular networks, namely vehicular content download algorithm (VCDA). The work was extended by employing different power management schemes in the CPs with additional studies that evaluate the impact of varying the portion of the total BS capacity allocated for vehicular applications.
- f. Evaluating and comparing the performance of all scenarios/setup in terms of total network power consumption, number of active CPs/BSs, average piece delay and average content delay at each hour of the day.

5. Developing an analytical queuing model for the Wi-Fi CPs within the CDN where each CP takes vacations (switch to sleep mode) to save energy during its inactivity period. Each CP with a wireless link to vehicles is modelled as a single server queue ($M/det-Neg/1/\infty$). The performance of the system was evaluated in terms of energy savings, average queue size, average piece delay, and average content delay. The performance results of the system are verified with simulations with respect to varying vehicular load according to real vehicular traffic profiles.

These contributions are supported by the following publications:

1. Hamdi Idjmayyel, Bilal R. Qazi and Jaafar M. H. Elmirghani, "Energy Efficient Double Cluster Head Routing Scheme in a City Vehicular Network," *in the 27th International Conference on Advanced Information Networking and Applications Workshops (WAINA), 25-28 March, 2013.*
2. Hamdi Idjmayyel, Wanod Kumar, Bilal R. Qazi and Jaafar M. H. Elmirghani, "Energy and QoS — A new perspective in a city vehicular communication network," *in the IEEE Globecom 2011 Workshops, 5-9 December, 2011.*
3. Hamdi Idjmayyel, Wanod Kumar, Bilal R. Qazi and Jaafar M. H. Elmirghani, "Saving energy with QoS for vehicular communication," *in the 8th International Conference on Wireless and Optical Communications Networks (WOCN), 24-26 May, 2011.*

4. Hamdi Idjmayyel, Bilal R. Qazi and Jaafar M. H. Elmirghani, "A geographic based routing scheme for VANETs," *in the 7th International Conference on Wireless and Optical Communications Networks (WOCN), 6-8 September, 2010.*
5. Hamdi Idjmayyel, Bilal R. Qazi and Jaafar M. H. Elmirghani, "Position Based Routing Protocol for a City Environment," *in the 4th International Conference on Next Generation Mobile Applications, Services and Technologies (NGMAST), 27-29 July, 2010.*

1.3 Thesis Outline

Following the introduction, the thesis is organised as flows:

Chapter 2 summarises vehicular network applications, architectures, technologies, standards, and environments. The chapter also presents an overview of routing protocols, energy efficiency, content caching and distribution, queuing theory modelling and MILP for vehicular networks.

Chapter 3 details the design and implementation of a V2V communication network (VANET) including traffic generation and QoS parameters calculation. The chapter also describes the MH routing protocol, PRMFR, and PRNFP along with their simulator designs. The performance of the aforementioned routing protocols is evaluated in terms of QoS parameters.

Chapter 4 presents the SCH, DCH, and SCF routing protocols and their simulation implementation. This chapter also describes two pure V2R communication scenarios in addition to a hybrid communication scenario comprising the proposed routing protocols. Furthermore, physical channel modelling and energy modelling for both networks are detailed. The system performance is evaluated in terms of QoS and energy.

Chapter 5 presents a MILP model that optimises the number and locations of CPs and BSs in a city vehicular environment. The proposed scenario is described, the chapter develops the optimisation models, uses the vehicular traffic profiles and introduces the concept of virtual traffic points (TPs) which is utilised for optimisation. This chapter also details the heuristics for the CDN and the cellular network.

Chapter 6 Introduces the VCDA along with its simulation implementation. Different power management schemes are also studied to save energy at CPs. The impact of varying BSs' resources allocated for vehicular communications is analysed. The performance of both (CDN and cellular) setups is evaluated in terms of QoS and energy for varying vehicular load and compared with that of the MILP models.

Chapter 7 proposes a detailed queuing model for the Wi-Fi CPs within the CDN, where each CP takes vacations (switches to sleep mode) to save energy during its inactivity periods. The performance of the system is evaluated in

terms of QoS and energy savings and the results are verified through simulations.

Chapter 8 summarises the major contributions of this thesis and highlights the recommendations for future investigations.

2 Vehicular Communication

Networks

2.1 Introduction

This chapter presents a summary of vehicular network applications, architectures, technologies, standards, and environments. The chapter also provides an overview, in the context of vehicular networks, of routing protocols, energy efficiency, content caching and distribution, queuing theory models, and MILP.

2.2 Vehicular Networks: An Overview

The rapid growth in the number of vehicles and the need to develop and deploy safety and non-safety (infotainment) related applications envisaged through vehicular networks have recently become the main drivers for research in this area. Due to this growth, the size of vehicular networks will be arguably equivalent, if not larger than that of the traditional cellular network [31]. Therefore, the incumbent cellular networks may not be able to cope with the demands of vehicular users. Hence a distinct setup is required which can support safety-related applications but also fulfil the ever-growing demand for

multimedia services while on the move. An intelligent vehicle within a vehicular network, is typically fitted with an OBU with wireless communication and computing capabilities, in addition to a GPS device allowing the vehicle to follow its spatial and temporal trajectory [7]. Intelligent vehicles might also have pre-stored digital maps and sensors that can be used to report accidents. Intelligent vehicles are a key part of ITS [8], where they share the goal of both enhancing safety and reducing congestion. Applications that intelligent vehicles can benefit from are categorised as either safety- or non-safety related applications (Infotainment). Collision avoidance and cooperative driving are among the safety-related applications [32,33], whereas internet access [34], multimedia streaming and gaming are examples of non-safety related applications. Other applications, such as toll services, parking, and travel information can also be offered by intelligent vehicles. V2V or IVC systems can be used for direct information exchange between vehicles; however, they do not offer access to external online resources, including the Internet [7].

Generally, cost and performance tradeoffs in a given environment are among the main factors that influence the design and implementation of any communication system. Urban areas demand wide deployment of the wireless infrastructure as the main goal is to provide high bandwidth and ubiquitous connectivity. On the other hand, infrastructure-less V2V communication can provide services where the roadside communications infrastructure is not available or is scarce for example in rural and sparsely populated areas. The

different nature of each of the aforementioned environments may lead to different network architectures being deployed, where utilising several wireless technologies in a certain environment is also a viable option. For example, cellular services are common in urban areas as they offer very good coverage, in addition to the Wi-Fi-based services that are highly popular at hot spots such as shopping centres and airports for high bandwidth applications [7].

2.3 Challenges of Vehicular Networks

Vehicular networks pose many challenges in terms developing designs that offer robustness, reliability and low delay. Some of the common challenges associated with vehicular networks are discussed, here.

- **High mobility**

Catering for high mobility is the most fundamental challenge in vehicular networks. Vehicles usually move at high speeds, which results in a frequent change in the network topology and hence network partitioning [35].

- **Lack of centralised management entity**

Vehicular ad hoc networks operate without the presence of a centralised entity to coordinate and manage the transmissions over the shared medium. This leads to inefficient access to the channel, and as a result collisions between unsynchronised packets are highly probable [36].

- **Transmission power**

Transmission power should be managed well in order to increase the throughput. Node density is an important factor when controlling the transmission power; if the density of nodes is low, the power should be increased so that messages are able to reach their destinations. In contrast, the transmission power should be decreased in high density environments to reduce the effect of interference and minimise channel congestion [37].

- **Radio channel characteristics**

Initiating wireless communication in a harsh environment such as the vehicular environment is a challenging task. Multipath propagation due to physical obstacles is one of the issues which results in degrading the strength and quality of the received signal. Moreover, fading might also be experienced due to the mobility of the surrounding objects and the movement of the sender/receiver themselves [36]. However, increasing the transmission power may help minimise the effect of fading.

2.4 Vehicular Network Applications

The emergence of robust wireless technologies, smart devices and sensors has contributed to the significant growth in vehicular network applications. These applications can be classified as safety or non-safety related applications and are installed on vehicles' OBUs and on RSUs. Due to the time sensitivity of safety information, safety-related messages have priority over non-safety

related messages. In [38], the authors divided safety information into two categories: event-driven and periodic-based information. The former type of information was offered the highest priority, where such information is generated and disseminated by the vehicles involved in an accident. This type of information is to be delivered to vehicles driving towards the area of the accident. In contrast, the latter type of information is disseminated by vehicles to provide status updates (e.g., velocity, direction and acceleration) to neighbouring vehicles and is broadcasted at specific intervals as a precautionary approach. Furthermore, RSUs deployed at intersections can also disseminate periodic information to vehicles, such as intersection conditions. The non-safety related applications aim to provide value added applications to passengers, such as transportation management, infotainment and music download to mention just a few. However, they have a lower priority than the safety-related applications, hence can tolerate higher delay.

2.4.1 Safety related applications

The most important goal of the safety-related applications in vehicular networks is to enhance the safety of passengers and pedestrians as well as the overall safety of the transportation infrastructure [4]. As mentioned earlier, safety-related data must be conveyed to the desired receivers within a certain time limit in order to take full advantage of the data. The vehicle safety communication (VSC) project proposed 34 applications under the safety-related category, which were carefully analysed in order to determine the possible

advantages of such applications [39,40]. The VSC rated these safety applications based on certain criteria [4]. For example, the applications were categorised based on their timely relevance for their commercial deployment. Another criterion worth mentioning is the efficiency of these applications in terms of preventing crashes. Some of the safety applications proposed by the VSC are presented in this thesis.

Lane-changing warning: This application is rated under the mid-term category, where the deployment date was set to be between 2012 and 2016 [4]. The aim of the lane-changing application is to help drivers in the process of changing lanes where periodic broadcasts are received by vehicles from nearby vehicles. In order for this application to be efficiently executed, each vehicle should maintain a table that keeps information about neighbouring vehicles, such as their locations. The data stored in these tables is used by the OBU to check if the road condition is suitable to change lanes. A warning is generated if the lane change poses a danger to the driver. One of the major disadvantages of the lane-changing warning application is its ineffectiveness in the presence of a low vehicular communications penetration ratio.

Traffic signal violation warning: Intersections are among the most hazardous parts of a road; hence, minimising the number of accidents at intersections is the main aim of this application. As shown in Figure 2.1, vehicles receive frequent updates about the traffic signal conditions through infrastructure-to-vehicles (I2V) communication via the RSU deployed near the intersection. Such

updates include the location of the traffic signal and its status. Thereafter, the OBU processes the updates received and determines if a warning message should be generated to the driver based on the nature of the update [4].

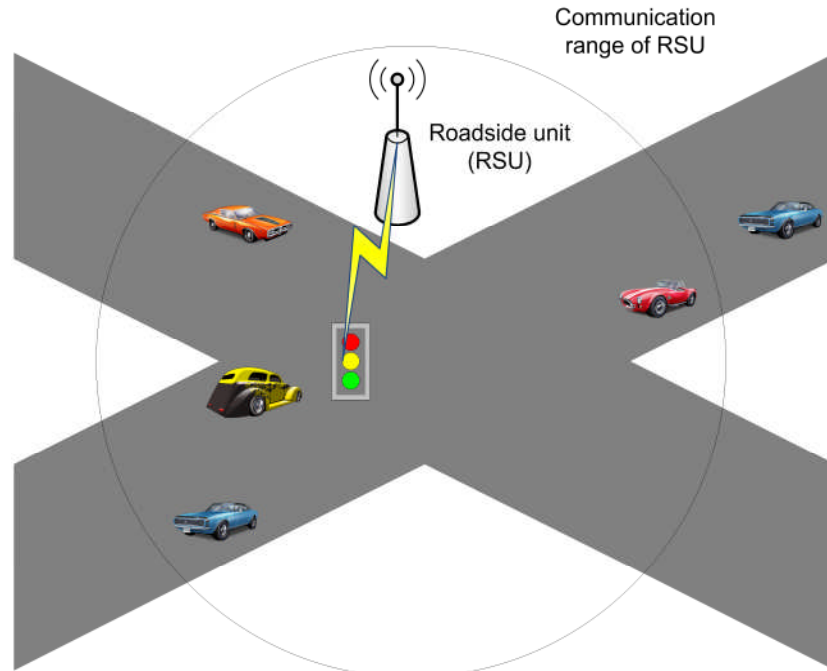


Figure 2.1: Traffic signal violation warning

Pre-crash warning: This application warns the driver when there is a very high probability of a crash which is likely unavoidable. In order to minimise the effect of an accident, V2V and I2V communication cooperate by frequently exchanging messages to enable the efficient use of the vehicle's equipment, such as air-bags and seat belt pre-tightening [2,41]. Such messages include precise information about the vehicle's location and size [2].

Control loss warning: The 'control-loss' warning application is triggered when a driver loses control of his/her vehicle. A message is broadcast to the neighbouring vehicles warning them about the 'control-loss' incident, where the

OBUs of the receiving vehicles assess the relevance of the information received and alert the drivers if needed [2,39].

Emergency electronic brake lights: Rear brake lights are not always enough to alert trailing vehicles about the deceleration of vehicles ahead, especially in poor visibility conditions. The emergency electronic brake light application [2,4] is used to broadcast information to other vehicles within range. Such information includes the deceleration rate and location of the vehicle applying its brakes [4]. Upon receiving the information, the OBUs of vehicles assess the significance of the received information and alert the drivers accordingly. Figure 2.2 depicts a scenario where this application may be used.

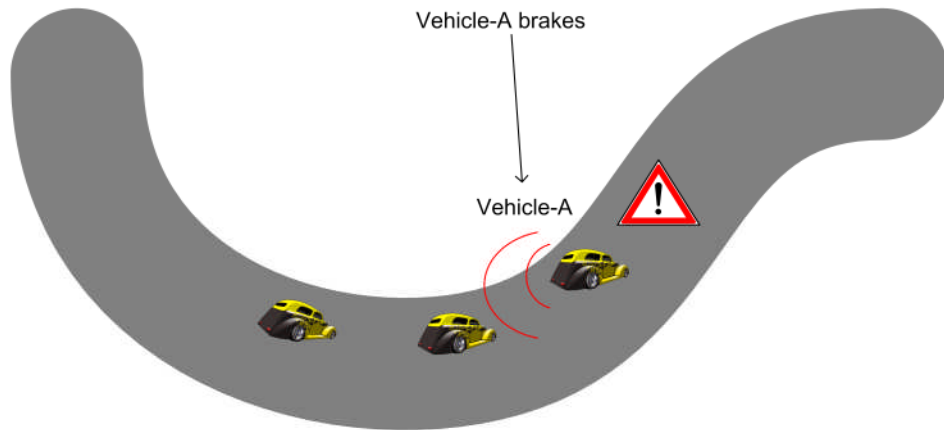


Figure 2.2: Emergency electronic brake light

2.4.2 Non-safety related applications

The goal of the non-safety related applications is to offer a more comfortable and efficient journey to drivers and passengers [42,43]. Several non-safety related applications have been proposed in the literature. The location of the

closest point of interest (POI), weather forecast, and electronic toll collection are examples of some of these applications. The latter application is an efficient way to collect payments electronically, without causing the driver to stop at a toll station for payment [9]. Furthermore, online gaming and instant messages in addition to downloading multimedia files are among the onboard entertainment applications. However, such applications tend to consume a considerable share of network resources [4]. Another interesting application is 'wireless advertising', in which businesses such as shopping malls, restaurants, and hotels can deploy gateways to broadcast advertisements about their products and services to nearby customers [44].

In order to avoid the interference that might occur with safety-related applications, separate physical channels should be used for the non-safety related applications. Moreover, safety-related communication traffic would always be prioritised over the non-safety related communication traffic [44].

2.5 Vehicular Network Architectures

Vehicular networks can support short-to-medium range wireless communication between vehicles within range or between vehicles and RSUs [7]. Vehicles should be equipped with OBUs in order to communicate with other vehicles and RSUs. Vehicular networks have three main architectures as mentioned below. These are:

- 1) Vehicle-to-vehicle (V2V) networks
- 2) Vehicle-to-roadside (V2R) networks
- 3) Hybrid vehicular networks

2.5.1 Vehicle-to-vehicle (V2V) networks

In this type of architecture, vehicles that are within radio range and are equipped with the appropriate OBUs can form a VANET [4,7]. Many researchers envision VANETs as the most feasible architecture for vehicular communication due to the low latency offered by them, in addition to the low cost associated with deploying such networks [7,45]. VANETs do not rely on any infrastructure to support the communication between vehicles (i.e., V2V), and hence, they are easy to deploy. Vehicles exchange different types of information (e.g., location and speed), and so local traffic information is gathered to provide safer roads for drivers, passengers, and pedestrians.

The authors in [9] categorised IVC systems as either single-hop IVC (SIVC) or multihop IVC (MIVC), depending on the way in which the data is delivered from the source vehicle to the destination vehicle. In SIVCs, the data is transmitted via a single hop from the source node to the destination node. On the other hand, in MIVCs, an intermediate node contributes to the delivery of the data between the source node and the destination node. SIVC systems are suitable for applications that demand short-range communication, while MIVC systems are used for applications that need long-range communication. Figure 2.3 and

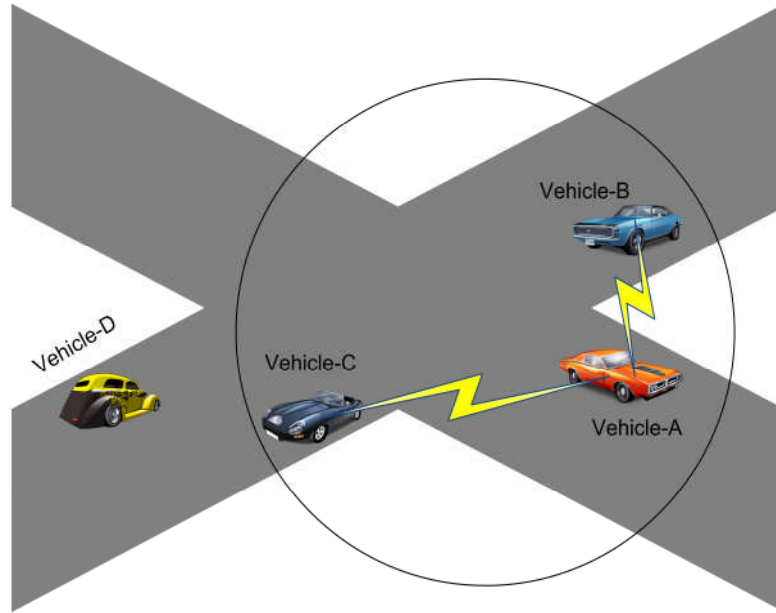


Figure 2.3: Single-hop inter-vehicle communication system

Figure 2.4 illustrate examples of the SIVC and the MIVC systems, respectively. In the SIVC system shown in Figure 2.3, vehicle-A is only capable of sending data to vehicle-B and vehicle-C, as they both are within vehicle-A's communication range. However, if vehicle-A wants to send data to vehicle-D, which is out of its communication range, vehicle-C, which is within the communication range of both vehicle-A and vehicle-D, can relay the data to vehicle-D under MIVC as shown in Figure 2.4.

There are major problems that need to be addressed in V2V systems, such as scalability, MPR, and network availability [7,9]. Moreover, due to network partitioning, ubiquitous network connectivity cannot be guaranteed.

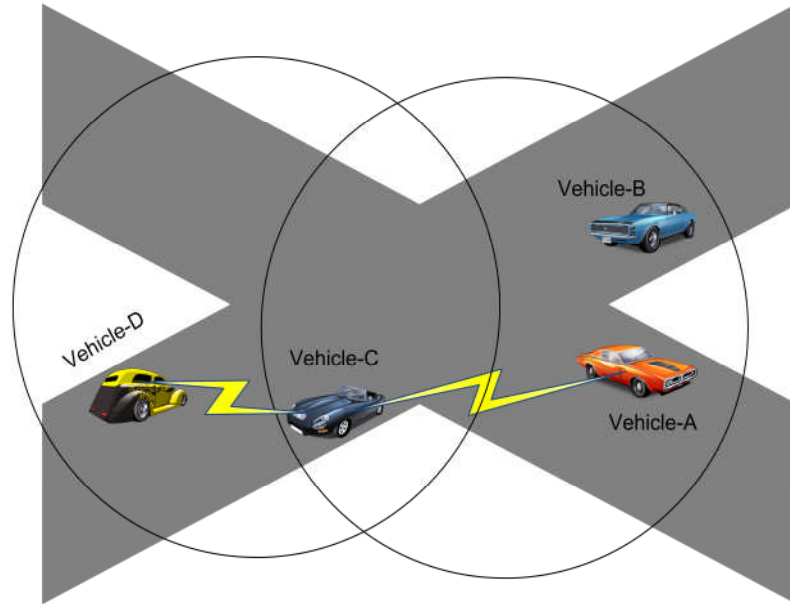


Figure 2.4: Multihop inter-vehicle communication system

2.5.2 Vehicle-to-roadside (V2R) networks

As mentioned in the preceding section, V2V systems have a number of advantages and could often be a viable approach for vehicular communication. However, V2V networks can be unreliable, especially in a low market penetration situation, which makes them unsuitable for several scenarios and applications. Moreover, V2V systems do not offer access to external online resources (e.g., the Internet). Thus, deploying V2R networks that are used for connecting vehicles to fixed infrastructures, such as RSUs, is needed at least in some areas. The V2R network offers reliable broadband communication services and access to online resources and local services, such as traffic information and tourist information [7]. There are two types of services that can be offered by the RSUs; the first type of RSU is deployed to perform certain tasks, such as supporting ramp meter controller functions, and parking payment

collectors, while the other type provides network access via wireless local area network (WLAN) access points (APs) and wireless wide area network (WWAN) BSs [7].

The traditional deployment of a wireless infrastructure in certain hot spots, such as in airports and buildings, is not suitable for vehicular environments where vehicles are distributed widely on roads. Furthermore, the high costs of deploying a wireless infrastructure to support vehicular communication, in addition to the large geographical scale of vehicular networks, are among the challenges faced in the deployment of a V2R network [7]. However, from a commercial point of view, the use of a wireless vehicular infrastructure could follow the footsteps of cellular and WLAN services, where it can be offered as a premium service to the subscribers for a certain fee. On the other hand, on-road services, such as traffic monitoring and management, could also be provided by the government. Recently, public states and private companies (e.g., automotive, communication, ITS equipment manufacturers) have started to cooperate to deploy a wireless vehicular infrastructure [46,47].

In order to benefit from V2R communication, the authors in [48] presented a novel vehicular networking architecture by incorporating various wireless technologies together, such as 3G cellular systems, long-term evolution (LTE), IEEE 802.11, and IEEE 802.16e. The V2R communication systems provide a practical solution to the problem of network fragmentation caused by the mobility of vehicles, through the installation of a wireless infrastructure [49].

However, achieving seamless connectivity in a V2R network calls for wide installation of wireless infrastructure, which is considered a costly approach. Figure 2.5 illustrates a V2R system with online RSUs connected through a wired connection.

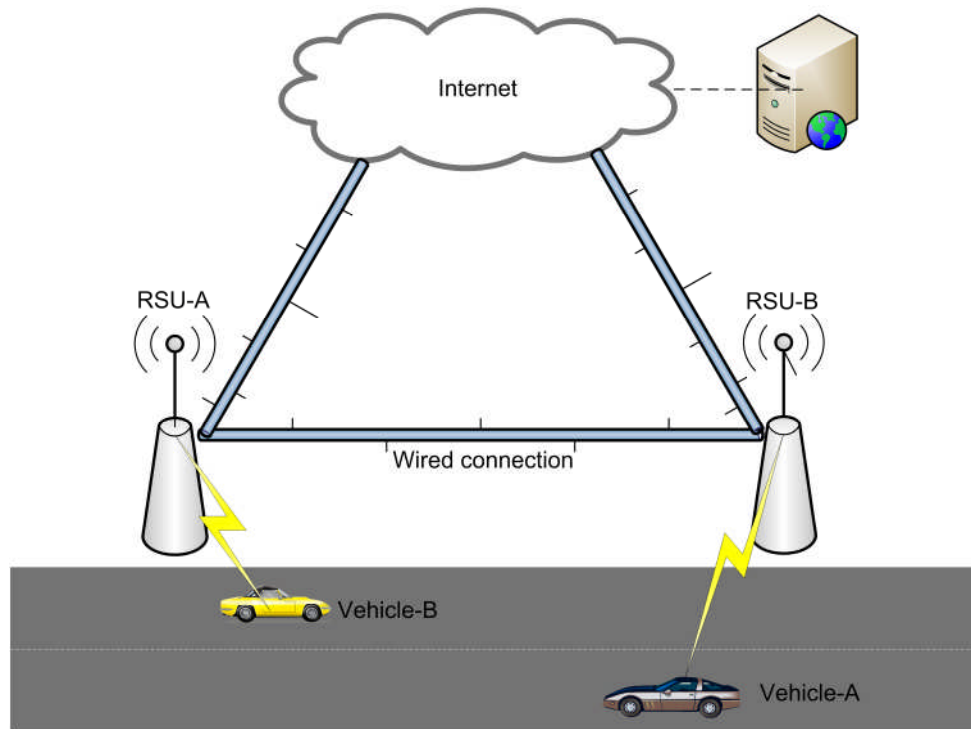


Figure 2.5: Vehicle to roadside (V2R) network

2.5.3 Hybrid vehicular networks

A hybrid vehicular network exploits both V2V and V2R communications in which the cooperation of these two systems guarantees seamless connectivity independent of the traffic scenario. For example, in a low vehicular density scenario where V2V communication is not present all the time, the vehicles communicate with the available RSUs to prevent connection loss [50-54]. Hybrid vehicular communication networks extend the range of traditional V2R

systems by allowing vehicles to communicate with the out-of-range RSUs via other vehicles. This approach reduces the infrastructure requirements and hence the cost [9]. Figure 2.6 shows a scenario in which vehicles warn other vehicles about a dangerous situation that could be avoided, with two interconnected RSUs cooperating in delivering the alert messages to out-of-range vehicles.

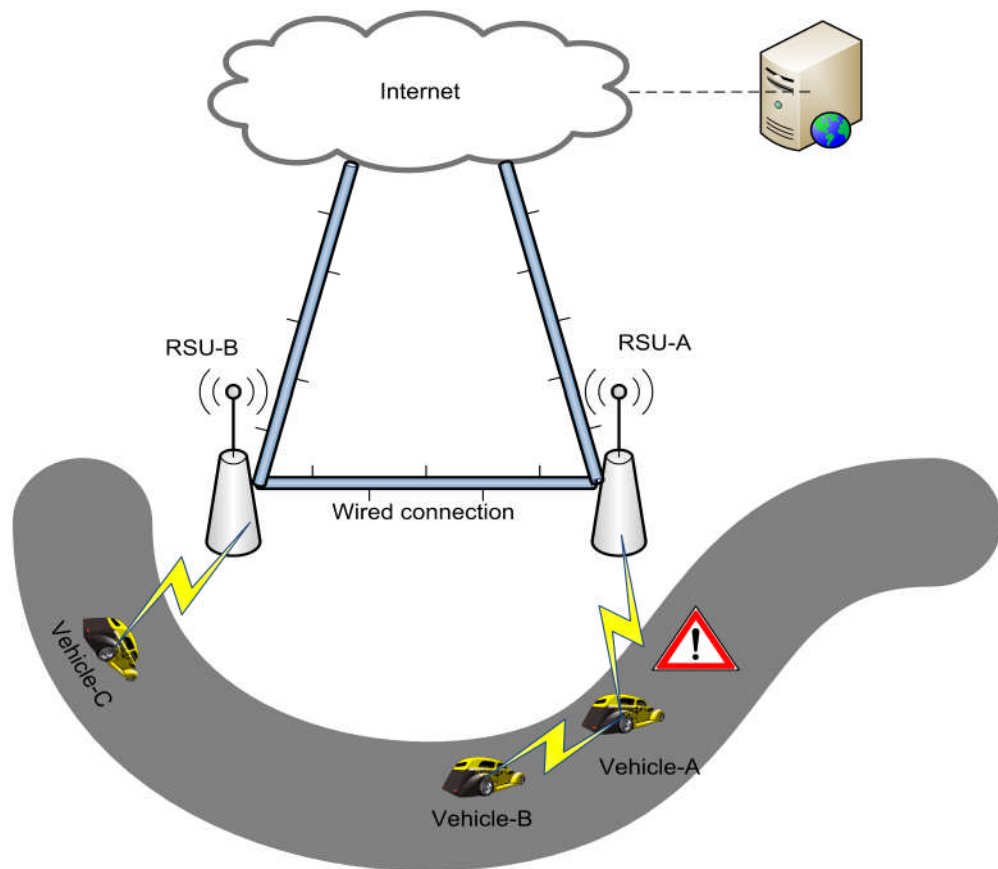


Figure 2.6: Hybrid vehicular communication system

2.6 Vehicular Networks Technologies and Standards

A variety of wireless technologies support vehicular communication. Initially, vehicular communication systems were operated at 915 MHz with up to two

channels in the 12 MHz spectrum. The maximum data rate supported was 0.5 Mbps with a communication range of only 30 m [55]. Thereafter, the U.S. federal communication commission (FCC) allocated 75 MHz band of wireless spectrum at 5.9 GHz solely for dedicated short range communication (DSRC). The allocated wireless spectrum can be used to organise and enhance traffic situations by allowing vehicles to exchange information among themselves and the infrastructure [55,56]. The DSRC and other wireless standards and technologies that can be used to support vehicular communication are detailed in this thesis.

2.6.1 Dedicated short range communications (DSRC)

The DSRC technology is used to offer secure and reliable V2V and V2R communication allowing the exchange of important information for various vehicular applications. The DSRC is developed to adapt to the frequent topology change caused by the mobility of vehicles and to provide low delay. The main aim of DSRC is to ensure a reliable service for safety-related applications; however, non-safety related applications that demand a certain level of QoS can also be supported by DSRC [38].

As mentioned earlier, the FCC allocated a 75 MHz band of the wireless spectrum at 5.9 GHz for DSRC to support public safety and commercial applications for vehicular communication. The 75 MHz band of spectrum (at 5.850-5.925 GHz) is divided into seven non-overlapping 10 MHz channels as

depicted in Figure 2.7 [2,4,6,33,57], where the first 5 MHz “guard channel” is reserved [58]. The seven channels consist of one control channel (CCH_178) and six service channels (SCH_172, SCH_174, SCH_176, SCH_180, SCH_182, and SCH_184). The control channel is dedicated to the broadcast of safety-related messages, such as warnings of hazardous situations, where it can also be used for service announcements [38,57,59,60]. SCH_172 is reserved for high-priority safety-related applications, whereas SCH_184 is reserved for long-range and high-power transmissions for intersection coordination applications. The remaining four service channels are unreserved and are used for exchanging safety and non-safety related information, such as store advertisements and multimedia downloads. The data rates supported using the 10 MHz channels are 3, 6, 9, 12, 18, 24, and 27 Mbps [38]. However, higher data rates of up to 54 Mbps can be achieved by utilising the optional 20 MHz channels (combining SCH_174 and SCH_176 or SCH_180 and SCH_182) [61]. Changing the modulation schemes and the channel code rate allows switching between the achievable data rates to occur [9].

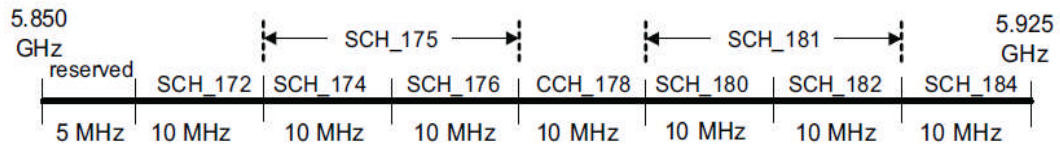


Figure 2.7: DSRC spectrum [38]

2.6.2 Wireless access in vehicular environments (WAVE)

The fundamental building blocks of the WAVE system are the OBUs and the RSUs, in which a WLAN can be established without the need for authentication [62]. While operating under the WAVE system, vehicles can exchange information with other vehicles through their OBUs or with RSUs via the wireless interface of the WAVE standards [63].

The physical and the medium access control (MAC) layers of the WAVE system are described in the IEEE 802.11p [64] standard. The physical layer is based on the IEEE 802.11a [65] standard, which uses orthogonal frequency division multiplexing (OFDM) technology with 10 MHz channels and a maximum data rate of 27 Mbps [63]. The IEEE 802.11 distributed coordination function (DCF), which is based on the carrier sense multiple access with collision avoidance (CSMA/CA) scheme, is used in the MAC protocol for the WAVE standard [63].

The IEEE 1609 working group [6,66] has standardised the higher protocol layers. The IEEE 1609.1 [66,67] is the resource manager at the application layer. It allows the communication between remote applications that might be located outside the vehicular environment and vehicles that are equipped by WAVE-enabled devices [68]. Moreover, the IEEE 1609.2 [69] is the security standard that provides privacy to the users and offers protection against spoofing and eavesdropping. The IEEE 1609.3 [70] defines the networking services standard that deals with connection configuration and management. It introduces the WAVE short message protocol (WSMP) that allows applications

to manage physical parameters, such as data rate, channel number and transmitter power [68]. It also offers a reliable broadcast service with low delay [63]. Finally, the IEEE 1609.4 [71] is the multi-channel operation standard. The IEEE 802.11p and the IEEE 1609 standards make up the WAVE protocol stack shown in Figure 2.8. The WAVE management handles system setup and maintenance [45].

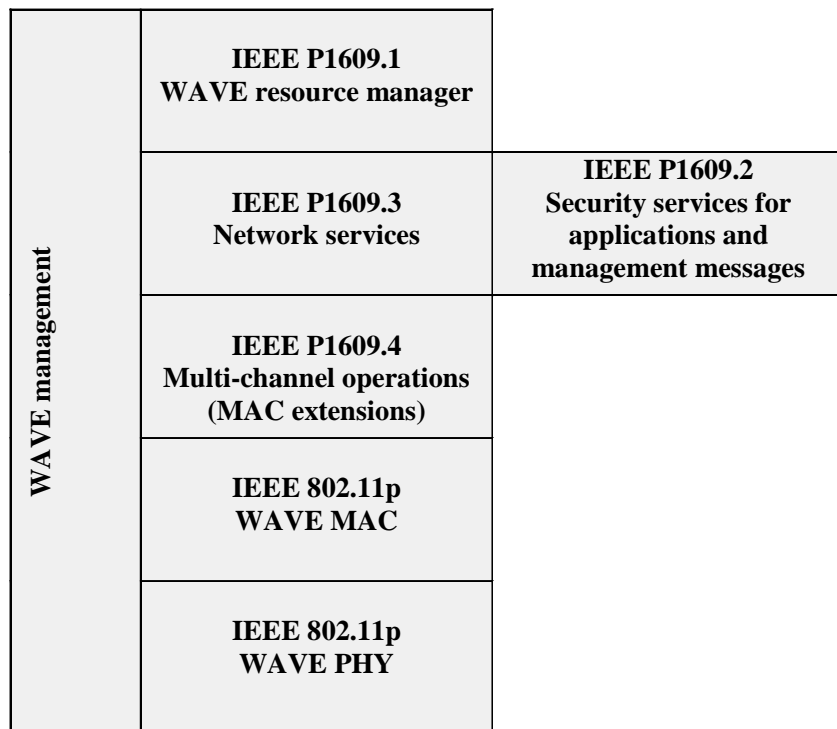


Figure 2.8: WAVE protocol stack [72]

2.6.2.1 IEEE 802.11p standard

The IEEE 802.11 [73] is the most commonly used WLAN standard, as the cost of the high performance equipment that supports the standard is relatively low. Most network simulators have implemented the IEEE 802.11 MAC layer, which makes testing the performance of IVC systems based on IEEE 802.11

hardware easy. However, the IEEE 802.11 standards do not suit vehicular networks' requirements due to the physical and MAC layer limitations. For example, the IEEE 802.11 physical layer is not suitable for high speed moving nodes (vehicles), whereas the MAC protocol cannot guarantee a reliable multicast/broadcast service [74]. One of the proposed solutions is to employ the flooding and retransmission process, but this has an undesirable effect on the throughput and may cause broadcast storm problems [75].

The IEEE 802.11 standard body has issued a new standard, namely, IEEE 802.11p [64], which is an amendment of the physical and MAC layers of the IEEE 802.11a standard. It supports V2V communication with vehicles moving at up to 200km/h with a communication range of up to 1000 m [64]. IEEE 802.11p is standardised and is based on the OFDM physical layer but now with 10MHz channels rather than 20MHz as in the IEEE 802.11a standard. This amendment alone is not enough to provide an appropriate QoS to support traffic safety related applications. Thus, it should be combined with adaptive transmission power and rate control to avoid channel congestion. Moreover, the IEEE 802.11a MAC is not suitable for vehicular communications due to hop unfairness in addition to the lack of MAC stability. Hence, the IEEE 802.11p MAC layer was proposed to allow an efficient communication group setup without much of the overhead typically needed in the current IEEE 802.11a MAC. Such an adjustment is easy to make, as it involves only software updates. On the other hand, at a physical level, the aim is to make the minimum

necessary changes to the IEEE 802.11a physical layer in order to avoid designing a new wireless air-link technology [76].

2.6.3 Cellular systems

A cellular network with its existing infrastructure can be used for longer range vehicular communication, where it also guarantees ubiquitous connectivity. However, the low data rates supported by the cellular network and the associated operational fee and licence make it unsuitable for vehicular environments [77].

2.6.4 IEEE 802.11x

The IEEE 802.11x standards are commonly used in LANs. Data rates of 54 Mb/s can be achieved by the IEEE 802.11g [78] standard where the recently standardised IEEE 802.11n allows data rates of up to 600 Mb/s [79]. These standards are not intended for use in vehicular environments as they cannot handle the mobility of vehicles [77]. Hence, efforts have been made in the amendment of the IEEE 802.11a to make it suitable for vehicular communication leading to the IEEE 802.11p standard discussed in Section 2.6.2.1.

2.6.5 Infrared (IR)

The advantages of Infrared (IR) technology [80] lie in using unlicensed bandwidth, in addition to the fact that secure connections can be established

with ranges of up to 100 m and a data rate of 1 Mbps [77]. Moreover, unlike in radio systems, interference is not an issue in IR systems so that the transmission power can be increased to any level permitted by the eye safety standards [81]. However, IR-based communication can be easily affected by the noise induced at the receiver due to the extreme solar radiation which results in range restrictions [77]. It is worth mentioning that IR technology has been successfully used in vehicular environments, such as the truck tolling scheme in Germany [78].

2.6.6 Millimetre waves (MM)

Unlike IR, millimetre waves (MM) operating at 60 GHz are not affected by artificial light and sunlight; they can also establish links in the absence of a line-of-sight (LOS) because of multipath propagation [77]. On the other hand, MM wave technology is not suitable for high mobility and long-distance communication, as its performance is degraded due to the fast movement of vehicles and the relatively high attenuation at these high frequencies. Hence, it is more practical for short- to medium-range transmissions [78].

2.6.7 Communication air-interface long and medium (CALM)

Communication air-interface long and medium (CALM) is a set of heterogeneous carriers integrated together to support medium- and long-range high-speed vehicular communication [78]. Among the carriers used in CALM

are 2G, 3G, WiMAX, IEEE 802.11p, and IEEE 802.20 in which the aforementioned carriers are used in packet-switched networks in mobile environments [66]. The main advantage of CALM lies in its ability to operate in various countries at any time, due to the multiple carriers included in the CALM framework. Moreover, it can also adapt to the requirements of different types of applications by utilising the carrier most suited for each application [78].

2.7 Vehicular Environments

Generally, cost and performance tradeoffs in a given environment are among the main factors that influence the design and implementation of any communication system. This section discusses the attributes of three different vehicular environments along with their suitable network configurations.

2.7.1 City environment

Providing seamless connectivity in a city vehicular environment is challenging. This is mainly due to the buildings and large objects that might obstruct signals and degrade the wireless channel [82]. Moreover, the packets might also suffer collisions in such an environment, especially in high traffic situations, as a single channel is shared among all users. However, the slow speed of vehicles in a city environment helps maintaining seamless wireless connections for longer periods of time. Heterogeneous deployment of wireless infrastructure is usual for city environments, where cellular services provide ubiquitous connectivity in addition to the recent inclusion of Wi-Fi APs for data offloading

[83]. Figure 2.9 illustrates the vehicular communication scenario in a typical city environment.

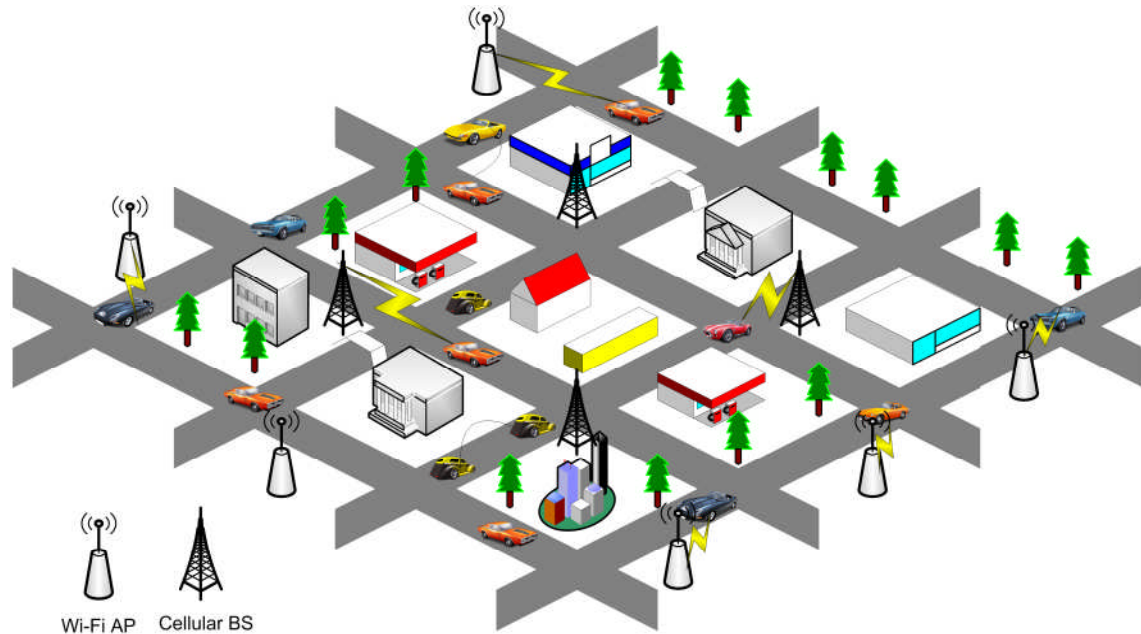


Figure 2.9: City environment

2.7.2 Highway environment

On highways, RSUs might be deployed at regular intervals to provide sufficient connectivity. However, scalability, short connection periods, and the relative speed difference between the vehicles and the RSUs due to the high mobility of the vehicles are some of the typical challenges faced in such environments [45]. The typical vehicular communication setup on highways is hybrid consisting of V2V and V2R communications. An example of a highway environment is shown in Figure 2.10.

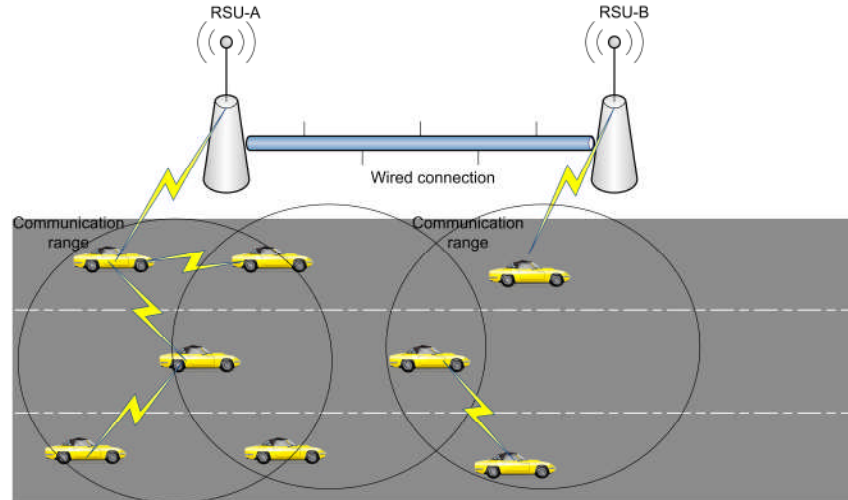


Figure 2.10: Highway environment

2.7.3 Rural environment

To achieve wide coverage through infrastructural deployments in rural and remote areas, a large number of RSUs is needed, which may become expensive. A cost-effective solution to provide good coverage is to deploy a small number of RSUs in suitable places along with ad hoc networks among the vehicles within communication range. However, terrain introduces further challenges in rural areas, where vehicles might lose LOS to other vehicles or RSUs due to winding roads and mountains, resulting in intermittent connectivity [84].

2.8 Vehicular Mobility and Communication Simulators

A vehicular communication network simulator should include a communication layer that takes care of data dissemination and routing, and a vehicular mobility layer which deals with vehicular movement, speed control, and the road

network. Hence, both vehicular mobility and network layer models are needed to accurately evaluate and analyse the performance of a vehicular communication system. However, designing such models should be carefully undertaken as various factors such as road network, accidents, number of vehicles and their speed need to be considered in order to achieve an accurate evaluation of a vehicular communication system.

According to [85], vehicular mobility models can be classified as either macroscopic or microscopic. The macroscopic simulators consider the vehicular traffic flow as a whole, where the flow is treated according to fluid dynamics [86]. On the other hand, microscopic simulators consider each vehicle as a separate entity, modelling its behaviour explicitly. Although the microscopic approach considers the behaviour of each vehicle at a high level of detail, which is desirable, the computational cost associated with it is high [86]. The microscopic models are commonly used nowadays due to their flexibility in manipulating each entity independently. SHIFT [87] is one of the known microscopic simulators introduced by California partners. However, the aforementioned classifications are broad and do not accurately describe the functionality of each type of model. In [86], mobility models are analysed by identifying their main functional blocks: motion constraints, traffic generator, time, and external influences. Motion constraints present the amount of freedom each vehicle possesses, where from a macroscopic point of view, roads and buildings are considered as motion constraints. On the other hand,

neighbouring vehicles and pedestrians are considered as microscopic motion constraints. The traffic generator describes various types of vehicles and takes care of their interactions according to the considered environment. Traffic densities, vehicle speed and flow are macroscopically modelled, where the distance between vehicles, overtaking, acceleration and deceleration are microscopically modelled. Time is one of the most important factors that needs to be considered when modelling realistic vehicular motion, where various mobility configurations are defined for a certain time of the day or weekday. The last functionality block is the external influence, which models the impact of a communication protocol on the motion patterns.

In addition to vehicular simulators, communication simulators such as OPNET [88], network simulator (NS-2) [89], QualNet [90], and OMNet++ [91] are also available to model communication network topology. OPNET and QualNet are professional simulation packages that are capable of modelling large number of communication networks but are expensive due to their advanced features. On the other hand, NS-2 and OMNet++ are freeware simulation packages which support useful modelling features. Leveraging and improving existing simulators such as transportation simulators and wireless communication simulators [89-91] is one of the most practical approaches. It allows the reuse of models that have been previously developed and verified, and then integrate these simulators to operate together and execute flawlessly. Though, the latter process is not easy and may lack scalability.

In order to easily integrate the different network layers and to accurately evaluate their performance under different vehicular densities, a city vehicular simulator (discussed in Appendix A) has been developed, rather than using existing ones such as NS-2 and OMNet++.

2.9 Routing Protocols

Establishing an efficient route for information from source to sink is called routing [92]. There are many routing protocols available in the literature, with each one being targeted for a certain kind of network according to its characteristics.

Due to the hybrid network architecture and the nodes' mobility in vehicular communication, the design of an efficient routing protocol for VANETs is very crucial. The key requirement of any routing protocol is to achieve minimal communication latency with minimum consumption of network resources [14]. The ad hoc nature (i.e. not relying on fixed infrastructure) is shared between VANETs and mobile ad hoc networks (MANETs). Moreover, low bandwidth and short communication range are also considered as similarities between both [14]. As a result, most general ad hoc routing protocols are still valid in VANETs, such as ad hoc on-demand distance vector (AODV) [93] and dynamic source routing (DSR) [94]. These types of protocols operate in a reactive manner, that is, they do not establish routes until such routes are needed and hence reduce the network overheads [95]. However, the simulation results of

these protocols when applied to VANETs showed poor performance in terms of route convergence and low communication throughput [14]. The poor performance is attributed to the fast movement of vehicles and dynamic information exchange through highly unreliable channels. Furthermore, the availability of a realistic mobility model is also an important factor in the design and performance evaluation of routing protocols for VANETs. A number of routing protocols have been proposed for VANETs [21], [96-100]. A few of the most relevant protocols are discussed in this thesis.

2.9.1 Flooding based routing protocols

Flooding is one of the most common approaches followed in order to achieve almost seamless connectivity in vehicular networks [101]. Flooding is achieved by broadcasting the information to all nodes within the transmission range, in which these nodes further transmit the received information to other nodes until the information reaches its intended destination [101]. The drawback of this mechanism is the excessive retransmissions that result in collisions between packets resulting in a broadcast storm [75]. Flooding achieves low latency due to the large number of information carriers (vehicles) compared to other routing techniques, but suffers from higher packet dropping probability (PDP) and a higher number of transmissions in the network [15,16].

2.9.1.1 Multihop (MH) routing protocol

Multihop (MH) routing is one of the flooding-based techniques. In MH routing, the source node forwards a packet to an out-of-range destination via a number of intermediate nodes, where these intermediate nodes exchange and further forward packets among themselves [15,16]. However, an intermediate node only shares a packet with another node if it does not have the same packet to avoid duplication [102]. Moreover, MH routing requires a large buffer in order to avoid packets being blocked due to buffer overflow. For example, if the buffer of a node is small, the old packets will be removed from the buffer when a new packet is received according to a first-in-first-out (FIFO) process.

2.9.1.2 Epidemic routing protocol

Communication networks can be compared to the epidemiology of directly transmitted infectious diseases. Normally, each individual in a certain population has a number of contacts to whom they can pass or from whom they can receive the infection. This creates a network called a 'Mixing Network'. A disease can spread between infected individuals and susceptible individuals in a population. The pattern of the disease-causing contacts forms a network [103].

Epidemic network models, social network models and many others can be used to model the data dissemination in VANETs [104]. Epidemic models are used to analyse the propagation of information in a network of vehicles, where the

information (the illness or epidemic) propagation from one vehicle to the next through proximity is examined. Moreover, the goal of epidemic networks is to stop the spread of a disease, whereas the goal in vehicular communication networks is to maximise it.

In epidemic routing, each node keeps a summary vector of the packets it holds, and whenever two nodes meet, they exchange the summary vectors. Thereafter, each node checks if it has any packet missing in its vector, whereupon it requests the missing packets, if any, from the other node [104]. This process minimises packet duplication. However, due to the flooding nature of epidemic routing, many unnecessary packets are replicated in the network causing high routing overheads [105].

2.9.2 Store-carry and forward (SCF) routing protocol

Considering the nature of vehicular communication environments, spatial and temporal communication patterns, SCF relaying were originally studied to solve the problem of end-to-end connectivity in delay tolerant networks (DTNs) [97]. In SCF routing [106], data packets are propagated from source vehicles to all neighbouring vehicles. However, if the destination is in the range of the source, packets are directly transmitted and subsequently removed from the source node's buffer. On the other hand, if the source vehicle is not capable of reaching the intended destination, it transmits the packets to all of its one-hop neighbours within the communication range. Relay vehicles store the packets

and forward them only if they encounter the destination node. In [18], the SCF routing for a city scenario to reduce flooding has been introduced. However, it suffers from slightly higher delay compared to flooding-based routing.

2.9.3 Geographic based routing protocols

Geographic-based routing has attracted considerable attention recently, due to the availability of low power, inexpensive, and portable GPS. Unlike flooding-based routing protocols, geographic-routing protocols take advantage of the geographic location of the nodes instead of topological connectivity. They use the geographic position information (coordinates) of certain nodes to establish efficient routes [15]. Geographic routing has more than one forwarding strategy, such as greedy forwarding [15,16] and compass routing [107], where both strategies demand the same information at any point in time. The source node knows its geographical location, which can be acquired from a GPS or any external source; its neighbours' locations, by exchanging messages; and finally, the destination node's location, where this can be obtained by a location service [108]. Other geographic-based routing protocols, such as geographic source routing (GSR), anchor-based street and traffic aware routing (A-STAR), have also been proposed in the literature [14].

In most greedy algorithms, the source node selects the next hop according to a specific criterion before starting the actual forwarding process. Some of the greedy algorithms use geometric calculations to choose the next hop, such as

the most forward within radius (MFR) [16] and the nearest forward progress (NFP) [15] algorithms. Another variant of geographic-based routing is compass routing [107], where the source node sends the packet to the neighbour who has the smallest angle with respect to source and destination. The associated problem with such forwarding strategies is the *dead-end* problem [109], where a closer node to the destination does not exist. On the other hand, the merits of such algorithms lie in their easy adaptation to the changing network topology that occurs due to the high mobility of the vehicles. Moreover, there is no need to generate global routes between the source and the destination [110].

2.9.4 Ad hoc on-demand distance vector (AODV) routing protocol

On-demand routing protocols are designed for general use in MANETs, which does not maintain a route to the destination until needed. As a result, their benefit lies mainly in reducing the routing overhead [9].

In AODV [9,93] routing, the source node starts the route discovery process by disseminating route request (RREQ) messages to the desired destination throughout the network. Upon RREQ reception, the receiving nodes update their routing tables with information about the source node and then rebroadcast the RREQ. Thereafter, the destination node unicasts a route reply (RREP) back to the source node acknowledging the RREQ. The RREP will be reversely delivered back to the source node via the same path that the RREQ traversed. Finally, when the source node receives the RREP, a path to the

destination will be set up, to initiate the transmission process. Furthermore, if a link breaks while transmission is taking place, a route error (RERR) is propagated back to the source node, which in turn, reinitiates the route discovery process [93].

As mentioned earlier, AODV routing was initially designed for MANETs, but it is also used for VANETs [111,112]. However, some modifications of the original AODV protocol in such scenarios are needed in order to make it suitable for V2V communications. For example, the authors in [113] modified the AODV protocol so that RREQs are transmitted only within the zone of relevance (ZOR). Experimental results show that the AODV protocol is suitable for small networks, while for larger networks, the route discovery stage may result in network congestion and become unreliable due to broken links [9,114].

2.9.5 Cluster based routing protocols

Cluster-based routing protocols were initially designed for MANETs [115-117]. However, since the nodes (vehicles) in VANETs have different characteristics to those in MANETs, such as driver behaviours and movement patterns, cluster-based routing protocols should be enhanced for use in VANETs in order to be able to form clusters that provide scalability with low communication overheads [14]. In cluster-based routing, a virtual infrastructure is formed by the clustering of the nodes to provide scalability. In a cluster, nodes are classified as follows: the cluster-head (CH) maintains information about its members and gateways in

addition to performing inter-cluster communication. Further, the gateway is connected to more than one cluster. Finally, all other nodes in the cluster are known as members [18].

In a typical cluster-based routing protocol, the network is divided into clusters where each cluster acts as a separate entity, so that updates within a cluster are not shared with other clusters [77]. As a result, cluster members need to maintain less information, hence, have lower overheads. Clustering techniques enhance the system performance in terms of resource utilisation such as frequency re-use in distant clusters [118].

The authors in [119] proposed a cluster-based routing protocol, namely, clustering for open IVC networks (COIN). Unlike in the classical cluster-based routing protocols, where cluster heads are elected based on relative mobility or ID, cluster heads in COIN are elected according to the driver's intention and vehicular dynamics. The studies conducted reveal that COIN performs well in VANETs in terms of cluster stability and the incurred overhead. Moreover, COIN maintains clusters for longer durations. On average, the cluster lifetime increases by 192% while the number of changes in cluster membership decreases by approximately 46% [119]. In [120], the location-based routing algorithm with cluster-based flooding (LORA_CBF) was presented for VANETs, where nodes can have a CH, gateway, or cluster member status. There is only one CH in each cluster maintaining information about the members and gateways within its cluster, whereas a gateway connects more than one cluster.

In LORA_CBF, data packets are delivered from the source node to the destination node through a greedy-like routing protocol. However, if the destination node's location is missing, the source node transmits a location request (LREQ) packet. The route discovery process associated with the AODV routing protocol is similar to the one used by LORA_CBF. However, the dissemination of LREQ and location reply (LREP) packets is restricted to CHs and gateways only. The performance of LORA_CBF has been evaluated in urban and highway vehicular environments and has been compared with the performance of AODV and DSR. The results show that the performance of AODV and DSR have been affected more by the size and mobility of the network than by the performance of LORA_CBF. In order to balance the load and improve QoS, a DCH routing protocol for a city vehicular network has been proposed in [19]. Simulation results demonstrate that the DCH protocol outperforms the SCH routing protocol in terms of average end-to-end packet delay and PDP.

2.9.6 Auction/credit based routing protocols

MANETs and VANETs inherit some uncertain factors, such as willingness to cooperate, unconditional forwarding of packets and honesty in revealing information [121]. Moreover, ad hoc networks were initially used for military purposes, where a single authority coordinates all the participating nodes in the network, and all the nodes have common goals to achieve [122]. On the contrary, in civilian applications of ad hoc networks [123-129], and more

specifically, VANETs, the participating nodes are considered to be selfish as they are not related to the same authority. Moreover, they have no common goal to achieve. As a result, cooperation cannot be presumed in such applications, as each node is working for its own benefit. An efficient solution for these challenges is to implement an auction-based routing protocol with a credit system in order to enhance the payoffs of the transmitter and the receiver [121, 126], [130-132].

The authors in [126] proposed a routing protocol to stimulate cooperation among selfish nodes in MANETs known as Sprite: a simple, cheat-proof, credit-based system for MANETs. In Sprite, the delivery of packets costs money (credits) where the source node pays a certain number of credits to all nodes that participate in the delivery of its packets. Hence, the source node decides how many packets to transmit depending on the asking price of the relay nodes that will forward its packets to the destination node. For example, if the asking price is high, the source node does not transmit many packets and vice versa. Upon delivery, all the nodes that were part of the delivery process including the source node and the destination node will have benefited [121]. Although the above-mentioned routing protocols were initially proposed for MANETs, they are also useful in improving the performance of VANETs.

2.10 Energy Efficiency in Wireless Networks

There were various efforts in the recent past to make wireless networks energy efficient. While one of the views is to optimise RF output power [12,133], others [134] found it little useful as the power consumption of the circuitry is much higher than the transmitter output power. However, collectively energy savings can be obtained with reduced transmission power and optimised operational power. Furthermore, energy savings can be achieved by introducing sleep strategies at wireless nodes in the idle state [135,136]. An energy efficient cluster-based scheme, namely a low-energy adaptive clustering hierarchy (LEACH) was introduced in [133], where a randomised cyclical election of local CHs is performed in order to distribute the energy load uniformly between the participating nodes. The transmission power consumption of a node consists of two elements: (i) the power consumption of the transmitter circuitry and (ii) the power consumption of the output amplifier. The results show that optimising the transmit power level at the source nodes leads to power savings during the period when the nodes are in the transmitting state. In [135], two sleep based semi-asynchronous power saving protocols were proposed. The performance of the semi-asynchronous power saving protocols is compared with that of the asynchronous power saving protocols, where the results reveal that the semi-asynchronous protocols achieve better performance than the asynchronous of protocols. In [137], the authors proposed three asynchronous power saving schemes, known as dominating-awake-interval, periodically-fully-awake-interval

and quorum-based schemes. These proposed schemes address the power management problem in IEEE 802.11-based MANETs that are usually associated with several challenges, such as unpredictable mobility, multihop communications, and the lack of clock synchronisation. Moreover, the authors studied common problems associated with the direct adoption of the power saving (PS) mode defined in the IEEE 802.11 [62] protocol, such as neighbour discovery and network partitioning. The neighbour discovery problem occurs when a node in the PS mode (sleep mode) is not able to inform other nodes about its existence in the network. Thus, routing protocols that are based on neighbour information may not be able to execute the route discovery process efficiently leading to high packet latency and network partitioning. To solve these problems, the proposed protocols force the PS nodes to transmit beacon packets more frequently than the traditional IEEE 802.11 standard does. Furthermore, the wake-up and sleep of nodes are carefully arranged so that any node (including the nodes in sleep mode) is guaranteed to be detected by other neighbouring nodes within an acceptable time. The simulation results reveal that the proposed schemes achieve considerable power savings while maintaining acceptable neighbour discovery time.

2.10.1 Energy efficiency in vehicular networks

Energy efficiency in vehicular networks has been a focal point in research recently [10-13], [18-20]. The authors in [11] proposed a cross-layer optimisation framework to enhance the power efficiency in V2R networks. A

joint power and sub-carrier assignment policy was derived based on the proposed framework, while considering the delay requirement of each vehicle in order to achieve the desired improvement in energy consumption. The results prove that the proposed scheme outperforms other existing schemes in terms of energy savings. In [10], the authors mentioned that cooperative relaying is a key approach towards achieving energy efficiency in vehicular communication networks. Moreover, the authors in [21] used the delay tolerance of networks as a resource to achieve savings in energy expenditure. They perturbed the delay (increase) in order to physically (using vehicles) propagate the packets to the desired location to save communication energy. However, energy savings were achieved in V2V communications only, without affecting active BSs. To achieve energy savings at both vehicles and BSs, a cluster-based routing scheme has been proposed in [18,19] by allowing cluster members and BSs to operate sleep modes to save energy. Simulation results prove that the proposed cluster-based schemes outperform other schemes in terms of network energy consumption, however, this was achieved at the expense of QoS.

2.11 Content Distribution Networks (CDNs) and Node Placement

Due to the overwhelming interest in media-rich content downloading, CDNs have drawn considerable attention in recent days. For example, IPTV, VoD and CuTV are among the services offered by these CDNs [27]. Such content delivery demands high bandwidth for transmission and a large storage capacity

for audio and video files. According to [29], by 2014, more than 91% of the global IP traffic is going to be in the form of videos, with an annual growth rate of 33%.

Content caching methods were initially used for web caching [138,139]. Nowadays, the use of web caching extends to wireless and mobile networks [140] with the aim of reducing the load on the network, thus, enhancing end to end delay and throughput. Two types of content caching are available: cooperative caching [141] and non-cooperative caching [142]. In the former scheme, nodes can share cached information and unanimously take decisions on the type of information to be cached and the longevity of the cached data. On the other hand, the nodes in the non-cooperative caching schemes are independent, where they take uncoordinated decisions on whether to cache currently used routing paths and data. Moreover, content caching is commonly used in communication networks to reduce end-to-end delay, enhance capacity (higher data rate), and minimise network congestion [143]. By using caching techniques, the network congestion is reduced as the traffic served by a BS is reduced. Moreover, by placing content close to the end users, energy consumption in transmission is reduced as roadside CPs are installed at locations where signals from the BS are weak [143]. Further, I2V communication is based on high data rate technologies capable of efficiently transferring media-rich files (e.g., high definition videos and real-time gaming) to vehicular nodes.

Due to the aforementioned advantages, content caching and distribution are attracting considerable attention in vehicular networks [83], [144-147]. In [144], the authors proposed a content distribution scheme for VANETs with the aim of achieving low latency content distribution in a dense vehicular highway network. RSUs are used to distribute the content to vehicles in a unidirectional highway network, with the help of V2V communication to achieve better connectivity and lower latency. The authors in [145] proposed a push-based popular content distribution (PCD) scheme in which RSUs proactively broadcast popular content to the vehicles in an area of interest. The vehicles that are within the range of each other form a VANET to distribute the received content among them. A symbol-level network coding (SLNC) technique is used to address the network fragmentation problem and reduce the overheads while maintaining the desired performance levels. Simulation results show that the proposed scheme in [145] performs better than other network coding-based PCD schemes in terms of average downloading delay, protocol efficiency, and fairness.

Energy-efficient caching was proposed in [148] and [149]. The authors studied different caching strategies to reduce the energy consumption in ad hoc networks. However, the node placement problem is one of the most important issues in terms of network planning and deployment. The location problem is usually formulated to determine the locations of communication networks' equipment, such as BSs, relay stations (RSs) and gateways. For example, to minimise the access latency in multi-hop wireless networks, the authors in [150]

implemented a scheme for caching server content at selected nodes in the network. The available studies on energy-efficient node placement mostly concentrate on sensor nodes [151]. In the case of relays, the authors in [152] studied the joint RS placement in order to maximise the sensor network lifetime. Furthermore, some studies have introduced RS placement to maximise the capacity of the network [153], whereas others have claimed to minimise the average probability of error [154].

2.12 Queuing Theory Based Analysis

Queuing theory can be used as a tool to model a number of stochastic problems related to communication networks [155]. Limited use of queuing theory in the context of vehicular networks has been witnessed. However, it has been widely used in analysing and predicting the QoS of access networks [156]. In [157], QoS parameters, such as throughput, PDP and end-to-end delay were evaluated using queuing models. The authors in [158] introduced a generic model based on [157] to optimise the buffer size while keeping the throughput above a certain threshold. In [159], the authors proposed a queuing analytical framework that combines priority queuing and vacation queuing to evaluate the performance of a multihop relay network in terms of QoS and energy efficiency. The vacation queuing model deals with the sleep mechanism of the node while the priority queuing model is formed at a node to differentiate between source packets and relayed packets which are waiting for processing and further transmission. The framework has been utilised to evaluate the performance of

the 802.11 DCF MAC protocol and the energy-aware S-ALOHA MAC protocol where a trade-off between QoS parameters and energy savings has been studied.

An M/M/1 queuing model was proposed in [160] to study the performance of a collision warning protocol in which the delay of warning messages and the throughput were evaluated. The authors in [161] studied the feasibility of using vacant UHF television white space for vehicular dynamic access through a queuing theory for multiserver, multipriority, preemptive queues. The performance was evaluated using M/M/c and M/G/c queues, where the results prove that the proposed approach is feasible for vehicular communication in rural and suburban areas, and meets the QoS requirements of DSRC.

2.13 Mixed Integer Linear Programming (MILP)

Optimisation techniques such as mathematical programming are used to maximise or minimise an objective function while satisfying a number of constraints [162]. Among the applications of mathematical programming is the design and management of communication networks, where such networks may have a large number of nodes/links, highly dynamic environment and extremely variable (spatial and temporal) load. For instance, a common problem in communication networks is to find an optimum set of routes that maximises the traffic flow between a pair of nodes when the capacity of each link is known [162]. The aforementioned problem can be solved using various

mathematical programming techniques such as linear programming (LP) [162]. In LP, the objective function and the constraints are given as linear functions. MILP [163] has been used as an optimisation tool for over 50 years in various fields such as engineering and business [164]. The merits of MILP lie in the availability of dedicated solvers and its modelling flexibility [164]. There are a number of MILP solvers in the literature [165-167], where they utilise various techniques [168,169].

MILP has been used in wireless networks for maximising data rates and minimising total network power consumption [170]. MILP formulation is also used in vehicular networks [171,172]. In [171], the authors have developed energy efficient scheduler which meets traffic demand generated by vehicles, with the help of a MILP model. The authors have derived an upper bound on the energy consumed by the scheduler which can be used as a bench mark for comparison with other scheduling algorithms. In [172], the authors proposed a content downloading system with the objective of maximising the aggregate throughput for a vehicular network. In order to achieve this, they have optimised the number and locations of RSUs, while considering various deployment strategies such as density-based, and different data transfer schemes such as relays. Their approach is based on processing a road layout and a vehicular mobility trace that produce a graph representing the temporal network evolution. Using this graph, the authors have formulated a MILP model to solve the max-flow problem, which utilises the optimised number of RSUs obtained

through different deployment strategies, however it identifies the optimum deployment to achieve the maximum throughput. The results revealed that a density-based RSU deployment has achieved performance comparable with the optimum (i.e. max-flow), and that multi-hop traffic delivery is a viable option, however, not beyond 2 hops from the RSU.

2.14 Summary

In this chapter, various challenges associated with vehicular networks, different types of vehicular network applications, architectures, technologies, and environments have been reviewed. Studies related to routing protocols, energy efficiency, content caching and distribution, queuing theory analysis and MILP for vehicular networks have been introduced.

3 Vehicular Ad hoc Network

3.1 Introduction

A vehicular communication network usually needs a vehicular mobility layer and a communication layer that interoperate in order to accurately evaluate its performance. Having discussed the design of the vehicular mobility model in Appendix A, in this chapter, the design and implementation of the V2V communication network including traffic generation and QoS parameters calculation are detailed. Secondly, the MH routing protocol and two position-based routing protocols, namely PRMFR and PRNFP along with their simulator design are described. Thirdly, these routing protocols are integrated with the city vehicular simulator (described in Appendix A) where their performance is evaluated under varying vehicular loads, and the impact of vehicular node's buffer size (*bSize*) on the performance is also studied. Finally, the impact of greedy nodes (GNs) on the performance of the three routing protocols is studied.

3.2 Vehicular Ad hoc Network Simulator

A simulator for the VANET has been developed in JAVA using one class that is ***AdhocSimulator***. However, the classes that were developed in the city

vehicular simulator (Appendix A), namely, **Vehicle** class, **Road** class, and **VehicularSim** class were also integrated to complete the system. The **AdhocSimulator** class defines a number of variables and vectors. Two variables *cr* and *mpr* are used for the communication range of vehicles and the market penetration ratio, respectively. The variable *bSize* is used to assign the buffer size of a vehicular node. The variable *dRate* is used to represent the traffic generation rate. The variable *totalPktsDropped* counts the total number of packets dropped and the variable *receivedPkts* counts the number of successfully received packets. The *totDelay* variable records the total delay experienced by all successfully delivered packets. The packet IDs and the total number of packets generated are stored in the *pktID* and *totalPkts* variables, respectively. The variable *totalPktsInNetwork* counts the total number of packets in the network (original and replicated packets).

Three global vectors are defined in the **AdhocSimulator** class: *vectPktID*, *vectPktTime*, *vectDestID*. The *vectPktID* and *vectPktTime* vectors store the ID and generation time of each packet, while the *vectDestID* vector keeps the ID of the vehicle that the packet should be delivered to (i.e. destination vehicle). These three vectors are used for the packet retrieval process which are discussed later in the chapter. The final stage of the vehicular ad hoc network simulator development is the routing protocol used. Three routing protocols are designed and integrated to interoperate in the vehicular simulator (discussed in

Appendix A). A flowchart for the VANET simulator is illustrated in Figure B.1 in Appendix B.

3.3 Traffic Generation

The traffic generation follows a constant bit rate (CBR) at 2 kb/s. Although the traffic generation rate is much higher in practice, a low rate has been chosen to demonstrate the principles and maintained acceptable computational burden. Moreover, the total simulation duration (*TotSimTime*) is set to 1500 seconds which is sufficient to study vehicle's mobility. Each packet generated is assigned a random source vehicle and a random destination vehicle from the total vehicles that are assigned in the simulation (*TOTAL_VEHICLES*). However, if the source vehicle and the destination vehicle have the same ID or the source vehicle is not equipped with an OBU (in the case where the MPR is not 100%), a new pair of source and destination is chosen for that packet. The packet size is represented by the variable *PktSize* that is set to 512 bytes, where packets are continuously generated throughout the simulation runtime. Hence, the total number of packets generated over 1500 seconds is given by

$$totalPkts = \frac{dRate \times TotSimTime}{PktSize \times 8} \quad (3.1)$$

The *pktID* of each generated packet is stored in the chosen source vehicle's vector (*srcPktID*) and in the global vector *vectPktID*. Moreover, the destination vehicle's ID of that packet and the time at which the packet was generated are

stored in the global vectors *vectDestID* and *vectPktTime*, respectively. Figure 3.1 gives an illustration of how each generated packet is maintained, whereas a flowchart showing the traffic generation mechanism is shown in Figure B.2 in Appendix B. Note that the same traffic generation mechanism is followed for all the routing protocols discussed in this chapter.

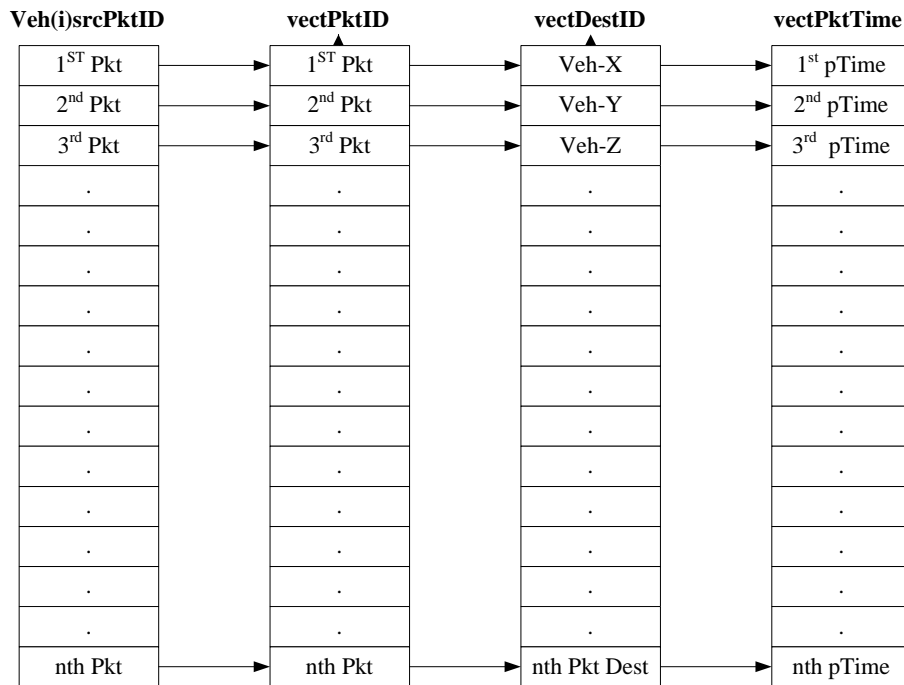


Figure 3.1: Storing procedure of packets

3.4 Multihop Routing Protocol and Its Implementation

This part of the simulator describes the packet propagation and the routing protocol used to deliver packets from their sources to their destinations. The first routing protocol designed was the MH routing protocol. In MH routing, the source vehicle floods the network with the packet to be transmitted. If any vehicle comes into the communication range of another it receives a replica of

the packet. This process continues until the packet reaches its destination or is dropped due to buffer overflow of vehicular nodes. The total number of transmissions in the network under the MH routing is very high as each vehicle forwards the packet to all the vehicles in its vicinity. However, the average end-to-end (E2E) delay is low compared to other routing schemes. The network topology of a flooding-based routing network is shown in Figure 3.2.

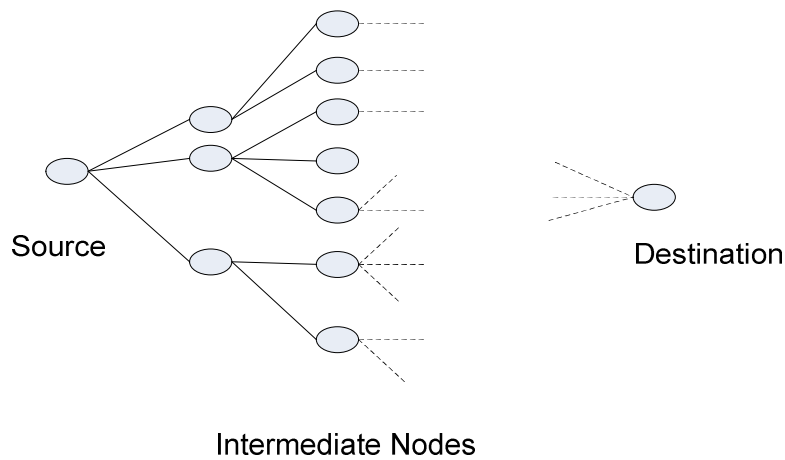


Figure 3.2: MH routing topology

As mentioned before, the number of vehicles in the network to be considered in simulation can be inserted by the user in the *TOTAL_VEHICLES* field. However, for simplicity, the MH simulation mechanism will be explained for a single vehicle. Firstly, the vehicle checks all other vehicles within its range and checks if these vehicles are equipped with OBUs. If these two checks are satisfied, the vehicle exchanges all its packets with the neighbouring vehicles and stores them in its *relayPktID* vector. However, a dedicated method is executed to check against packet duplication. Moreover, the vehicle keeps

checking the size of its buffer so that if it is full, the first packet stored in the buffer is dropped according to the FIFO mechanism as shown in Figure 3.3.

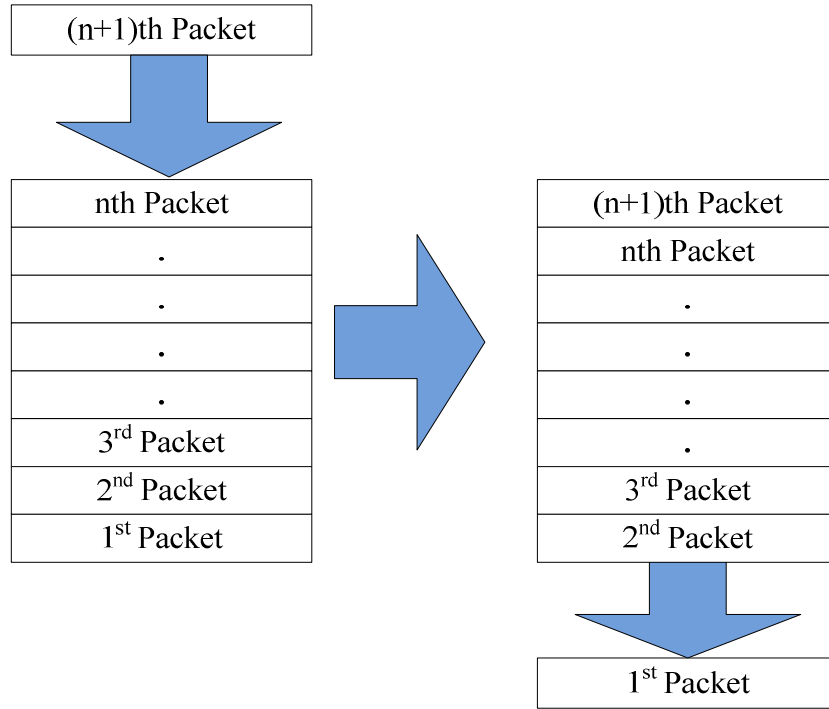


Figure 3.3: Packet dropping mechanism (FIFO)

Secondly, the E2E delay experienced by each successfully received packet is calculated. All other packets are kept in the vehicle's buffer and are further transmitted to any other vehicle that it encounters. The vehicle checks each packet stored in its *relayPktID* vector and retrieves its generation time (*pTime*) from the *vectPktTime* vector (see Figure 3.1). The delay for each packet (*pDelay*) is given by

$$pDelay = SysTime - pTime \quad (3.2)$$

The *receivedPkts* variable is incremented with each successfully received packet where the E2E delay for these packets is added to the *totDelay* to

calculate the average packet delay experienced in the network. When the simulation ends, the average E2E delay, PDP, and the total number of transmissions in the network (*totalPktsInNetwork*) are determined. The system parameters used in simulations are given in Table 3.1. A snapshot of MH routing in the city scenario is depicted in Figure 3.4, where a flowchart for MH routing simulation is depicted in Figure B.3 in Appendix B.

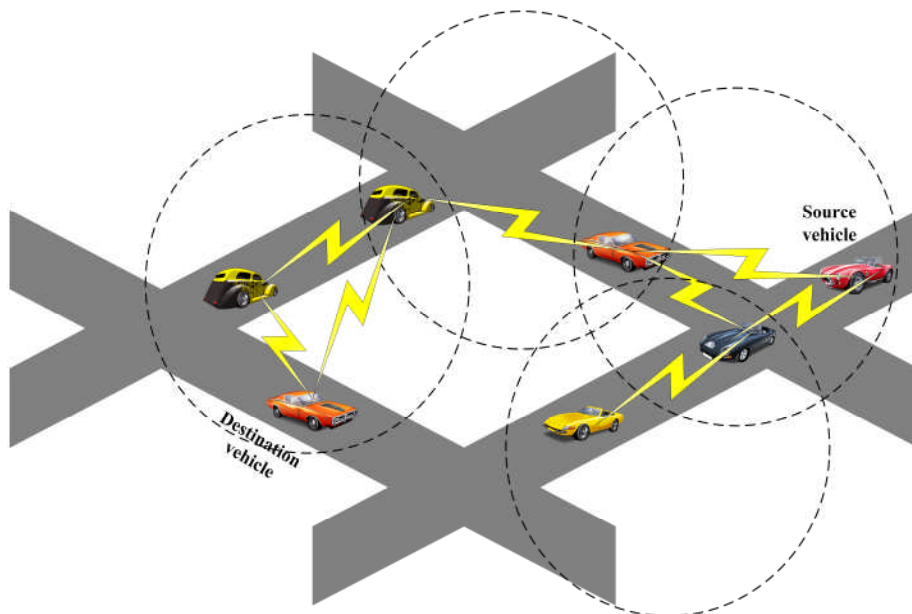


Figure 3.4: A snapshot of MH routing

3.5 Geographic (Position)-based Routing

In MH routing, the information is carried by all the vehicles in the city achieving low E2E delay. However, this causes the network to be flooded by packet replicas, which in turn, results in wasting network resources. Therefore, two position-based routing protocols are proposed here, namely, PRMFR and

PRNFP to reduce the number of packets in the network and the percentage of dropped packets.

In the two proposed routing protocols, it is assumed that a vehicle knows its own location using GPS, the locations of other nodes and the location of the destination. This is done through each vehicle periodically broadcasting its location using low data rate transmission but longer range (i.e.1 km in our case). Collisions are avoided by utilising random back-offs and multiple channels. Moreover, the movements of the vehicles are predictable, but their direction cannot be predicted once they arrive at a junction.

3.5.1 Position-based routing with most forward within radius (PRMFR) protocol and its implementation

In PRMFR protocol, the aim is to achieve the maximum forward progress within the communication range while minimising the total number of transmissions in the network and reducing the PDP. If the destination vehicle is in the source vehicle's vicinity, the source vehicle forwards the packet directly to the destination vehicle without the aid of any relay vehicle. But due to the large area of the city model (discussed in Appendix A) used in simulations and the small communication range (250 m communication range assumed), this situation rarely happens. However, if the destination vehicle is not in the vicinity of the source vehicle, the distance between the destination and the in-range neighbouring vehicles is determined using the *findHypotenuse()* method. However, only the nearest vehicle to the destination but within the

3.5 Geographic (Position)-based Routing

communication range of the source vehicle (determined by *findMinDistance()* method) gets a copy of the packet. Figure 3.5 gives a better picture of how the proposed routing scheme operates. As depicted in Figure 3.5, Vehicle-A, Vehicle-B, Vehicle-C, and Vehicle-D are all within the communication range of the source vehicle. However, Vehicle-A and Vehicle-B are immediately ignored as they are not in the direction of the destination vehicle. The distance between the destination vehicle and Vehicle-C (d_1) and the distance between the destination vehicle and Vehicle-D (d_2) are calculated, and hence the packet is forwarded to Vehicle-D as it is closer to the destination vehicle than Vehicle-C.

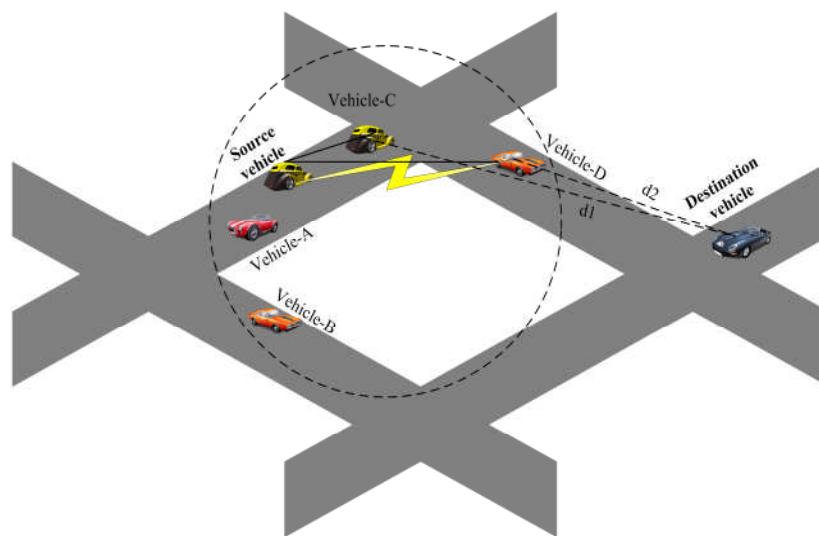


Figure 3.5: A snapshot of PRMFR and PRNFP

As soon as Vehicle-D receives the packet, the PRMFR algorithm is executed along the forwarding path until the packet either reaches the destination vehicle or is dropped due to buffer overflow. The *pDelay* is calculated in the same way mentioned earlier. The advantage of such a routing scheme is the minimisation of the number of hops traversed by each packet, hence decreasing the number

of packet replicas in the network. The simulation mechanism of the PRMFR protocol is shown in Figure B.4 in Appendix B, and the system parameters used in simulations are given in Table 3.1.

Variable	Value
Simulation area	3x3 km ²
Number of runs	50
Number of vehicles	20 to100
Simulation duration	1500 seconds
Traffic source	CBR
Sending rate	2 kb/s
Packet size	512 bytes
MAC protocol	802.11
Node buffer size	10, 50
Greedy nodes percentage	25%

Table 3.1: System parameters

3.5.2 Position-based routing with nearest forward progress (PRNFP) protocol and its implementation

The PRNFP protocol operates in the same manner as the PRMFR protocol. However, the source vehicle opts to forward the packet to the nearest neighbour within the transmission radius instead of the farthest neighbour. The motivation behind designing the PRNFP protocol is also to minimise the total number of transmissions in the network and to reduce the number of dropped packets compared to the MH routing. The distance between the source vehicle and all neighbouring vehicles is determined using the *findHypotenuse()* method, where the nearest neighbouring vehicle to the source vehicle, determined by the *findMinDistance()* method, gets a replica of the packet. The PRNFP algorithm repeats itself until the packet reaches the desired destination vehicle.

In Figure 3.5, using the PRNFP protocol, the distance between the source vehicle and all its neighbours (Vehicle-C and Vehicle-D) is determined, where node C is chosen as the next hop according to the NFP algorithm. As soon as node C receives the packet, the same algorithm is executed along the forwarding path until the packet either reaches the destination or gets dropped due to buffer overflow. The simulation mechanism of the PRNFP protocol is shown in Figure B.4 and the system parameters used in simulations are given in Table 3.1.

3.6 Greedy Nodes (GNs) Integration

In the three routing protocols presented in this chapter, it is assumed that all vehicles act fairly in terms of relaying packets. However, the behaviour of vehicles is different in practice, where some vehicles may opt to drop packets rather than forwarding them to the next vehicle towards the destination. This behaviour has a negative impact on the system performance which has to be studied. Hence, a percentage of GNs is introduced to the network and their impact on the performance of the routing protocols is studied. Simulation results show that GNs have a significant effect on the performance of MH routing in terms of PDP and total number of transmissions in the network. On the other hand, GNs have marginally affected the performance of the PRMFR and PRNFP protocols. Figure 3.6 depicts a snapshot of MH routing with GNs. The source vehicle forwards the packet to all its neighbours (Vehicle-A and Vehicle-B). However, only Vehicle-A forwards the packet to other vehicles

within its communication range. Similarly, when Vehicle-C receives the packet from Vehicle-A, it forwards the packet to the destination vehicle. Note that Vehicle-B and Vehicle-D hold the received packet which eventually gets dropped due to finite buffer size, rather than being forwarded to the next hop.

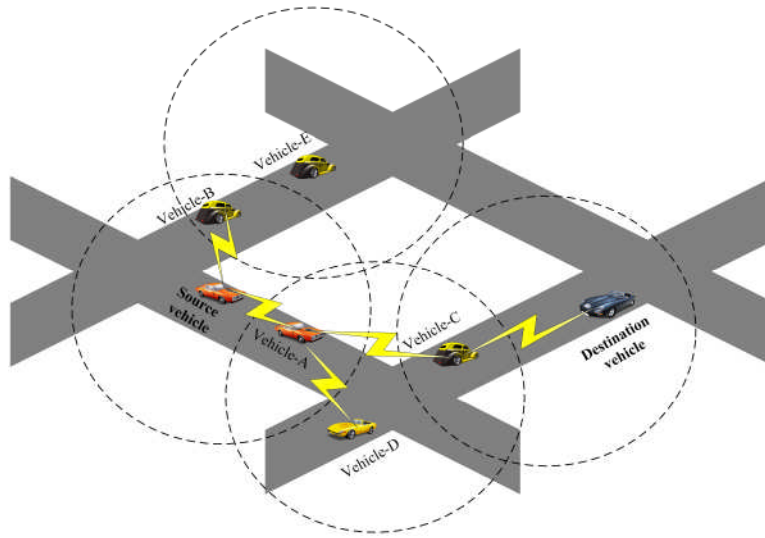


Figure 3.6: A snapshot of MH routing with GNs

3.7 Performance Evaluation

The performance of the three routing protocols has been evaluated in terms of QoS parameters, namely, E2E delay, PDP, and total number of transmissions in the network. The developed city vehicular simulator (discussed in Appendix A) encompasses a 3×3 km² city environment, which is used to evaluate the performance of the routing protocols discussed in this chapter. Moreover, the impact of vehicular node's buffer size, *bSize*, on the performance has been studied by varying the buffer size (10 and 50 packets). Further, the effect of GNs on the performance of the routing protocols has been considered. Moreover, the traffic generation rate and total simulation duration are set to 2

kb/s and 1500 seconds, respectively. The reason behind such a low rate is to enable us to demonstrate the principles and maintain acceptable computational burden, whereas the chosen total simulation duration is sufficient to study the vehicles mobility in an effective manner. The system parameters are described in Table 3.1.

3.7.1 Average end-to-end delay

The average E2E delay is an important measure of the system performance which describes the average delay experienced by a packet to be delivered from the source vehicle to the destination vehicle. The average E2E delay is only determined for the successfully received packets and can be calculated as

$$E2E\ Delay = \frac{totDelay}{receivedPkts} \quad (3.3)$$

where *totDelay* refers to the summation of the delay experienced by each successfully received packet (i.e. *pDelay*), which can be computed using Equation 3.2, and *receivedPkts* denotes the total number of successfully received packets. Figure 3.7 shows that the E2E delay for all the three protocols decreases with an increase in the number of vehicular nodes with a buffer size of 50 packets. With a buffer size of 10 packets, MH routing outperforms PRMFR and PRNFP protocols. This is because delay is only calculated for successfully received packets where with a small buffer (i.e. 10), packets will either be dropped (and hence do not contribute to the total delay) or

will reach their destinations with low latency. Note that for a buffer of size 10, the delay significantly increases with the increase of number of vehicles for the PRMFR and PRNFP. This is mainly because the number of successfully received packets also increases significantly while the number of vehicles is still relatively low (i.e. 40) and hence the higher delay. Moreover, PRMFR achieves lower delay than MH with a buffer of size 50 especially with high number of vehicles. This is because with higher number of vehicles, the connectivity in the network is improved in addition to the fact that in PRMFR, the packet is only forwarded in the direction of the destination. Figure 3.8 shows a comparison of the E2E delay for the three protocols with and without 25% GNs with a buffer size of 50 packets. The E2E delay decreases with an increase in the number of vehicular nodes for the three protocols. However, it is almost the same for all the protocols.

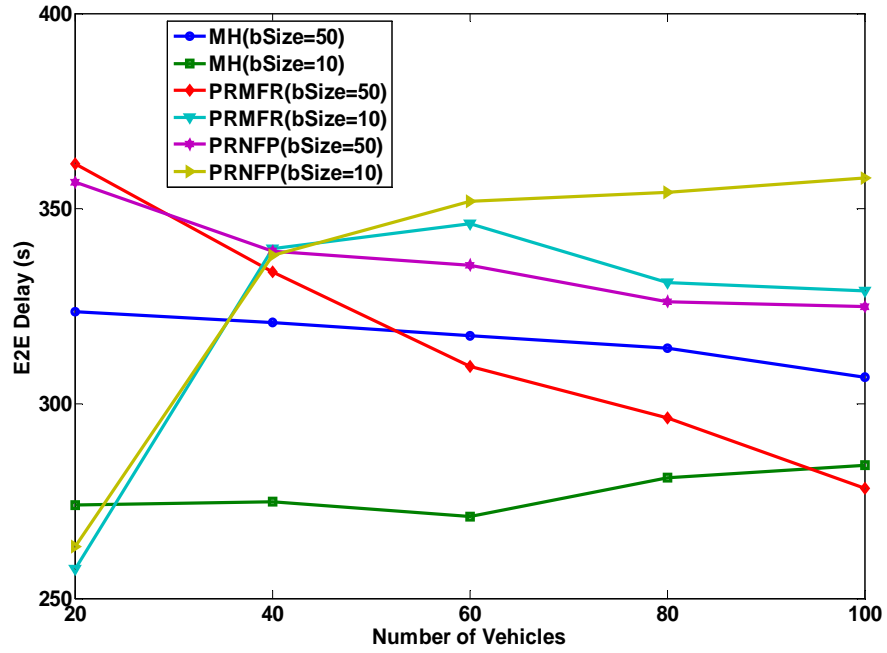


Figure 3.7: Average E2E delay with varying vehicular load

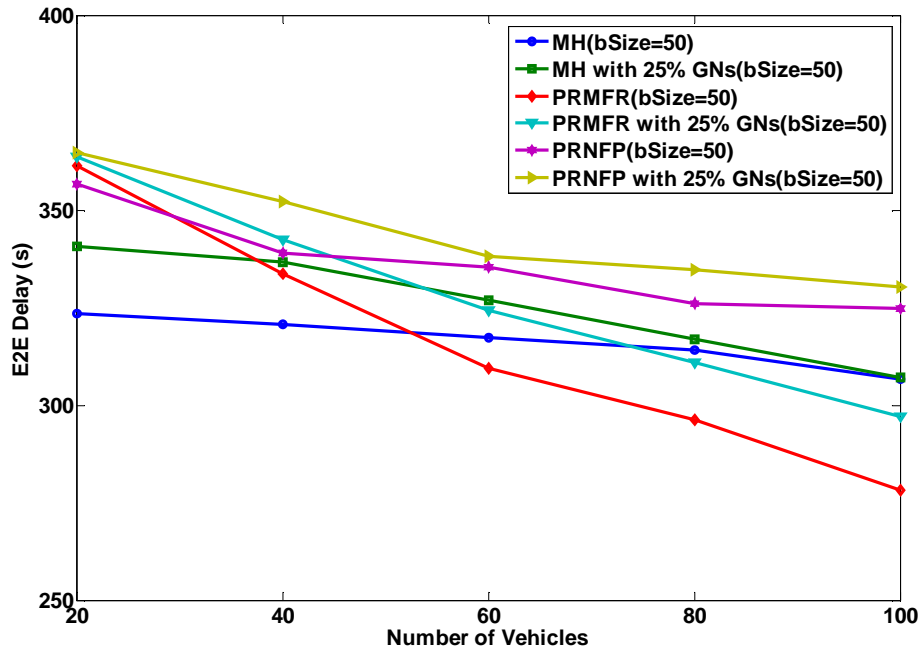


Figure 3.8: Average E2E delay with GNs with varying vehicular load

3.7.2 Packet dropping probability

The PDP is another key parameter used for performance evaluation and can be calculated as

$$PDP (\%) = \frac{totalPktsDropped}{totalPkts} \times 100 \quad (3.4)$$

where *totalPktsDropped* are the packets which have been dropped due to vehicular nodes' buffer overflow, and *totalPkts* refers to the total number of packets generated during simulation. Figure 3.9 shows the PDP under the three routing protocols with different buffer size. The PDP decreases with an increase in the number of vehicular nodes. Both PRMFR and PRNFP perform better than MH routing particularly for a buffer size of 10 packets, where the percentage of dropped packets is 50% less compared to MH routing. However, employing larger buffers gives the opportunity for vehicular nodes to hold more packets and thus experience a lower PDP.

Figure 3.10 shows the PDP for all three protocols in the presence and absence of 25% GNs. In MH routing, the effect of GNs is clear as the percentage of dropped packets has increased by approximately 18%. On the other hand, the effect of GNs is negligible on both PRMFR and PRNFP. This is because under these protocols, only few selective nodes (according to their distances from the source) receive the packets.

3.7 Performance Evaluation

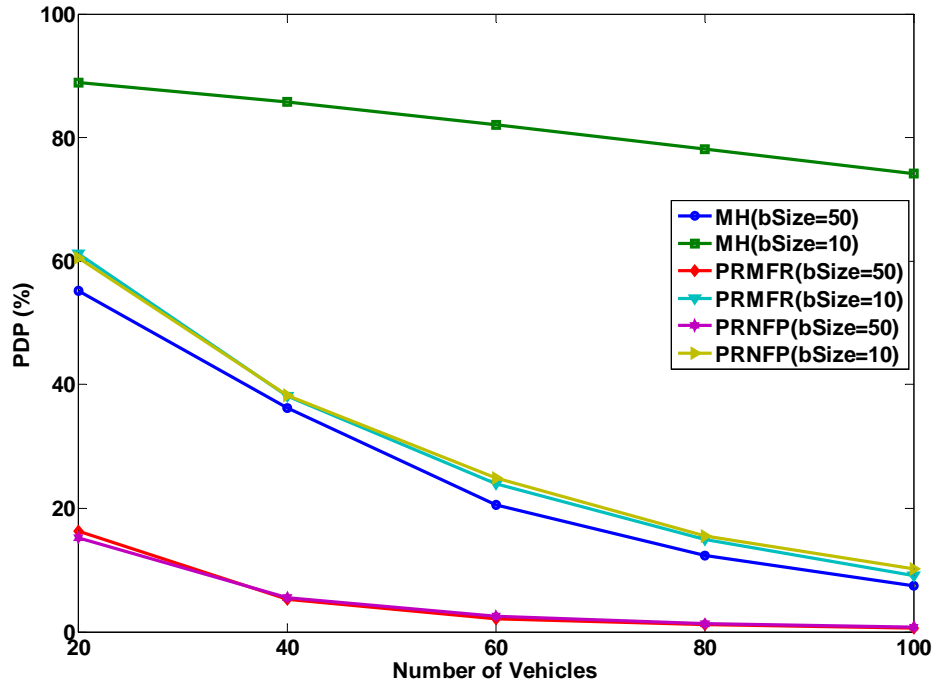


Figure 3.9: PDP with varying vehicular load

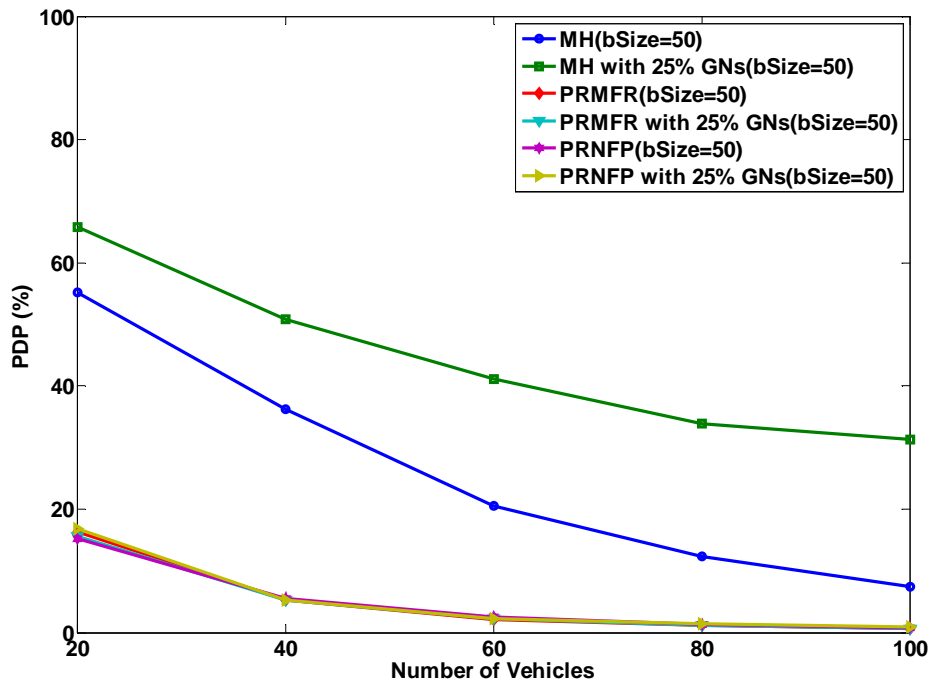


Figure 3.10: PDP with GNs with varying vehicular nodes

3.7.3 Total number of transmissions in the network

The third important parameter used for performance evaluation is the total number of transmissions in the network which denotes the summation of the total number of original packets and the replicated packets in the network (*totalPktsInNetwork*). Figure 3.11 shows that the total number of transmissions in the network increases with an increase in the number of vehicular nodes. In MH routing, the total number of transmissions is much higher compared to the PRMFR and PRNFP protocols. Moreover, for a buffer of size 10, the total number of transmissions with 60 vehicles is more than 1 million packets for MH routing compared to 394k packets and 400k packets for PRMFR and PRNFP, respectively. Figure 3.11 also shows that PRMFR and PRNFP have generated 63% and 65% less packets than MH routing, respectively. Note that in the PRNFP and PRMFR protocols, a replica of the packet is only transmitted to one node at a time where the relay node is chosen according to a specific forwarding criterion (closest or farthest from source). On the other hand, the network is flooded with packet replicas in the case of MH routing and hence the large number of packets in the network.

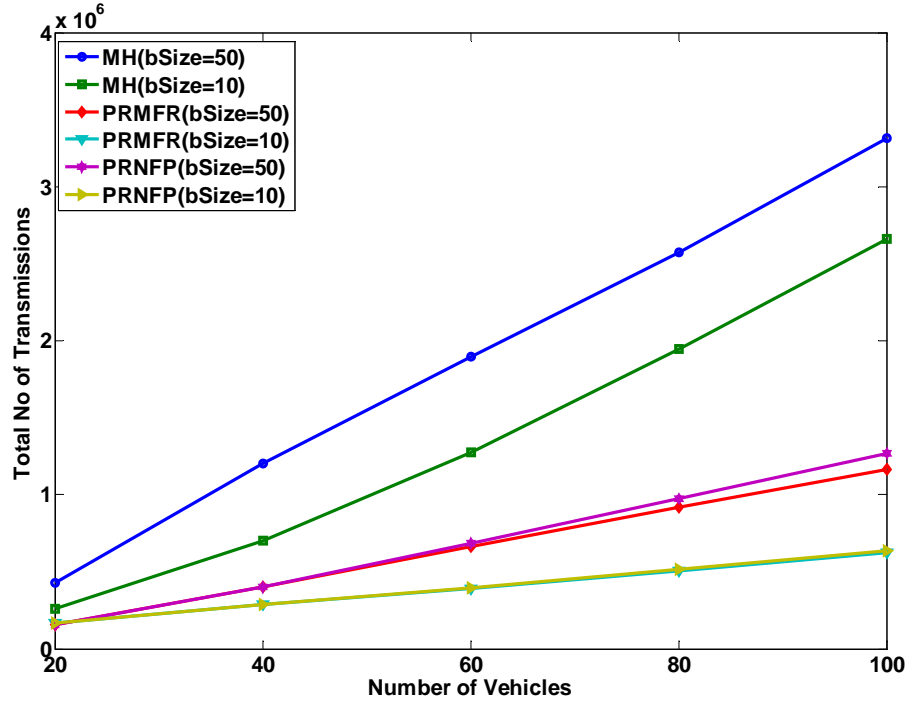


Figure 3.11: Total number of transmissions in the network with varying vehicular load

With 25% GNs incorporated, the total number of transmissions is reduced by almost 50% under MH routing as shown in Figure 3.12. The significant reduction in the number of packets is attributed to the nature of GNs and their behaviour in the network. Similar to PDP, for PRMFR and PRNFP with GNs, the total number of transmissions is marginally reduced.

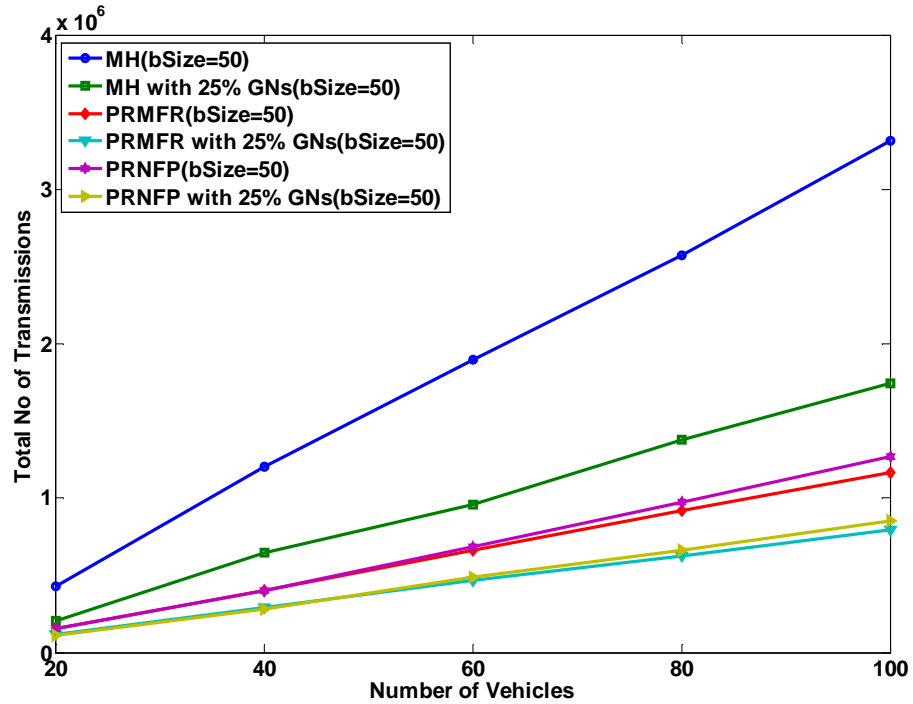


Figure 3.12: Total number of transmissions in the network with GNs with varying vehicular load

3.8 Summary

In this chapter, VANETs and their simulation implementation are described. Further, the MH routing, PRMFR, and PRNFP protocols are studied along with their simulation implementation. A realistic scenario is introduced where the effect of greedy nodes on the proposed routing protocols has been discussed. The performance of the three routing protocols is analysed in terms of average E2E, PDP, and total number of transmissions in the network. Furthermore, the impact of introducing 25% greedy nodes on the performance of the routing protocols is studied.

3.8 Summary

The simulation results showed that the PRMFR and PRNFP protocols outperform the MH routing protocol especially in terms of PDP and total number of transmissions in the network. Both PRMFR and PRNFP generated approximately 70% less packets than MH routing while the percentage of dropped packets decreased by almost 53%.

The impact of GNs was more significant on the MH routing protocol than on the PRMFR and PRNFP protocols. MH routing protocol experienced a significant reduction in the number of transmissions in the network in the presence of GNs. However, this has been achieved at the expense of higher packet dropping probability.

4 Energy Efficient Hybrid Vehicular Network in a City Environment

4.1 Introduction

Since almost 80% of the power is consumed by the BSs hardware and accessories [21], a pure V2R network in a city environment is considered very costly in terms of power consumption. The total energy consumption of a V2R network can be reduced by limiting the number of BSs and with a suitable selection of a routing protocol in lieu of extensive BS coverage.

To demonstrate the difference in terms of energy expenditure and QoS parameters, in this chapter, two pure V2R scenarios are studied, where the first one provides full coverage with 9 BSs (one BS per rectangular city block, see Figure 4.1) while the other studied scenario utilises 4 BSs. While operating under 4 BSs a significant amount of energy is saved however at the expense of degraded QoS. To restore the performance, different routing schemes have been examined / developed namely, MH (described in Chapter 3), SCF, SCH, and DCH routing. Following the introduction, the studied scenario is introduced.

Thereafter, the two pure V2R communication systems and the four routing schemes are discussed along with their simulation implementation. These communication schemes are integrated with a city vehicular simulator (described in Appendix A). Moreover, a physical propagation model¹ and a detailed energy model specifically derived for the studied dynamic scenario have been incorporated to analyse a more realistic representation of the communication layer which allows an accurate performance evaluation of the system in terms of QoS and energy consumption.

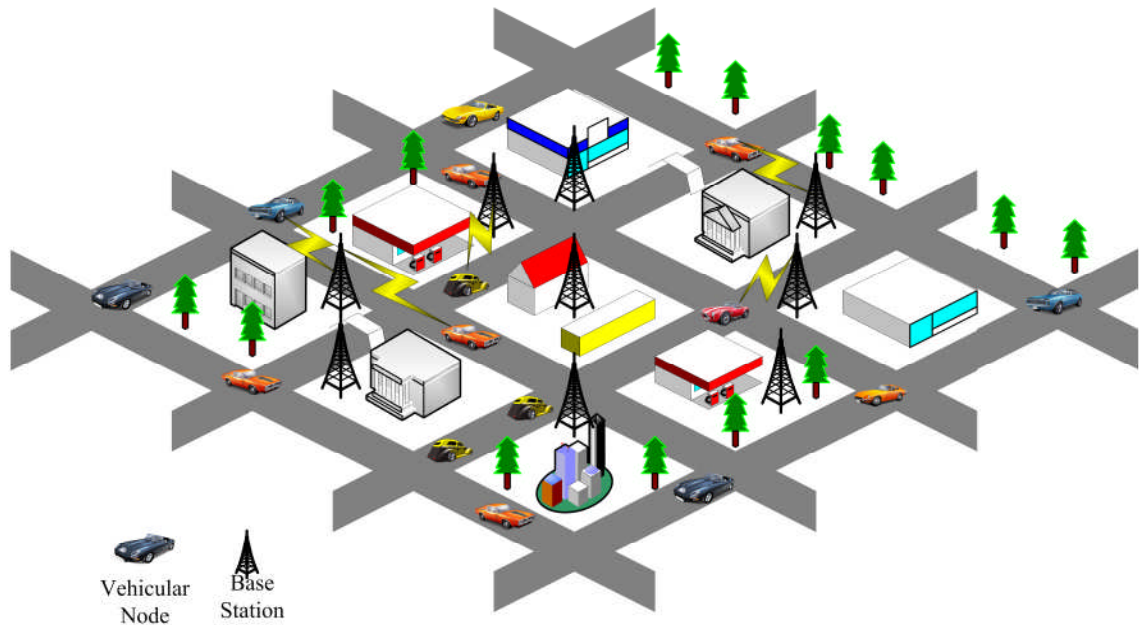


Figure 4.1: The studied city scenario

¹ Note that this piece of work was carried out in collaboration with a former PhD student, Dr. Wanod Kumar of School of Electronic and Electrical Engineering, University of Leeds, United Kingdom.

4.2 The Studied City Scenario

The studied scenario is a 3x3 km² city with 48 roads and 16 junctions (discussed in Appendix A) and 9 BSs installed in the 9 blocks as shown in Figure 4.1.

4.3 Vehicle-to-Roadside (V2R) Scenarios and their Simulation Implementation

In this scenario, the city network shown in Figure 4.1 is divided into nine equally sized blocks where one BS is installed in each block (formed between four roads) to serve the traffic (9BS_V2R scenario). A dedicated class for BSs (class **Basestation**) is designed and integrated with the city vehicular simulator and the VANET simulator (described in Chapter 3). Class **Basestation** creates a BS object along with its attributes which are: *BSID*, location of BS in road i.e. *BSRoad*, the location of the BS i.e. *BSLoc*, and the cluster ID of the BS i.e. *BSCID*. The traffic generation follows the same process discussed in Chapter 3. However, the traffic generation rate used in this chapter is set to 1 kb/s in order to avoid prohibitive simulation time due to the number of packets generated over the 1500 seconds network evaluation period. Each generated packet is assigned a random source vehicle and is stored in its buffer as discussed in Chapter 3. The destination node for each packet generated in the V2R scenario is the nearest BS to the source vehicle which is determined using the

findHypotenuse() method. The communication range of the V2R scenario is 800 m. The system communication parameters are given in Table 4.1.

Note that it is a pure V2R scenario in which no V2V communication takes place. Due to the ubiquitous coverage achieved by the 9BS_V2R scenario, the E2E delay, packet loss ratio (PLR), and the total number of transmissions in the network are very low. However, this comes at the expense of total network energy consumption. Hence, using the developed city vehicular simulator (discussed in Appendix A), five of the nine fully functional BSs are put into sleep mode to save significant amount of energy. The corresponding impact on QoS is studied (4BS_V2R scenario).

4.4 Hybrid Scenario, Routing Protocols and their Simulation Implementation

Routing is one of the essential functions in vehicular networks as its main task is to efficiently deal with the frequent topology changes and fragmented network. Several routing protocols have been proposed in the literature. The majority of these protocols focuses on QoS and energy efficiency separately. However, due to the increased use of the road network, there is a need to study different routing protocols which offer QoS guarantees while minimising the energy consumption. Flooding based routing [101] relies on packet retransmissions so that once a packet has been generated and transmitted by a single node, it is retransmitted by all the receivers. Flooding offers low end to

end delay but suffers from large number of transmissions. SCF [106] is another routing protocol used in vehicular networks, in which a relay node stores the received packets and carries them until it detects an appropriate destination and forwards them. In cluster based routing schemes [96], the vehicles are divided into groups based on their geographical locations. Under a cluster structure, vehicles are assigned a different status, such as CH and cluster member. Clustering reduces routing overheads as only CHs spread data, but experience higher delay.

While operating under the 4BS_V2R scenario, significant energy savings is achieved compared to the 9BS_V2R scenario. However, this is achieved at the cost of QoS as the 4BS_V2R scenario does not offer seamless connectivity. Hence, an ad hoc setup which comprises four routing schemes is introduced which restores the performance and the trade-off between energy and different QoS parameters is studied in detail. The four routing schemes are integrated with the city vehicular simulator and with the communication simulator (described in Chapter 3), including the **Basestation** class, to form a hybrid communication system. The vehicles that are not within the BSs' range deliver their packets to the BSs via other relay vehicles according to different routing protocols. The buffer of a vehicular node can store up to 100 messages where the V2V communication range is set to 200 meters. The system communication parameters are given in Table 4.1. Note that MH routing was discussed in

Chapter 3 along with its simulation implementation, however, the only difference here is that the destination node is a BS instead of a vehicle.

System Communication Parameters	V2R	V2V
Channel bit rate	1 Mb/s	1 Mb/s
Data generation	1 kb/s	1 kb/s
Simulation area	$3 \times 3 \text{ km}^2$	$3 \times 3 \text{ km}^2$
Simulation duration	1500 s	1500 s
No. of simulation runs	50	50
No. of vehicles	100 to 500	100 to 500
Transmission range	Up to 800 m	Up to 200 m
Packet size	512 bytes	512 bytes
Maximum tolerable delay	N/A	500 s
Buffer size	N/A	100 messages

Table 4.1: System communication parameters

4.4.1 Store-carry and forward (SCF) routing

In SCF or two-hop routing, data packets are propagated from source vehicles to all neighbouring vehicles or BSs. If one of the BSs is in the V2R range of the source vehicle, packets are directly transmitted and subsequently removed from the source vehicle's buffer. However, if the source vehicle is not capable of reaching any BS, it transmits the packets to all its one hop neighbours within the V2V range. Relay vehicles store the packets and forward them only if they encounter a BS as shown in Figure 4.2. The SCF routing is primarily introduced to reduce flooding experienced in the MH routing protocol discussed in Chapter 3. However, it suffers from higher delays.

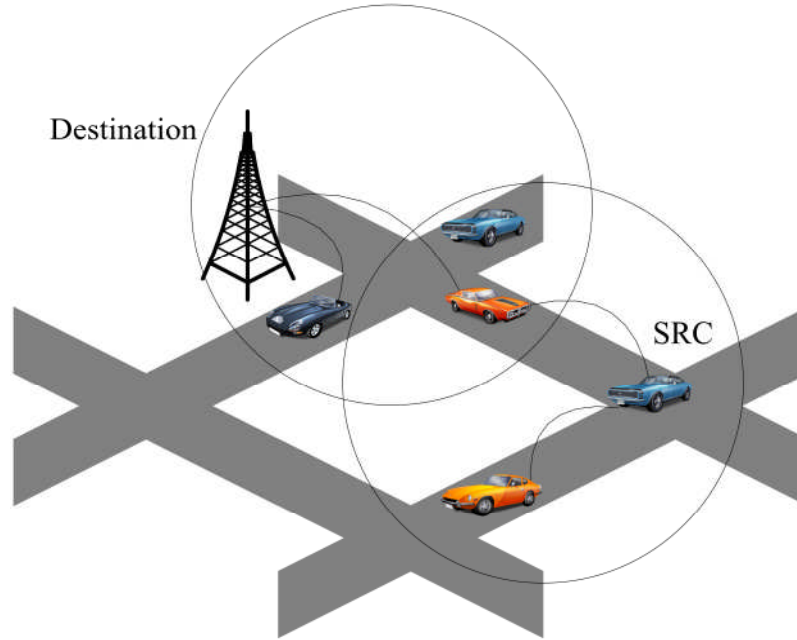


Figure 4.2: A snapshot of the SCF routing

4.4.2 Single cluster-head (SCH) based routing

The main motivation behind utilising the SCH routing scheme in this environment is to save energy by putting the maximum number of vehicles possible into sleep mode. It also reduces the total number of transmissions (flooding) in the network by allowing only CHs to perform out of range communications. In this scheme, the city network is divided into nine clusters where a random vehicle from each cluster is elected as a CH using the *setCH()* method. All other vehicles in each cluster are classified as cluster members. The *updateCH()* method is executed periodically to check if any CH has moved out of its cluster and elects a new one if needed. When a new CH is elected, all the packets stored in the old CH's buffer are transmitted to the new CH. The packets are then removed from the buffer of old CH. The *msgPropagation()* method deals with the actual transmission of the packets.

Similar to the MH and SCF routing, if the source vehicle is in the range of one of the BSs it transmits all its packets directly to the BS. However, if the source vehicle cannot reach any of the BSs, the packet is forwarded to the CH responsible for the source's cluster if they are in each other's range which can be determined using the *getCH()* method. The packet is carried by a CH until it gets to the BS's range and is hence transmitted. Clustering provides a relatively low number of transmissions but suffers higher E2E delay. Figure 4.3 presents a snapshot of SCH routing. A flowchart for SCH routing representing the simulation mechanism for a single vehicle (Veh[i]) is depicted in Figure B.5 in Appendix B.

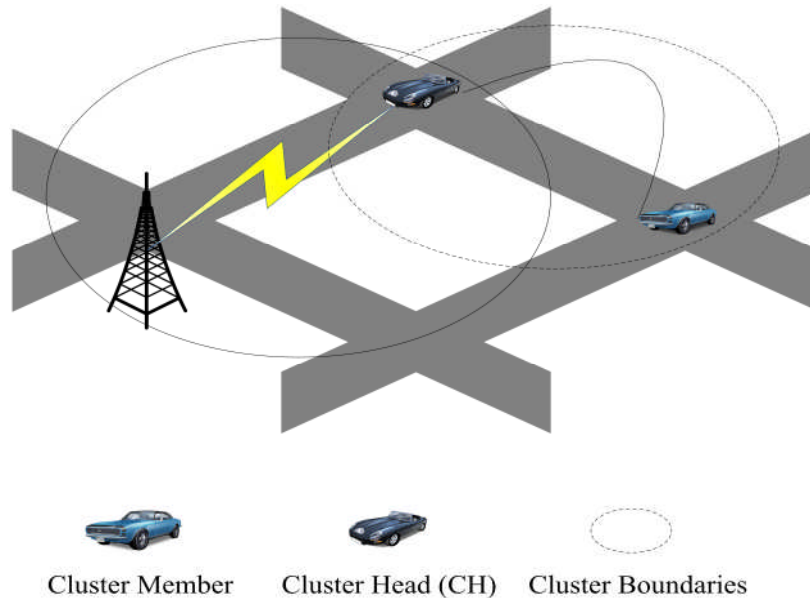


Figure 4.3: A snapshot of the SCH based routing

4.4.3 Double cluster-head (DCH) based routing

In order to enhance the performance of the proposed SCH routing in terms of QoS, a DCH routing scheme is proposed where two CHs are elected in each

cluster to perform inter cluster communications. Using the *setCH1()* and *setCH2()* functions, two distinct cluster heads are elected in each cluster where the *updateCH1()* and *updateCH2()* functions are executed every second to check if any CH gets out of its cluster boundaries and elect new CH/CHs if needed. In the *msgPropagation()* function, if the source vehicle is in the vicinity of any BS, it forwards its packets to that BS, otherwise, the source vehicle transmits its packets to the two cluster heads (acquired using the *getCH1()* and *getCH2()* methods) in its cluster. Both CHs carry the packets and as soon as one of the CHs gets into the range of any BS it transmits the packets to the BS. The advantage of the DCH scheme over the SCH scheme is the enhancement of the performance of the system in terms of E2E delay and PLR, where having two CHs in each cluster improves the connectivity of the network. In contrast having two CHs in each cluster increases the total energy consumption of the network as compared to the SCH scheme, where double the number of nodes is active, and hence consuming energy. Note that the energy levels of the DCH protocol are still lower than those of the MH and SCF schemes. A snapshot of the DCH scheme is depicted in Figure 4.4.

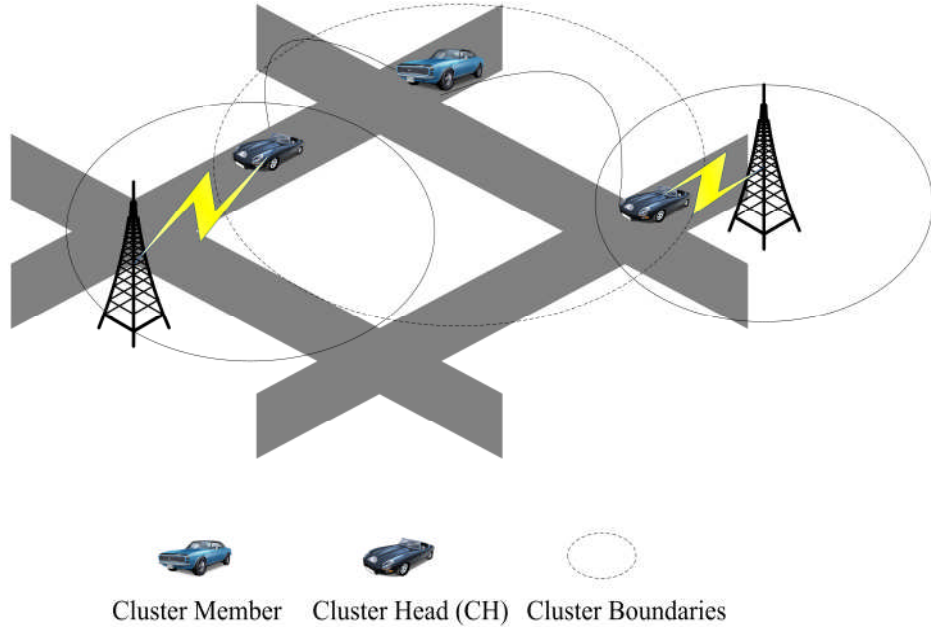


Figure 4.4: A snapshot of the double cluster-head (DCH) based routing

4.5 Physical Propagation Modelling

In a city/urban environment, for both V2R and V2V communication a LOS signal is typically not present. Hence, the signal envelope follows a Rayleigh distribution [173] and is given by

$$f_A(a) = \begin{cases} \frac{a}{\sigma^2} \exp\left(-\frac{a^2}{2\sigma^2}\right), & a \geq 0 \\ 0, & a < 0 \end{cases} \quad (4.1)$$

where σ is the root mean square (rms) value of the received signal amplitude.

The received power has an exponential distribution given by

$$f_P(p) = \begin{cases} \frac{p}{2\sigma^2} \exp\left(-\frac{p}{2\sigma^2}\right), & p \geq 0 \\ 0, & p < 0 \end{cases} \quad (4.2)$$

The mean received power can be predicted using deterministic propagation models such as free space (FS), two-ray ground and path loss models [173]. According to field measurements [174,175], the path loss model is more suitable to predict the mean received power in an urban environment and is given by

$$P_r(d) = P_r(d_{ref}) \left(\frac{d_{ref}}{d} \right)^v \quad (4.3)$$

where $P_r(d_{ref})$ is the reference power obtained with Friis formula and $P_r(d)$ is the mean received power at a distance d [173]. The power received, calculated using Equation (4.3), is used as average power in Equation (4.1). A propagation model based on attenuation and fading is used for both V2R and V2V communication systems. The probability of outage (P_{out}) can be expressed as

$$P_{out} = 1 - \exp\left(-\frac{P_{th}}{P_r(d)}\right) \quad (4.4)$$

where P_{th} is the receiver threshold power [174]. In this work, a 30 dBm transmit power is utilised for centralised communication, where BSs with antenna heights $h_b = 10$ m and gain 3 dBi [176] and vehicles with antenna height $h_v = 1.5$ m and gain 0 dBi are taken into account with an operating frequency of 2.4 GHz. A flat fading channel, which remains constant during a packet transmission, is assumed for both systems. A two slope model based on measurements [174,175] is utilised to characterise attenuation in both

scenarios. For V2V communication the mean received power decays with $\nu = 2$ for a distance $d \leq 100$ m and with $\nu = 3.8$ for other distances [174]. Similarly for centralised communication, path loss exponents $\nu = 2$ and $\nu = 4$ are used for $d \leq 300$ m and $d > 300$ m respectively [175].

To analyse the probability of outage (P_{out}) for a received packet with the above mentioned physical channel parameters, different threshold power (P_{th}) values have been taken into account at the receiver which accommodates different data rates for both scenarios. The P_{out} with different receiver threshold power (P_{th}) setups for V2R and V2V systems is shown in Figure 4.5 and Figure 4.6, respectively. It is evident from the results that the outage increases with the data rates hence, the communication range for an acceptable P_{out} decreases.

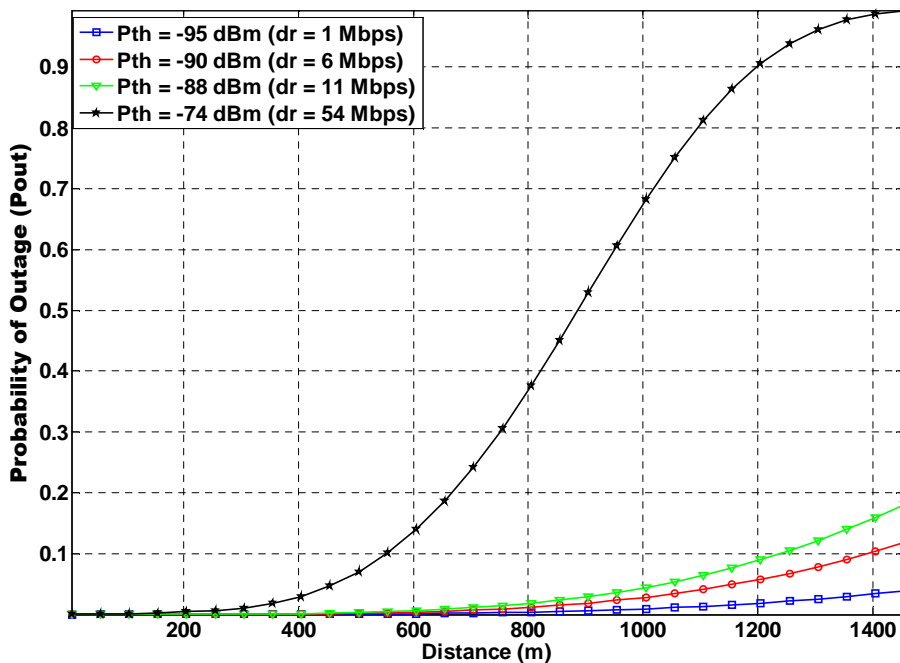


Figure 4.5: Probability of outage for a V2R system

It can be seen from Figure 4.5 and Figure 4.6 that a $P_{out} \leq 0.002$ can be achieved for all packets with a data rate of 1 Mbps (i.e. $P_{th} = -95$ dBm). Therefore, in this work a wireless link of 1 Mbps for V2V and V2R systems has been considered. Furthermore, the maximum communication range supported by a V2V system is set to 200 m. In case of a pure centralised system, the maximum range between a BS and a vehicle is set to 800 m.

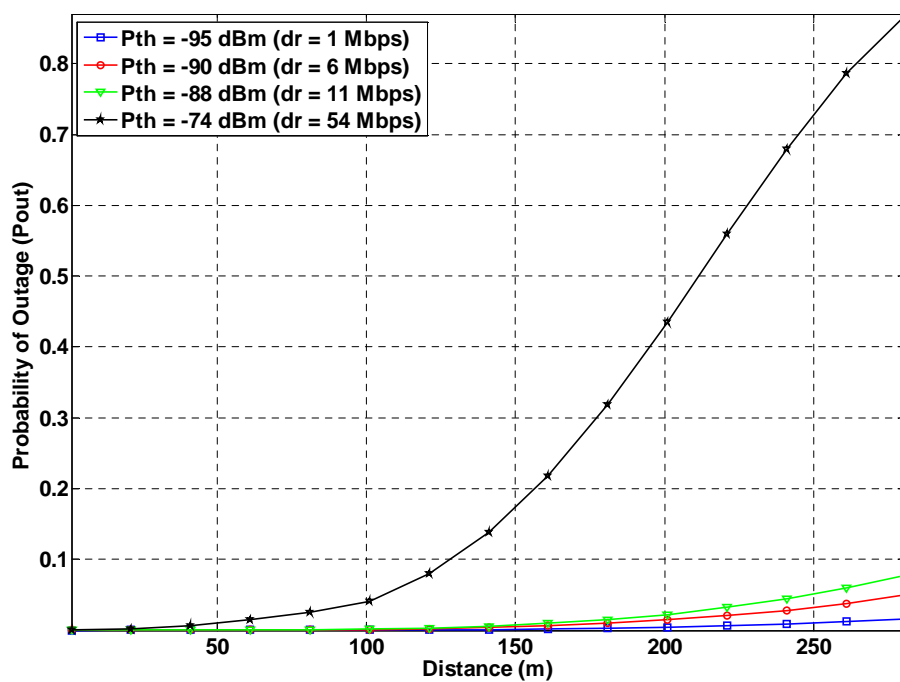


Figure 4.6: Probability of outage for a V2V system

4.6 Energy Modelling

The energy consumption in a wireless communication network can be computed as a sum of energies consumed in transmitting, receiving, listening, and operating states respectively [133,177]. The energy consumption in transmission of a bit (Ψ_t) is given by [18],

$$\Psi_t = \frac{P_{tc}}{d_r} = \frac{10 \text{ W}}{1 \times 10^6 \text{ bps}} = 1 \times 10^{-5} \text{ J/bit} \quad (4.5)$$

where P_{tc} is the total power consumed by the transmitter circuitry and d_r is the data rate. The power utilised by a receiver (P_{rc}) is up to 75% of P_{tc} [177]. Hence, the energy consumed for the reception of a bit (Ψ_r) is

$$\Psi_r = \frac{P_{rc}}{d_r} = \frac{7.5 \text{ W}}{1 \times 10^6 \text{ bps}} = 7.5 \times 10^{-6} \text{ J/bit} \quad (4.6)$$

The total energy consumed for the transmission of packets (Nps) from a BS to vehicles during the simulation time (1500 seconds) is

$$E_{t_BS} = \sum_{i=1}^{Nps} \Psi_t \times PktSize_i \quad (4.7)$$

and from vehicles to vehicles or to a BS

$$E_{t_Vehs} = \sum_{i=1}^k \Psi_t \times PktSize_i \quad (4.8)$$

where $PktSize_i$ is the size of the i^{th} packet in bits (512×8 bits) and k refers to the sum of the original packets (V2R) and the replicated packets (V2V). The total transmission energy (E_T) in the network can be calculated as

$$E_T = E_{t_BS} + E_{t_Vehs} \quad (4.9)$$

Similarly, utilising Equation (4.7) and Equation (4.9) in the context of Equation (4.6), the total reception energy (E_R) in the network can also be calculated. The listening energy for all the BSs ($E_{L_{BS}}$) deployed can be calculated as

$$E_{L_{BS}} = P_{lc} \times (1500 - T_{t_N} - T_{r_N}) \times M \quad (4.10)$$

where M is the number of BSs deployed and

$$T_{t_N} = T_{r_N} = \frac{PktSize \times Nps}{d_r \times M} \quad (4.11)$$

where P_{lc} is the power consumed in the listening state at the receiver which is same as P_{rc} , T_{t_N} and T_{r_N} correspond to the time taken for the transmission and the reception of the original packets for a BS in 1500 seconds duration. Similarly, the total listening energy for all the nodes ($E_{L_{Vehs}}$) can be calculated as

$$E_{L_{Vehs}} = P_{lc} \times (1500 - T_{t_k} - T_{r_k}) \times l \quad (4.12)$$

where l refers to the number of nodes in the listening state which varies according to the routing scheme employed. In the cases of MH and SCF, l refers to the total number of nodes (100 ~ 500) in the network whereas for SCH and DCH, it will be 9 and 18 (CHs), respectively. All the other nodes are put into sleep mode to save energy. Similarly, in a pure V2R system all the nodes are synchronised in such a way that they can be put into sleep mode. They only wake up at the time of transmission or reception. Therefore

$$T_{t,k} = T_{r,k} = \frac{PktSize \times k}{d_r \times n_{sim}} \quad (4.13)$$

where $T_{t,k}$ and $T_{r,k}$ correspond to the time taken for the transmission and the reception of total (original + replicated) packets in the network, n_{sim} refers to the number of nodes participating in the simulation. Therefore, total listening energy (E_L) in the network can be calculated as

$$E_L = E_{l_{BS}} + E_{l_{Vehs}} \quad (4.14)$$

Hence, the total network energy during the simulation time (1500 s) can be determined as

$$E_{TOTAL} = [M \times P_O \times 1500] + E_T + E_R + E_L \quad (4.15)$$

where P_O is the operational power consumption of a V2R BS and is assumed to be 100 W.

4.7 Performance Evaluation

The performance of both scenarios along with the four routing protocols has been evaluated in terms of QoS and energy consumption. The results reveal the deficiencies of a number of scenarios and schemes, such as the fully functional 9 BSs (9BS_V2R), fully functional 4 BSs (4BS_V2R), MH with 4 BS, SCF with 4 BS, (all in a $3 \times 3 \text{ km}^2$ city environment) compared to the SCH with 4 BS and DCH with 4 BS schemes with respect to energy consumption. The

vehicular nodes' buffer size is set to 100 messages while the traffic is generated at a rate of 1 kb/s. The system communication parameters are described in Table 4.1.

4.7.1 Average end-to-end delay

The average E2E delay results are illustrated in Figure 4.7 for different setups. The scenario with 9 BSs (9BS_V2R) deployed experiences a very low delay which shows the ubiquitous coverage available in the whole network. MH and SCF offer low delays that continue to decrease further with increase in the number of vehicles due to the connectivity achieved through these routing protocols. For example, the delay for MH with 300 vehicles is approximately 16 seconds compared to 37 seconds, 114 seconds and 137 seconds for the SCF, DCH and SCH schemes, respectively, as shown in Figure 4.7. The overall delay for the DCH (i.e. around 114 s) scheme is slightly higher but lower than that of the 4 BSs without any routing schemes scenario (i.e. 4BS_V2R).

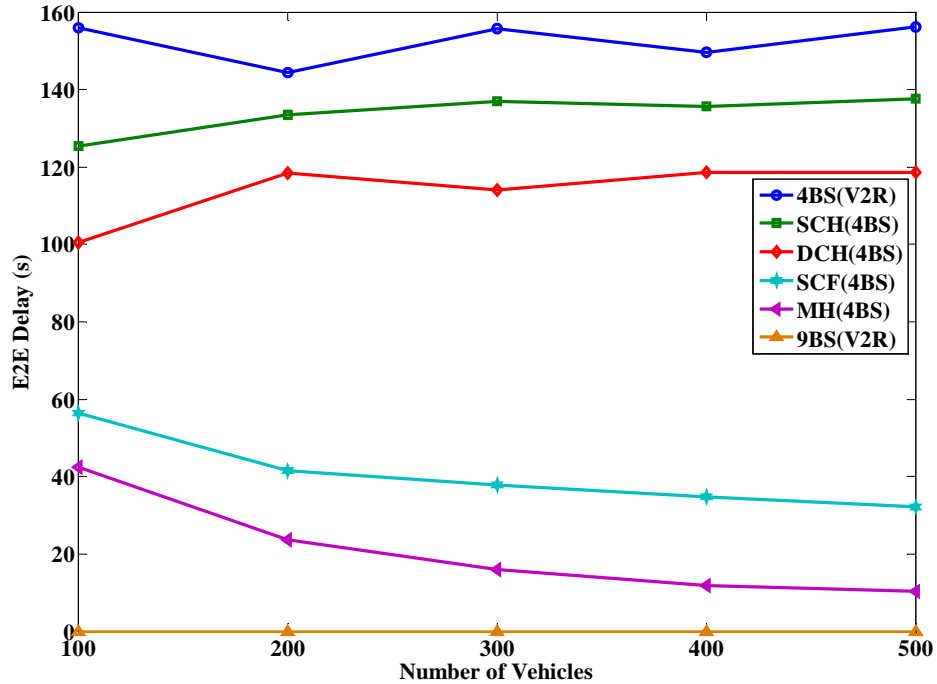


Figure 4.7: Average E2E delay with varying vehicular load

4.7.2 Packet loss ratio

The PLR results are shown in Figure 4.8. For the 9BS_V2R scenario, the PLR is also almost zero compared to the 4BS_V2R scenario where it almost reaches 0.05. Since the buffer size of 100 messages is large enough for MH and SCF, all the packets are successfully transmitted to the BSs however this is associated with significantly higher energy consumption. The PLR is slightly higher for the SCH and DCH (i.e. 0.026 and 0.019 respectively); however, significant listening and total energy savings are experienced while operating under these schemes. Note that the PLR for the SCH and DCH schemes is mainly due to the maximum tolerable delay (500 s) rather than the buffer overflow.

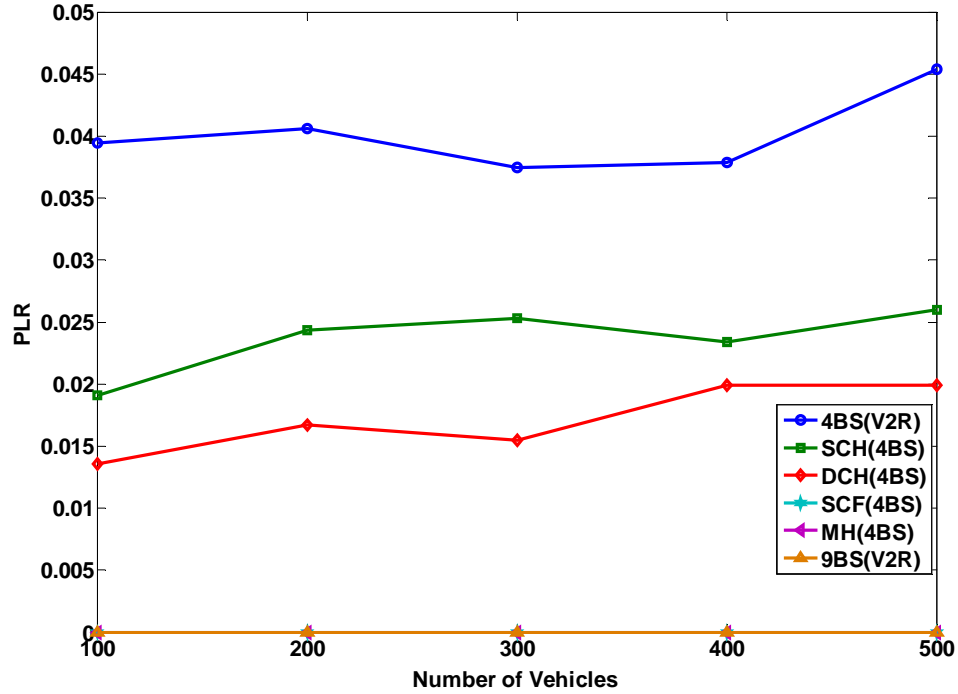


Figure 4.8: Packet loss ratio with varying vehicular load

4.7.3 Total number of transmissions

Figure 4.9 shows the total number of transmissions in the network for different scenarios. In 9BS_V2R, 4BS_V2R, SCH and DCH setups, the number of transmissions is very low for varying number of vehicles. However, in the MH scheme a large number of packets get replicated in the network due to its flooding nature especially with an increase in the number of vehicles. With only 400 vehicles in the system and 1 kb/s data rate, the total number of transmissions in the network reaches up to 19 million within 1500 seconds compared to approximately 9,000, 437 and 323 transmissions in the SCF, DCH and SCH, respectively.

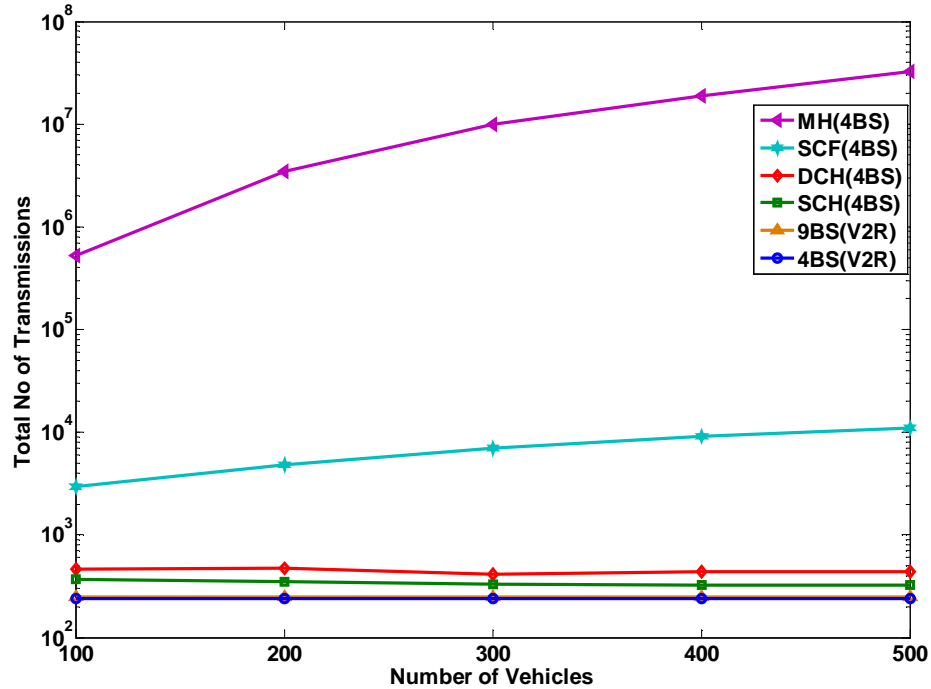


Figure 4.9: Total number of transmissions with varying vehicular load

4.7.4 Transmit and receive energies

The total transmitting (Tx) and receiving (Rx) energy shown in Figure 4.10 follows the same trend of the total number of transmissions (please see Figure 4.9) for different scenarios. Due to flooding in MH, the total energy (Tx + Rx) significantly increases with the number of vehicles. All other scenarios have significantly lower energy levels in terms of transmitting and receiving energy. For example, with 300 vehicles in the network, DCH consumes only 29 J of energy in transmitting and receiving compared to 696 kJ consumed in MH. This can be attributed to the fact that in DCH, only CHs perform inter-cluster communications.

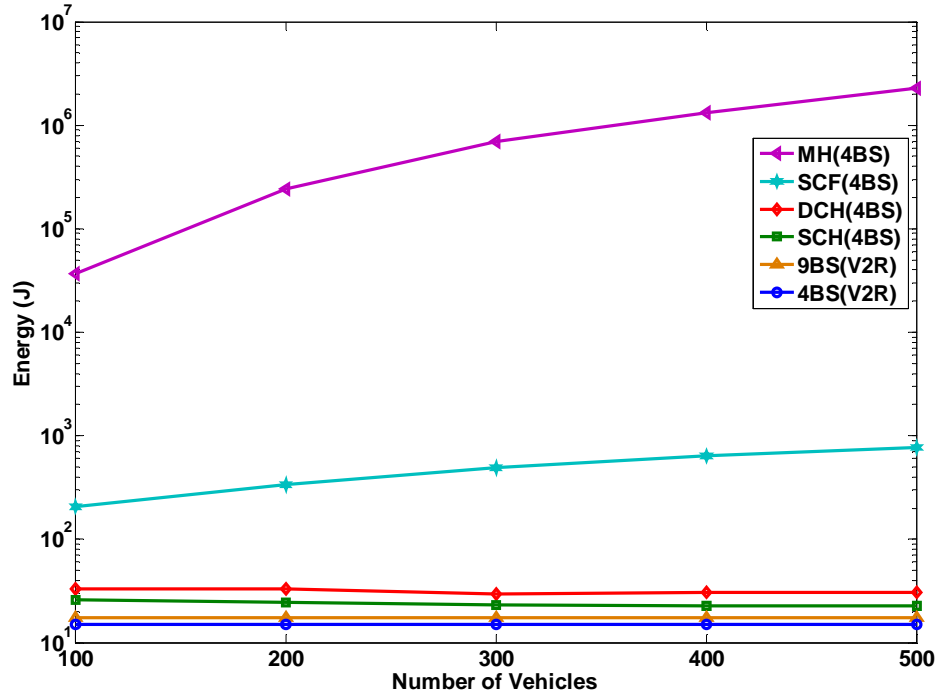


Figure 4.10: Total Tx and Rx energy with varying vehicular load

4.7.5 Listening energy

Since MH and SCF are schemes where all the vehicles need to continuously sense the medium in order to transmit or receive a packet, the listening energy is an essential element in estimating the total energy consumption in the network. Therefore, with an increase in the number of vehicles, the number of listening vehicles increases (particularly in the ad hoc setup). Note that in all the routing schemes considered in this chapter, the vehicles use carrier sense multiple access with collision avoidance (CSMA/CA) to sense (and access) the environment. Interestingly with 500 vehicles in the network, the SCF scheme consume 5.6 million J compared to 3.6 million J for the MH scheme as shown in Figure 4.11. This is due the fact that since the listening time is the remaining

time after the transmission and reception times (please see Equation (4.12)), the vehicles in MH have significantly higher number of transmissions compared to the SCF as shown in Figure 4.9, but SCF spends a significant amount of the time listening to the channel leading to the high listening energy consumption shown in Figure 4.11. As can be seen in Figure 4.11, the other routing schemes, such as DCH, consume significantly lower energy even with the higher number of vehicles in the system as in this case only cluster heads consume energy (i.e. are not in the sleep state).

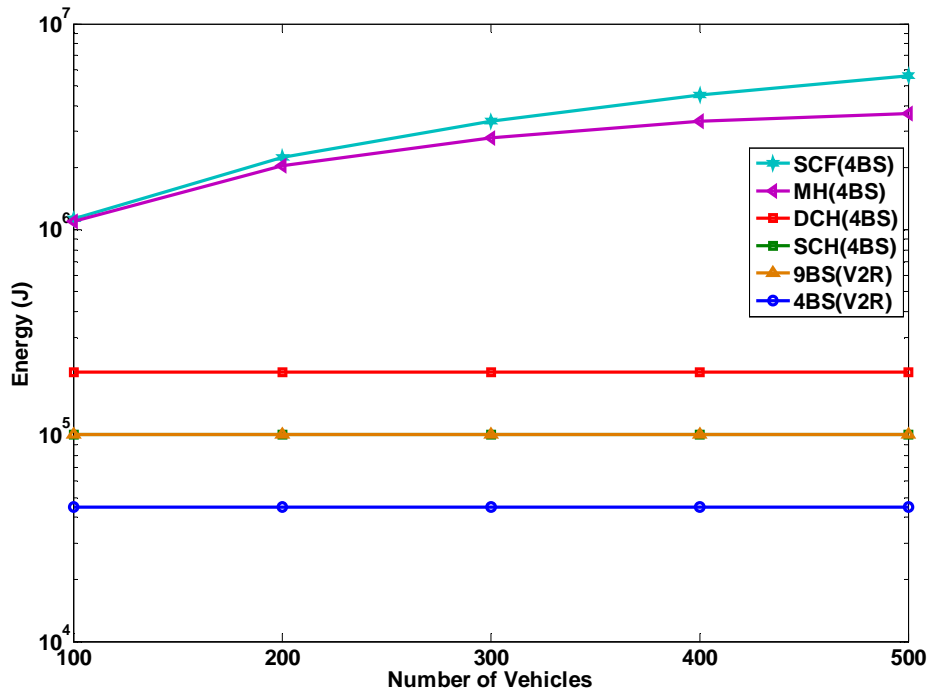


Figure 4.11: Total listening energy with varying vehicular load

4.7.6 Total network energy

The total network energy consumed in all the scenarios proposed is shown in Figure 4.12. The results clearly reveal that both MH and SCF with 4 BSs consume higher energy levels compared to the fully functional 9BS_V2R scenario. The higher network energy consumed in MH and SCF schemes primarily occurs due to the listening and transmission and receiving energy. Even though SCF is preferred over MH scheme from the network resources point of view, however, the results show that they consume almost the same amount of total network energy (over 6 million Joules) which is considerably higher than the fully operational 9 BS scenario (about 1.5 million). On the contrary, the SCH and DCH schemes save up to 2 times the total network energy compared to the fully operational 9 BS scenario and up to 9 times compared to MH and SCF while maintaining an acceptable level of QoS. The SCH and DCH schemes not only save significant amounts of energies, they also bring the PLR down to an acceptable level, as low as 0.014. It should be noted that the PLR of the SCH and DCH schemes are primarily higher. However, this is a trade-off that has to be made in order to achieve significant energy savings. On the other hand, the PLR can be decreased by marginally increasing the V2V range.

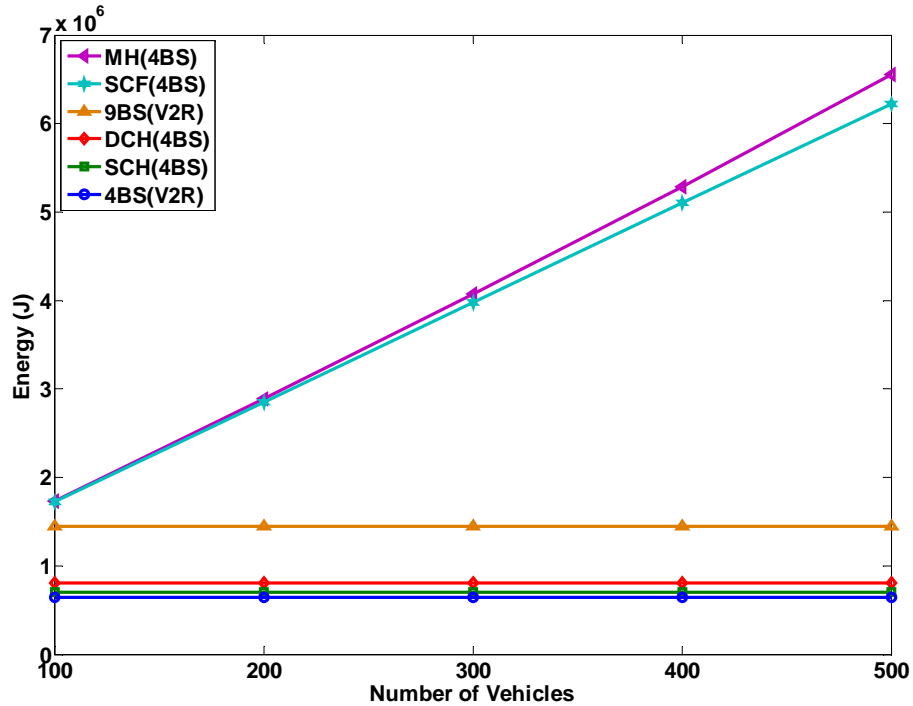


Figure 4.12: Total network energy with varying vehicular load

4.8 Summary

In this chapter, the performance of two pure V2R communication systems, in terms of QoS and energy consumption, has been evaluated in a city environment. Further, a hybrid communication system, comprising 4 BSs and an ad hoc setup with 4 routing schemes has been proposed to restore the performance of the pure V2R network with 4BS. An analysis of the physical propagation and energy model has been presented. The QoS parameters including average E2E delay, PLR, and total number of transmissions in the network have been evaluated. Moreover, the performance of the scenario has been evaluated in terms of energy consumption where the trade-off between the QoS parameters and energy consumption has been studied.

4.8 Summary

The results showed that the SCH and DCH schemes achieve 52% and 45% energy savings compared to the 9BS_V2R scenario, and 83% and 80% energy savings compared to the MH and SCF scenarios, respectively. However, these are achieved with marginally higher average E2E delay and PLR. In SCH and DCH schemes, the PLR can be further decreased through a small increase in V2V range.

5 Power Efficient Content Distribution Network for a City Vehicular Environment

5.1 Introduction

Due to the increased interest in media-rich files, content distribution networks (CDNs) have recently drawn considerable attention. Such services demand high bandwidth for transmission and large storage capacity for audio and video files. According to [29] more than 91% of the global IP traffic is going to be a form of video by 2014, with an annual growth of 33%. These growing figures coupled with a desire by vehicular users to download media-rich content (multimedia files) aggravate the problem of providing the required QoS in such a dynamic environment while saving significant amount of energy.

In this chapter, firstly a MILP model is developed which minimises the power consumption of the city vehicular network by optimising the number and locations of standalone Wi-Fi content CPs. The performance of the proposed CDN is compared with that of a traditional cellular network, where the number and locations of cellular BSs are also optimised for two operating scenarios,

namely highly dense and light load city scenarios. Secondly, the results of the MILP model are verified by developing a full simulation, and a heuristic that mimics the behaviour of the MILP model. Finally, the performance of the system is evaluated in terms of total network power consumption and number of active CPs/BSs.

5.2 The Studied Scenario

The proposed setup is examined in a $3 \times 3 \text{ km}^2$ Manhattan type city scenario with 48 roads and 16 junctions, as shown in Figure 5.1.

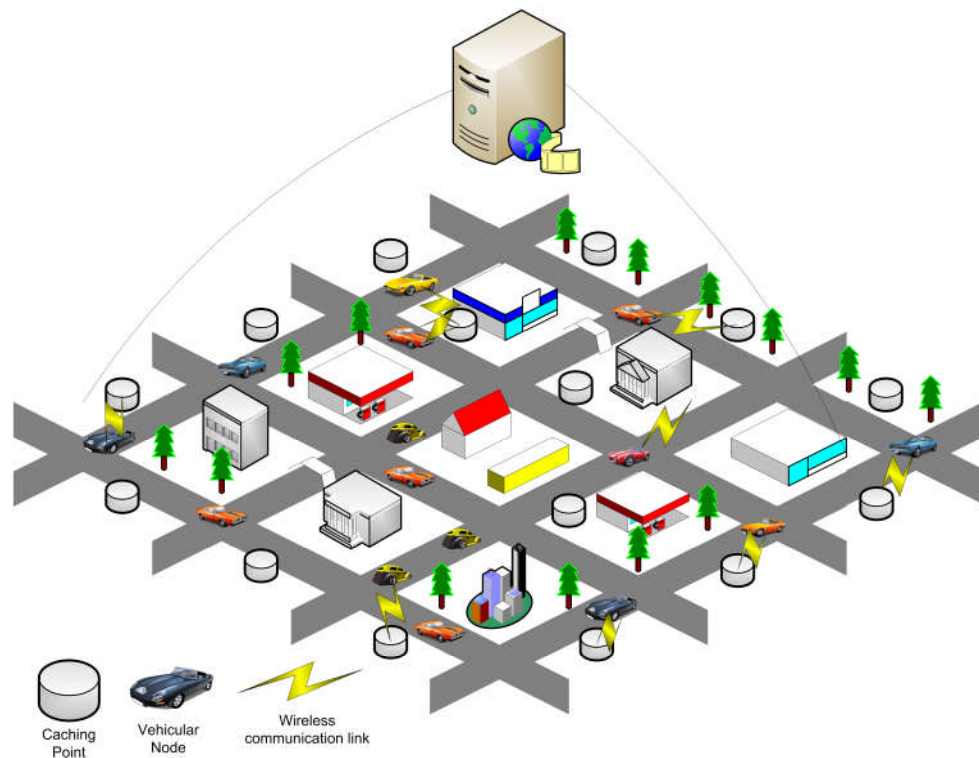


Figure 5.1: The studied city scenario

5.2.1 Vehicular traffic profiles

To understand the mobility and traffic characteristics of vehicles in a city network, statistical analysis should be carried out on measured vehicular traffic flow profiles. The Transportation Branch of the Infrastructure Services Department, Canada has carried out a detailed statistical analysis on the city of Saskatoon [30]. Their study offers vital mobility characteristics that can help develop an accurate vehicular traffic model, and determine the intensity of load at different hours of the day. In this chapter, the data of October 15th, 2009 has been used, and restricted to a coverage area of $3 \times 3 \text{ km}^2$ resulting in a maximum of 500 vehicles in an hour. The number of vehicles is large enough to analyse the performance at peak hours, while keeping the simulation time acceptable. The original trend of vehicular flow during different times of the day is however maintained. Vehicular traffic from other days was also analysed but similar trends were observed. Figure 5.2 shows hourly vehicular flow where business hours observe moderate traffic and late afternoon hours (16:00 hr - 18:00 hr) represent peak traffic.

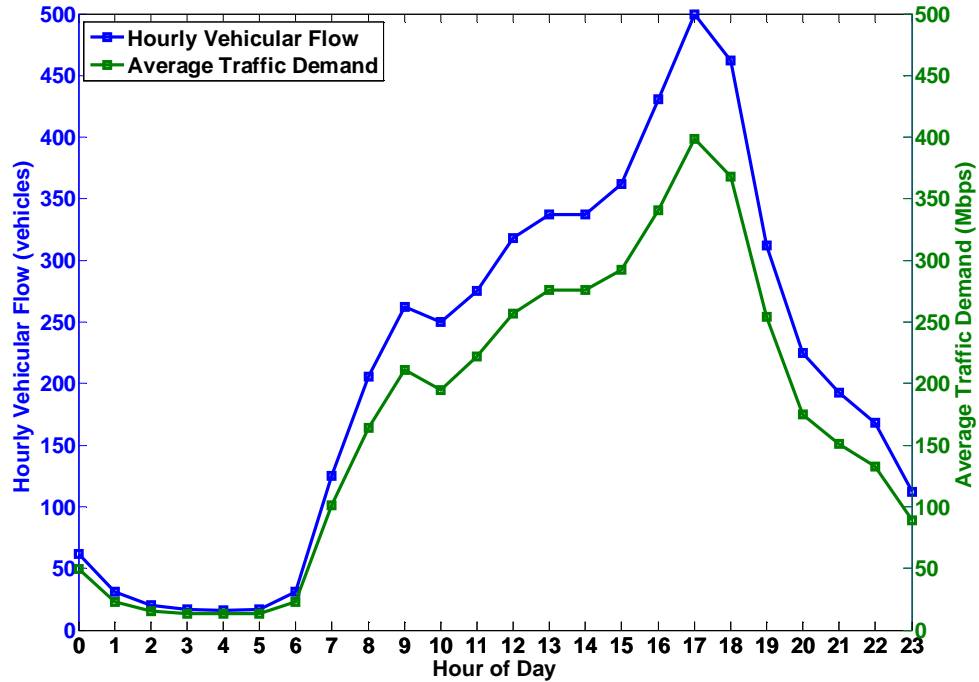


Figure 5.2: Hourly vehicular flow and demand

5.2.2 Vehicular mobility simulator

Based on the vehicular flow profiles, a bespoke vehicular mobility simulator has been developed. Vehicles move at a speed that varies between 0 and 13 m/s (maximum speed limit in a typical city) with an acceleration/deceleration of 2 m/s². Upon reaching a junction, vehicles choose one of the three directions based on a certain probability, where the probability of choosing a direction leading towards the city centre) is much higher (0.7 based on typical city data [30]) than that of leaving (i.e. 0.3) especially during business hours.

The vehicular simulator which incorporates real vehicular mobility is run for 24 hours to generate traffic at different locations within a city at each hour of the day. To maintain a balance between accuracy and computational complexity (in

MILP, heuristics and simulations), data traffic is generated based on the number of vehicles, reflecting vehicular traffic at each hour of the day. The arrival of a content request, generated by a vehicle, follows a Poisson distribution with a mean inter arrival time (τ) of 2000 seconds. The data traffic generated by vehicles is aggregated and used to generate data traffic snapshots in the city every 40 seconds resulting in 90 time points (data traffic snapshots) within one hour. Figure 5.2 represents the average traffic demand which varies between 25 Mb/s to 400 Mb/s. The traffic demand files are used as an input to the proposed MILP model to find the optimum number and locations of CPs/BSs. As the MILP model is unable to handle the movement of vehicles, a set of traffic points (TPs) that represent traffic centroids which account for the content/data traffic requested by nearby vehicles is assumed. Hence, a set of fixed traffic-generating points in the city space is seen by the MILP model. Vehicular mobility (and vehicular data generation) causes the level of traffic (in Mb/s) at each of these traffic centroids to vary. If a large number of such TPs is adopted, the impact of discretisation is reduced. Each bi-directional road has one TP, amounting to a total of 24 TPs in the city vehicular network. Moreover, the traffic demand of each TP and consequently the load on neighbouring CPs/BSs increase and decrease according to the number of vehicles entering or leaving the TP catchment area due to vehicular mobility.

5.3 Wi-Fi based CDN

Instead of a traditional cellular network for content downloading in a city vehicular environment, a power efficient Wi-Fi based CDN is introduced where its results are compared to those of a cellular network. The Wi-Fi CDN employs a number of CPs containing popular multimedia content. Typical examples of such content include advertisements for stores in a city, trailers of movies available at nearby cinemas, short videos about free parking spaces and city events, YouTube and BBC iPlayer videos. Such a Wi-Fi CDN setup can provision higher data rates and can achieve better power efficiency compared to traditional cellular networks. In such a setup, one main cellular BS can be employed for coverage, i.e. signalling, and for voice-type services (very low data rates) while small BSs, such as CPs, operate under its coverage and are activated and deactivated to save energy according to traffic requirements, a scenario envisaged in energy efficient 5G networks [178].

To optimise the number and locations of these CPs in a city vehicular network, a set of 192 candidate sites (CSs) is defined. These 192 CSs are uniformly distributed in the city, where each road has four CSs. Note that on each pair of roads (i.e. one road in each direction), a total of 8 CSs are available (i.e. four in each direction) so that each TP has a large enough number of possible neighbouring CSs to serve its demand even at peak hours. A large number of candidate sites is important to maintain fairness as it enables the proposed MILP model to select the optimal locations for CP. Each CP is installed with an

IEEE 802.11p radio, where the capacity of the CP is 30 Mb/s (see Table 5.1) and each user typically achieves a data rate that varies between 3-18 Mb/s, depending upon the communication range and the channel reliability [179]. According to [179], the typical communications range in vehicular networks is up to 300 meters (radius). However, considering a typical outdoor environment in a city vehicular network, a range of 100 meters (radius) is assumed. This lower range will result in a higher number of CPs, hence higher power consumption, it however represents a more realistic/practical scenario. Each content file is 200 MB which is a typical size of a BBC iPlayer video [180]. Along with a Wi-Fi transceiver, each CP is also equipped with a hard disk which has a storage capacity of 50 content files, a microcontroller that acts as an interface with applications where it coordinates piece requests and orders files, and a MAC and algorithm unit (such as VCDA presented in Chapter 6). A block diagram for a CP is illustrated in Figure 5.3. Due to the limited storage capacity of the CPs, only the most popular videos, which attract the interest of the users in the target area (i.e. city), are stored. Moreover, these CPs are connected to the server via a passive optical network (PON), where the power consumption of an optical network unit (ONU) is also considered for each active CP. The power consumption of the transceiver, hard drive, microcontroller, MAC and algorithm unit, and ONU are given in Table 5.1.

Due to the mobility of vehicles and the short communications range of CPs, file downloads may be interrupted and hence a complete file will be downloaded

from multiple CPs during a journey. To solve the download interruption problem, each file is divided into multiple smaller pieces where a vehicle finishes downloading the complete file when it has received all the pieces of that file from potentially multiple CPs. For example, the transmission range of a CP is 100 meters (i.e. 200 meters in diameter) and the maximum speed of a vehicle is 13 m/s, hence, a vehicle stays in the range of a CP for approximately 16 seconds. At a download rate of 3 Mb/s, a piece with a size of 6 MB can be downloaded (during the 16 seconds), where a video consists of 33 pieces.

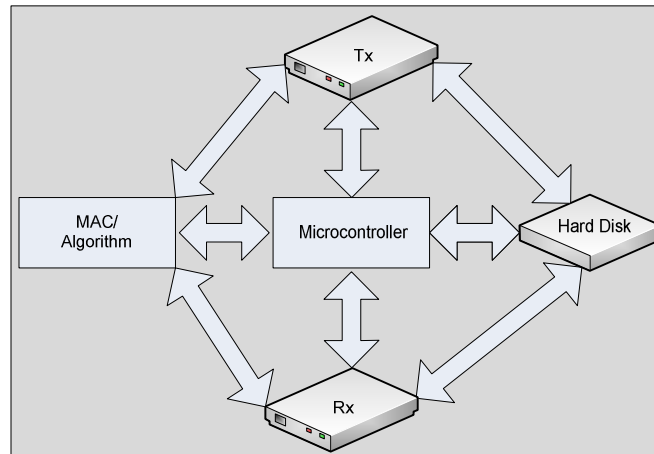


Figure 5.3: CP block diagram

5.4 Cellular Network

To examine the power consumption of cellular networks and the need to introduce CDN for such a dynamic environment, a similar MILP model for a cellular network is defined which optimises the number and location of BSs. Similar to the CDN, the same number of CSs (192) is considered for BSs number and location optimisation; however the transmission range is set to 500 m for BSs [181]. The data rate of a cellular BS is set to 1 Mb/s/user [181] which

can be achieved even at cell edges due to the relatively short transmission range. The total node capacity in both cellular and Wi-Fi networks is set to 30 Mb/s (Table 5.1). Note that the capacity of a cellular BS can be much higher (e.g. 100 Mb/s [182]), however, it is anticipated that the network operators will be inclined to allocate only a small portion (for example 30%) of the full capacity for vehicular applications. Similar to the Wi-Fi CDN scenario, each video is also divided into multiple smaller pieces, however, due to the larger transmission range of a BS, a vehicle can download multiple pieces while it is under the coverage of a single BS. The average power consumption of a BS is set to 500 W [23] compared to just 15 W for a typical Wi-Fi access point [183]. To maintain fairness, the power consumption of the hard drive, microcontroller, and MAC and algorithm unit are also considered in the cellular network. The same data traffic and virtual TPs in the case of CDN are used for the cellular network. Moreover, the same analysis is undertaken for the cellular network in a lightly dense environment, where data rates of 3 Mb/s [184] can be achieved by each user and BSs can cover up to 800 m [18]. The performance of this scenario is compared with the Wi-Fi network and the cellular network under a highly dense building setup.

Since in this work the main interest lies in finding the limits of power consumption of such networks, an idealistic MAC protocol is assumed where transmission without any contention or collision is considered. As this is a content distribution network instead of a network that provides real-time voice or

video related services, delays associated with handoffs between CPs/BSs are not included. The impact of handoffs is expected to be low as the content file is divided into smaller pieces in such a way that typical vehicular mobility and download rates result in vehicles being within the range of a CP/BS until a piece is typically completely downloaded even when vehicles travel at the maximum legal speed in the city.

Communication System Parameters:	Wi-Fi	Cellular
Data rate	3 Mb/s/user	1 Mb/s/user, 3 Mb/s/user
MILP modelling area / Simulation area	$3 \times 3 \text{ km}^2$	$3 \times 3 \text{ km}^2$
No. of vehicles (V)	16 to 500	16 to 500
Transmission range (radius)	100 m	500 m, 800 m
Object size	200 MByte	200 MByte
Piece size (P_s)	6 MByte	6 MByte
Number of pieces per object	33	33
CP storage capacity	50 Objects	N/A
Inter arrival time of content requests (τ)	2000 seconds (mean)	2000 seconds (mean)
Inter arrival time of piece request (σ)	16 seconds	16 seconds
Simulation duration per run	3600 seconds	3600 seconds
Wireless node capacity (B)	30 Mb/s	30 Mb/s
Sets:		
V	Set of vehicles	
TP	Set of traffic points	
CP	Set of caching point candidates	
BS	Set of base station candidates	
N_p	Set of neighbouring TPs	
N_{pc}	Set of neighbouring CPs	
T	Set of time points within one hour i.e. 90	
Parameters:		
$P_{CP_{TX}ct}$	Transmitter power consumption of CP c at time t	
$P_{V_{RX}it}$	Transceiver's power consumption of vehicle i i.e. 15 W [183]	
$P_{CP_{min}_{OP}}$	Operational power consumption of CP i.e. 47 W	

	$(P_C+P_{HD}+P_{ONU}+P_{MC}+P_{MAC/ALG})$
P_C	CP's circuitry power consumption i.e. 15 W [183]
P_{HD}	Hard drive power consumption i.e. 10 W [185]
P_{ONU}	ONU power consumption i.e. 2 W [186]
P_{MC}	Microcontroller power consumption i.e. 10 W
$P_{MAC/ALG}$	MAC and algorithm processor unit power consumption i.e. 10 W
P_{BS}	Operational power consumption of BS i.e. 500 W [23]
$P_{BS_{min_OP}}$	Total operational power consumption of a BS including all elements i.e. 530 W $(P_{BS} + P_{HD} + P_{MC} + P_{MAC/ALG})$
P_a	Power amplifier power consumption i.e. 2 mW [173]
λ_{tj}	TP j demand at time t
A	Large number for MILP constraint, set to 10000 here
H	Large number for MILP constraint, set to 100 here
Variables:	
$P_{CP_{TX_{cjt}}}$	Distance dependent transmitting power consumption of CP c to TP j at time t
$P_{CP_{RX_{ct}}}$	Receiver power consumption of CP c at time t , i.e. 0 in our case
$P_{V_{TX_{it}}}$	Transmitter power consumption of vehicle i at time t
α_c	Equals 1 if CP c is ON, equals 0 otherwise
λ_{cjt}	Traffic between CP c and TP j at time t
δ_{cjt}	Equals 1 if CP c is transmitting content to TP j , equals 0 otherwise
d	Distance between CP/BS and TP
v	Path loss exponent i.e. 2 for $d \leq 300$ and 4 for $d > 300$ [175]
Indices:	
c	Index of caching point (CP)
j	Index of traffic point (TP)
t	Index of time point (T)
i	Index of vehicle (V)
Pseudo-codes notations:	
P_N	Total network power consumption
\emptyset	Average content delay
ϑ	Average piece delay
$R[x]$	Request of content x
x	Content ID
$\zeta[x]$	Request generation time of content x
K	Piece request
n	Piece number
γ	Request generation time of piece

N	Total number of pieces per content i.e. 33
$TP_j[v]$	Nearest TP j to vehicle v
Δ_v	Waiting timer of vehicle v

Table 5.1: Communication System Parameters and List of notations

5.5 A Linear Programming Model for CP/BS Number and Location Optimisation

The proposed mixed integer linear programming (MILP) model aims to reduce the power consumption of the two networks: Wi-Fi and cellular. To evaluate the two networks, a MILP model is developed to minimise the total power consumption of a city vehicular network by optimising the number and locations of CPs/BSs while serving varying amounts of traffic demand representing different vehicular densities at each hour of the day. The MILP model uses a number of sets, parameters and variables which are defined in Table 5.1. Note that the MILP model is valid for both networks but with different parameters and notations. The cellular scenario can be implemented by replacing each CP c by BS b .

The power consumption of the network consists of:

The transmitter power consumption of CP c at time t :

$$\sum_{c \in CP} P_{CP_{TX}ct} \tag{5.1}$$

Equation (5.1) describes the distance dependent power consumption of CP c at time t and can be calculated using Equations (5.7) and (5.8).

The receiver power consumption of CP c at time t :

$$\sum_{c \in CP} P_{CP_{RX}ct} \quad (5.2)$$

The receiver power consumption of a CP is not considered in this work, as it is a cloud based content distribution scenario and vehicles do not generate content and upload to CP. However, Equation (5.2) is included to make the MILP model generic and applicable to all scenarios.

The power consumption of CP c at time t if CP c is switched ON:

$$\sum_{c \in CP} \alpha_c \cdot P_{CP_{min}OP} \quad (5.3)$$

This is the minimum operational power consumption of a CP if it is switched ON. It includes the power consumption of circuitry, the power consumption of hard drive used for storing content, the power consumption of the microcontroller, the power consumption of the MAC and algorithm unit, and the power consumption of the ONU, as shown in Table 5.1.

The transmitter power consumption of vehicle i at time t :

$$\sum_{i \in V} P_{V_{TX}it} \quad (5.4)$$

The vehicle transmitter power is not considered in this work, as this is a cloud based content distribution scenario where vehicles (users) only generate

requests and the power associated with transmitting a request is negligible. However, it can be calculated, if required, using Equation (5.8) by replacing each CP c by Vehicle i and each TP j by CP c .

The receiver power consumption of vehicle i at time t :

$$\sum_{i \in V} P_{V_{RX}it} \quad (5.5)$$

The receiver power consumption of vehicles is considerable and its amount can be found in Table 5.1. Note that the amount of power consumed by the vehicle's transceiver in the idle (operational) and receiving state is the same [18].

The MILP model is defined as:

Objective: Minimise

$$\sum_{t \in T} \left(\sum_{c \in CP} P_{CP_{TX}ct} + P_{CP_{RX}ct} + \alpha_c \cdot (P_{CP_{min_OP}}) + \sum_{i \in V} P_{V_{TX}it} + P_{V_{RX}it} \right) \quad (5.6)$$

The objective is to minimise the total network power consumption over all 90 time points in set T , representing one hour. The MILP model ensures that the system works at every point in time using the following constraints.

Subject to:

$$P_{_CP_{TX}ct} = \sum_{j \in TP} (P_{_CP_{TX}cjt} \cdot \delta_{cjt}) \quad (5.7)$$

$$\forall c \in CP, \forall t \in T$$

The transmitting power must be calculated as a single CP can connect to multiple TPs simultaneously, and hence the proportion of the CP transmitter power used to link to TP j (according to the distance) is given by $P_{_CP_{TX}cjt}$. Note that it is multiplied by the binary variable δ_{cjt} , so that the transmitting power is only calculated if there is traffic between CP c and TP j at time t .

Equation (5.8) calculates the distance dependent power consumed by CP c transmitting to TP j at time t which is calculated according to the path loss model given by [173]:

$$\sum_{j \in TP} P_{_CP_{TX}cjt} = P_a \cdot d_{cj}^v \quad (5.8)$$

$$\forall c \in CP, \forall t \in T$$

where P_a is the power used by the power amplifier and defined in Table 5.1. Note that Equation (5.8) can also be used to calculate the power consumed by vehicle i transmitting to CP c at time t by replacing each CP c by vehicle i and each TP j by CP c .

$$\begin{aligned} \lambda_{tj} &= \sum_{c \in N_{pc}[j]} \lambda_{cjt} \\ \forall t \in T, \forall j \in TP \end{aligned} \quad (5.9)$$

Equation (5.9) is the flow conservation constraint which ensures that at each time point the total traffic is served. Note that the set of neighbourhood of a TP (i.e. $c \in N_{pc}[j]$) is constructed based on the limited range of the CP, and hence it only includes the CPs that are within range of that TP. Therefore, Equation (5.9) ensures that the total demand of a TP is only served by neighbouring CPs.

$$\begin{aligned} \sum_{j \in N_p[c]} \lambda_{cjt} &\leq B \\ \forall c \in CP, \forall t \in T \end{aligned} \quad (5.10)$$

Equation (5.10) is the capacity constraint which ensures that at each time point the capacity of the CP is not violated. The MILP model will install another cache to serve the remaining traffic of the TP if the CP has already reached its full capacity (i.e. 30 Mb/s).

$$\begin{aligned} \lambda_{cjt} &\leq \delta_{cjt} \cdot A \\ \forall c \in CP, \forall j \in TP, \forall t \in T \end{aligned} \quad (5.11)$$

Equation (5.11) ensures that if the traffic is non-zero between CP c and TP j i.e. $\lambda_{cjt} \neq 0$, then $\delta_{cjt} = 1$ i.e. the TP is connected to a CP.

$$\begin{aligned} \lambda_{cjt} &\geq \delta_{cjt} \\ \forall c \in CP, \forall j \in TP, \forall t \in T \end{aligned} \quad (5.12)$$

Equation (5.12) ensures that if the amount of traffic between CP c and TP j is zero i.e. $\lambda_{cjt} = 0$, then there is no connection i.e. $\delta_{cjt} = 0$.

$$\sum_{t \in T} \sum_{j \in Np[c]} \delta_{cjt} \geq \alpha_c \quad \forall c \in CP \quad (5.13)$$

$$\sum_{t \in T} \sum_{j \in Np[c]} \delta_{cjt} \leq \alpha_c \cdot H \quad \forall c \in CP \quad (5.14)$$

Equations (5.13) and (5.14) ensure that if there is a connection between CP c and TP j at any time point t i.e. $\delta_{cjt} = 1$, then CP c is switched ON for all time points i.e. $\alpha_c = 1$.

5.6 CDN/Cellular Heuristic

In order to verify the results of the MILP model, a heuristic is developed, presented as Pseudo-code 5.1, to mimic the behaviour of the MILP model. Pseudo-code 5.1 illustrates how the CDN heuristic works for the Wi-Fi network, however it can also be utilised for the cellular network by replacing each CP c by BS b . The heuristic begins with 192 CSs (4 on each road) distributed uniformly around the city, where all the CSs are initially inactive. Similar to the MILP model, the requested (generated) traffic at virtual TPs is utilised to optimise the number and locations of the CPs/BSs. The heuristic starts by creating a CP and BS neighbourhood list for each TP in which any CP/BS CS

that is within range of a TP is added to the neighbourhood list of that TP as given by lines 1-5 of Pseudo-code 5.1. Thereafter, each vehicle generates a request for certain content ($R[x]$) and subsequently records the request generation time ($\zeta[x]$) as given in lines 7-8. Before generating a request for an individual piece, the vehicle searches for the nearest TP as given by line 10. The request for a piece (n) is then generated ($K_x[n]$) where the piece request generation time ($\gamma_x[n]$) is recorded as given by lines 11-12. Thereafter, the nearest TP to that vehicle automatically searches for an active CP/BS within its neighbourhood list. If an active CP/BS is available and it has enough capacity to serve the vehicle's request, the piece is downloaded and the piece delay and power consumption are computed as given in lines 13-16. However, if no active CP/BS is within TP's range or if a neighbouring CP/BS is operating at its full capacity, a new neighbouring candidate CP/BSs is activated. The content delay (ϕ_x) is computed after the vehicle has downloaded the whole content as given by line 18. The heuristic is run at each hour of the day to obtain results which will be compared with the ones achieved by the MILP model.

Pseudo-code 5.1 CDN/Cellular heuristic

Input: $\forall v \in V, \forall j \in TP, c \in CP$ **Output:** $P_N, \emptyset, \vartheta$

```
1  for all  $j \in TP$  do
2    for all  $c \in CP$  do
3      create neighbourhood list;
4    end for
5  end for
6  for all  $v \in V$  do
7    generate  $R[x]$ ;
8    record  $\zeta[x]$ ;
9    for all  $n = 1, 2, 3, \dots, N$  do
10   find nearest  $TP_j[v]$ ;
11   generate  $K_x[n]$ ;
12   record  $\gamma_x[n]$ ;
13   find appropriate CP or activate new CP;
14   download  $K_x[n]$ ;
15   compute  $\vartheta_x[n]$ ;
16   compute  $P_N[n]$ ;
17   end for
18   compute  $\emptyset_x$ ;
19 end for
```

5.7 Performance Evaluation

The power consumption of both (Wi-Fi and cellular) networks is calculated by the proposed MILP model which optimises the number and locations of CPs/BSs. The MILP model is solved using the 32 bit AMPL/CPLEX software on a Core2, 2.8 GHz PC with 4 GB memory. Having determined the optimised number and locations of CPs/BSs using the MILP model, a heuristic is implemented to mimic the behaviour of the MILP model in order to verify the results achieved. The heuristic runs for each hour of the day with the same number of CSs, TPs and parameters utilised in the MILP model.

From the results obtained by the MILP model and shown in Figure 5.4, it is found that the optimum number and locations' of CPs/BSs vary according to vehicular density and hence data traffic demand, allowing the network operators to switch the CPs/BSs ON or OFF accordingly. Note that Figure 5.4 shows all the CPs that were activated throughout the whole day, where red CPs correspond to the ones activated during the hours labelled in the figure.

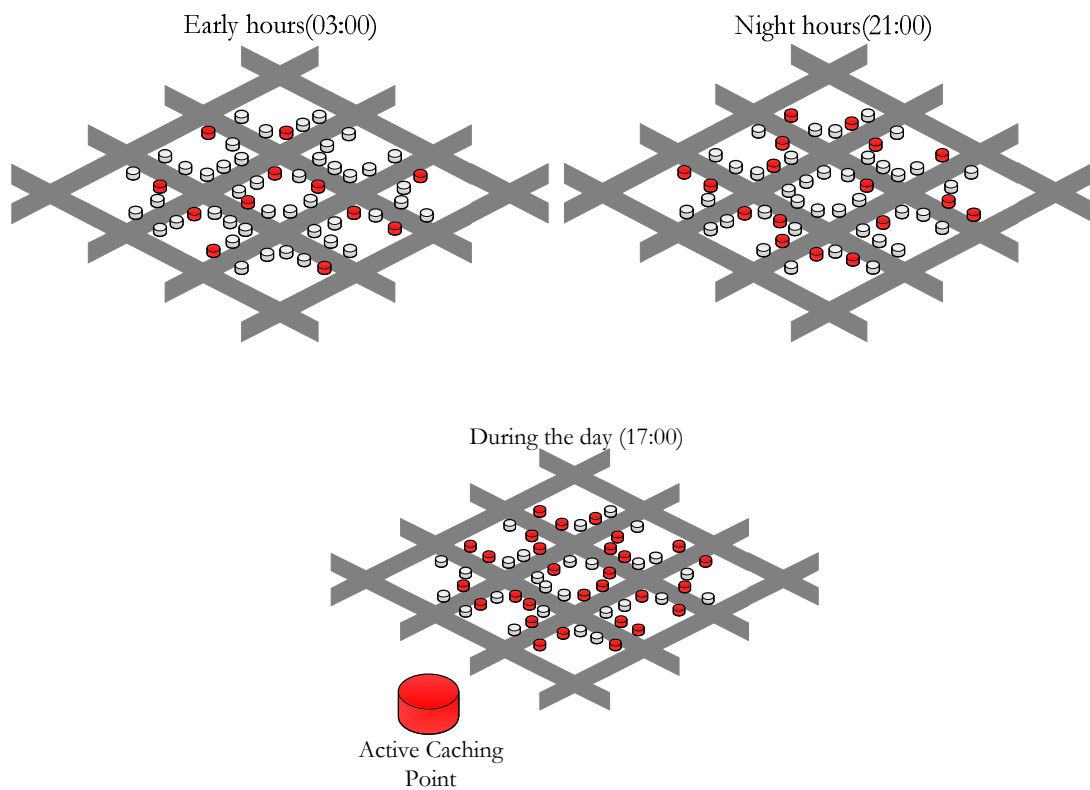


Figure 5.4: Optimised locations of the CPs through the MILP model at different hours of the day

5.7.1 Total network power consumption

Figure 5.5 shows the total power consumption of the network obtained through the MILP model and the heuristic for the CDN and the cellular network in a city vehicular environment. The figure shows two scenarios for the cellular network,

one in highly dense building environment (such as Manhattan) where each user can achieve a data rate of 1 Mb/s and BSs can only cover up to 500 m, whereas the second scenario describes a less dense building environment where each user can achieve a data rate of 3 Mb/s and BSs can cover up to 800 m. The power consumption results for both networks follow the same trend as the hourly vehicular flow (Figure 5.2) as higher vehicular traffic (i.e. higher content demand) contributes to higher total network power consumption due to the large number of CPs/BSs required to fulfil traffic demand during peak hours of the day. The power consumption of vehicles' transceivers during these (peak) hours also contributes to the total network power consumption. The figure reveals that the cellular network under both scenarios consumes significantly more power than that of the Wi-Fi network. This is mainly due to the higher operational power consumption of a BS utilised in the cellular network compared to a Wi-Fi enabled CP utilised in the CDN, where a BS consumes 530 W (including all the components) compared to just 47 W consumed by a CP. The power consumption of the Wi-Fi network during off-peak hours, for example at 04:00 hr, is about 1.2 kW compared to 7.08 kW and 2.9 kW consumed by the cellular network under the highly dense and less dense building environments, respectively. This can be attributed to the fact that a higher number of BSs are required when lower range BSs are utilised, resulting in 6x higher power consumption than that of the CDN. Even at peak hours (for example 17:00 hr), the CDN consumes 1.5 times lower power than that of the cellular network under the highly dense environment. The reduction

in power consumption after business hours is due to the lower content demand. On average, the total power consumption of the Wi-Fi network during the whole day is half the total power consumption of the cellular network under highly dense environment and 1.4 times less than that of the lightly dense environment. Note that the power consumption of the cellular network under the highly dense environment is higher than that under the less dense environment throughout the whole day. This is mainly because of the higher transmission range of the BSs, in which a single BS can cover more than 1 TP simultaneously. For example, the cellular network under the lightly dense environment achieves power saving of up to 2.5x over the cellular network under the highly dense environment at early hours of the day.

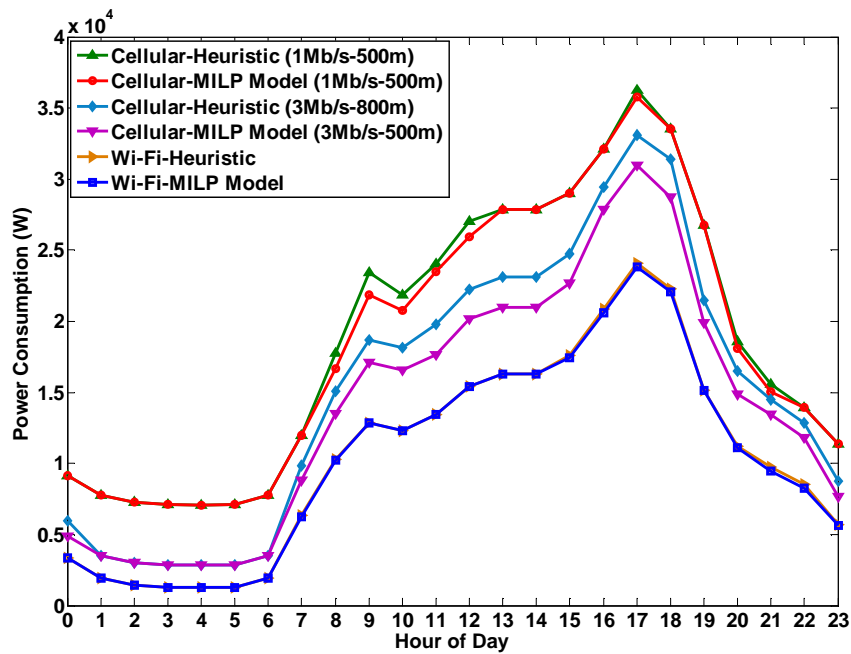


Figure 5.5: Total network power consumption (Cellular vs. Wi-Fi)

Figure 5.5 also shows a comparison of power consumption between the heuristics and the MILP models of both networks. It can be observed that the results of the heuristics follow the same trends as the MILP models. The power consumption of the heuristic driven Wi-Fi network is almost the same as the one achieved by the MILP model. For example, the power consumption evaluated by the MILP model at 17:00 hr is 23.8 kW compared to 24 kW achieved by the heuristic. Moreover, the power consumption results achieved by the heuristic under the cellular network are also comparable with the ones achieved by the MILP model. However, the difference between the MILP model and the heuristic's results in the case of cellular network, especially after 07:00 hr, is evident due to the higher power consumption of a BS compared to a CP. For example, if the heuristic activates only one extra BS than the MILP model, this contributes an extra 530 W to the results compared to those achieved by the MILP model. On the other hand, the heuristic achieves almost identical results at early hours of the day (01:00 hr – 06:00 hr) when the vehicular density is low. Moreover, the difference between the MILP model's results and the heuristic's results for the cellular network under the less dense environment is more evident than the difference under the highly dense environment. This is mainly due to the higher transmission range of the BSs utilised in the former environment, where higher BS range allows a single BS to serve more than 1 TP. Further, as the heuristic operates in real time as opposed to the MILP model that has a global knowledge of the whole traffic demand, the heuristic

does not always activate the BSs at their optimum locations and hence the slight deviation in the results.

5.7.2 Number of active CPs/BSs

Figure 5.6 and Figure 5.7 show the total number of active CPs and BSs in both networks achieved by their respective MILP model and the heuristic at each hour of the day. The number of BSs/CPs needed to serve the content demand varies during the day. The number of active BSs/CPs is directly proportional to the traffic demand (please see Figure 5.2). The results show that the number of BSs and CPs activated under both networks remain fixed during the lower traffic periods (00:00 hr – 06:00 hr) as at least 12 CPs, 12 BSs, and 4 BSs are required to serve the demand during that period under the Wi-Fi network, cellular network under highly dense environment, and cellular network under less dense environment, respectively. As traffic demand increases (after 06:00 hr), the number of BSs/CPs increases as well. For example, the number of active CPs in the Wi-Fi network at the highest load (17:00 hr) is 29 compared to 25 BSs and 16 BSs activated in the cellular network under the highly dense environment and the lightly dense environment, respectively (attained by the MILP model). Although the traffic demand gets slightly lower between 09:00 hr and 10:00 hr as shown in Figure 5.2, the number of CPs stays the same. This is because even though the CPs are underutilised during these periods due to the distribution of traffic, they are still required at some instances. Note that despite the larger number of active CPs in the Wi-Fi network, the power consumption of

the cellular network is much higher than the power consumed by the Wi-Fi network. This is because a BS consumes approximately 12 times more power than a CP.

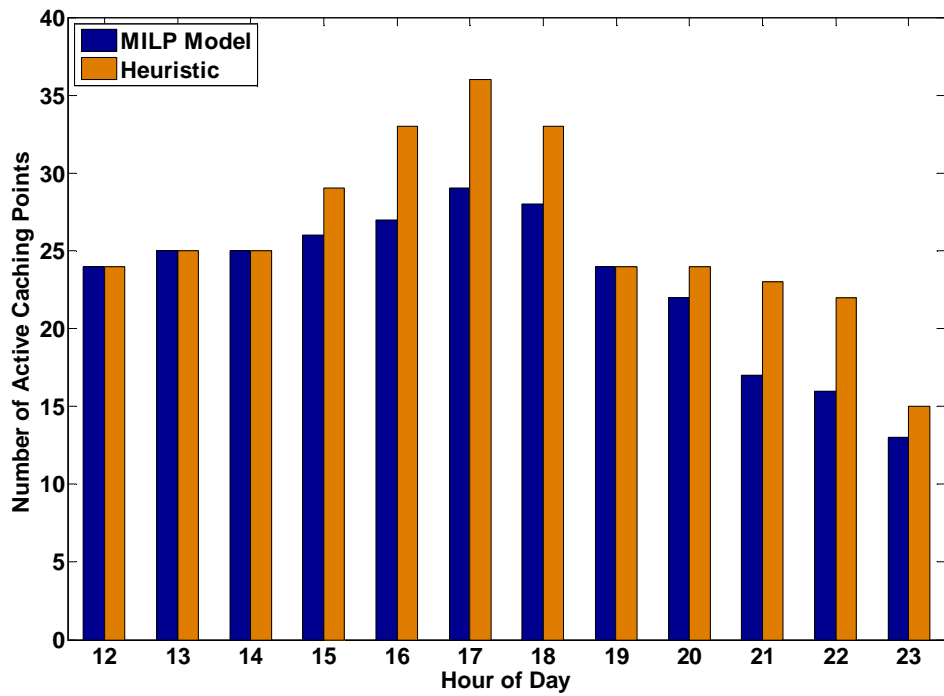
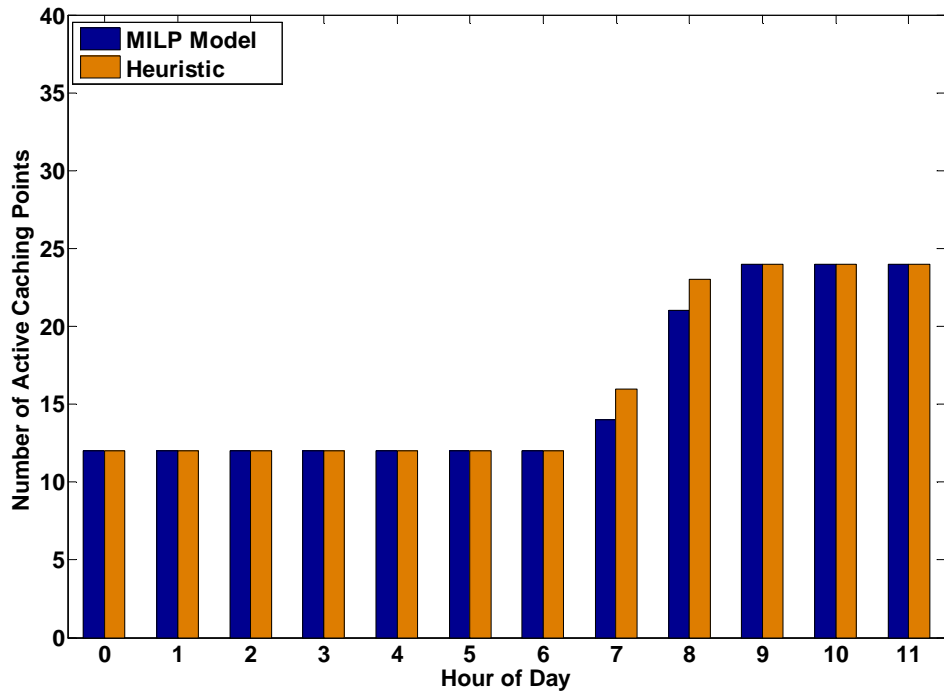


Figure 5.6: Number of active CPs

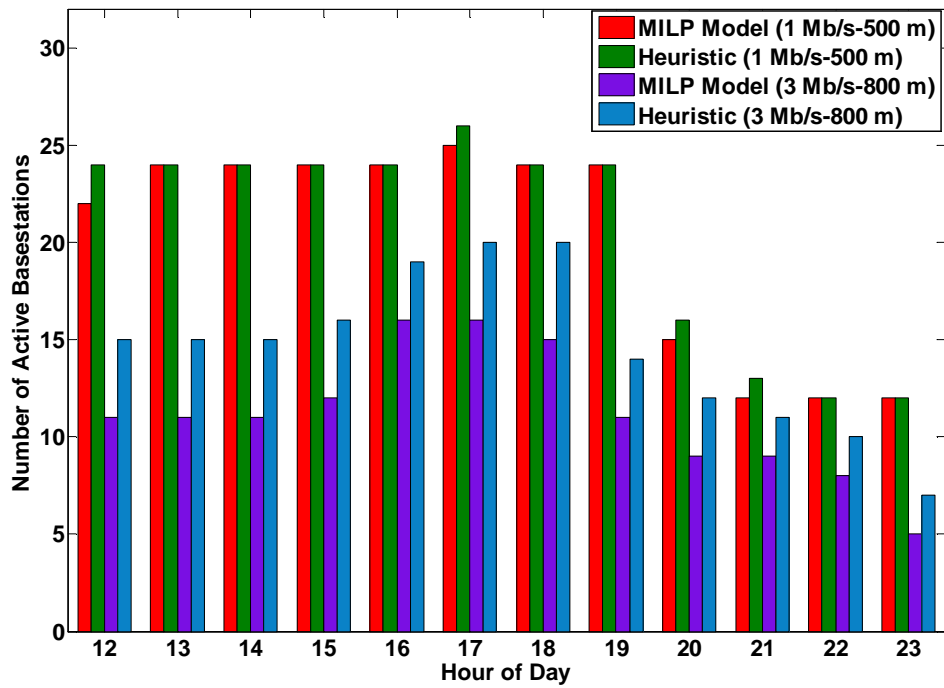
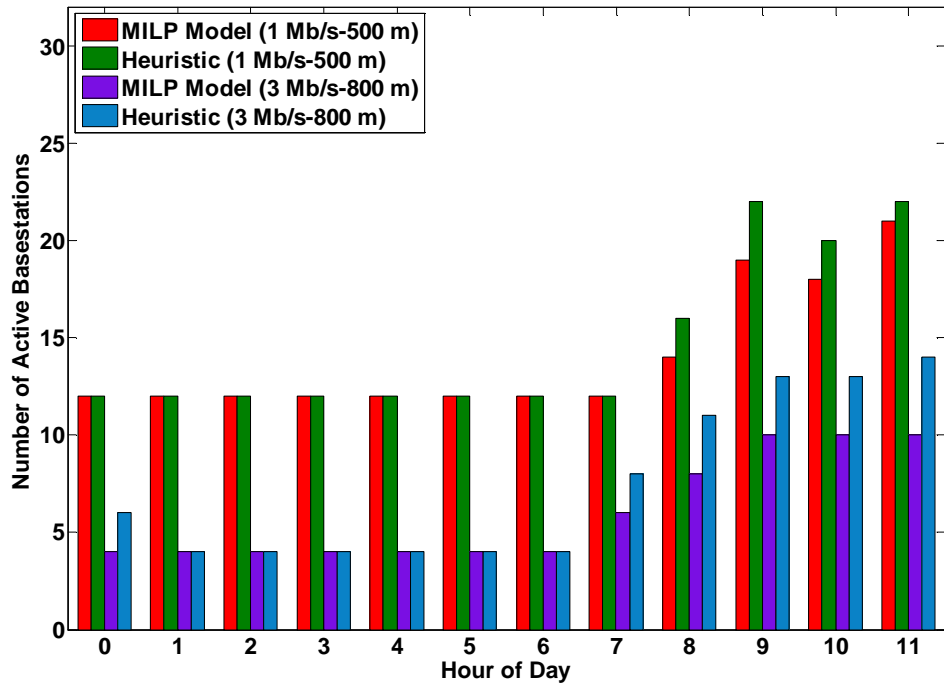


Figure 5.7: Number of active BSs

5.7.3 Root mean square deviation between MILP model and heuristic

Figure 5.8 and Figure 5.9 show the root mean square deviation in the number and location of CPs or BSs between the MILP model and the heuristic, respectively. Figure 5.8 shows that the results of both the MILP model and heuristic under the Wi-Fi network and the cellular network are in good agreement. However, the deviation in the number of CPs is slightly higher than the deviation in the number of BSs due to the higher data rate per user achieved by the Wi-Fi network in which a CP can serve up to 10 simultaneous requests whereas a BS can serve up to 30 users simultaneously (data rate per user is 1 Mb/s). Hence, the slight deviation in the arrival of requests between the MILP model and the heuristic (traffic is generated offline for MILP model and online for heuristic) has affected the Wi-Fi network more than the cellular network. For example at 17:00 hr, the difference between the number of CPs activated by the MILP model and the heuristic is 7 (shown in Figure 5.6) and the total number of TPs in the network is 24 leading to the root mean square number deviation of 1.42 as shown in Figure 5.8. Moreover, the root mean square deviation in the location of CPs or BSs has high values due to the distribution of CPs or BSs CS in the city. For example, if the heuristic activates a different CP or BS than the ones activated by the MILP model they will have a root mean square deviation of at least 50 m and 100 m, respectively.

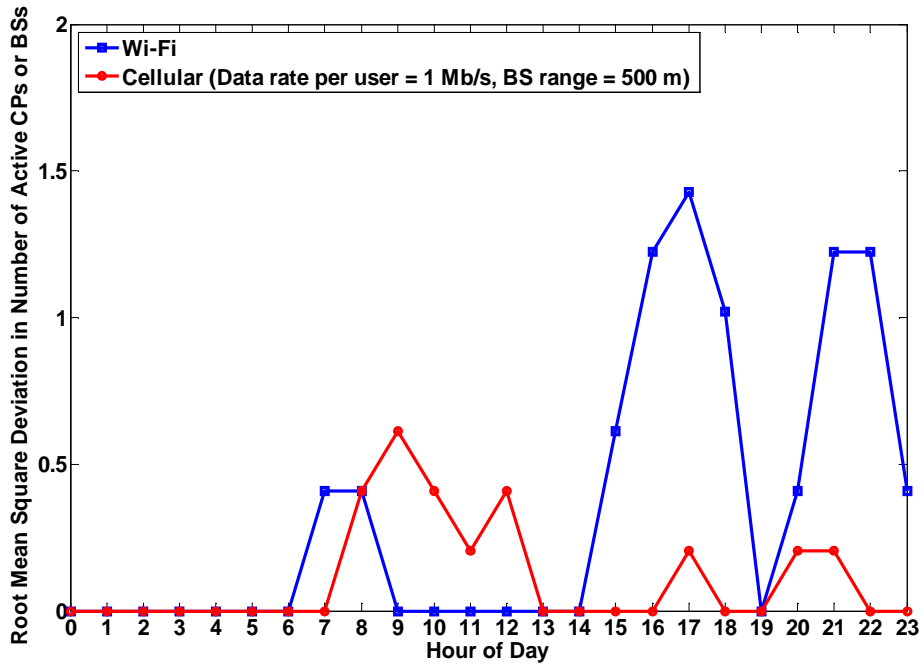


Figure 5.8: Root mean square number deviation of active CPs or BSs

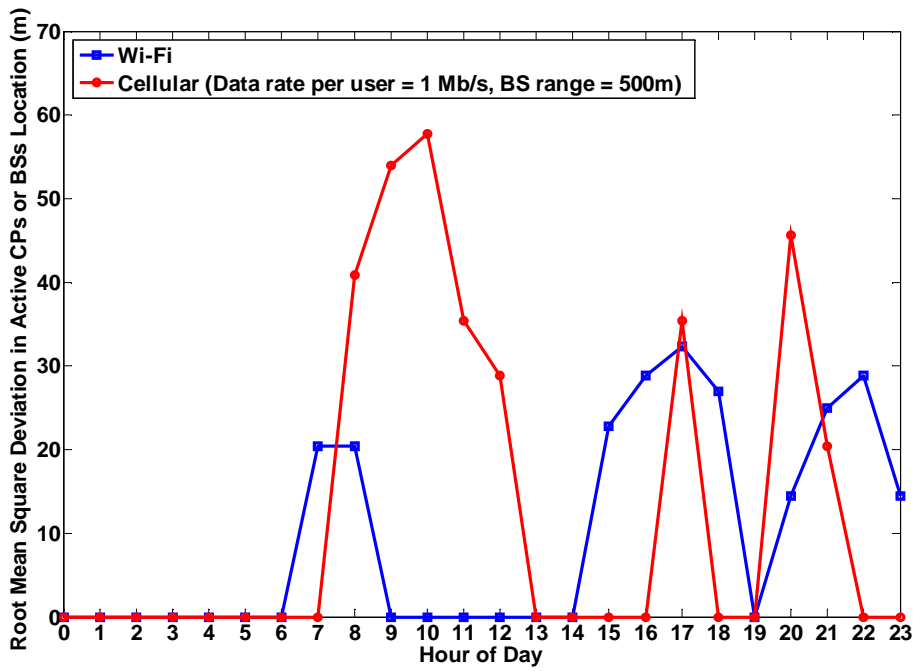


Figure 5.9: Root mean square location deviation of active CPs or BSs

5.8 Summary

In this chapter, the feasibility of a power-efficient content distribution network in a typical city vehicular environment is studied. The proposed Wi-Fi CDN has been compared with a cellular network in terms of total network power consumption and the number of active CPs and BSs. A MILP model has been developed with the objective of minimising the total network power consumption by optimising the number of CPs/BSs and their locations for both networks in such a dynamic environment. Based on the insights obtained through the results of the MILP model, a heuristic has been developed to mimic the MILP model's behaviour and verify its results and comparable power savings have been achieved. This validates the accuracy of the proposed approach and provides a simple algorithm for practical operation.

The results computed by the MILP model revealed that the Wi-Fi CDN has achieved considerable power savings over the cellular network, where the latter consumes up to 6 times more power than the former during the early hours of the day, and up to 1.5 times during peak hours.

These results also highlight the merits of deploying such a Wi-Fi content caching and distribution network instead of a traditional cellular network in an environment where a large volume of traffic is to be served over a wide spatial coverage and particularly if a limited content vocabulary (such as YouTube, BBC iPlayer etc) is to be shared among a large number of vehicular users.

6 Impact of Vehicular Mobility on the Performance of the City Vehicular Content Distribution Network

6.1 Introduction

In the previous chapter, static TPs (but with varying traffic volume) were used in both MILP model and the heuristic to facilitate mathematical tractability, hence, the impact of real vehicular mobility could not be studied in detail. Therefore, an algorithm, namely vehicular content download algorithm (VCDA) is developed for both Wi-Fi and cellular networks and is presented in this chapter, where each vehicle is served in real space and time instead of spatially static aggregation TPs (which nonetheless exhibit temporal variation). An important performance parameter, waiting duration (W_d), is also introduced where vehicles wait for a maximum amount of time before requesting the activation of a CP/BS that is in the sleep state if no active CP/BS was within their vicinity.

Further, utilising VCDA, different power management mechanisms are employed on CPs and the impact of such power management schemes are studied on the total network power consumption. The portion of the total BS capacity that is allocated to vehicular applications is varied and the impact on the content being distributed is studied. Finally, the performance of the system is evaluated in terms of total network power consumption and the number of active CPs/BSs, average piece delay, and the average content delay. These results are compared to those of the MILP model, presented in Chapter 5.

6.2 The Studied Scenario

The proposed setup is examined in a $3 \times 3 \text{ km}^2$ Manhattan type city scenario with 48 roads and 16 junctions, as shown in Figure 5.1 (in Chapter 5). Moreover, the same vehicular traffic profiles that were utilised for the analysis undertaken in Chapter 5 are used in this work. The hourly vehicular flow and the average traffic demand are shown in Figure 5.2.

6.3 Vehicular Content Download Algorithm (VCDA)

In both MILP model and the heuristic discussed in the previous chapter, the number and the locations of CPs/BSs were optimised. The total network power consumption based on a fixed network topology using TPs which act as vehicles' traffic demand aggregation points was evaluated. To have a more realistic scenario, and study the impact of vehicular mobility on the total network power consumption, the VCDA is developed in this chapter to optimise the

number and locations of CPs/BSs where vehicles roam freely and directly communicate with CPs/BSs, instead of utilising any virtual TPs. Furthermore, a performance parameter, namely W_d , is introduced, where vehicles wait for a maximum amount of time after requesting a content before activating a new CP/BS if there is no available/active CP/BS. Moreover, vehicles generate requests in a similar fashion as generated for the MILP model and heuristic (discussed in Chapter 5), however aggregation points i.e. TPs are not considered in this case and the traffic demand of each vehicle individually needs to be fulfilled along with the CPs/BSs capacity constraints, so that the actual impact of vehicular mobility can be studied. The same parameters used for the work in Chapter 5 including data rates and communication range are utilised in this chapter and are presented in Table 5.1 (in Chapter 5).

Pseudo-code 6.1 illustrates how the VCDA works for the Wi-Fi CDN, however it can also be utilised for the cellular network by replacing each CP c by BS b . Note that the notations used in Pseudo-code 6.1 are also described in Table 5.1. The VCDA starts with an inactive set of CSs. Upon generating a request for content, it records the request time to eventually calculate content delay as given by lines 2-3. Thereafter, the vehicle starts to generate requests for individual pieces and records the request time of each piece in order to calculate the individual piece delay as given by lines 4-6. Regardless of the value of W_d , as soon as a vehicle generates a piece request, it sets the waiting timer (Δ_v) to 0 as given by line 7. Thereafter, it scans for an active CP/BS within

its vicinity. If an active CP/BS with available capacity is discovered, the vehicle is served immediately and the piece delay and power consumption of the serving CP are computed as given by lines 8-11. However, if there is no active CP/BS in the vicinity of a vehicle, or the active CP/BS is operating at its maximum capacity, the vehicle waits for a maximum amount of time, i.e. W_d , before a new neighbouring CP/BS candidate is activated. The content delay (ϕ_x) is computed after the vehicle has downloaded the whole content as given by line 13. The W_d quantity is varied between 0 seconds and 120 seconds in order to study its effect on power consumption, where an inverse relation between W_d and the power consumption is observed.

In addition to evaluating the number and locations of CPs/BSs and the total network power consumption, the VCDA also determines the average piece delay and the average content delay experienced by vehicles under varying values of W_d , where the trade-off between delay and power consumption is studied.

Pseudo-code 6.1 VCDA

Input: $W_d, \forall v \in V$ **Output:** $P_N, \emptyset, \vartheta$

```
1  for all  $v \in V$  do
2      generate  $R[x]$ ;
3      record  $\zeta[x]$ ;
4      for all  $n = 1, 2, 3, \dots N$  do
5          generate  $K_x[n]$ ;
6          record  $\gamma_x[n]$ ;
7          set  $\Delta_v = 0$ ;
8          find suitable CP or wait for a maximum of  $W_d$  then activate new CP;
9          download  $K_x[n]$ ;
10         compute  $\vartheta_x[n]$ ;
11         compute  $P_N[n]$ ;
12     end for
13     compute  $\emptyset_x$ ;
14 end for
```

6.4 Performance Evaluation

The performance of the Wi-Fi CDN and the cellular network is evaluated under the VCDA. In addition to the evaluation of the number of active CPs/BSs and the total network power consumption, the average piece delay and the average content delay experienced by vehicles are also calculated for different values of W_d i.e. 0, 30, 60, 90 and 120 seconds.

The VCDA is employed in both networks (Wi-Fi and cellular) to study a more realistic scenario by taking real vehicular mobility into account. As expected, the impact of vehicular mobility on the performance is clearly evident under the VCDA than in the MILP model. As detailed earlier, W_d is varied between 0 and 120 seconds to study its effect on the performance of the network. The average

piece and content (video) delay are calculated, in addition to the total network power consumption and the number of active CPs/BSs. The performance of the VCDA with different W_d is also compared with the MILP model presented in Chapter 5. Further, the performance of the Wi-Fi network under VCDA has been evaluated under different power management schemes. Two different operating scenarios have been studied in the case of the cellular network. The first scenario assumes a dense environment (e.g. Manhattan) where buildings have a considerable effect on the channel allowing users to only achieve data rates of 1 Mb/s/user and a BS range of up to 500 m. The second scenario assumes a less dense environment (e.g. Leeds) where each user can achieve a data rate of 3 Mb/s and a BS can cover up to 800 m. Moreover, the impact of varying allocated resources (i.e. bandwidth) on the performance has also been studied under the cellular scenario (vehicular network content download application).

6.4.1 Total network power consumption

Figure 6.1 shows the total network power consumption of the Wi-Fi network under VCDA with different waiting times with no power management mechanism employed compared to the total network power consumption of the MILP model. The results of the VCDA follow the same trend as that of the MILP model. The power consumption with no W_d (i.e. 0 seconds) is the highest. This is because as soon as a vehicle generates a request for content, a CP is immediately activated to serve it unless there was an active CP in range which had enough bandwidth available to serve the vehicle's demand. Eventually, this mechanism activates a large number of CPs corresponding to individual vehicle's request rather than any TP's request as vehicles are highly mobile compared to the static TPs. With this configuration, the power consumption at 4:00 hr is approximately 4 kW compared to 1.2 kW attained by the MILP model, as shown in Figure 6.1. As can be noticed from the figure the total network power consumption decreases with increase in the waiting time. This is mainly due to the lower number of active CPs required as vehicles start to wait until they find an active CP before activating a new one. Hence the chances of vehicles getting into the range of an already active CP are high. Furthermore, the VCDA through flexible W_d provides an opportunity to an active CP operating at its highest capacity to finish serving some requests during the waiting time of another vehicle and hence can eventually serve the waiting vehicle instead of activating a new CP. The results also show that a W_d of 60 seconds achieves comparable power consumption to that of the MILP model, while maintaining

acceptable delay. For instance, the power consumption at 17:00 hr is approximately 24 kW when vehicles wait for 60 seconds before being served compared to 23.8 kW attained by the MILP model. Note that the VCDA with 120 seconds W_d outperforms the MILP model in terms of power consumption during some periods of the day. For example, the total network power consumption of VCDA with a W_d of 120 seconds at 10:00 hr is 12 kW compared to approximately 12.3 kW achieved by the MILP model.

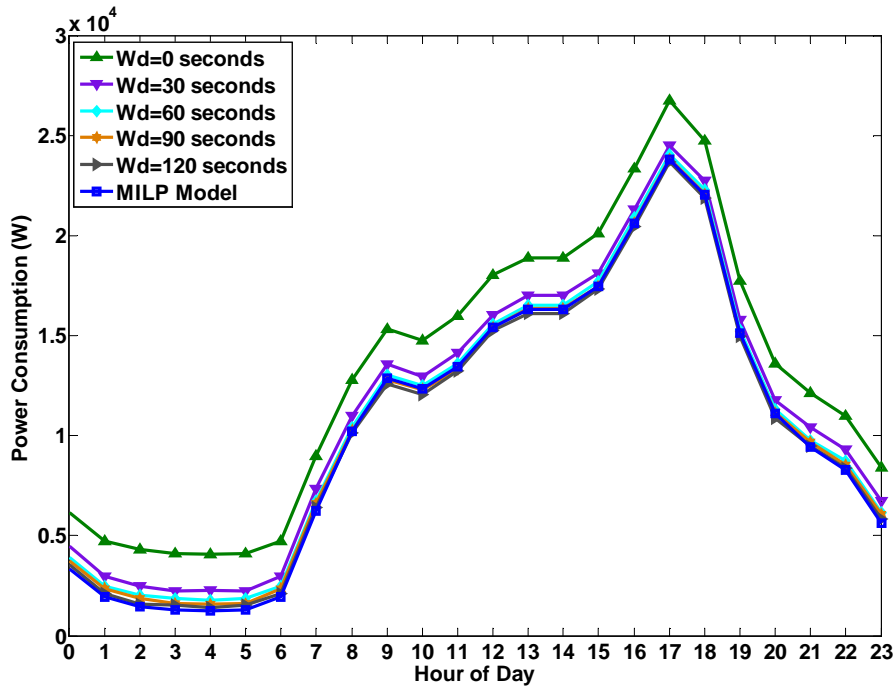


Figure 6.1: Total network power consumption (Wi-Fi)

Figure 6.2 shows the total network power consumption of the Wi-Fi network under VCDA with W_d of 0 seconds with two power management (namely semi and perfect) mechanisms employed and without a power management mechanism compared to the total network power consumption of the MILP model (with no power management mechanism). Note that the MILP model

operates in such a way that if a CP/BS is switched ON for any time point, it stays ON throughout the entire hour (i.e. it stays ON for all 90 time points). The VCDA with no power management mechanism consumes the most power compared to the MILP model and the other two scenarios. This is mainly because CPs are not switched OFF or even put into low power mode when they are in an idle state and hence considerable amount of power is wasted during these periods. On the other hand, by employing the semi power management mechanism (i.e. put CPs to low power mode during idle state) power saving of up to 2x is achieved over VCDA with no power management mechanism especially at the early hours of the day. This is because the CPs are underutilised during early hours of the day and hence can be put into low power mode for longer periods. Note that by putting CPs into low power mode, only the hard drive and the MAC and the algorithm unit are switched OFF to enable fast start-up upon receiving a new request. The figure also shows that the maximum power savings are achieved by employing VCDA with perfect power management mechanism, where CPs are completely switched OFF during idle periods. Power savings of up to 5x and 2x are achieved by employing VCDA with perfect power management and semi power management respectively compared to the VCDA with no power management.

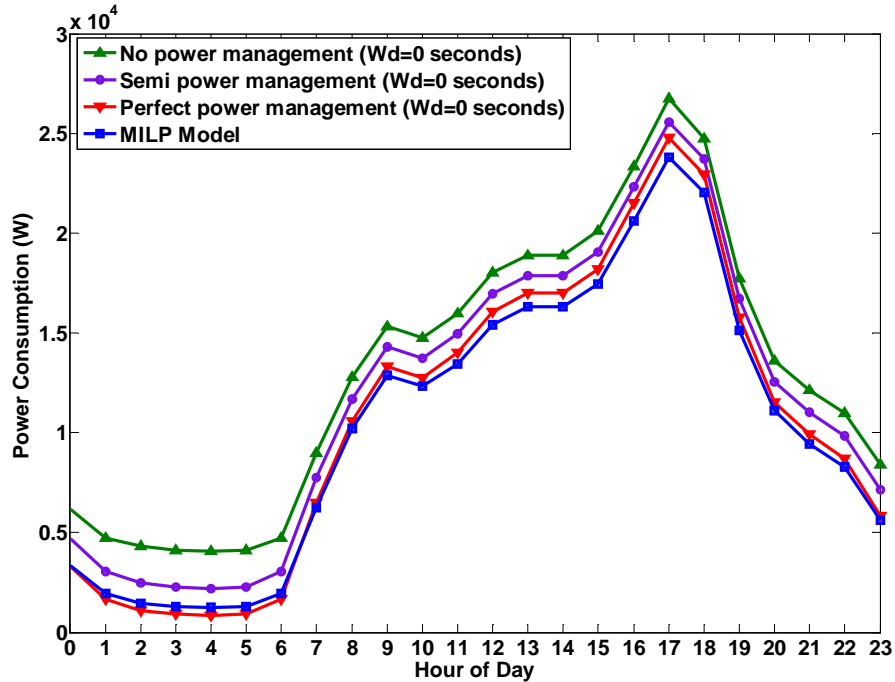


Figure 6.2: Total network power consumption with different power management mechanisms (Wi-Fi)

Figure 6.3 and Figure 6.4 shows the total network power consumption of the cellular network under VCDA with different W_d where both highly (Figure 6.3) and lightly (Figure 6.4) dense environments are considered. Similar to the Wi-Fi network, the VCDA results follow the same trend as that of the MILP model. Figure 6.3 shows that the VCDA with W_d of 0 seconds consumes the highest power compared to the other waiting times (i.e. W_d) and to the MILP model, as one of the inactive BSs is activated as soon as a vehicle generates a request and if there is no active BS in the vicinity. However as vehicular density increases, the power consumption achieved by the MILP model gets higher than that of the VCDA regardless of the value of W_d . This is due to the difference between how the MILP model and the VCDA operate, where in the MILP model, the traffic demand by vehicles was assembled at TPs, whereas in

the VCDA vehicles flow freely and download their requests directly from the BSs. Hence, with TPs uniformly distributed in the city and a BS transmission range of only 500 m due to the dense environment considered, each BS can only serve a single TP so that if a request is generated at another TP an additional BS has to be switched ON leading to higher total network power consumption. On the other hand, due to the mobility of vehicles and their non-uniform distribution in the city, a single BS can serve a number of vehicles and hence the lower number of active BSs required under the VCDA, resulting in lower power consumption (Figure 6.3). Since the data rate is set to 1 Mb/s/user and the BS capacity for vehicular content downloading is assumed to be 30 Mb/s, a single BS can serve up to 30 vehicles simultaneously compared to only 1 TP (which might have only a few vehicles under its coverage). For example, at 12:00 hr, the total network power consumption achieved by the MILP model is approximately 26 kW compared to 25 kW achieved by the VCDA with W_d of 0 seconds. Note that the VCDA can achieve power savings of up to 2x compared to the MILP model. However, this is achieved at the expense of higher average piece and content delay.

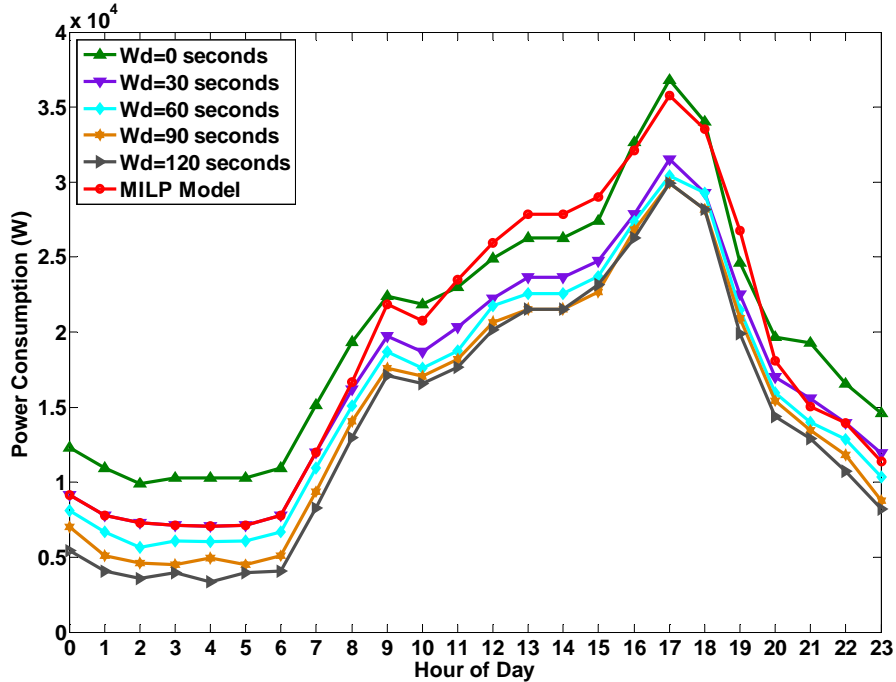


Figure 6.3: 1 Mb/s/user & 500 m BS range - Total network power consumption (Cellular – 30 Mb/s for vehicular content downloading)

Figure 6.4, which considers lightly dense environment, also shows the total network power consumption of the cellular network under the VCDA with different W_d and compares the results with those of the MILP model. Since data rates of 3 Mb/s/user [184] and a BS coverage of 800 m [18] are utilised, the figure shows that the MILP model achieves better results compared to the VCDA regardless of the value of W_d . This is mainly due to the fact that each BS can serve more than one TP due to the higher coverage of each BS leading to a lower total network power consumption. With a BS capacity of 30 Mb/s, each BS can serve up to 10 users (each operating at 3 Mb/s) simultaneously compared to 30 users at 1 Mb/s/user. This figure, i.e. 10, is comparable to the average number of vehicles under a TP. For example, the total network power consumption at 12:00 hr achieved by the MILP model is approximately 20 kW

compared to approximately 27 kW achieved by the VCDA with W_d of 0 seconds. However, by allowing vehicles to wait for the maximum W_d i.e. 120 seconds, significant power savings could not be achieved. For example, the total network power consumption achieved by the MILP model at 16:00 hr is 27.9 kW compared to 27.3 kW achieved by the VCDA with W_d of 120 seconds. Moreover, waiting for up to 2 minutes before starting to download content may not be acceptable to a number of users.

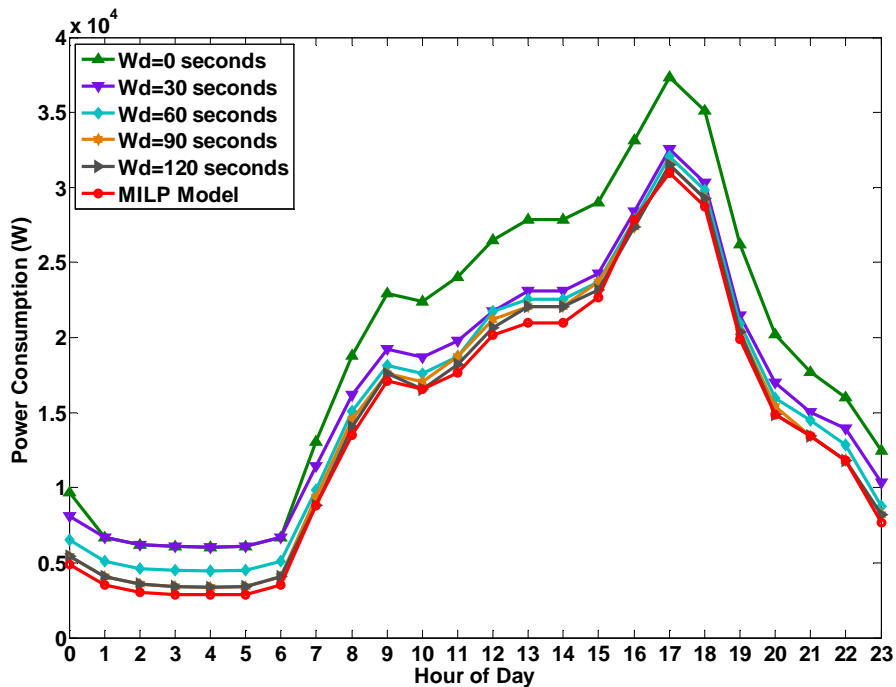


Figure 6.4: 3 Mb/s/user & 800 m BS range - Total network power consumption (Cellular – 30 Mb/s for vehicular content downloading)

Different maximum downloading resources (data rates or proportion of the BS 100 Mb/s capacity) can be allocated by an operator to vehicular applications ensuring fair resource allocation to other services (such as voice and cellular data). Figure 6.5 shows the impact of varying allocated resources (i.e. BS

resources of 30 Mb/s, 50 Mb/s and 70 Mb/s) on the total network power consumption achieved by the VCDA and compares the performance to that of the MILP model, where the MILP model has 30 Mb/s BS capacity. Studying this impact is important to evaluate both current and futuristic trends in vehicular applications. The data rate per user is 3 Mb/s, W_d is 0 seconds and the BS transmission range is set to 800 m. At the early hours of the day, increasing the capacity has negligible effect on power consumption as both vehicular density and traffic demand are low. As a result, only the minimum number of BSs are activated (i.e. 10 in the case of VCDA and 4 in the case of MILP model) to meet minimum traffic demand. As the vehicular density increases, the load on BSs also increases leading to a higher network power consumption. However, the power consumption achieved by the VCDA with higher BS capacity employed is lower than that achieved by the VCDA with BS of lower capacity. This is because more users can simultaneously be served by one BS with the higher capacity. For example, the power consumption at 17:00 hr with a BS capacity of 70 Mb/s is 30.5 kW compared to 37.3 kW when the BS capacity is set to 30 Mb/s. Note that the VCDA with a 70 Mb/s BS capacity consumed less power than the MILP model at 17:00 hr because of the aforementioned reason.

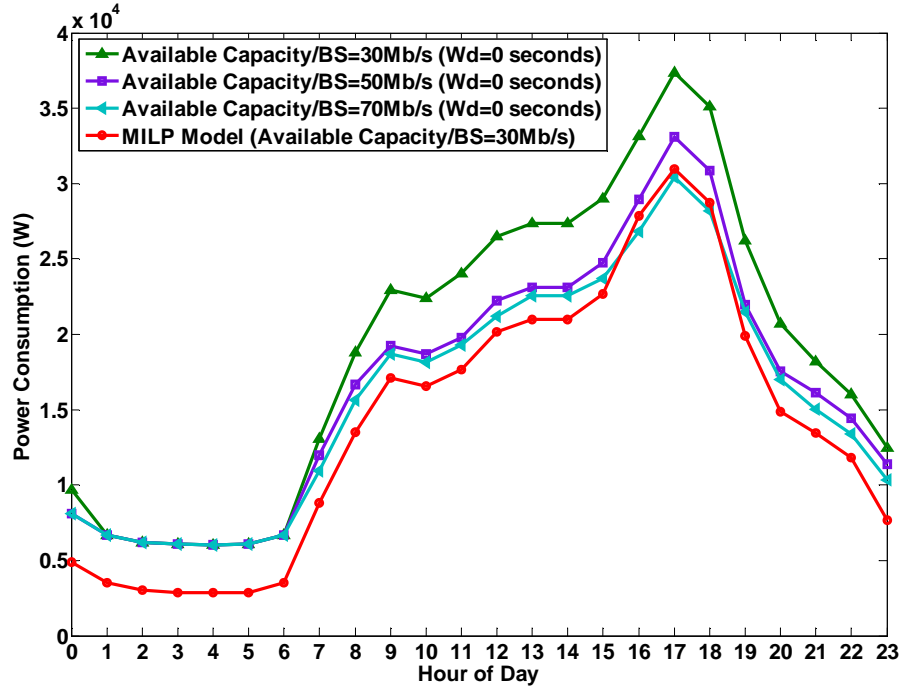


Figure 6.5: Power consumption with variable BS capacity for vehicular applications (Cellular- 3 Mb/s/user, 800m BS range & $W_d = 0$)

6.4.2 Number of active CPs/BSs

The number of active CPs/BSs at each hour of the day under the VCDA has been evaluated. Figure 6.6 shows the number of active CPs throughout the 24 hours for varying W_d . The results are compared with those of the MILP model. It is evident from Figure 6.6 that the number of active CPs increases as the W_d decreases. The number of active CPs is very high when utilising the VCDA with 0 seconds W_d , as vehicles are served as soon as they generate a request. The number of active CPs with 0 seconds W_d is much higher than that achieved by the MILP model due to the mobility of vehicles. For example, 94 CPs are active at 17:00 hr while utilising the VCDA with a W_d of 0 seconds compared to just 29 active CPs attained by the MILP model. This huge difference is reflected in the

total network power consumption (see Figure 6.1). Moreover, this large number (i.e. 94 active CPs) reduces to as low as 26 active CPs when the vehicles start to wait for a maximum of 120 seconds. However, considerable amount of delay is experienced to achieve these low numbers of active CPs (i.e. lower power consumption).

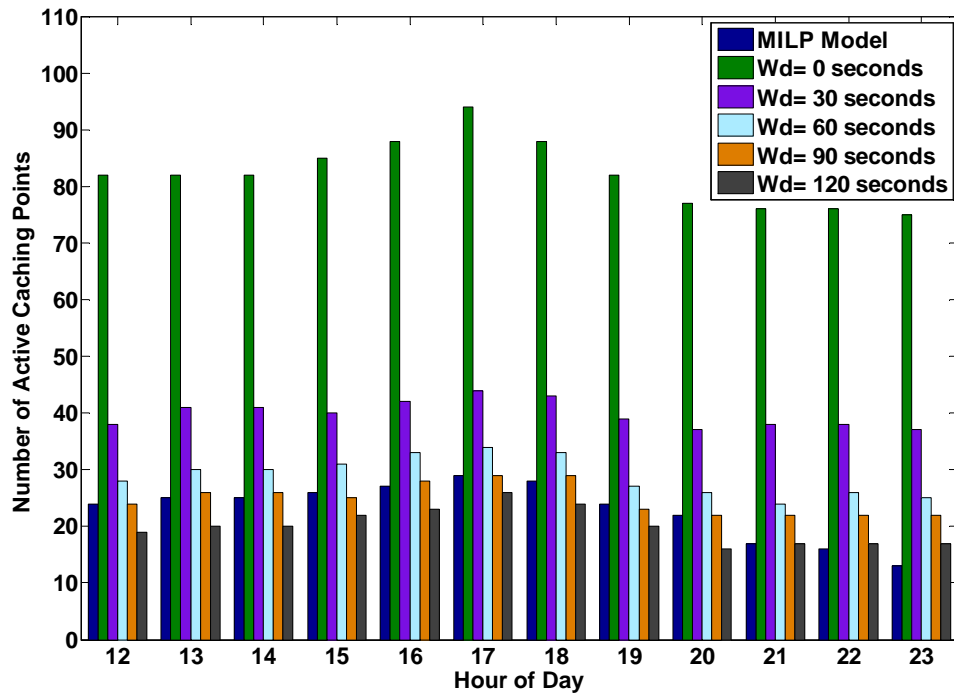
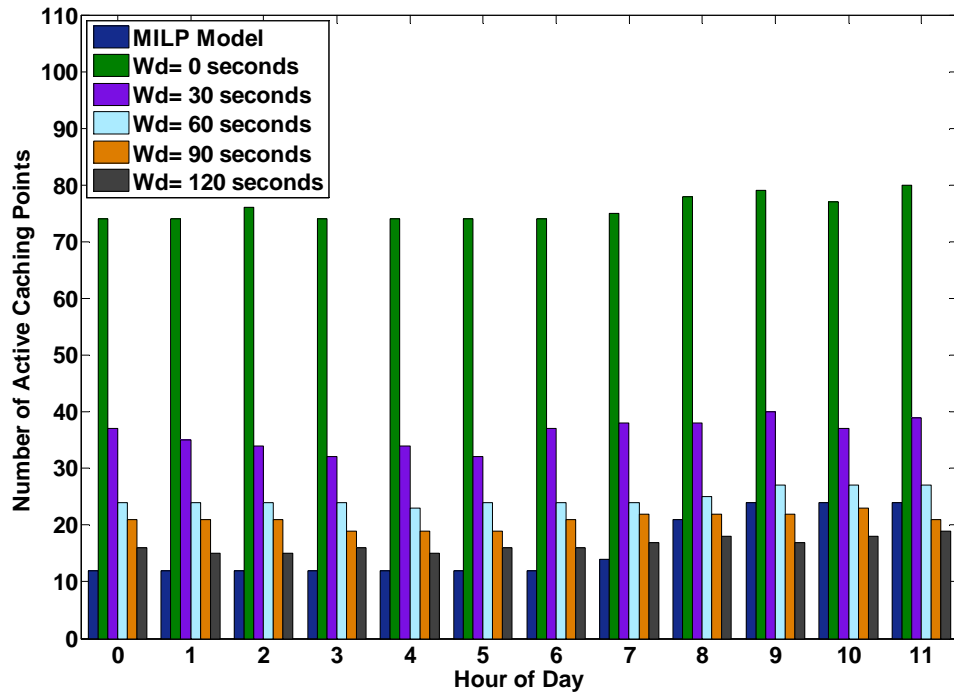


Figure 6.6: Number of active CPs (Wi-Fi)

Figure 6.7 and Figure 6.8 depict the number of active BSs in the cellular network under the VCDA and the MILP model. Figure 6.7 shows the number of active BSs where the data rate is set to 1 Mb/s/user, the capacity and the transmission range of a BS are 30 Mb/s and 500 m, respectively. Similar to the Wi-Fi network the number of active BSs decreases with increase in W_d . At the early hours of the day, the number of active BSs is the highest for the case of 0 seconds W_d , where a BS is activated as soon as a vehicle generates a request. For example, the number of active BSs at 4:00 hr is 18 compared to 12 achieved by the MILP model. However as the vehicular density increases, the number of active BSs increases for all configurations. Due to the lower range of the BSs and the way both VCDA and the MILP model operate, the number of active BSs achieved by the MILP model at some points throughout the day exceeds that achieved by the VCDA even with W_d of 0 seconds. For example, the number of active BSs achieved by the MILP model at 12:00 hr is 22 compared to 20 achieved by the VCDA with W_d of 0 seconds. Furthermore, the number of active BSs reaches as low as 5 at 04:00 hr when vehicles wait for up to 120 seconds before starting to download the requested content. However, this is achieved at the cost of high average piece and content delay.

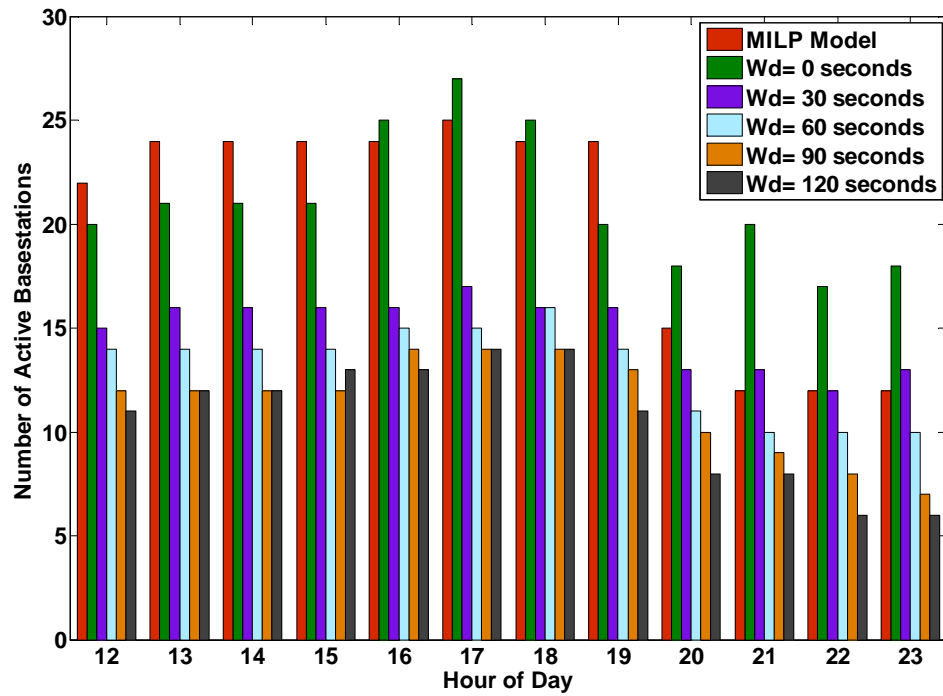
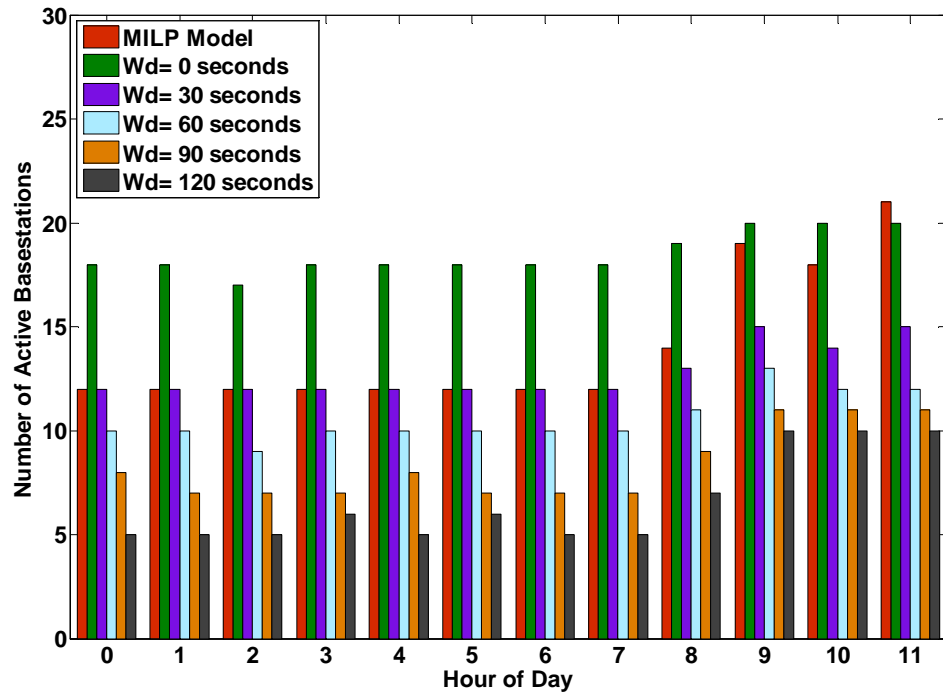


Figure 6.7: 1 Mb/s/user & 500 m BS range - Number of active BSs (Cellular – 30 Mb/s for vehicular content downloading)

Figure 6.8 illustrates the number of active BSs in the cellular network where the data rate is set to 3 Mb/s/user, the capacity and the transmission range of a BS are 30 Mb/s and 800 m, respectively. The number of active BSs is the highest for the case of 0 seconds W_d , where it reaches 28 active BSs at 17:00 hr compared to the 16 active BSs achieved by the MILP model. However, the number of active BSs gets significantly lower with increase in W_d . Due to the higher transmission range of a BS and the higher data rate per user utilised in this scenario, the MILP model performs better than the VCDA with W_d of 0 seconds throughout the day. However, the VCDA achieves a lower number of active BSs when vehicles wait for long periods before activating a BS. For example, the number of active BSs achieved by the MILP model at 16:00 hr is 16 compared to 15 achieved by the VCDA with W_d of 120 seconds. This is achieved at the expense of higher content and piece delay.

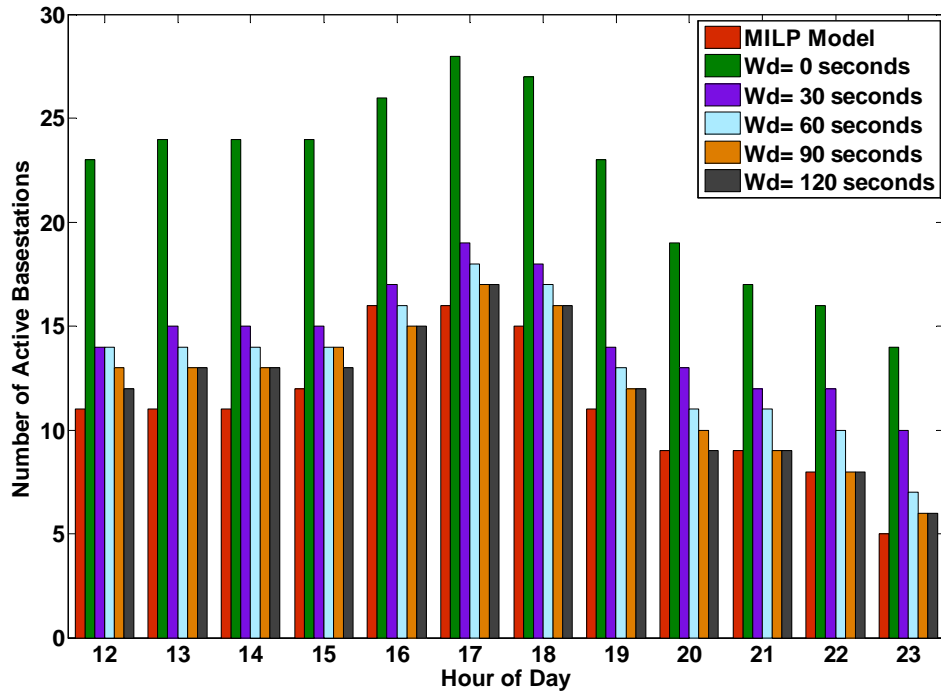
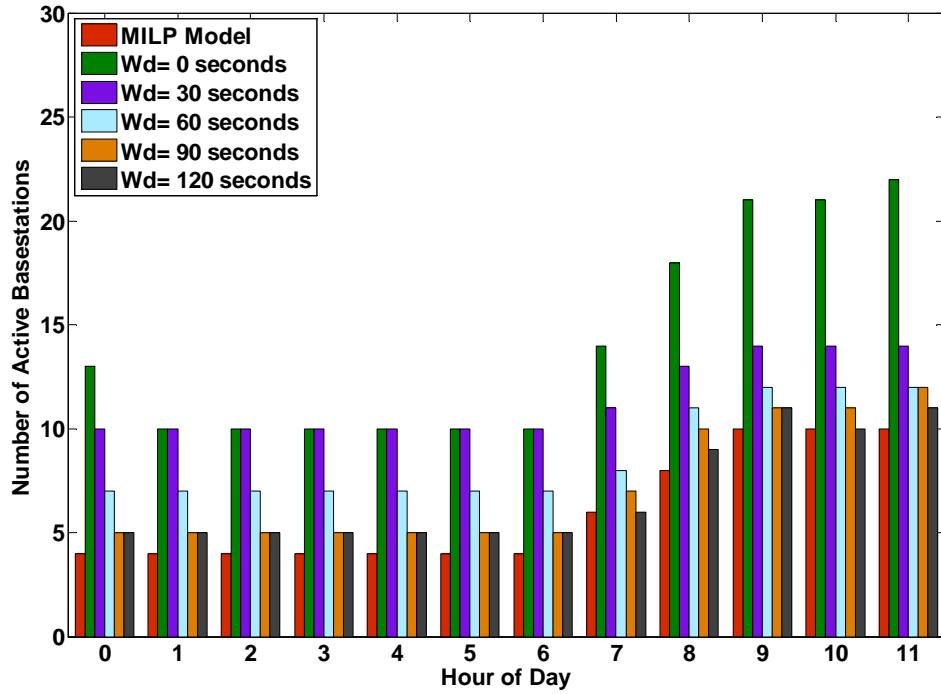


Figure 6.8: 3 Mb/s/user & 800 m BS range - Number of active BSs (Cellular – 30 Mb/s for vehicular content downloading)

Figure 6.9 shows the number of active BSs under the VCDA with W_d of 0 seconds with varying BS capacity (i.e. 30, 50, 70 Mb/s) compared to the MILP model, where BS capacity is 30 Mb/s. The data rate per user is 3 Mb/s, the BS transmission range is 800 m and W_d is 0 seconds. The figure shows that increasing the BS capacity does not affect the number of active BSs during early hours of the day. This is due to the low vehicular traffic and hence only the minimum number of BSs is activated to meet traffic demand. As vehicular traffic increases, the number of active BSs also increases for both MILP model and the VCDA with a BS capacity of 30 Mb/s. Moreover, as the capacity of a BS increases, the number of active BSs decreases as BSs can serve a large number of vehicles simultaneously. For example, the number of active BSs achieved by the VCDA with a BS capacity of 30 Mb/s at 17:00 hr is 28 compared to the 15 achieved by the VCDA with a BS capacity of 70 Mb/s. Note that the number of active BSs under the VCDA with a BS capacity of 70 Mb/s does not vary considerably during the whole day. This shows that under the VCDA, 70 Mb/s is the optimum BS capacity to serve all the users during the whole day with the minimum power consumption for the set of system parameters considered.

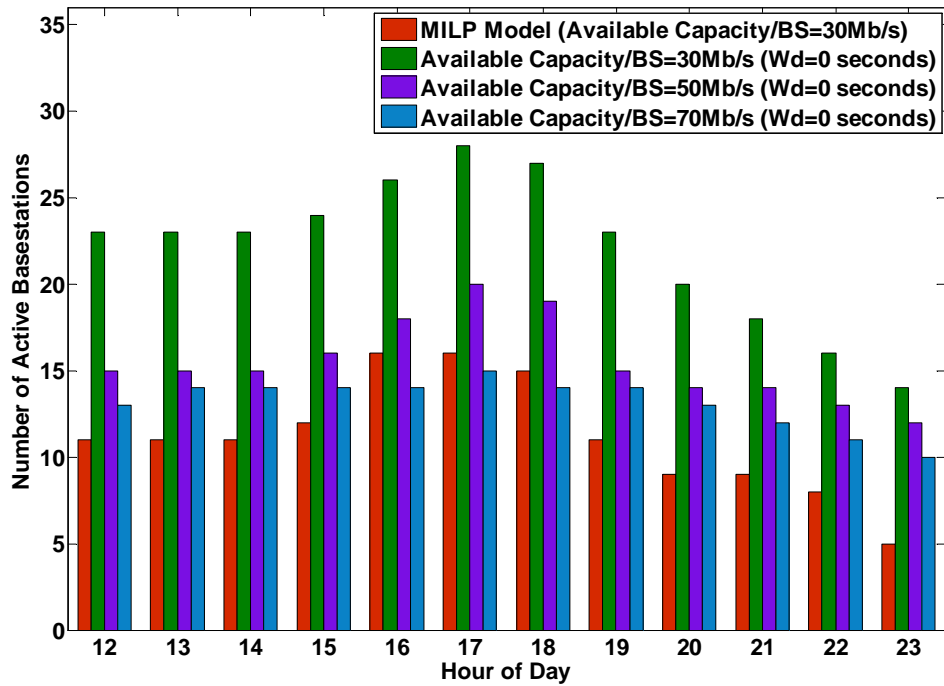
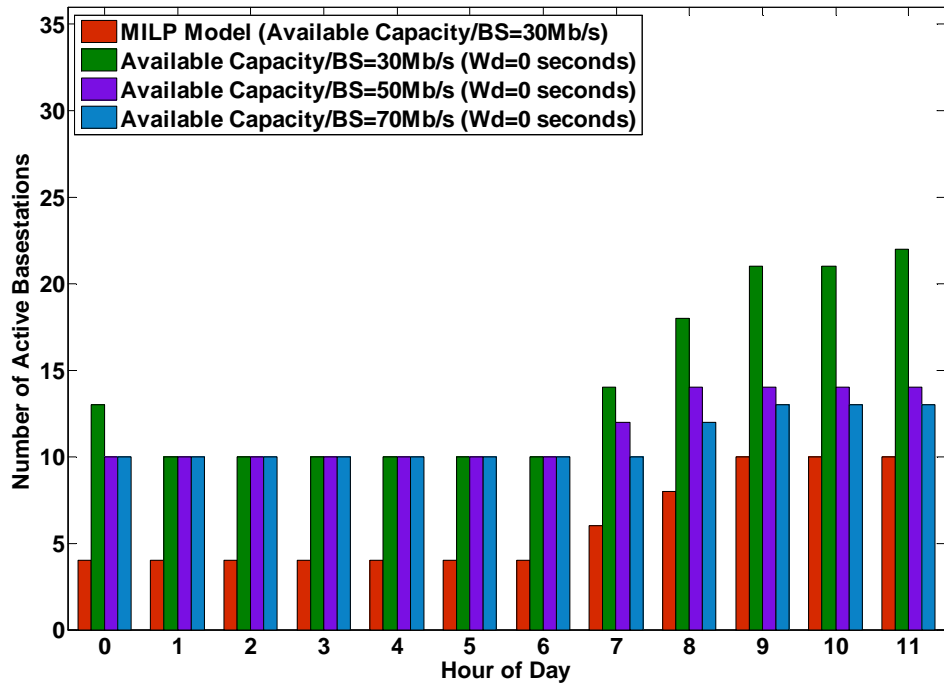


Figure 6.9: Number of BSs with variable BS capacity for vehicular applications (Cellular- 3 Mb/s/user, 800m BS range & Wd = 0)

6.4.3 Average piece delay and average content delay

As mentioned earlier, the VCDA determines the average piece delay as well as the average content delay experienced by the vehicles throughout the day. Figure 6.10 shows the average piece delay attained throughout the 24 hours for the Wi-Fi network for varying W_d . The figure also shows a comparison of the aforementioned results with those obtained through the MILP model. It is evident from the figure that with an increase in W_d , the average piece delay also increases. This is due to the fact that vehicles wait for a certain amount of time before being served if they did not discover an active CP to serve them. It can be noticed that the average piece delay is higher at low traffic loads (early morning hours and late night). This can be attributed to the fact that the number of active CPs during these hours is very low, hence the vehicles in that hour wait much longer before they get served. For example, the average piece delay at 04:00 hr with vehicles waiting a maximum of 120 seconds is approximately 42 seconds, whereas it reaches 29 seconds at 17:00 hr for the same W_d . Moreover the average piece delay achieved by the VCDA (with 0 seconds W_d) corresponds to the one achieved by the MILP model. This is because they both behave in the same manner, where vehicles are served immediately after they generate a request. As the MILP model is unable to provide the average piece delay, it is computed by dividing the piece size over data rate per user and is found to be 16 seconds as this is the amount of time needed to download a piece (service time). Although the VCDA with 0 seconds W_d achieves very low

delay (service time only), it comes at the cost of very high total network power consumption (Figure 6.1).

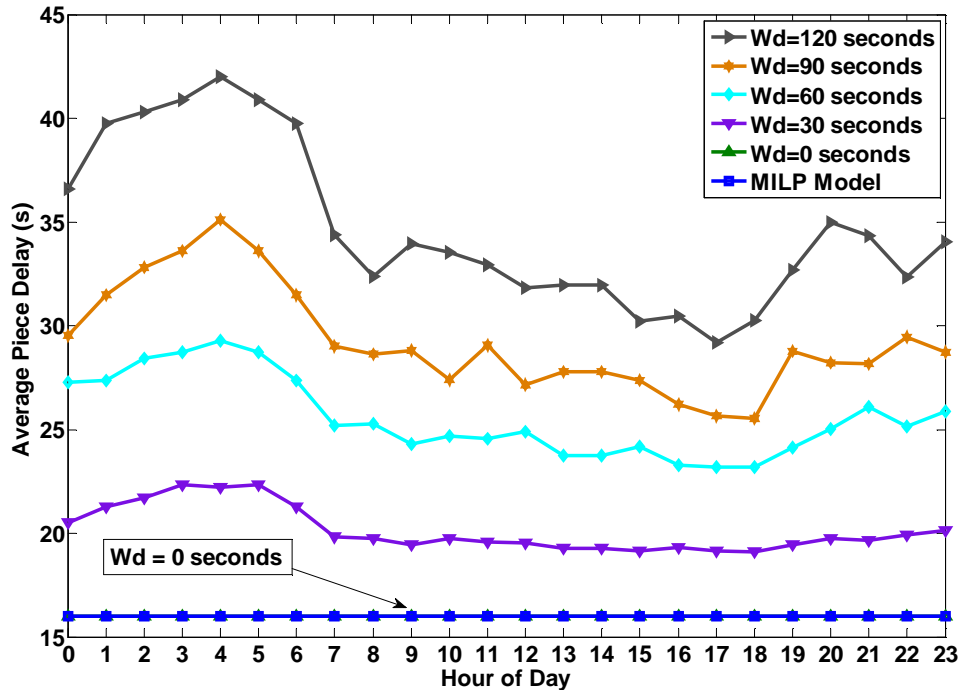


Figure 6.10: Average piece delay (Wi-Fi)

Figure 6.11 illustrates the average content delay for the Wi-Fi network. The results show the average content delay for the VCDA with varying W_d along with the average content delay achieved by the MILP model. Similar to the average piece delay through the MILP model, the average content delay is also computed by multiplying the average piece delay (i.e. 16 seconds) by the number of pieces in each content (i.e. 33). This is because each downloaded piece does not experience any additional delay other than the service time, as an idealistic MAC is assumed in this work, as a first step. As the content size is fixed (i.e. 200 MB) along with the download rate of 3 Mb/s/user, the content

delay achieved by the MILP model is 528 seconds (i.e. 8.8 minutes). Hence, a 200 MB video, approximately 33 minutes long is downloaded in 8.8 minutes (i.e. standard quality BBC iPlayer video of 800 kb/s bit rate [187]). However the IEEE 802.11ac [188], to be standardised soon, can achieve download rates of up to 1.3 Gb/s. Hence, in the future, a 200 MB video could be downloaded in 0.02 minutes. The VCDA with 0 seconds W_d has almost constant content delay throughout the day, however, it is higher than the content delay achieved by the MILP model because the content delay in this case is evaluated for each specific content individually rather than any 33 pieces making a content. For example, if a vehicle generates a request for content while downloading another content, the second request will be downloaded as soon as the first one is completely downloaded, and hence extra delay experienced. As W_d increases the average content delay increases. For example, the delay at 17:00 hr is approximately 1200 seconds with 120 seconds W_d , while it is about 800 seconds for a W_d of 30 seconds at the same hour. Similar to the average piece delay, the average content delay is higher at low traffic as the number of active CPs is lower during that period and vehicles have to wait before they get served.

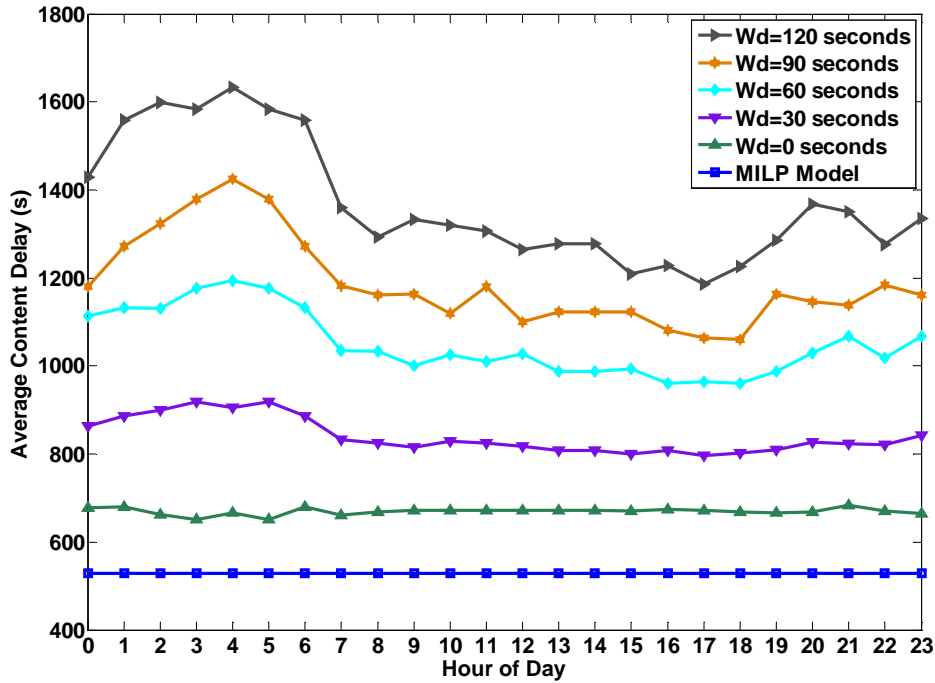


Figure 6.11: Average content delay (Wi-Fi)

Figure 6.12 shows the average piece delay under the cellular network (30 Mb/s BS capacity, 3 Mb/s/user & 800 m BS range) for the VCDA with varying W_d along with the one achieved by the MILP model. Similar to the Wi-Fi network, the average piece delay of the VCDA with 0 seconds W_d is in good agreement with the one achieved by the MILP model. Moreover, Figure 6.12 shows that the average piece delay experienced under the cellular network is lower than that of the Wi-Fi network. This is mainly due to the larger communication range of a BS compared to a CP, where vehicles rarely wait before being served as the already active BSs can cover wide areas. However, lower the average piece delay experienced while operating under the cellular network is associated with very high total network power consumption as shown in Figure 6.4.

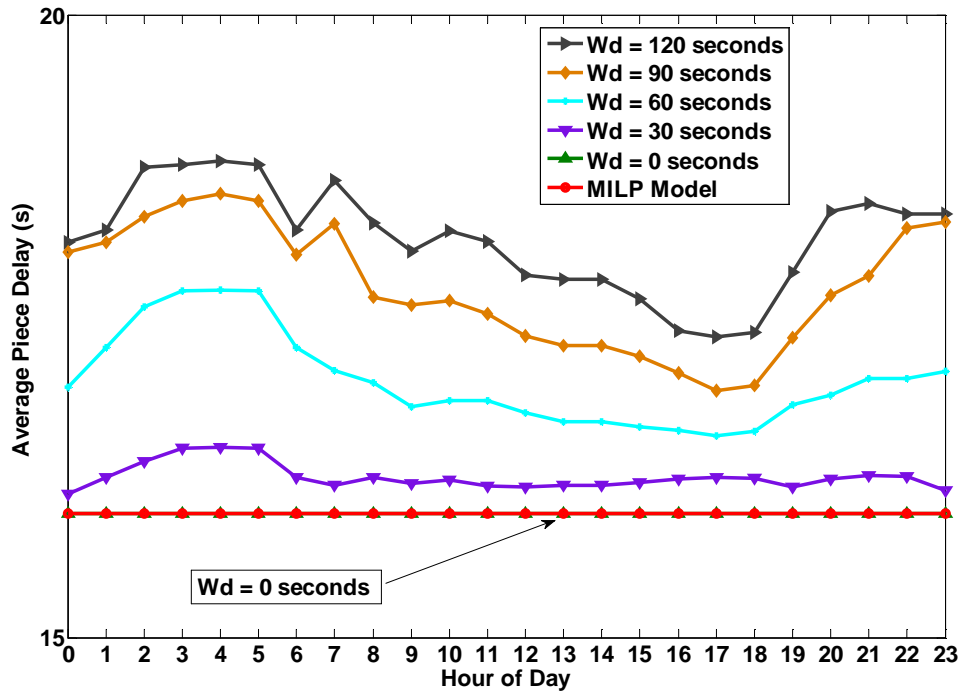


Figure 6.12: Average piece delay (Cellular-30 Mb/s BS capacity, 3 Mb/s/user & 800 m BS range)

The average content delay for the VCDA with varying W_d and the MILP model is shown in Figure 6.13 under the cellular network (30 Mb/s BS capacity, 3 Mb/s/user & 800 m BS range). The content delay of the MILP model is constant throughout the day which is because the requests are served immediately as soon as they get generated. The average content delay while operating under the VCDA increases with an increase in W_d . The average content delay experienced by vehicles, if they wait 30 seconds, is very close to the one with no waiting; however, considerable amount of power is saved in the former scenario. Moreover, when the waiting time increases, the average content delay increases as well. Similar to Figure 6.11 (in the case of Wi-Fi), there is a significant difference between the average content delay obtained through

computation (MILP model) and the VCDA with $W_d = 0$ under the cellular network. This is because the average content delay in the case of VCDA with $W_d = 0$ is evaluated for each specific content individually rather than any 33 pieces making a content, which is carried out in the case of MILP model.

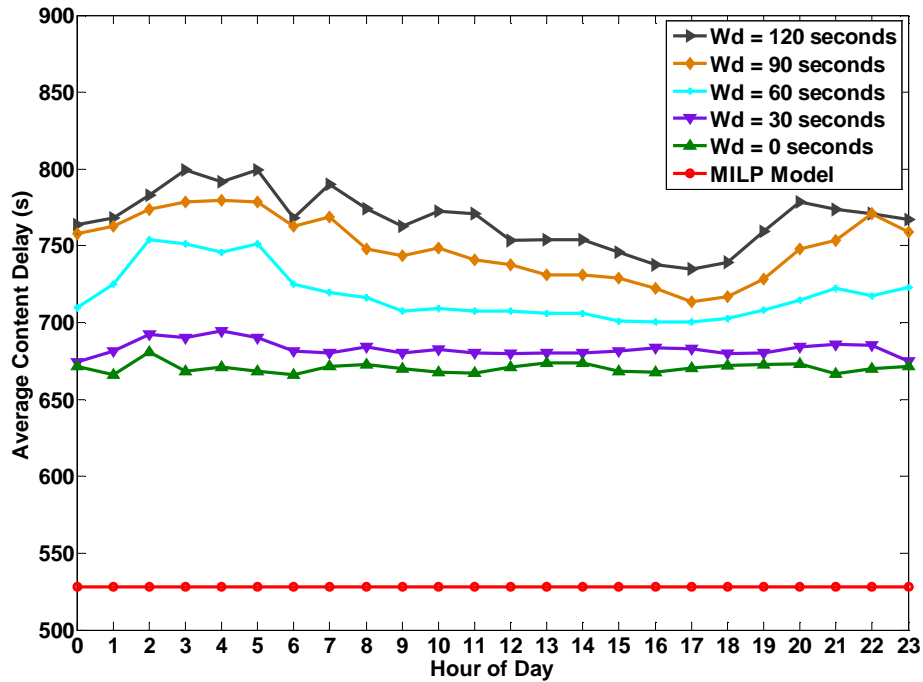


Figure 6.13: Average content delay (Cellular-30 Mb/s BS capacity, 3 Mb/s/user & 800 m BS range)

6.5 Summary

In this chapter, the impact of vehicles' mobility on the performance of the Wi-Fi CDN and cellular network has been studied. To perform such analysis, the VCDA has been proposed where each vehicle is served in real space and time instead of spatially static aggregation TPs (which nonetheless exhibit temporal variation) that was presented in Chapter 5. An important performance parameter, waiting time, was introduced where vehicles waited for a maximum

amount of time if no active CP/BS was within their vicinity before requesting the activation of a new CP/BS.

The results of the VCDA revealed that power savings comparable with the ones obtained through the MILP model could be achieved with acceptable performance degradation in terms of average piece and content delay. The results also showed that by employing power management mechanisms on CPs under the VCDA, power savings of up to 5x were achieved during the early hours of the day, whereas power savings of up to 1.3x were achieved on average throughout the entire day as shown in Figure 6.2.

Moreover, the results of the cellular network showed that the VCDA outperformed the MILP model under highly dense environments due to the shorter transmission range and the lower data rate per user. Finally, increasing the BS capacity from 30 Mb/s to 70 Mb/s has achieved power saving of up to 1.2x during peak hours, and up to 1.1x on average throughout the entire day as shown in Figure 6.5, which allowed serving a large number of users simultaneously, hence reducing the number of active BSs.

7 Sleep Enabled Wi-Fi Caching

Points in a City Content

Distribution Network

7.1 Introduction

The performance of an energy efficient vehicular communication network heavily relies on the vehicular profile and the communication infrastructure associated with it. In a V2R communication network, vehicles communicate with RSUs, which can be used as CPs for offloading multimedia content such as videos. Such an infrastructure is known as CDN. Maintaining the required levels of QoS while keeping the energy consumption low is essential in CDN. For example, in Chapter 5, energy savings of up to two times have been achieved by optimising the number and locations of Wi-Fi enabled CPs in a city CDN compared to a traditional cellular network. A further reduction of energy consumption may be possible with the introduction of sleep cycles at each CP, where the CP switches to sleep mode during its inactivity period. Therefore, it is important to analyse the system for maximising energy savings through sleep cycles at each CP, whose location is already optimised and study the effect on

QoS for content distribution. In Chapter 5, hourly analysis has been done with steady state parameters. For example, a CP is either switched ON or OFF in an hour and it remains in that state for the entire hour. In practice, there could be some instances within an hour, where a CP has no request to serve. By switching OFF its transmitting circuitry while inactive, a further reduction of energy consumption is possible. This is performed at the cost of degraded QoS. Therefore it is worthwhile to study the trade-off between QoS and energy savings through transient analysis of the system instead of day wise or hourly steady state analysis. The introduction of random sleep cycles at the CPs redefines its performance in terms of QoS and energy savings, hence the focus of this chapter.

In this chapter, the performance analysis of the CDN is carried out from a CP's perspective instead of the users (vehicles/traffic points) perspective as was the case in the previous chapters. Traffic gets bifurcated to a secondary CP, when primary CP reaches its maximum capacity of 10 connections. Thus, both primary and secondary CP were considered for the analysis, where applicable. The scheme is analysed with vacation queuing model and an event driven simulator. The QoS parameters considered for evaluations are average piece delay, sleep count, average content delay and energy savings.

7.2 The Studied Scenario

The studied scenario consists of a centralised city vehicular communication system, shown in Figure 5.1 (Chapter 5), where communication between vehicles and a CP is enabled through a wireless link utilising 802.11p [64]. Having determined the optimum number and locations of CPs for a content distribution scheme in such an environment (in Chapter 5), the analysis has been carried out for each CP separately. For analysis, a highly loaded CP (primary) with multiple random sleep cycles is considered first as shown in Figure 7.1. Later the secondary CP which handles the bifurcated (over flown) traffic from primary CP is also analysed. Let us consider the primary CP now. The generated requests (for individual piece of content) by vehicles arrive at the input buffer of the CP in order to be served (i.e. accessed and downloaded by the vehicle). When the CP is idle (i.e. its buffer is empty) it switches to sleep mode for a random amount of time with a certain mean duration in order to save transmission energy. Upon return from sleep, if there are requests waiting in the buffer to be served, the CP starts to serve them, otherwise, the CP switches to sleep mode again. This process is called sleep cycle. The transient behaviour of the CP is analysed by studying the performance within an hour instead of the steady state analysis undertaken in the previous chapters.

The data rate per user is assumed to be 3 Mb/s [179], and the transmitter power consumption of a CP is determined as $P_{MAX} - P_{MIN} = 7.8 W$ [31]. Moreover, the CP can serve at data rates between 3 Mb/s and 30 Mb/s

depending on the number of users (vehicles) connecting to it simultaneously, where it can handle up to a maximum of 10 simultaneous connections. The mean inter arrival time of piece requests is considered as 16 seconds (from Chapter 5) and is negative exponentially distributed. This number was chosen due to the fact that each content is divided into 33 pieces of 6 MB of size, where each piece takes 16 seconds to download at a rate of 3 Mb/s. Since it is assumed that the CP provides coverage of 200 meters (diameter), and the maximum speed of vehicle in a typical city is 13 m/s, a vehicle stays in the range of a CP for approximately 16 seconds. Hence, the vehicle can download a piece of 6 MB size while in the range of a CP. All system parameters are summarised in Table 5.1 (in Chapter 5). Since the main interest lies in finding the analytical bounds of QoS and energy savings, an idealistic MAC protocol between the vehicles and the CP is assumed in this work where transmission occurs without any contention or collision. The impact of handoffs is expected to be low and is not considered. This is because the content file is divided into smaller pieces in such a way, that, typical vehicular mobility and download rates result in vehicles being within the range of a CP until a piece is completely downloaded. This can be achieved even when vehicles travel at the maximum legal speed in the city.

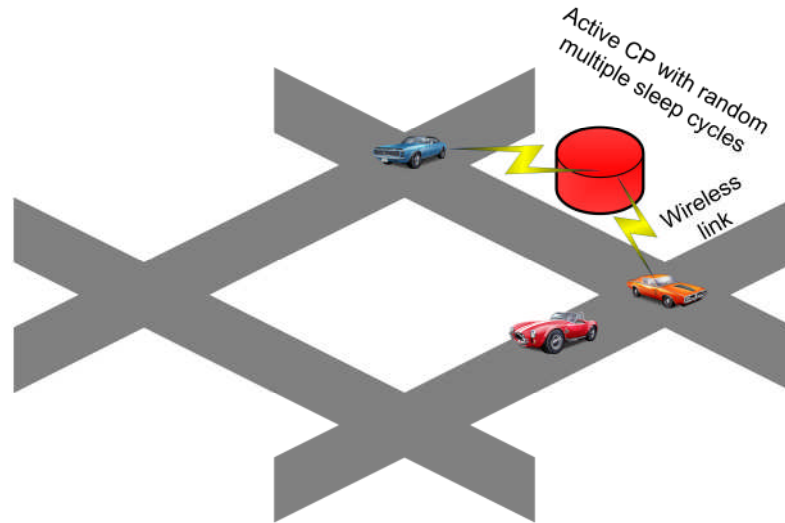


Figure 7.1: The studied scenario

7.3 Analytical Modelling of CP with Multiple Random Sleep Cycles

The CP transmitter can effectively be treated as a server which has a variable aggregated data rate. The aggregated data rate varies transiently depending upon number of requests (users) that are processed in parallel. Since a deterministic piece size is considered, the service duration can be represented as det-Neg distribution [189], where the data rate varies stochastically from 3 Mb/s to 30 Mb/s (corresponding to 1 to 10 simultaneous connections). Furthermore, the arrival of requests is a Poisson process with a mean arrival rate (as discussed in Chapter 5) and the CP transceiver is considered to have a large buffer. Therefore, the CP can be modelled as a $M/det-Neg/1/\infty$ ² queue. The CP, in addition, saves energy by going into sleep mode [190], (which

² The arrival of requests follows a Poisson distribution (M), the service follows a deterministic-negative distribution (det-Neg) with a single server and a large buffer.

switches OFF the transmitter) when it is inactive for a randomly distributed time duration. When the duration elapses, the CP returns from the sleep mode and checks if there is any request in the buffer waiting to be processed. If a request has arrived, it starts serving the request or else it switches to sleep mode again as before. This process is called sleep cycle. Therefore, the CP with sleep cycles can be modelled as a M/det-Neg/1/ ∞ queue which takes queue length dependent vacations. Two events can represent the sleep process: a) the time epoch where the CP becomes inactive when there is no request to be served and b) The duration of sleep through which the CP will be inactive. The former relies on the stochastic property of the system i.e. arrival and service of the requests, and the hardware. Hence, it is not controllable. However, the latter is exponentially distributed with mean value and can be controlled. Each sleep cycle is associated with a wake-up overhead (E_{wo}). This accounts for circuitry initialisation, synchronisation etc. The key parameters are also shown in Table 7.1.

Variable	Notation	Value
Piece Size	$Piece_Size$	6 MByte
Content Size	$Content_Size$	200 MByte
Data Rate	d_i	3,6,9,12,15,18,21,24,27, and 30 Mb/s
Transmit Power of CP	P_{ct}	7.86 W [31]
Energy for wake-up overhead	E_{wo}	0.0175 J [31]

Table 7.1: System parameters

The service duration of the CP is det-Neg distributed with mean, $\bar{X} = \mu^{-1}$ and variance $Var(X)$. Further, the sleep cycles are negative exponential distributed

with mean \bar{S} . The CP is assumed to have infinite buffer. The service durations and sleep cycle times are independent and identically distributed (iid) random variables which are also independent of each other.

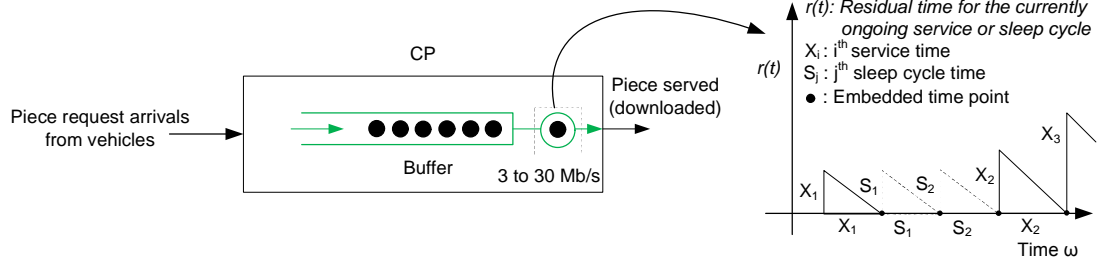


Figure 7.2: M/det-Neg/1/∞ queues with sleep cycles to represent CP operation

The queuing model is solved with residual life approach as illustrated in Figure 7.2.

Let $r(\omega)$ be the residual time for the ongoing service or sleep.

Time average of $r(\omega)$, ($0 \leq \omega \leq t$)

$$\bar{R} = \frac{1}{t} \int_0^t r(\omega) d\omega = \frac{1}{t} \sum_{i=1}^{N_\lambda(t)} \frac{1}{2} X_i^2 + \frac{1}{t} \sum_{j=1}^{N_s(t)} \frac{1}{2} S_j^2 \quad (7.1)$$

where $N_\lambda(t)$ is the number of piece requests that arrive within $(0, t)$, and ω is the instantaneous time.

$N_s(t)$ is the number of sleep cycles (sleep count) within $(0, t)$.

Therefore,

$$\begin{aligned}
 \bar{R} &= \lim_{t \rightarrow \infty} \left[\frac{1}{t} \sum_{i=1}^{N_\lambda(t)} \frac{1}{2} X_i^2 + \frac{1}{t} \sum_{j=1}^{N_s(t)} \frac{1}{2} S_j^2 \right] \\
 &= \lim_{t \rightarrow \infty} \left[\frac{N_\lambda(t)}{t} \frac{\sum_{i=1}^{N_\lambda(t)} \frac{1}{2} X_i^2}{N_\lambda(t)} \right] + \lim_{t \rightarrow \infty} \left[\frac{N_s(t)}{t} \frac{\sum_{j=1}^{N_s(t)} \frac{1}{2} S_j^2}{N_s(t)} \right] \\
 &= \frac{1}{2} \lambda \bar{X}^2 + \frac{1}{2} \lim_{t \rightarrow \infty} \frac{1}{\frac{t(1-\rho)}{N_s(t)}} \bar{S}^2 (1-\rho) \\
 &= \frac{1}{2} \lambda \bar{X}^2 + \frac{1}{2} (1-\rho) \frac{\bar{S}^2}{\bar{S}}
 \end{aligned} \tag{7.2}$$

where the offered load ρ , is defined as

$$\rho = \lambda \bar{X} = U_s \quad \text{[System utilisation]} \tag{7.3}$$

Since

$$\frac{t(1-\rho)}{N_s(t)} = \bar{S} \tag{7.4}$$

The average waiting time for a piece at the CP can be computed using Little's theorem as

$$\begin{aligned}
 W_q &= N_q \bar{X} + \bar{R} \\
 &= \lambda W_q \bar{X} + \bar{R}
 \end{aligned}$$

where N_q represents the number of piece requests waiting in the queue.

Therefore,

$$W_q = \frac{\bar{R}}{(1 - \rho)} \quad (7.5)$$

Since $\rho = \lambda \bar{X}$

Using Equation (7.2) and Equation (7.3) give

$$W_q = \frac{\lambda \bar{X}^2}{2(1 - \rho)} + \frac{\bar{S}^2}{2\bar{S}} \quad (7.6)$$

The average delay of a piece (W) including the waiting delay (W_q) and the service time (\bar{X}) can be computed as

$$\begin{aligned} W &= W_q + \bar{X} \\ &= \bar{X} + \frac{\lambda \bar{X}^2}{2(1 - \rho)} + \frac{\bar{S}^2}{2\bar{S}} \end{aligned} \quad (7.7)$$

The average number of pieces in the system (N_{sys}) from Little's theorem can be written as

$$\begin{aligned} N_{sys} &= \lambda W \\ &= \lambda \bar{X} + \frac{\lambda^2 \bar{X}^2}{2(1 - \rho)} + \frac{\lambda \bar{S}^2}{2\bar{S}} \end{aligned} \quad (7.8)$$

The energy savings (E_s) per hour through sleep cycles for the CP can be expressed as

$$\begin{aligned}
 E_s &= (1 - U_s) \times P_{ct} \times 3600 - (E_{wo} \times N_s) \\
 &= (1 - \rho) \times P_{ct} \times 3600 - (E_{wo} \times N_s) \\
 &= N_s \bar{S} \times P_{ct} - (E_{wo} \times N_s) \\
 &= N_s (\bar{S} P_{ct} - E_{wo})
 \end{aligned} \tag{7.9}$$

where,

U_s is the system utilisation.

P_{ct} is the CP's transmitter circuitry power consumption.

E_{wo} is the CP's wake-up overhead.

The number of sleep cycles (N_s) can be computed from Equation (7.4) as

$$\lim_{t \rightarrow \infty} \frac{N_s(t)}{t} = N_s = \frac{(1 - \rho)}{\bar{S}} \tag{7.10}$$

The average content delay (\bar{D}) can be computed as

$$\bar{D} = \frac{E(Content_Size)}{Piece_Size} \cdot W \tag{7.11}$$

where $Content_Size$ is exponentially distributed with mean (see Table 7.1):

$$\bar{C} = E(Content_Size) \tag{7.12}$$

For det-Neg distribution of service time (considering fixed piece size and generally distributed data rate), the probability density function (pdf) can be expressed as

$$\begin{aligned} x(t) &= p\delta\left(t - \frac{1}{\mu}\right) + (1 - p)\mu e^{-\mu t} \\ &= p\delta(t - \bar{X}) + (1 - p)\frac{1}{\bar{X}}e^{-\frac{t}{\bar{X}}} \end{aligned} \quad (7.13)$$

where,

$$\mu = \frac{1}{\bar{X}} \quad (7.14)$$

and δ is the Dirac-delta function and ($0 \leq p \leq 1$), p is the parameter which determines the degree of superposition of deterministic and negative exponential pdf.

$$\begin{aligned} E(x(t)) &= p\bar{X} + (1 - p).\bar{X} \\ &= \bar{X} = \frac{1}{\mu} \end{aligned} \quad (7.15)$$

$$\begin{aligned} Var(x(t)) &= p.0 + (1 - p).\bar{X}^2 \\ &= (1 - p)\bar{X}^2 \\ &= \frac{1 - p}{\mu^2} \end{aligned} \quad (7.16)$$

$$\begin{aligned}
 Var(X) &= E(X - \bar{X})^2 \\
 &= E(X^2) - [E(x)]^2 \\
 &= \overline{X^2} - \bar{X}^2
 \end{aligned} \tag{7.17}$$

Therefore,

$$\begin{aligned}
 \overline{X^2} &= Var(X) + \bar{X}^2 \\
 &= (1 - p)\bar{X}^2 + \bar{X}^2 \\
 &= (2 - p)\bar{X}^2
 \end{aligned} \tag{7.18}$$

Note that \bar{X} and $E(X)$ are identical because this is an Ergodic stochastic process.

$$\overline{S^2} = Var(S) + \bar{S}^2 = 2\bar{S}^2 \tag{7.19}$$

Simplifying Equation (7.7) yields

$$\begin{aligned}
 W &= \bar{X} + \frac{\lambda(2 - p)\bar{X}^2}{2(1 - \rho)} + \frac{2\bar{S}^2}{2\bar{S}} \\
 &= \bar{X} + \frac{\lambda(2 - p)\bar{X}^2}{2(1 - \rho)} + \bar{S}
 \end{aligned} \tag{7.20}$$

Simplifying Equation (7.8) yields

$$N_{sys} = \lambda\bar{X} + \frac{\lambda^2(2 - p)\bar{X}^2}{2(1 - \rho)} + \frac{\lambda \cdot 2\bar{S}^2}{2\bar{S}}$$

$$= \lambda \bar{X} + \frac{\lambda^2(2-p)\bar{X}^2}{2(1-p)} + \lambda \bar{S} \quad (7.21)$$

Since the developed queuing model is Ergodic, the service time parameters can be computed as below.

$$\text{Service time } (\bar{X}) = E[X_1, X_2, \dots, X_n]$$

where,

$$X_i]^{n} = \frac{\text{Piece_Size}}{d_i} \quad (7.22)$$

where d_i are the data rates (see Table 7.1)

Therefore,

$$\bar{X} = \frac{\text{Piece_Size}}{\text{Mean}(d_i)} = \text{Mean}\left(\frac{\text{Piece_Size}}{d_i}\right) \quad (7.23)$$

$$\text{Var}(X) = \text{Var}\left(\frac{\text{Piece_Size}}{d_i}\right)$$

$$(1-p) = \frac{\text{Var}(X)}{\bar{X}^2}$$

Therefore,

$$p = 1 - \frac{\text{Var}(X)}{\bar{X}^2} \quad (7.24)$$

7.4 Performance Evaluation

The performance of the system has been evaluated in terms of E_s , W , and \bar{D} with respect to different hours of the day reflecting varying vehicular density shown in Figure 5.2 in Chapter 5. Moreover, the performance has been evaluated with different sleep cycle durations (100 ms, 1 s). Both analytical and simulation results are found to be in good agreement. Note that the buffer size is set to a very large number. The system parameters are given in Table 7.1.

7.4.1 Energy savings

Figure 7.3 illustrates the energy savings achieved by both CPs throughout the entire day by operating multiple random sleep cycles with different mean duration. The figure shows that the energy savings achieved at the early hours of the day is higher than that achieved at later hours of the day. This is due to the low vehicular load at the early hours that leads to lower number of generated requests. This allows the CP to switch into sleep mode more often (i.e. longer total sleep duration) and hence the higher energy savings. For example, the energy savings achieved by the primary CP at 03:00 hr is 23 kJ compared to the 4 kJ achieved at 17:00 hr. Moreover, the figure also shows that the secondary CP achieves higher energy savings as compared to the primary CP. This is because the load on the primary CP is much higher than that on the secondary CP (please see Figure 7.5) where only the extra load is bifurcated to the secondary CP. The secondary CP was switched ON only after the primary

CP was fully utilised, i.e. after 07:00 hr, as demonstrated by the MILP model results presented in Chapter 5. Note that before 08:00 hr, the secondary CP was achieving maximum energy savings because it was sleeping for almost the entire duration (between 00:00 hr and 07:00 hr), where the primary CP was able to handle all the traffic generated during that period. The energy savings achieved by the secondary CP between 00:00 hr and 07:00 hr is approximately 28 kJ compared to the 11 kJ achieved at 17:00 hr. The figure also demonstrates that the sleep cycle duration has insignificant effect on the results of both CPs. This is mainly because the piece size (i.e. 6 MB) and the service time (i.e. 16 seconds) are relatively large. Hence, the CPs spend significant amount of time serving each request. Furthermore, the time between the arrivals of consecutive requests is high in which the CP can take multiple vacations before the arrival of the next request. Therefore, the total sleep duration throughout the entire hour is the same. Note that the waking up overhead is very small so that the effect of the sleep cycle duration on the energy savings is negligible.

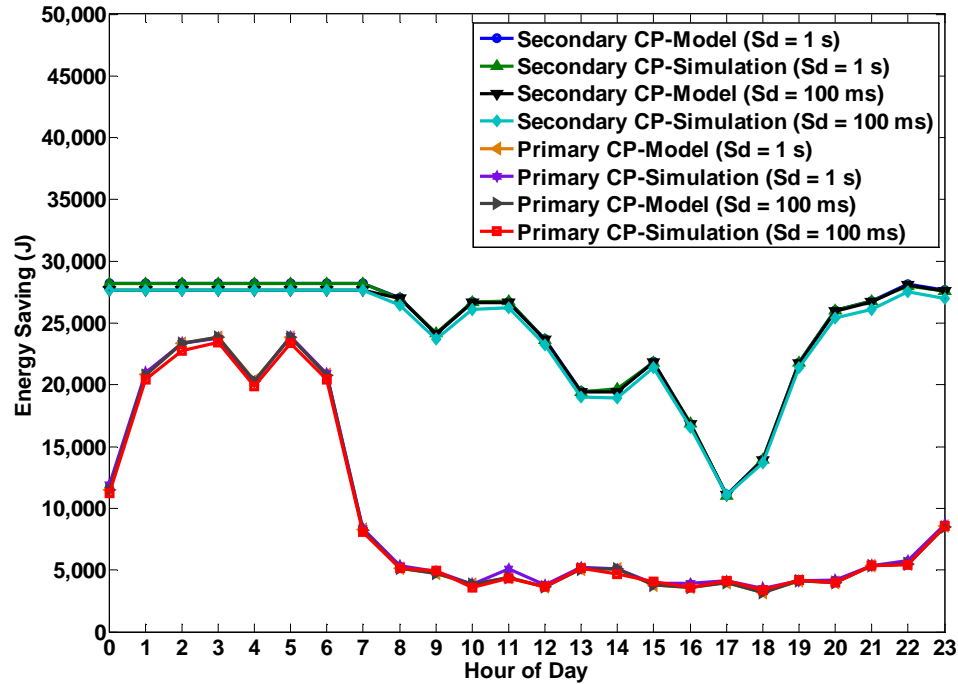


Figure 7.3: Energy savings

7.4.2 Average piece delay

Figure 7.4 shows the average piece delay experienced by the primary and secondary CP throughout the entire day with different sleep cycle durations employed. In traditional access networks, packet size can be fixed/variable but the data rate is fixed. However, in our study, pieces with fixed size are served with a variable data rate. This is because the performance of the system is evaluated from the CP's perspective, where a CP can serve up to 10 simultaneous connections. Hence, at a data rate of 3 Mb/s/user, the CP can serve at data rates that vary between 3 Mb/s and 30 Mb/s depending on the number of simultaneous connections. Therefore, the average piece delay does not follow the trend of the load (Figure 7.5) as is the case with traditional networks that operate at a fixed data rate as shown in Figure 7.4. At 08:00 hr,

the number of connections (i.e. load) increases, therefore, the secondary CP is activated as suggested by the MILP model (presented in Chapter 5). shown in Figure 7.5. Since the number of simultaneous connections (hence the operating data rate) and the queue size affect the average piece delay, the irregularities in delay response were observed. The corresponding pdf of the number of simultaneous connections and queue size for the primary CP and secondary CP are shown in Figure 7.6 and Figure 7.7, respectively, which depict irregular pattern throughout. Moreover, these indicate that during the 13:00 hr, the secondary CP is being consistently utilised. This is because the maximum number of simultaneous connections (i.e. 10) was achieved at the primary CP (Figure 7.6), validating the findings of the MILP model presented in Chapter 5. Note that similar analysis has been carried out at different hours of the day, and similar trends were observed.

7.4 Performance Evaluation

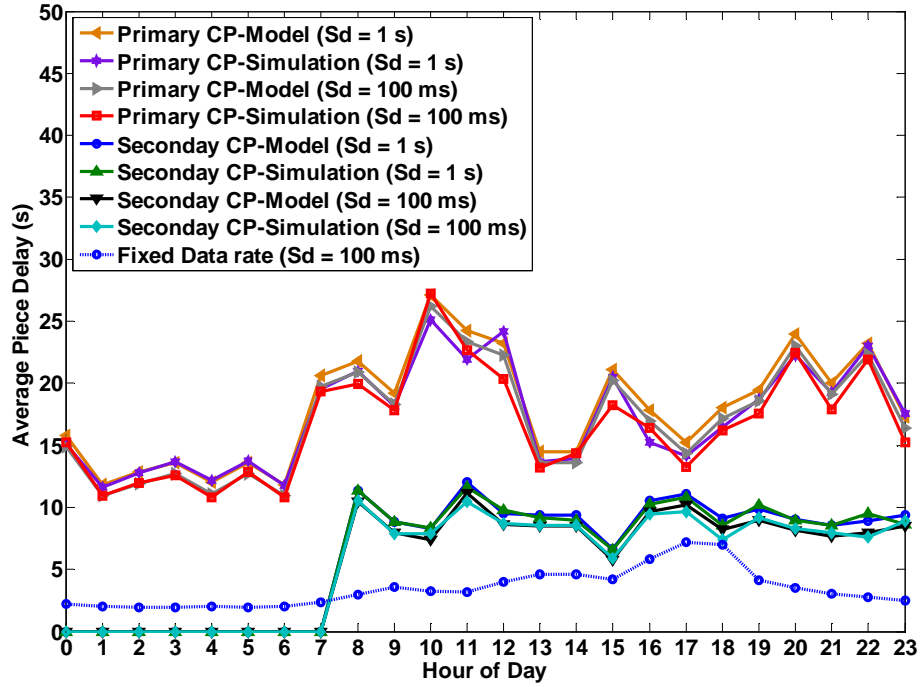


Figure 7.4 Average piece delay

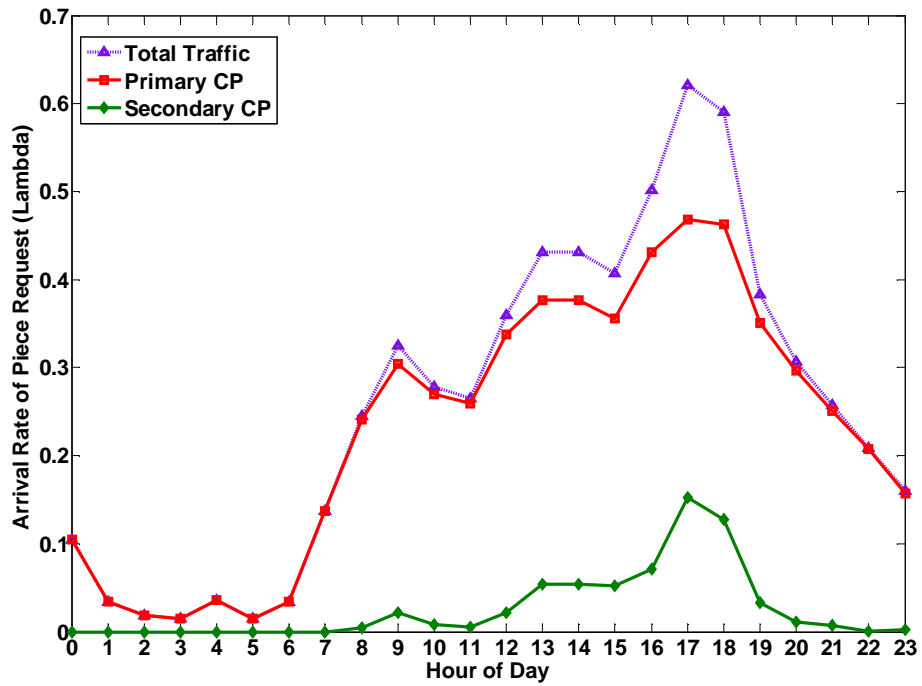


Figure 7.5: Load on CPs

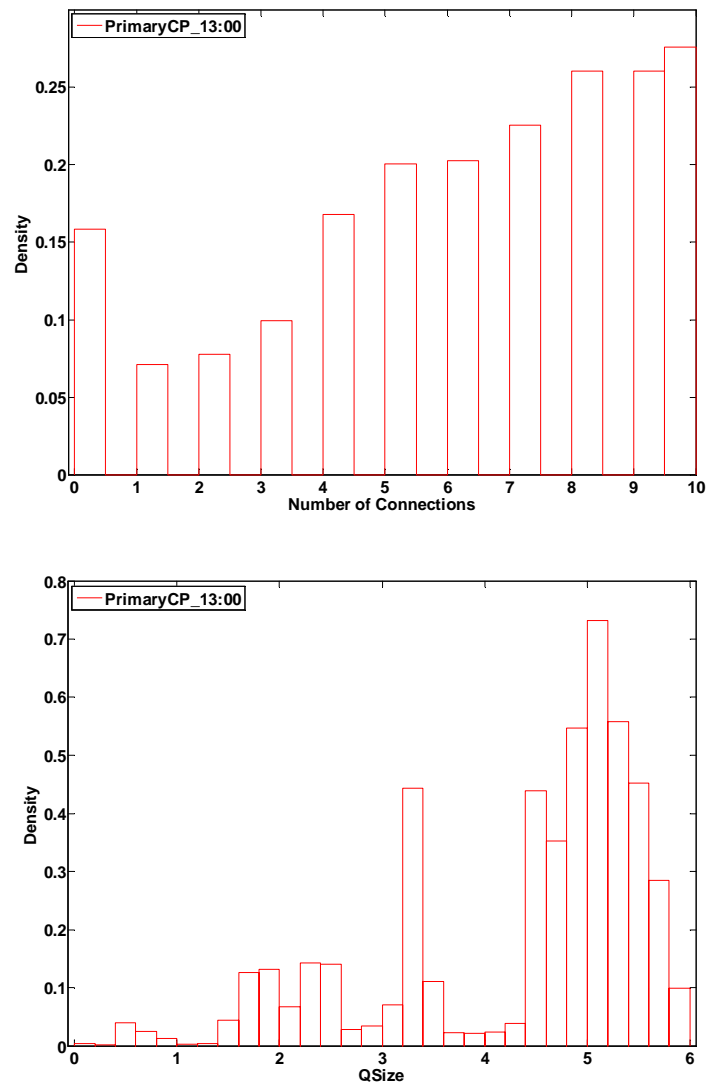


Figure 7.6: Number of simultaneous connections and queue size pdf (primary CP)

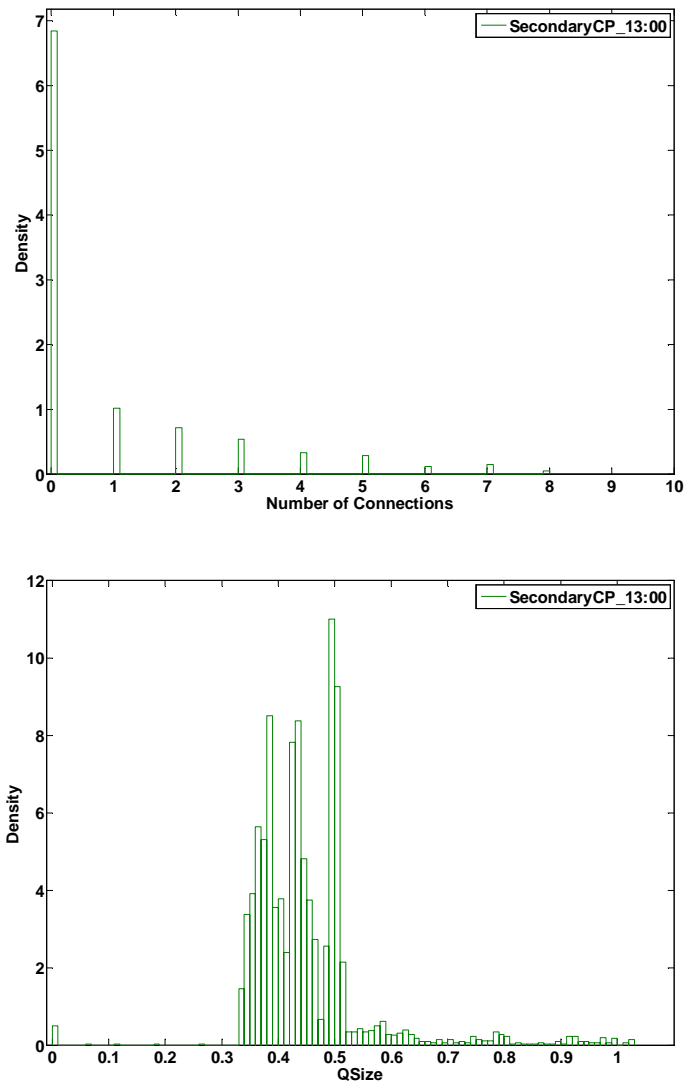


Figure 7.7: Number of simultaneous connections and queue size pdf (secondary CP)

7.4.3 Average content delay

To analyse content delay, it is simplistically assumed that a vehicle traverses through in such a way that it is served by similarly loaded CPs in its path (which is not an accurate mobility pattern).

Figure 7.8 shows the average content delay experienced by both CPs at each hour of the day. The figure shows the average content delay has a similar behaviour as that of the average piece delay. This is because a content consists of 33 pieces, where the average content delay is computed as the sum of the average piece delay of 33 pieces. Moreover, since the average content delay depends on the average piece delay and the latter is governed by the queue size and the number of simultaneous connections, the irregularities in the average content delay is observed as well.

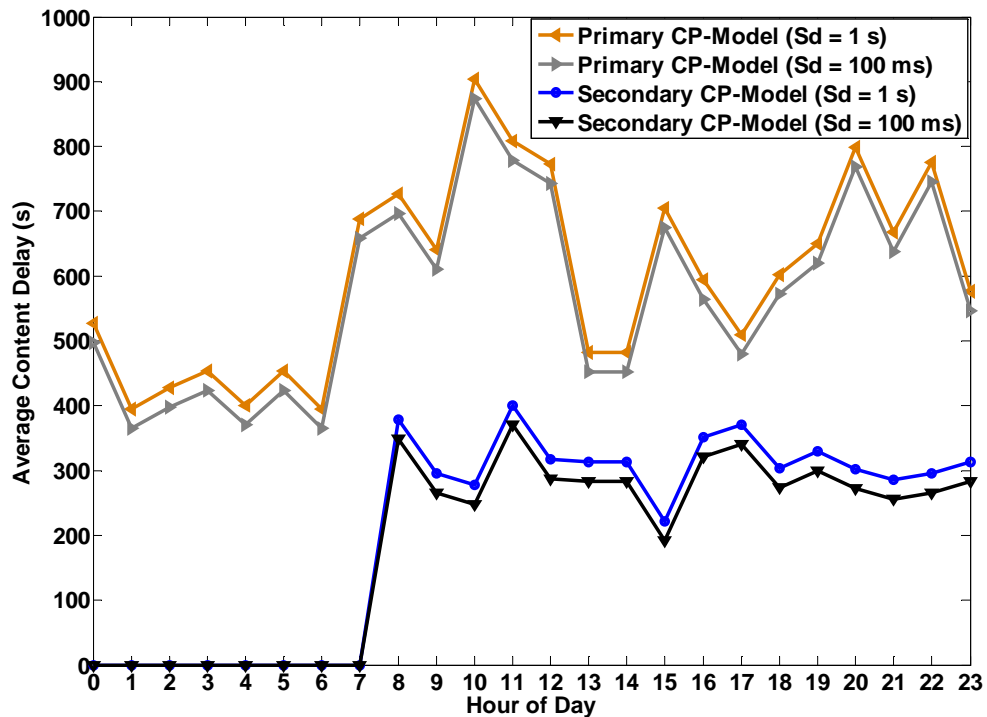


Figure 7.8: Average content delay

7.5 Summary

Building on the steady state MILP analysis in Chapter 5, a transient (sleep, queuing) performance analysis of the CDN is carried out in this chapter

addressing each CP with its traffic load, instead of the users (vehicles/traffic points) perspective. Traffic load is bifurcated to a secondary CP (switched on), when the primary CP reaches its maximum capacity of 10 connections. Thus, both primary CP and secondary CP were considered for the analysis, where applicable. In order to save energy while maintaining QoS, random sleep cycles are introduced at each CP, where the CP switches to sleep mode during its inactivity period. The CP with sleep cycles was modelled as a $M/det-Neg/1/\infty$ queue which takes queue length dependent vacations.

The results revealed that up to 84% energy savings were achieved during the early hours of the day (i.e. low traffic volumes), and up to 33% energy savings were achieved on average throughout the entire day. Moreover, the secondary CP has achieved higher energy savings during its operating span compared to that achieved by the primary CP. This is because the load on the primary CP was much higher than that on the secondary CP, where only the extra load was bifurcated to the secondary CP. Furthermore, the results revealed that the mean sleep cycle duration has insignificant effect on the energy savings of both CPs. This is due to the large piece size (i.e. 6 MB), long service time (i.e. 16 seconds) and low wake-up overhead.

Interestingly, it is revealed that the average piece delay and average content delay do not follow the trend of the load which is usual for fixed data rate operation. This occurs because of the variable data rate (due to variation in number of simultaneous connections), queue size and the number of

7.5 Summary

simultaneous connections. The analytical results were validated by simulations and both are found to be in good agreement.

8 Conclusions and Future Work

8.1 Conclusions and Key Findings

This thesis is concerned with the characterisation and design of routing protocols for a vehicle-to-vehicle (V2V) communication system and a hybrid communication system in a city vehicular network. It also evaluates the performance of these protocols from both quality of service (QoS) and energy perspectives. Moreover, it studies the feasibility of having a power efficient content distribution network (CDN) by optimising the number and locations of caching points (CPs) in this environment.

Firstly, a city vehicular mobility simulator was developed, which utilises some key parameters such as vehicular flow and variable speeds of vehicles in a typical city. The simulator is based on a 3x3 km² Manhattan grid, with 48 roads and 16 junctions, representing a road network topology in this environment. The development of the simulator was an important step to evaluate the communication protocols developed in this thesis.

A vehicular ad hoc network (VANET) utilising a flooding based routing protocol, namely multihop (MH) routing, was developed and integrated into the city vehicular mobility simulator as a communication layer to facilitate delay tolerant

communication in a city environment. The simulation implementation of the VANET and the MH routing protocol was detailed. The performance of the system was analysed in terms of average end-to-end (E2E) delay, packet dropping probability (PDP), and the total number of transmissions in the network for varying vehicular loads and different buffer sizes. The simulation results reveal that the MH routing protocol achieved lower E2E delay; however, due to its flooding nature, the PDP and the number of transmissions in the network were unacceptable.

In order to reduce flooding, two position-based routing protocols, namely position based with most forward within radius (PRMFR) and position based with nearest forward progress (PRNFP) were developed, and their simulation implementations were also presented. The performance of the two routing protocols was analysed in terms of the QoS parameters mentioned above, and compared with MH routing. The results reveal that PRMFR and PRNFP outperformed the MH routing protocol, especially in terms of PDP and the total number of transmissions in the network. The two position based routing protocols generated approximately 70% less packets than the MH routing protocol, while the PDP was reduced by 53% compared to MH routing.

Moreover, the impact of greedy nodes (GNs) on the routing protocols was studied. It was observed that the impact of GNs was considerably significant on the MH protocol compared to the other (PRMFR and PRNFP protocols). The

results also revealed that the PDP improved significantly by utilising a larger buffer for vehicles.

To extend the work, a pure V2R communication system was developed utilising nine basestations (BSs) to provide ubiquitous coverage over the entire city area. The performance of the system was evaluated in terms of QoS parameters including average E2E delay, packet loss ratio (PLR), total number of transmissions, and energy consumption. The simulation results revealed that the V2R communication system achieved enhanced QoS due to the ubiquitous coverage offered by this system; however, it was achieved at the expense of very high energy consumption.

In order to save energy, five of the nine fully functioning BSs were switched into sleep mode and the impact on QoS was studied. Although significant energy was saved by the new setup, the QoS deteriorated considerably due to the low connectivity achieved under the V2R communication system with only four BSs. To restore the performance, an ad-hoc setup comprising MH and store-carry and forward (SCF) routing protocol was introduced to cooperate with the four BSs, forming a hybrid communication system. The performance of the two routing protocols from both QoS and energy perspectives was evaluated and compared with the V2R communication systems. The results reveal that the MH and SCF routing protocols enhanced the performance of the V2R system with four BSs in terms of average E2E delay and PLR. However, due to the flooding nature of MH routing and the fact that vehicles under SCF and MH protocols

spend a significant amount of time listening to the channel, the total network energy consumption was significantly high. Hence, a cluster-based routing protocol was developed, namely single cluster-head (SCH), in which the maximum number of vehicles possible were put into sleep mode, only allowing cluster-heads (CHs) to perform out of range communications. The results indicate that a considerable amount of energy was saved, while acceptable levels of QoS were maintained.

Another cluster-based routing protocol was introduced, namely double cluster-head (DCH), to improve the QoS performance of the SCH while keeping energy consumption low. The communication scenarios were described, along with the routing protocols, their simulation implementations, and analyses of the physical propagation and energy models. The performance of the abovementioned systems was evaluated and compared for varying vehicular loads. The results show that the SCH and DCH routing protocols saved up to two times the total network energy compared to the pure V2R communication system with nine BSs, and up to nine times compared to the MH and SCF routing protocols with four BSs, while maintaining an acceptable level of QoS. The higher network energy consumed under the MH and SCF protocols is mainly due to listening and transmitting, and receiving energies by vehicles. Under the SCH and DCH protocols, the PLR can be further reduced by slightly increasing the V2V range.

The feasibility of a Wi-Fi-based power efficient CDN was studied and compared with a traditional cellular network in a city vehicular environment. A mixed

integer linear programming (MILP) model was developed and used to optimise the number of caching points (CPs)/BSs and their locations, with the objective of minimising the total power consumption of both networks. To solve the mobility problem which leads to dynamic topology change, a set of traffic points (TPs) was assumed and used to represent traffic centroids which account for the content; data traffic requested by nearby vehicles. A bespoke simulator was developed to generate traffic at each hour of the day, incorporating real city vehicular traffic profiles (from the city of Saskatoon). Furthermore, based on the insights obtained through the MILP model results, a heuristic was developed to mimic the behaviour of the MILP model and comparable power savings were achieved, which also verified the accuracy of the current approach and provided a simple algorithm for practical operation. Both networks were described, along with their models and heuristics implementations.

The performance of the systems in terms of total network power consumption and the number of active CPs/BSs was evaluated for each hour of the day. The results computed by the MILP model revealed that the Wi-Fi CDN achieved considerable power savings over the cellular network, where the latter consumed up to 6 times higher power than the former at the early hours of the day, and up to 1.5 times at peak hours. The results also showed that the hourly vehicular flow and traffic demand had a significant effect on power consumption, since higher content demand means higher power consumption due to the larger number of vehicular nodes and larger number of active

BSs/CPs. The significant power savings achieved by the Wi-Fi network over the cellular network was mainly due to the lower operational power consumption of a CP (47 W) compared to a cellular BS (500 W). This justified the fact that, even with a higher number of CPs, the cellular network consumed significantly higher power.

The work on the power efficient CDN was further extended by developing the vehicular content download algorithm (VCDA). Since static TPs (but with varying traffic volume) were used in both the MILP model and the heuristic to facilitate mathematical tractability, there was a need to study the impact of real vehicular mobility on the performance. Therefore, the VCDA was developed whereby each vehicle is served in real space and time instead of spatially static aggregation TPs (which nonetheless exhibit temporal variation). An important evaluation factor, waiting time, was introduced where vehicles waited for a maximum amount of time if no active CP/BS was within their vicinity before requesting the activation of a new CP/BS. In addition to the total network power consumption and the number of active CPs/BSs, key QoS parameters, average piece delay and average content delay, were determined for both networks.

The impact of different power management schemes on total network power consumption was studied for the Wi-Fi CDN under the VCDA. Furthermore, the performance of the cellular network was evaluated under two different scenarios: a highly dense environment and a lightly dense environment. The former scenario utilised a data rate of 1 Mb/s/user and a BS coverage of 500 m,

whereas the latter utilised a data rate of 3 Mb/s/user and a BS coverage of up to 800 m. The impact of varying the portion of the total BS capacity allocated for vehicular applications on the total network power consumption of the cellular network (lightly dense scenario) was also investigated.

The results of the VCDA revealed that power savings comparable with those achieved by the model can be attained with acceptable performance degradation in terms of average piece and content delay. The results also suggested that if vehicles waited for a maximum of 60 seconds before being served while operating under the Wi-Fi network, comparable power consumption with the model was achieved with an average piece delay of 25 seconds. On the other hand, if vehicles waited for 90 seconds while operating under the cellular network, the power consumption was very close to the one obtained through the MILP model with an acceptable average piece delay of 17 seconds.

The results also emphasised that by employing power management mechanisms on CPs under the VCDA, power savings of up to 5 times could be achieved during the early hours of the day and up to 1.3 times on average throughout the entire day. Moreover, the results of the cellular network showed that the VCDA outperformed the model under the highly dense environment due to the shorter transmission range and the lower data rate per user. This contributed to a decrease in power consumption (i.e. a lower number of active BS) under the VCDA, as vehicles could move freely compared to the static

virtual traffic aggregation points, TPs, taken into account in the MILP model. Finally, increasing the BS capacity from 30 Mb/s to 70 Mb/s achieved power savings of up to 1.2 times during peak hours and up to 1.1 times on average throughout the entire day, which allowed a large number of users to be served simultaneously; hence, a lower number of active BSs was required.

These results highlighted the merits of deploying such a Wi-Fi content caching and distribution network instead of a traditional cellular network in an environment where a large volume of traffic is to be served over a wide area of spatial coverage, particularly if a limited content vocabulary (such as YouTube, BBC iPlayer etc.) was to be shared among a large number of mobile users.

To achieve further energy savings, sleep cycles were introduced at the CP and an analytical queuing model for the Wi-Fi CDN was developed, where a CP takes vacations (switches to sleep mode) during its inactivity period. The CP with a wireless link to vehicles was modelled as a single server queue ($M/det-Neg/1/\infty$). The performance of the system was evaluated in terms of energy savings, average queue size, average piece delay and average content delay. The performance results of the system were verified with simulations with respect to varying vehicular load according to real vehicular traffic profiles. The performance results revealed that the system was able to fulfil traffic demand, while saving up to 84% energy during off-peak hours and 33% during the whole day in a city vehicular environment.

8.2 Future Work

The pieces of work carried out in this thesis open a number of new avenues for future research. A few of them are listed below:

1. The work presented in Chapter 3 can be improved by designing a MAC protocol along with a detailed mathematical model so the actual performance of the system could be evaluated in such a dynamic environment.
2. The contributions of Chapter 4 can further be enhanced by incorporating a detailed queuing model for the SCH and DCH routing protocols so that the CHs can be put into sleep mode during their inactivity periods. This would achieve significant power savings. Another extension of this work could be the study of different types of traffic classes in this network. This will significantly alter the performance in a way that the system is able to maintain individual QoS parameters for these traffic classes.
3. The work in Chapter 5 and Chapter 6 can be further extended by incorporating a vehicular distributed cloud system, where each vehicle has storage and wireless capabilities so that it can share or /and relay pieces/content to other vehicles. This will reduce the load on CPs and can even save energy by reducing the number of CPs in the city. However, this system can significantly benefit from a realistic MAC protocol, which also allows hand-offs between two cells. Detailed

analytical and simulation models for such a MAC protocol are needed to evaluate the performance of the system accurately.

4. The work in Chapter 4, Chapter 5, and Chapter 6 can be extended by employing renewable energy sources such as wind and solar energy for CPs and BSs. A detailed analysis of renewable energy profile can help determine the available power and attempt to match it to load through energy storage (batteries), and hence reduce the carbon footprint of the network significantly at a given power consumption level.

References

- [1] N. F. M. X. Shen and L. Cai, "Special section on vehicular communication networks," *IEEE Transactions on Vehicular Technology*, vol. 56, no. 6, pp. 3241–3243, 2007.
- [2] G. Karagiannis et al., "Vehicular networking: A survey and tutorial on requirements, architectures, challenges, standards and solutions," *IEEE Communications Surveys Tutorials*, vol. 13, no. 4, pp. 584–616, 2011.
- [3] C. Han, M. Dianati, R. Tafazolli, R. Kernchen, and X. Shen, "Analytical study of the IEEE 802.11p MAC sublayer in vehicular networks," *IEEE Transactions on Intelligent Transportation Systems*, vol. 13, no. 2, pp. 873–886, June 2012.
- [4] J. Guo and N. Balon, "Vehicular ad hoc networks and dedicated short-range communication," University of Michigan, Dearborn, USA, Tech. Rep June 2006.
- [5] H. Kawashima, "Japanese perspective of driver information systems," *Transportation*, vol. 17, no. 3, pp. 263–284, 1990.
- [6] R. Stanica, E. Chaput, and A.-L. Beylot, "Properties of the MAC layer in safety vehicular Ad Hoc networks," *IEEE Communications Magazine*, vol. 50, no. 5, pp. 192–200, May 2012.

- [7] H. Wu, "Analysis and design of vehicular networks," Department of Computer Science, Georgia Institute of Technology, PhD Thesis, December 2005.
- [8] S. McNeil, W. (A). Wallace, and T. F. Humphrey, "DEVELOPING AN INFORMATION TECHNOLOGY ORIENTED BASIC RESEARCH PROGRAM FOR SURFACE TRANSPORTATION SYSTEMS," National Science Foundation and US Department of Transportation, Chicago, Illinois, Report, 2000.
- [9] M. Sichitiu and M. Kihl, "Inter-vehicle communication systems: a survey," *IEEE Communications Surveys and Tutorials*, vol. 10, no. 2, pp. 88–105, 2008.
- [10] T.-D. Nguyen, O. Berder, and O. Sentieys, "Energy-efficient cooperative techniques for infrastructure-to-vehicle communications," *IEEE Transactions on Intelligent Transportation Systems*, vol. 12, no. 3, pp. 659–668, September 2011.
- [11] H. Zhang, Y. Ma, D. Yuan, and H.-H. Chen, "Quality-of-service driven power and sub-carrier allocation policy for vehicular communication networks," *IEEE Journal on Selected Areas in Communications*, vol. 29, no. 1, pp. 197–206, January 2011.
- [12] P. Kolios, V. Friderikos, and K. Papadaki, "Ultra lower energy store-carry and forward relaying within the cell," in *IEEE 70th Vehicular Technology Conference Fall (VTC-Fall)*, September 2009, pp. 1–5.

- [13] S.-H. Wu, C.-M. Chen, and M.-S. Chen, "An asymmetric and asynchronous energy conservation protocol for vehicular networks," *IEEE Transaction on Mobile Computing*, vol. 9, no. 1, pp. 98–111, January 2010.
- [14] F.Li and Y.Wang, "Routing in vehicular ad hoc networks: A survey," *IEEE Vehicular Technology Magazine*, vol. 2, no. 2, pp. 12-22, June 2007.
- [15] H. Idjmayyel, B.R.Qazi, and J.M.H.Elmirghani, "A geographic based routing scheme for VANETs," in *2010 Seventh International Conference On Wireless And Optical Communications Networks (WOCN)*, Colombo, September,2010, pp. 1-5.
- [16] H. Idjmayyel, B.R. Qazi, and J.M.H. Elmirghani, "Position Based Routing Protocol for a City Environment," in *2010 Fourth International Conference on Next Generation Mobile Applications, Services and Technologies (NGMAST)*, Amman, July, 2010, pp. 174-179.
- [17] "GeSI SMARTer 2020:The Role of ICT in Driving a Sustainable Future," Tech Rep., (Visited September 2013). [Online]. http://www.smart2020.org/assets/files/02_Smart2020Report.pdf
- [18] H. Idjmayyel, W. Kumar, B.R. Qazi, and J.M.H. Elmirghani, "Energy and QoS — A new perspective in a city vehicular communication network," in *2011 IEEE GLOBECOM Workshops (GC Wkshps)*, December 2011, pp. 327-331.
- [19] H. Idjmayyel, B.R. Qazi, and J.M.H. Elmirghani, "Energy Efficient Double

- Cluster Head Routing Scheme in a City Vehicular Network," in *2013 27th International Conference on Advanced Information Networking and Applications Workshops (WAINA)*, Barcelona, March, 2013, pp. 1594-1599.
- [20] Y. Liu et al., "Multi-layer clustering routing algorithm for wireless vehicular sensor networks," *IET Communications*, vol. 4, no. 7, pp. 810-816, April 2010.
- [21] P. Kolios, V. Friderikos, and K. Papadaki, "Look-Ahead Strategies Based on Store-Carry and Forward Relaying for Energy Efficient Cellular Communications," *Future Internet*, vol. 2, no. 4, pp. 587-602, November 2010.
- [22] O. Arnold, F. Richter, G. Fettweis, and O. Blume, "Power consumption modeling of different base station types in heterogeneous cellular networks," in *19th Future Network and Mobile Summit*, 2010.
- [23] P. Grant and S. Fletcher, "Mobile basestations: Reducing energy," *Engineering and Technology Magazine*, vol. 6, no. 2, February 2011.
- [24] H. Idjmayyel, W. Kumar, B.R. Qazi, and J.M.H. Elmirghani, "Saving energy with QoS for vehicular communication," in *Eighth International Conference on Wireless and Optical Communications Networks (WOCN)*, May 2011, pp. 1-5.
- [25] F.J.Martinez, J.-C.Cano, C.T.Calafate, and P.Manzoni, "CityMob: A Mobility Model Pattern Generator for VANETs," in *IEEE International*

- Conference on Communications Workshops (ICC Workshops '08)*, 2008, pp. 370-374.
- [26] V.D.Khairnar and S.N.Pradhan, "Mobility models for Vehicular Ad-hoc Network simulation," in *IEEE Symposium on Computers & Informatics (ISCI)*, 2011, pp. 460-465.
- [27] F. Thouin and M. Coates, "Video-on-Demand Networks: Design Approaches and Future Challenges," *IEEE Network*, vol. 21, no. 2, pp. 42-48, March-April 2007.
- [28] N.I. Osman, T.E.H. El-Gorashi, and J.M.H Elmirghani, "Caching in green IP over WDM networks," *Journal of High Speed Networks*, vol. 19, no. 1, pp. 33-53, 2013.
- [29] CISCO., "Cisco Visual Networking Index: Forecast and Methodology, 2009 - 2014," 2011.
- [30] "Traffic Characteristics Report, City of Saskatoon," 2009.
- [31] W. Kumar, S. Bhattacharya, B.R. Qazi, and J.M.H. Elmirghani, "A Vacation-based Performance Analysis of an Energy-Efficient Motorway Vehicular Communication System," *Submitted to the IEEE Transaction on Vehicular Technology*, 2013.
- [32] P. Morsink, C. Cseh, O. Gietelink, and M. Miglietta, "Design of an application for communication-based longitudinal control in the CarTALK project," *IT Solutions for Safety and Security in Intelligent Transport (e-*

Safety), 2002.

- [33] Q.Xu, T. Mak, J. Ko, and R. Sengupta, "Vehicle-to-Vehicle Safety Messaging in DSRC," in *1st ACM international workshop on Vehicular ad hoc networks* , 2004, pp. 19-28.
- [34] K. Kutzner et al., "Connecting Vehicle Scatternets by Internet-Connected Gateways," in *MMC'2003*, 2003.
- [35] H.Wu, R. Fujimoto, and G. Riley, "Analytical models for information propagation in vehicle-to-vehicle networks," in *IEEE 60th Vehicular Technology Conference (VTC2004-Fall)*, 2004, pp. 4548-4552.
- [36] M. Torrent-Moreno, M. Killat, and H. Hartenstein, "The challenges of robust inter-vehicle communications," in *IEEE 62nd Vehicular Technology Conference (VTC-2005-Fall)*, 2005, pp. 319-323.
- [37] J.J. Blum, A. Eskandarian, and L. Hoffman, "Challenges of intervehicle ad hoc networks," *IEEE Transactions on Intelligent Transportation Systems*, vol. 5, no. 4, pp. 347-351, December 2004.
- [38] Z.Y.Rawashdeh and S.M.Mahmud, "Communications in Vehicular Networks," Wayne State University, Detroit,Michigan,.
- [39] F. Report, "Vehicle safety communications," DOT HS 810 591, Tech. Rep., 2006.
- [40] H. Hartenstein and K. Laberteaux, "A tutorial survey on vehicular ad hoc networks," *IEEE Communications Magazine*, vol. 46, no. 6, pp. 164–171,

June 2008.

- [41] A.K.K.Aboobaker, "Performance Analysis of Authentication Protocols in Vehicular Ad Hoc Networks (VANET)," Royal Holloway, University of London, MSc Thesis, 2009.
- [42] P. Buccioli, E. Masala, and J. C. D. Martin, "Dynamic Packet Size Selection for 802.11 Inter-Vehicular Video Communications," in *Vehicle to vehicle communications workshop (V2VCOM)*, 2005.
- [43] A. Sugiura and C. Dermawan, "In traffic jam IVC-RVC system for ITS using Bluetooth," *IEEE Transactions on Intelligent Transportation Systems*, vol. 6, no. 3, pp. 302-313, September 2005.
- [44] J. Jakubiak and Y. Koucheryavy, "State of the Art and Research Challenges for VANETs," in *5th IEEE Consumer Communications and Networking Conference (CCNC)*, 2008, pp. 912-916.
- [45] W. Kumar, "Performance Evaluation of Energy Efficient Vehicular Networks with Physical Channel Impairments," University of Leeds, PhD Thesis, 2012.
- [46] J. Werner. More Details Emerge about the VII Efforts. Newsletter of the ITS Cooperative Deployment Network. [Online]. http://www.ntoctalks.com/icdn/vii_details_itsa04.html.
- [47] J. Werner. USDOT Outlines the New VII Initiative at the 2004 TRB annual meeting. Newsletter of the ITS Cooperative Deployment Network.

- [Online]. http://www.nawigts.com/icdn/vii_trb04.html.
- [48] K. Saravanan, A. Thangavelu, and K. Rameshbabu, "A Middleware Architectural framework for Vehicular Safety over VANET (InVANET)," in *First International Conference on Networks and Communications*, 2009, pp. 277-282.
- [49] V.Bychkovsky, B.Hull, A. Miu, H. Balakrishnan, and S.Madden, "A measurement study of vehicular internet access using in situ Wi-Fi networks," in *12th annual international conference on Mobile computing and networking*, 2006, pp. 50-61.
- [50] X.Ma, X.Chen, and H.H.Refaï, "Performance and Reliability of DSRC Vehicular Safety Communication: A Formal Analysis," *Journal on Wireless Communications and Networking*, 2009.
- [51] A.Mostafa, A.M.Vegni, T.Oliveira, T. D. C. Little, and D. P. Agrawal, "QoSHVCP: Hybrid Vehicular Communications Protocol with QoS Prioritization for Safety Applications," *Communications and Networking*, 2012.
- [52] N. Mejri, F. Kamoun, and F. Filali, "Cooperative infrastructure discovery through V2X communication," in *The 9th IFIP Annual Mediterranean Ad Hoc Networking Workshop (Med-Hoc-Net)*, 2010, pp. 1-8.
- [53] J.Seo, K.Park, W.Jeon, J. Kwak, and D.K. Kim, "Performance evaluation of V2X communications in practical small-scale fading models," in *IEEE 20th International Symposium on Personal, Indoor and Mobile Radio*

- Communications*, 2009, pp. 2434-2438.
- [54] A.M. Vegni and T. D C Little, "A message propagation model for hybrid vehicular communication protocols," in *7th International Symposium on Communication Systems Networks and Digital Signal Processing (CSNDSP)*, 2010, pp. 382-386.
- [55] L. Armstrong. Dedicated short-range communications project. (visited May 2010). [Online]. <http://www.learmstrong.com/Dsrc/>
- [56] Federal Communications Commission (FCC). (visited May 2010). [Online]. http://www.fcc.gov/Bureaus/Engineering_Technology/
- [57] D. Jiang, V. Taliwal, A. Meier, W. Holfelder, and R. Herrtwich, "Design of 5.9 ghz dsrc-based vehicular safety communication," *IEEE Wireless Communications*, vol. 13, no. 5, pp. 36-43, October 2006.
- [58] A.Meier, "Design of the Vehicular Safety Communication Architecture," Swiss Federal Institute of Technology Zurich, Master's Thesis 2005.
- [59] Y. Qian and N. Moayeri, "Design of Secure and Application-Oriented VANETs," in *IEEE Vehicular Technology Conference (VTC Spring)*, 2008, pp. 2794-2799.
- [60] J. Zhu and S. Roy, "MAC for dedicated short range communications in intelligent transport system," *IEEE Communications Magazine*, vol. 41, no. 12, pp. 60-67, December 2003.
- [61] H. Menouar, F. Filali, and M. Lenardi, "A survey and qualitative analysis of

- mac protocols for vehicular ad hoc networks," *IEEE Wireless Communications*, vol. 13, no. 5, pp. 30-35, October 2006.
- [62] IEEE 802.11 Working Group p, "IEEE p802.11ptm/d6.01 draft standard for IT - telecommunications and information exchange between systems - local and metropolitan area networks - specific requirements - part 11: WLAN MAC and PHY specifications amendment 7:WAVE," Institute of Electrical and Electronics Engineers, New York, Technical report 2009.
- [63] Y.Zang, B.Han, S.Sories, and G.Gehlen, "A Hybrid Solution for Vehicular Communications," in *ITS World Congress* , 2009.
- [64] IEEE P802.11p/D7.0, *Draft for wireless access in vehicular environments,Std.*, May 2009.
- [65] IEEE 802.11a, *Amendment 1: High-Speed Physical Layer in the 5 GHz Band, Std.*, September 1999.
- [66] K. Bilstrup, "A Survey Regarding Wireless Communication Standards Intended for a High-Speed Vehicle Environment," School of Information Science, Computer and Electrical Engineering, Halmstad, Sweden, Technical Report 2007.
- [67] IEEE 1609.1, Trial use standard for WAVE resource manager, *IEEE Vehicular Technology Society Std.*, October 2006.
- [68] M. T. Moreno, "Inter-Vehicle Communications: Achieving Safety in a DistributedWireless Environment: Challenges, Systems and Protocols,"

- Universitätsverlag Karlsruhe, Germany, Ph.D Thesis 2007.
- [69] IEEE 1609.2, Trial use standard for WAVE security services for applications, *IEEE Vehicular Technology Society Std.*, July 2006.
- [70] IEEE 1609.3, Trial Use standard for WAVE networking services, *IEEE Vehicular Technology Society Std.*, April 2007.
- [71] IEEE 1609.4, Trial-use standard for WAVE multi-channel operation, *IEEE Vehicular Technology Society Std.*, November 2006.
- [72] Y. Toor, P. Muhlethaler, and A. Laouiti, "Vehicle Ad Hoc networks: applications and related technical issues," *IEEE Communications Surveys & Tutorials*, vol. 10, no. 3, pp. 74-88, Third Quarter 2008.
- [73] Information technology Telecommunications and information exchange between systems Local and metropolitan area networks—Specific requirements—Part 11: Wireless LAN Medium Access Control (MAC) and Physical Layer(PHY) Specifications, *Std 802.11*, 1999.
- [74] F. Borgonovo, L. Campelli, M. Cesana, and L. Coletti, "MAC for ad-hoc inter-vehicle network: services and performance," in *IEEE 58th Vehicular Technology Conference (VTC 2003-Fall)*, 2003, pp. 2789-2793.
- [75] S.Y.Ni, Y.C.Tseng, Y.S.Chen, and J.P.Sheu, "The broadcast storm problem in a mobile ad hoc network," in *5th annual ACM/IEEE international conference on Mobile computing and networking* , 1999 , pp. 151-162.

- [76] D. Jiang and L. Delgrossi, "IEEE 802.11p: Towards an International Standard for Wireless Access in Vehicular Environments," in *IEEE Vehicular Technology Conference (VTC Spring)*, 2008, pp. 2036-2040.
- [77] B.R.Qazi, "Performance Evaluation of Vehicular Networks," University of Leeds, Ph.D Thesis 2010.
- [78] M. M. Morsi, I. Khalil, E. Uhlemann, and N. Nygren, "Wireless strategies for future and emerging ITS applications," in *15th World Congress on Intelligent Transport Systems*, New York, USA, 2008.
- [79] IEEE Std. 802.11n-2009: Enhancements for Higher Throughput.(visited August 2012). [Online]. <http://www.ieee802.org/>
- [80] J.M. Kahn and J.R Barry, "Wireless infrared communications," *Proceedings of the IEEE* , vol. 85, no. 2, pp. 265-298, February 1997.
- [81] Int.Electrotech. Commission, "CEI/IEC825-1:Safety of Laser Products," 1993.
- [82] B. A. Forouzan, *Data Communications and Networking*, 3rd ed.: McGraw-Hill, 2006.
- [83] J.Eriksson, H.Balakrishnan, and S.Madden, "Cabernet: vehicular content delivery using WiFi," in *14th ACM international conference on Mobile computing and networking* , 2008 , pp. 199-210.
- [84] S.Wan, J.Tang, and R.S. Wolff, "Reliable Routing for Roadside to Vehicle Communications in Rural Areas," in *IEEE International Conference on*

Communications (ICC '08), 2008, pp. 3017-3021.

- [85] D. Helbing, "Traffic and related self-driven many-particle systems," *Reviews of Modern Physics*, vol. 73, no. 4, pp. 1067–1141 , October 2001.
- [86] J. Harri, F. Filali, and C. Bonnet, "Mobility models for vehicular ad hoc networks: a survey and taxonomy," *IEEE Communications Surveys & Tutorials*, vol. 11, no. 4, pp. 19-41, Fourth Quarter 2009.
- [87] California PATH. (2010) SHIFT: The Hybrid System Simulation Programming Language. (Visited January 2010). [Online]. <http://www.path.berkeley.edu/shift/>
- [88] OPNET. (2008).(Visited January 2010). [Online]. <http://www.opnet.com/>
- [89] The Network Simulator (NS2). (2010) [Online]. <http://www.isi.edu/nsnam/ns/>
- [90] Scalable Network Technologies. (2010) QualNet. [Online]. <http://qualnetworld.com/>
- [91] OMNET++. (2010) [Online]. <http://www.omnetpp.org/>
- [92] J. Bernsen and D. Manivannan, "Greedy Routing Protocols for Vehicular Ad Hoc Networks," in *International Wireless Communications and Mobile Computing Conference (IWCMC '08)*, 2008, pp. 632-637.
- [93] C.E. Perkins and E.M. Royer, "Ad-hoc on-demand distance vector routing," in *Second IEEE Workshop on Mobile Computing Systems and*

- Applications*, 1999, pp. 90-100.
- [94] D.B. Johnson and D.A. Maltz, "Dynamic Source Routing in Ad Hoc Wireless Networks," in *Mobile Computing*, T.Imielinski and Henry F. Korth, Eds.: Springer US, 1996, pp. 153-181.
- [95] V.Namboodiri and L.Gao, "Prediction-Based Routing for Vehicular Ad Hoc Networks," *IEEE Transactions on Vehicular Technology*, vol. 56, no. 4, pp. 2332-2345, July 2007.
- [96] Z.Wang, L.Liu, M.Zhou, and N.Ansari, "A Position-Based Clustering Technique for Ad Hoc Intervehicle Communication," *IEEE Transactions on Systems, Man, and Cybernetics, Part C: Applications and Reviews*, vol. 38, no. 2, pp. 201-208, March 2008.
- [97] C.Chen and Z.Chen, "Exploiting Contact Spatial Dependency for Opportunistic Message Forwarding," *IEEE Transactions on Mobile Computing*, vol. 8, no. 10, pp. 1397-1411, October 2009.
- [98] J.Y.Yu, P. H J.Chong, and M.Zhang, "Performance of Efficient CBRP in Mobile Ad Hoc Networks (MANETS)," in *IEEE 68th Vehicular Technology Conference (VTC 2008-Fall)*, 2008, pp. 1-7.
- [99] C.E.Perkins and P.Bhagwat, "Highly dynamic Destination-Sequenced Distance-Vector routing (DSDV) for mobile computers," in *the conference on Communications architectures, protocols and applications (SIGCOMM '94)*, 1994, pp. 234 - 244.

- [100] A.S.Nargunam and M. P.Sebastian, "Fully distributed cluster based routing architecture for mobile ad hoc networks," in *IEEE International Conference on Wireless And Mobile Computing, Networking And Communications (WiMob'2005)*, 2005, pp. 383-389.
- [101] P.Muhlethaler, A.Laouiti, and Y.Toor, "Comparison of Flooding Techniques for Safety Applications in VANETs," in *7th International Conference on ITS Telecommunications (ITST '07)*, 2007, pp. 1-6.
- [102] S.K.Sarkar, T. G. Basavaraju, and C. Puttamadappa, *Ad Hoc Mobile Wireless Networks: Principles, Protocols and Applications*, 1st ed. Boston, MA,USA: Auerbach Publications, 2007.
- [103] M.J.Keeling and K.T.D Eames, "Networks and epidemic models," *J R Soc Interface*, vol. 2, no. 4, pp. 295–307, September 2005.
- [104] M. Zhang and R.S Wolff, "Routing protocols for vehicular Ad Hoc networks in rural areas," *IEEE Communications Magazine*, vol. 46, no. 11, pp. 126-131, November 2008.
- [105] H.Kang and D.Kim, "Vector Routing for Delay Tolerant Networks," in *IEEE 68th Vehicular Technology Conference (VTC 2008-Fall)*, 2008, pp. 1-5.
- [106] H. Oka and H. Higaki, "Multihop Data Message Transmission with Inter-Vehicle Communication and Store-Carry-Forward in Sparse Vehicle Ad-Hoc Networks (VANET)," in *New Technologies, Mobility and Security (NTMS '08)*, 2008, pp. 1-5.

- [107] B.R. Qazi and J. M H Elmirghani, "A Routing Scheme for VANETs in a City Environment," in *Third International Conference on Next Generation Mobile Applications, Services and Technologies (NGMAST '09)*, 2009, pp. 467-471.
- [108] C. Lochert, M. Mauve, H.Füßler, and H. Hartenstein, "Geographic routing in city scenarios," in *ACM SIGMOBILE Mobile Computing and Communications Review*, 2005, pp. 69-72.
- [109] P.Bose, P.Morin, I.Stojmenović, and J.Urrutia, "Routing with Guaranteed Delivery in Ad Hoc Wireless Networks," *Wireless Networks* , vol. 7, no. 6, pp. 609-616, November 2001.
- [110] H.Fussler, M.Mauve, H.Hartenstein, D.Vollmer, and M.Kaesemann, "A Comparison of Routing Strategies in Vehicular Ad-Hoc Networks," *REIHE INFORMATIK*, March 2002.
- [111] T. Kosch, C. Schwingenschlogl, and Li Ai, "Information dissemination in multihop inter-vehicle networks," in *The IEEE 5th International Conference on Intelligent Transportation Systems*, 2002, pp. 685-690.
- [112] T. Nishida et al., "Inter-vehicle P2P communication experimental on-board terminal," in *Second IEEE Consumer Communications and Networking Conference (CCNC)*, 2005, pp. 434-438.
- [113] Chia-Ching Ooi and N. Faisal, "Implementation of geocast-enhanced AODV-bis routing protocol in MANET," in *IEEE Region 10 Conference (TENCON 2004)*, 2004, pp. 660-663.

- [114] S.Y. Wang, C.C. Lin, Y.W. Hwang, K.C. Tao, and C.L. Chou, "A practical routing protocol for vehicle-formed mobile ad hoc networks on the roads," in *IEEE Intelligent Transportation Systems*, 2005, pp. 161-166.
- [115] C.R. Lin and M. Gerla, "Adaptive clustering for mobile wireless networks," *IEEE Journal on Selected Areas in Communications*, vol. 15, no. 7, pp. 1265-1275, September 1997.
- [116] B. Das and V. Bharghavan, "Routing in ad-hoc networks using minimum connected dominating sets," in *IEEE International Conference on Communications (ICC '97)*, 1997, pp. 376-380.
- [117] J.Wu and H.Li, "A Dominating-Set-Based Routing Scheme in Ad Hoc Wireless Networks," *Telecommunication Systems* , vol. 18, no. 1-3, pp. 13-36, September 2001.
- [118] H. Wu and A.A. Abouzeid, "Cluster-based routing overhead in networks with unreliable nodes," in *IEEE Wireless Communications and Networking Conference*, 2004, pp. 2557-2562.
- [119] J. Blum, A. Eskandarian, and L. Hoffman, "Mobility management in IVC networks," in *IEEE Intelligent Vehicles Symposium*, 2003, pp. 150-155.
- [120] R.A. Santos, A. Edwards, R. Edwards, and L. Seed, "Performance evaluation of routing protocols in vehicular adhoc networks," *The International Journal of Ad Hoc and Ubiquitous Computing*, vol. 1, no. 1/2, pp. 80–91, November 2005.

- [121] Z.Ji, W.Yu, and K.J.R.Liu, "A Game Theoretical Framework for Dynamic Pricing-Based Routing in Self-Organized MANETs," *IEEE Journal on Selected Areas in Communications*, vol. 26, no. 7, pp. 1204-1217, September 2008.
- [122] B. Xu, S. Hischke, and B. Walke, "The role of ad hoc networking in future wireless communications," in *International Conference on Communication Technology (ICCT 2003)*, 2003, pp. 1353-1358.
- [123] S.Marti, T.J. Giuli, K.Lai, and M.Baker, "Mitigating routing misbehavior in mobile ad hoc networks," in *The 6th annual international conference on Mobile computing and networking*, 2000, pp. 255-265.
- [124] P.Michiardi and R.Molva, "Core: a collaborative reputation mechanism to enforce node cooperation in mobile ad hoc networks," in *Sixth Joint Working Conference on Communications and Multimedia Security: Advanced Communications and Multimedia Security*, 2002, pp. 107-121.
- [125] S.Buchegger and J.Yves, "Performance Analysis of the CONFIDANT Protocol (Cooperation Of Nodes: Fairness In Dynamic Ad hoc NeTworks)," in *The 3rd ACM international symposium on Mobile ad hoc networking & computing*, 2002, pp. 226 - 236.
- [126] S. Zhong, J. Chen, and Y.R. Yang, "Sprite: a simple, cheat-proof, credit-based system for mobile ad-hoc networks," in *Twenty-Second Annual Joint Conference of the IEEE Computer and Communications (INFOCOM 2003)*, 2003, pp. 1987-1997.

- [127] W.Yu and K. J.R.Liu, "Attack-Resistant Cooperation Stimulation in Autonomous Ad Hoc Networks," *IEEE Journal on Selected Areas in Communications*, vol. 23, no. 12, pp. 2260-2271, December 2005.
- [128] Z. Ji, Wei Y., and K.J.R. Liu, "An optimal dynamic pricing framework for autonomous mobile ad hoc networks," in *25th IEEE International Conference on Computer Communications (INFOCOM 2006)*, 2006, pp. 1-12.
- [129] V. Srinivasan, P. Nuggehalli, C. -F Chiasserini, and R.R. Rao, "Cooperation in wireless ad hoc networks," in *Twenty-Second Annual Joint Conference of the IEEE Computer and Communications*, 2003, pp. 808-817.
- [130] L.Anderegg and S.Eidenbenz, "Ad hoc-VCG: a truthful and cost-efficient routing protocol for mobile ad hoc networks with selfish agents," in *The 9th annual international conference on Mobile computing and networking* , 2003, pp. 245-259.
- [131] S. Eidenbenz, G. Resta, and P. Santi, "COMMIT: a sender-centric truthful and energy-efficient routing protocol for ad hoc networks with selfish nodes," in *19th IEEE International Parallel and Distributed Processing Symposium*, 2005.
- [132] S.Zhong, L.E.Li, Y.G.Liu, and Y.R.Yang, "On designing incentive-compatible routing and forwarding protocols in wireless ad-hoc networks: an integrated approach using game theoretic and cryptographic

- techniques," *Wireless Networks*, vol. 13, no. 6, pp. 799-816 , December 2007.
- [133] W.R. Heinzelman, A. Chandrakasan, and H. Balakrishnan, "Energy-efficient communication protocol for wireless microsensor networks," in *The 33rd Annual Hawaii International Conference on System Sciences*, 2000, pp. 1-10.
- [134] E. Callaway, "Low power consumption features of the IEEE 802.15.4/Zigbee LRWPAN standard," in *Mini-tutorial, ACM Sensys 03*, Los Angeles, CA,USA, November 2003.
- [135] C.-S.Hsu and Y-C.Tseng, "Cluster-based semi-asynchronous power-saving protocols for multi-hop ad hoc networks," in *IEEE International Conference on Communications (ICC 2005)*, 2005, pp. 3166-3170.
- [136] L.Ning, X.Yuan, and X.Sheng-li, "A power-saving protocol for ad hoc networks," in *International Conference on Wireless Communications, Networking and Mobile Computing*, 2005, pp. 808-811.
- [137] Y-C.Tseng, C-S.Hsu, and T-Y.Hsieh, "Power-saving protocols for IEEE 802.11-based multi-hop ad hoc networks," in *Twenty-First Annual Joint Conference of the IEEE Computer and Communications Societies*, 2002, pp. 200-209.
- [138] J.Wang, "A Survey of Web Caching Schemes for the Internet," *ACM SIGCOMM Computer Communication Review* , vol. 29, no. 5, pp. 36-46, October 1999.

- [139] G. Barish and K. Obraczke, "World Wide Web caching: trends and techniques," *IEEE Communications Magazine*, vol. 38, no. 5, pp. 178-184, May 2000.
- [140] U. Niesen, D. Shah, and G.W. Wornell, "Caching in Wireless Networks," *IEEE Transactions on Information Theory*, vol. 58, no. 10, pp. 6524-6540, October 2012.
- [141] Z. Jing, Z. Ping, C. Guohong, and C.R. Das, "Cooperative Caching in Wireless P2P Networks: Design, Implementation, and Evaluation," *IEEE Transactions on Parallel and Distributed Systems*, vol. 21, no. 2, pp. 229-241, February 2010.
- [142] G.Cao, "Proactive power-aware cache management for mobile computing systems," *IEEE Transactions on Computers*, vol. 51, no. 6, pp. 608-621, June 2002.
- [143] X.Wang, Y.Bao, X.Liu, and Z.Niu, "On the design of relay caching in cellular networks for energy efficiency," in *IEEE Conference on Computer Communications Workshops (INFOCOM WKSHPS)*, 2011, pp. 259-264.
- [144] M. Johnson, L. De Nardis, and K. Ramchandran, "Collaborative Content Distribution for Vehicular Ad Hoc Networks," in *Allerton Conf. Communication, Control, and Computing*, 2006.
- [145] M. Li, Z. Yang, and W. Lou, "CodeOn: Cooperative Popular Content Distribution for Vehicular Networks using Symbol Level Network Coding," *IEEE Journal on Selected Areas in Communications*, vol. 29, no. 1, pp.

- 223-235, January 2011.
- [146] D.Zhang and C.K.Yeo, "Enabling Efficient WiFi-Based Vehicular Content Distribution," *IEEE Transactions on Parallel and Distributed Systems*, vol. 24, no. 3, pp. 479-492, March 2013.
- [147] U. Shevade et al., "Enabling High-Bandwidth Vehicular Content Distribution," in *ACM Int'l Conf. Emerging Networking EXperiments and Technologies (CoNEXT)*, 2010, pp. 1-12.
- [148] K-L. Wu, P.S. Yu, and M-S. Chen, "Energy-Efficient Caching for Wireless Mobile Computing," in *the Twelfth International Conference on Data Engineering*, 1996, pp. 336-343.
- [149] S.Doshi, S.Bhandare, and T.X.Brown, "An on-demand minimum energy routing protocol for a wireless ad hoc network," *ACM SIGMOBILE Mobile Computing and Communications Review* , vol. 6, no. 3, pp. 50-66, July 2002.
- [150] P. Nuggehalli, V. Srinivasan, C. Chiasserini, and R.R. Rao, "Efficient Cache Placement in Multi-Hop Wireless Networks," *IEEE/ACM Transactions on Networking*, vol. 14, no. 5, pp. 1045-1055, October 2006.
- [151] P. Cheng, C-N. Chuah, and X. Liu, "Energy-aware node placement in wireless sensor networks," in *IEEE Global Telecommunications Conference (GLOBECOM '04)*, 2004, pp. 3210-3214.
- [152] Y.T. Hou, Yi Shi, H.D. Sherali, and S.F. Midkiff, "On energy provisioning

- and relay node placement for wireless sensor networks," *IEEE Transactions on Wireless Communications*, vol. 4, no. 5, pp. 2579-2590, September 2005.
- [153] B. Lin, P-H. Ho, L-L. Xie, X. Shen, and J. Tapolcai, "Optimal Relay Station Placement in Broadband Wireless Access Networks," *IEEE Transactions on Mobile Computing*, vol. 9, no. 2, pp. 259-269, February 2010.
- [154] J. Cannons, L.B. Milstein, and K. Zeger, "An algorithm for wireless relay placement," *IEEE Transactions on Wireless Communications*, vol. 8, no. 11, pp. 5564-5574, November 2009.
- [155] G. Giambene, *Queueing Theory and telecommunications: Networks and Applications.*: Springer, 2005.
- [156] J.N. Daigle, *Queueing Theory with Applications to Packet Telecommunication.*: Springer, 2004.
- [157] J.M.Smith, "Optimal design and performance modelling of M/G/1/K queueing systems," *Mathematical and Computer Modelling: An International Journal* , vol. 39, no. 9-10, pp. 1049-1081 , May 2004.
- [158] F.R.B.Cruz, A.R. Duarte, and T. van Woensel, "Buffer allocation in general single-server queueing networks," *Computers and Operations Research* , vol. 35, no. 11, pp. 3581-3598 , November 2008.
- [159] A. Fallahi, E. Hossain, and A.S. Alfa, "QoS and energy trade off in distributed energy-limited mesh/relay networks: a queuing analysis," *IEEE*

- Transactions on Parallel and Distributed Systems*, vol. 17, no. 6, pp. 576-592, June 2006.
- [160] X. Yang, J. Liu, N.F. Vaidya, and F. Zhao, "A vehicle-to-vehicle communication protocol for cooperative collision warning," in *The First Annual International Conference on Mobile and Ubiquitous Systems: Networking and Services (MOBIQUITOUS 2004)*, 2004, pp. 114-123.
- [161] S. Chen, A. M. Wyglinski, S. Pagadarai, R. Vuyyuru, and O. Altintas, "Feasibility analysis of vehicular dynamic spectrum access via queueing theory model," *IEEE Communications Magazine*, vol. 49, no. 11, pp. 156-163, November 2001.
- [162] Eiji Oki, *Linear Programming and Algorithms for Communication Networks: A Practical Guide to Network Design, Control, and Management*: CRC Press, 2012.
- [163] M. Juenger et al., *50 Years of Integer Programming 1958-2008: From the Early Years to the State-of-the-Art*. New York: Springer-Verlag, 2010.
- [164] J.P.Vielma, "Mixed Integer Linear Programming Formulation Techniques," April 2013.
- [165] IBM ILOG. (2012, June) CPLEX High-performance mathematical programming engine. [Online]. <http://www-01.ibm.com/software/commerce/optimization/cplex-optimizer/index.html>
- [166] Gurobi Optimization. (2012, June) The Gurobi Optimizer. [Online].

<http://www.gurobi.com/>

- [167] Fair Isaac Corporation. (June, 2012) FICO Xpress Optimization Suite. [Online]. <http://www.fico.com/en/Products/DMTools/Pages/FICO-Xpress-Optimization-Suite.aspx>
- [168] W. Adams and R. Forrester, "A simple recipe for concise mixed 0-1 linearizations," *Operations Research Letters*, vol. 33, no. 1, pp. 55-61, January 2005.
- [169] R. Bixby, M. Fenelon, Z. Gu, E. Rothberg, and R. Wunderling, "Mixed-Integer Programming: A Progress Report," *The Sharpest Cut*, pp. 309-325, 2004.
- [170] R.Madan, S.Cui, S.Lall, and A.J. Goldsmith, "Mixed Integer-Linear Programming for Link Scheduling in Interference-Limited Networks," in *Resource Allocation in Wireless Networks (RAWNET)*, 2005, pp. 1-6.
- [171] A.A.Hammad, G.H.Badawy, T.D.Todd, A.A.Sayegh, and D.Zhao, "Traffic Scheduling for Energy Sustainable Vehicular Infrastructure," in *IEEE Global Telecommunications Conference (GLOBECOM 2010)*, 2010, pp. 1-6.
- [172] F.Malandrino, C.Casetti, C.Chiasserini, and M.Fiore, "Content downloading in vehicular networks: What really matters," in *IEEE INFOCOM*, 2011, pp. 426-430.
- [173] A. Goldsmith, *Wireless Communications.*: Cambridge University Press,

2005.

- [174] A. L. Cheng, B. Henty, D. Stancil, F. Bai, and P. Mudalige, "Mobile Vehicle-to-Vehicle Narrow-Band Channel Measurement and Characterization of the 5.9 GHz Dedicated Short Range Communication (DSRC) Frequency Band," *IEEE Journal on Selected Areas in Communications*, vol. 25, no. 8, pp. 1501–1516, October 2007.
- [175] E. Green and M. Hata, "Microcellular propagation measurements in an urban environment," in *IEEE International Symposium on Personal, Indoor and Mobile Radio Communications*, 1991, pp. 324 - 328.
- [176] HP A-802.11a/b/g Access Point Series. (visited June 2010). [Online]. <http://h20195.www2.hp.com/v2/GetPDF.aspx/4AA3-0791ENW.pdf>
- [177] L. Feeney and M. Nilsson, "Investigating the Energy Consumption of a Wireless Network Interface in an Ad Hoc Networking Environment," in *Twentieth Annual Joint Conference of the IEEE Computer and Communications Societies (INFOCOM 2001)*, 2001, pp. 1548 –1557.
- [178] A. Capone. (2012, June) Energy and mobility: Scalable solutions for the mobile data explosion. GreenTouch. Politecnico di Milano, (visited March 2013). [Online]. <http://www.greentouch.org>
- [179] S.T. Sheu, Y.C. Cheng, and J-S.Wu, "A Channel Access Scheme to Compromise Throughput and Fairness in IEEE 802.11p Multi-Rate/Multi-Channel Wireless Vehicular Networks," in *IEEE 71st Vehicular Technology Conference (VTC 2010-Spring)*, 2010, pp. 1-5.

- [180] BBC iPlayer. (Visited May 2013). [Online]. <http://www.bbc.co.uk/iplayer/>
- [181] J. Derksen, R. Jansen, M. Maijala, and E. Westerberg. (2006) HSDPA performance and evolution, (Visited March 2013). Ericsson Review, no. 03. [Online]. <http://www.ericsson.com>
- [182] P. Croy. (2012, June) LTE Backhaul Requirements: A Reality Check. Aviat Network Whitepaper, (visited July 2013). [Online]. <http://www.portals.aviatnetworks.com>
- [183] Ruckus ZoneFlex 7762 Access Point specification data sheet. (Visited January 2013). [Online]. <http://www.ruckuswireless.com/products/zoneflex-outdoor/7762>
- [184] Motorola Whitepaper. 2G and 3G cellular networks: their impact on today's enterprise mobility solutions and future mobility strategies. (Visited March 2013). [Online]. <http://www.motorola.com>
- [185] P. Schmid and A. Roos. Power consumption: conclusions, (Visited February 2013). [Online]. <http://www.tomshardware.com/reviews/-external-hard-drive,2045-16.html>
- [186] J. Kani, "Power Saving Techniques and Mechanisms for Optical Access Networks Systems," *Journal of Lightwave Technology*, vol. 31, no. 4, pp. 563-570, February 2013.
- [187] BBC iPlayer. (Visited May 2013). [Online]. http://iplayerhelp.external.bbc.co.uk/help/tablets/ipadapp_bitrate

- [188] Netgear Whitepaper. Next Generation Gigabit WiFi-802.11 ac,(Visited June 2013). [Online]. <http://www.netgear.com>
- [189] M. Rajaratnam and F. Takawira, "Two moment analysis of channel reservation in cellular networks," in *IEEE Africon*, 1999, pp. 257-262.
- [190] I. Haratcherev, M. Fiorito, and C. Balageas, "Low-Power Sleep Mode and Out-Of-Band Wake-Up for Indoor Access Points," in *IEEE GLOBECOM Workshops*, 2009, pp. 1-6.

Appendices

Appendix A: City Vehicular Simulator

A.1: Introduction

In this Appendix, the developed city vehicular mobility simulator is introduced that was integrated with the network layer models and has been used as a simulation tool to analyse and evaluate our work presented in this thesis.

A.2: Overview

The city vehicular simulator has been designed in JAVA, where a number of classes and variables have been defined to control the flow of the simulator, as well as to execute the required tasks for managing V2V and V2R communications. The simulator consists of three main classes. Class **Vehicle** is responsible for the vehicle object and its attributes, whereas class **Road** defines the road object along with its attributes. The third class **VehicularSim** carries

out the main tasks of the simulator such as initialising the roads and vehicles, and it deals with vehicles' movement and speed control. Each class will be discussed in detail in this Appendix. A flowchart for the city vehicular simulator is shown in Figure A.2. The variable *SysTime* controls any event during simulation run time. It also represents the duration (in seconds) that the simulation has been running for and is responsible for the movement of vehicles. The parameter *TOTAL_VEHICLES* indicates the number of vehicles in the network and is entered by a user to make the simulator run to represent different vehicular traffic densities. The city is based on a $3 \times 3 \text{ km}^2$ Manhattan grid with 48 roads and 16 junctions, where each road is 1000 meter long. Note that in this thesis, $3 \times 3 \text{ km}^2$ has been considered with 48 roads and 16 junctions, however, the developed vehicular simulator is extremely flexible, and allows any road topology (i.e. $1 \times 1 \text{ km}^2$, $2 \times 2 \text{ km}^2$, etc) to be represented in a Manhattan grid layout. The length of each road is divided by the variable *numberOfLocations*, where each location represents an index of an array and is 1 m in length. The city network is initialised using the *initialiseRoad()* method. Vehicles are introduced to the map each with a unique ID and are placed randomly on roads and locations using the *AssignRandVehicle()* method. Each vehicle occupies 5 m of a road (average vehicle length). The total simulation duration is indicated by *TotSimTime*. Vehicles keep a record of their speed (maximum speed is 13 m/s, speed limit in a typical city), road number, *vehRoad*, and location, *vehLocation*, and can accelerate/decelerate at a rate of 2 m/s^2 . Moreover, vehicles randomly (based on a uniform distribution) choose

one of the four directions (including U-turn) upon reaching a junction using the *getDirection()* method. The *setDirection()* and *checkAvailability()* methods are executed to ensure that vehicles do not overlap and that vehicles do not leave the road network. Being an event-driven simulator, every vehicle, at each iteration, computes the distance to the vehicle ahead in order to adapt its speed accordingly. The city vehicular network is illustrated in Figure A.1.

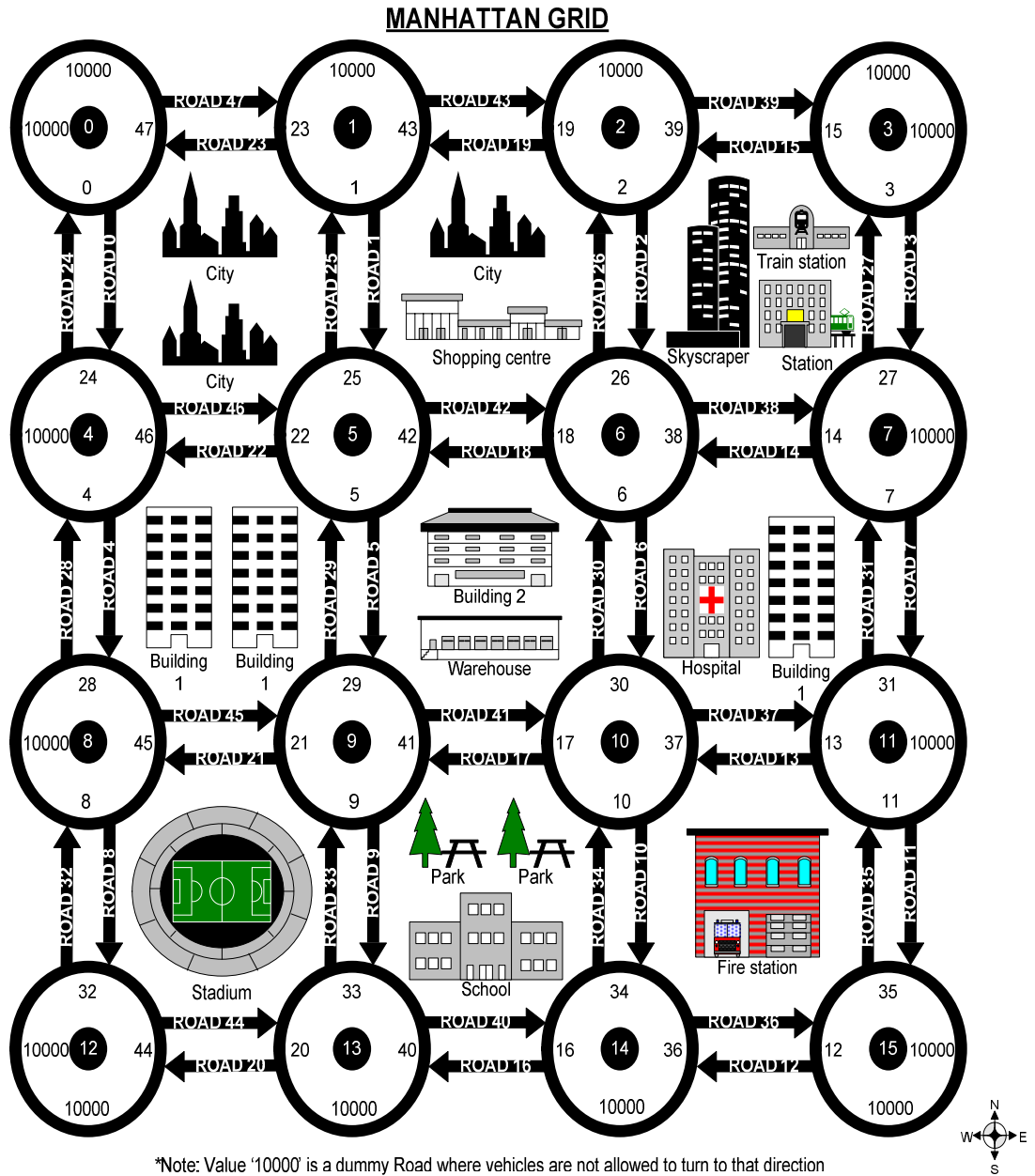


Figure A.1: 3x3 km² Manhattan grid

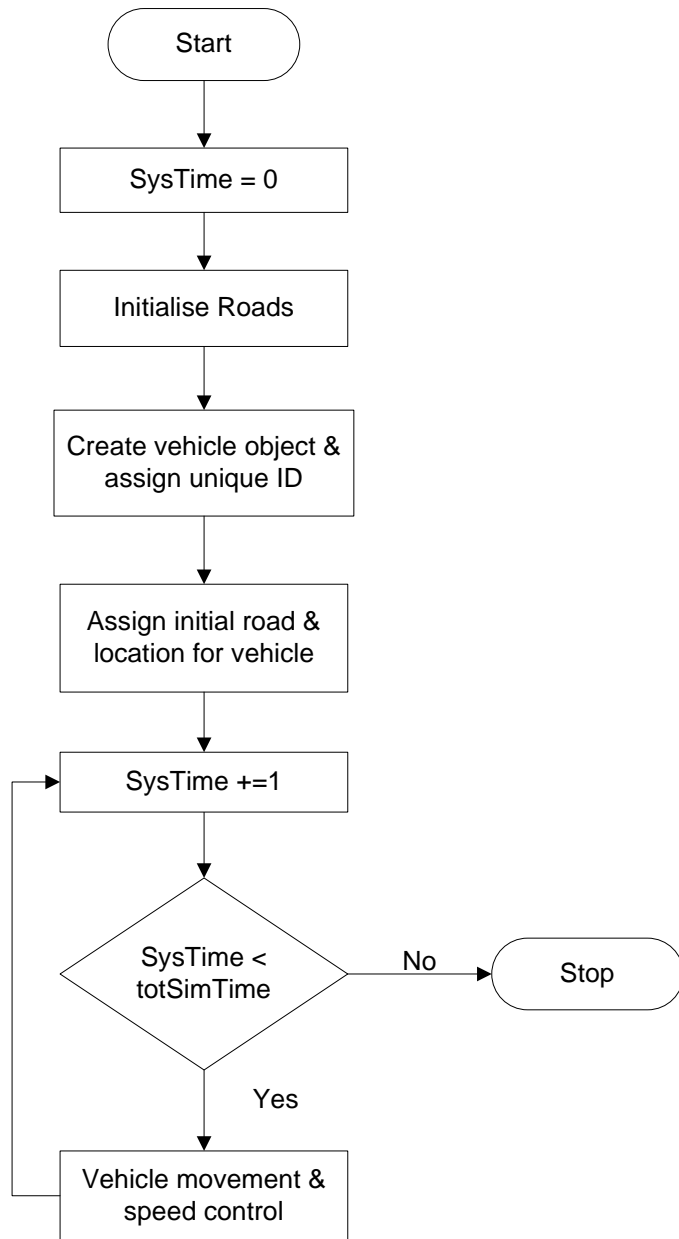


Figure A.2: City vehicular simulator flowchart

A.3 Simulator Design

A.3.1 Vehicle class

This class is responsible for creating a new vehicle object along with its attributes and parameters. Each vehicle created in the simulation is given a unique integer ID i.e. *VehID*, two integer variables that hold the vehicle's road and location, i.e. *VehRoad* and *VehLocation* respectively. Moreover, a Boolean variable *isEquipped* is initialised to false, which indicates if a vehicle is equipped with an OBU allowing it to communicate with other similarly equipped vehicles. Moreover, each vehicle is initialised with two vectors namely, *srcPktID* and *relayPktID*. The *srcPktID* vector stores the original packets generated by the vehicle itself, while the *relayPktID* vector keeps the packets received by other vehicles which might be further forwarded to other vehicles, depending upon the type of communication protocol integrated. These vectors are used while integrating the communication layer.

A.3.2 Road class

Class Road is responsible for the road's object and its attributes and parameters. There are 48 roads in our city vehicular network where each road is 1000 meters long. Each road is divided into an array of 1000 elements where each element in the array container refers to one location (i.e. 1 m) on that road. At the end of each road, a junction is placed with four possible directions that can be taken, i.e. straight, right, left and U-turn, hence, an integer variable

called *NO_EXITS* is initialised to four. There are 16 junctions in our city vehicular network where each is given a unique ID i.e. *JctID*. Each road object is initialised with: a unique integer ID, *RdID*, an integer that holds the ID of the junction where the road starts, *FromJctID*, and an integer that keeps the ID of junction to where the road is heading, *ToJct*. Moreover, an array of size 1000 Boolean elements namely, *RdArray* is initialised for all roads where it is set true if the location (i.e. array) is occupied by a vehicle, false otherwise, to keep track of the vehicles' locations.

A.3.3 Vehicular simulator class

Class ***VehicularSim*** is the main class in the city vehicular simulator. It consists of a number of methods each dedicated for a certain task. A number of variables have been defined to control the flow of the simulator procedure, as well as to execute the required tasks for managing vehicular movement. The parameter *TOTAL_VEHICLES* refers to the total number of vehicles in the network, where the variables *TOTAL_ROADS* and *TOTAL_JUNCTIONS* represent the number of roads and the number of junctions in the city network, respectively. Moreover, variable *SysTime* is responsible for generating and controlling any event during the simulation run time. It also represents the duration the simulation has been running for and is responsible for the vehicles movement. The variable *MPR* refers to the market penetration ratio, which indicates the ratio of the vehicles equipped with networking capabilities to the

total vehicles available in the network. All the important procedures along with their tasks are discussed in the following sections.

A.3.3.1 Road initialisation

The first procedure to be executed during the simulation (*initialiseRoad()*) is responsible for initialising the road network. To start the simulation process, 48 road objects are created where each road is given a unique ID (*RdID*) between 0 and 47. A text file *Roads.txt* is read by creating a new *FileReader* object to get the road numbers. Road IDs are stored sequentially and are represented by two integers representing the IDs of junctions connecting that road namely, *FromJct* and *ToJct*. For each of the 48 roads created, the *RdArray* Boolean variable is initially set to false indicating that there is no vehicle on any road. Similarly, a text file called *Junctions.txt* is read to get the data for each of the 16 junctions. The text file contains four integers for each junction indicating the four possible roads that each junction's exit leads to. Note that road number '10000' indicates an out of map boundary and thus a vehicle needs to choose another exit.

A.3.3.2 Vehicle assignment

This method (*AssignRandVehicle()*) is used to create new vehicle objects and subsequently place them on city roads. Depending on the user choice (vehicular density from real measurements), a number of vehicle objects are created and each is assigned a unique ID (*VehID*). Thereafter, each vehicle object created is located on a random road at a random location, i.e. *VehRoad*

and *VehLocaction*, respectively. Each vehicle occupies 5 meters on a certain road, setting *RdArray* Boolean variable to true. If another vehicle is present on the same road and is occupying any of the new vehicle's 5 meters space, a new pair of road and location will be selected. Finally, if another vehicle is present on the same road but is not occupying the new vehicle's space, the new vehicle's 5 meters space will be set as occupied. A flowchart explaining the flow of this method is presented in Figure A.3.

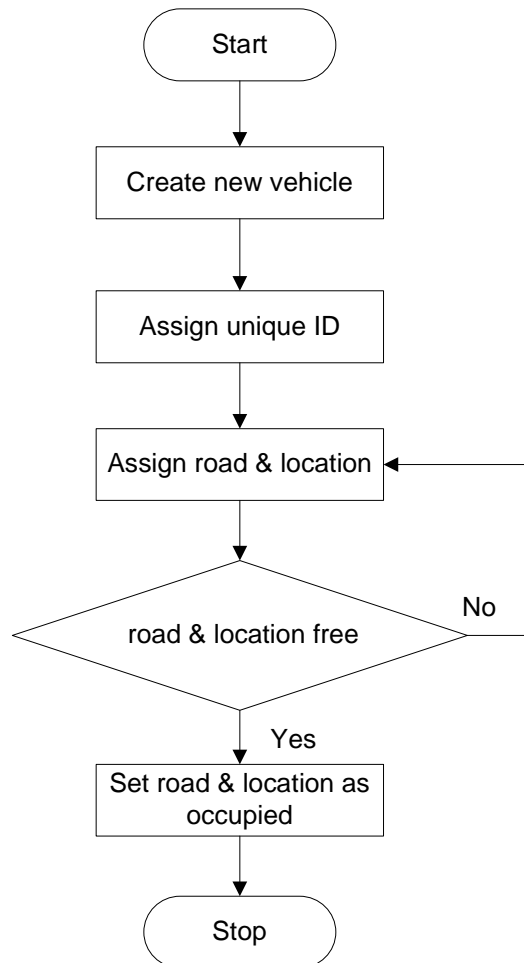


Figure A.3: Assign vehicle flowchart

A.3.3.3 Vehicular mobility

This procedure (method) deals with the vehicle's movement and speed control. Each vehicle chooses one of the 4 directions upon approaching a junction. The *GetDirection()* method is executed to return a random integer between 0 and 3 indicating the direction that a vehicle will take upon reaching a junction. Note that the direction is chosen according to uniform distribution. After choosing a certain direction, the *setDirection()* method is executed to check the available space of the road at its entry point. If the entry point is not occupied, it moves to the new location and set it as occupied after releasing its old location. On the other hand, if another vehicle occupies the desired location, it stays in its current location and waits until the location is made available (adjusting its speed accordingly).

The speed of vehicles is set according to the vehicular density of each road and the inter-vehicle spacing. The maximum speed limit in a typical city is 48 km/h (i.e. 13 m/s), where vehicles move at this speed representing free flowing traffic. The flowchart in Figure A.4 describes the procedure of this method.

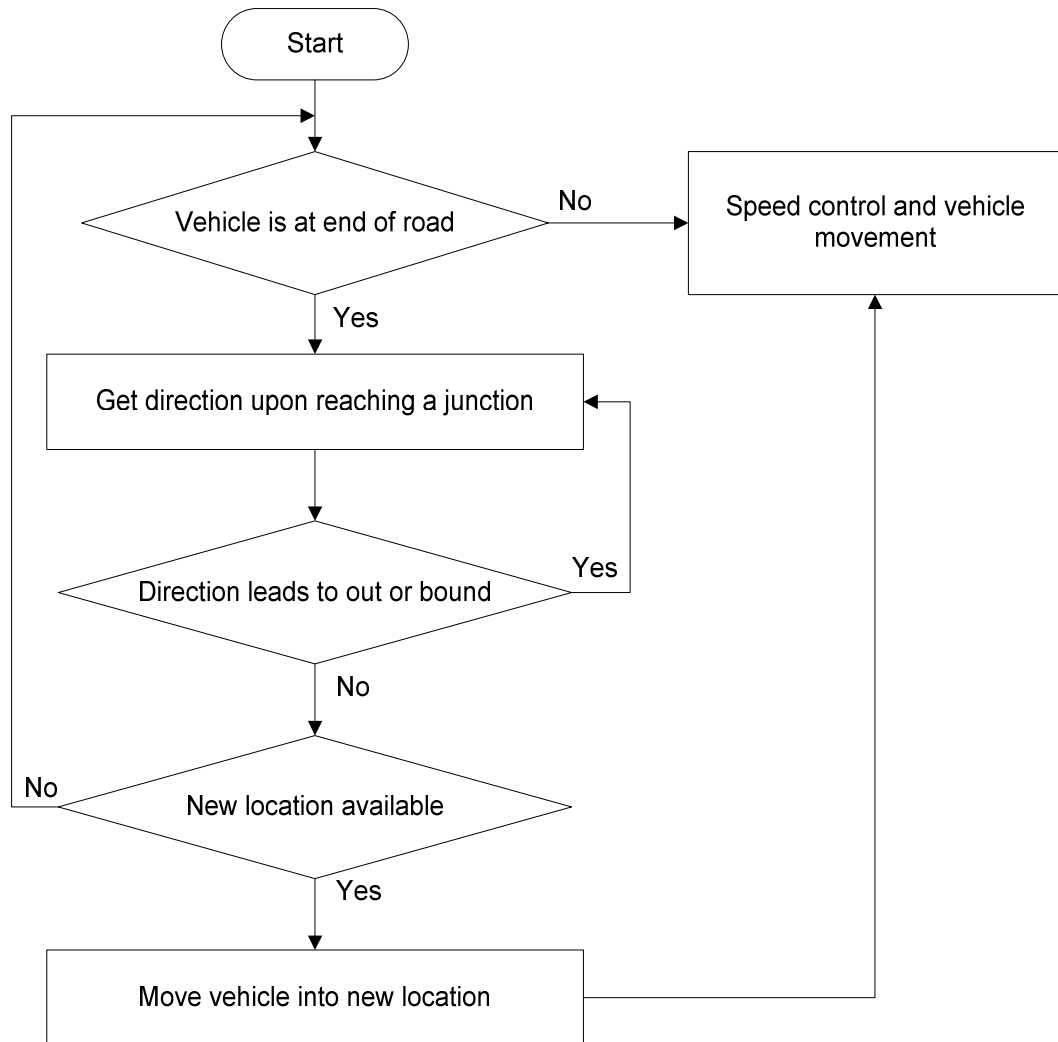


Figure A.4: Vehicular mobility flowchart

A.4 Summary

In this appendix, the city vehicular simulator that has been designed and implemented in JAVA along with its main classes and methods have been detailed. The simulator has been integrated with a set of communication protocols (discussed in this thesis), to study their performance in a city vehicular environment, under different communication scenarios, such as ad hoc, centralised and hybrid.

Appendix B: Flowcharts

B.1 VANET Simulator Flowchart

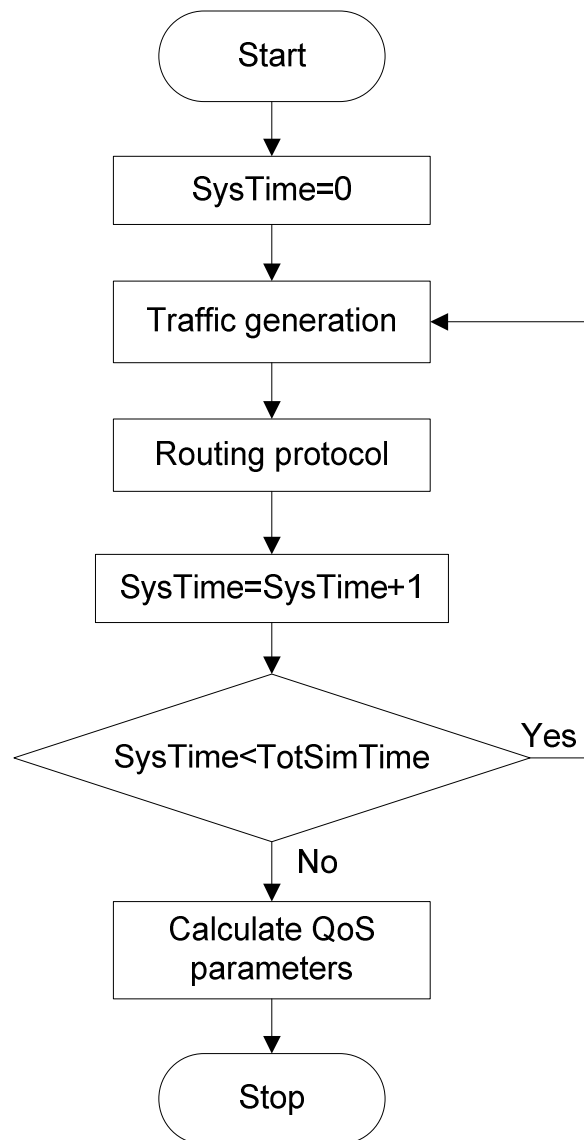


Figure B.1: VANET simulator flowchart

B.2 Traffic Generation Flowchart

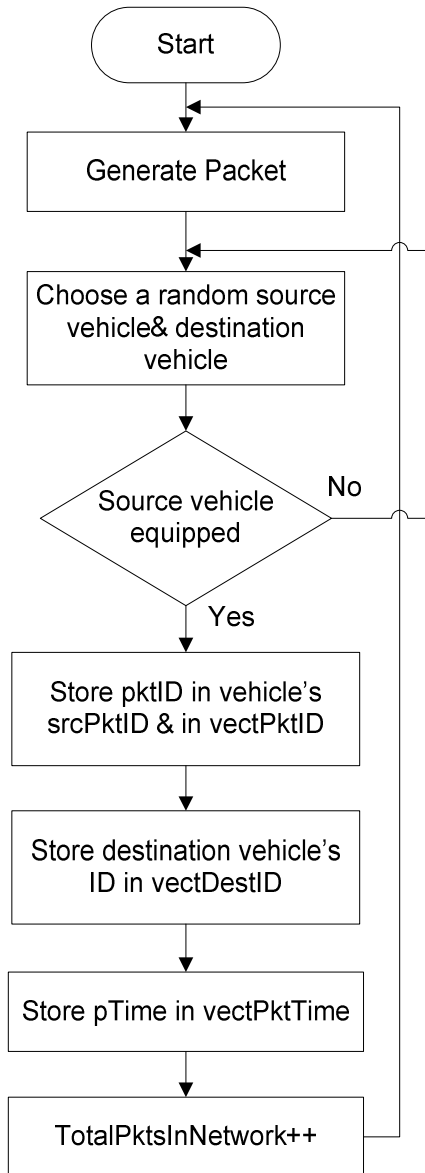


Figure B.2: Flowchart for traffic generation mechanism

B.3 Multihop Routing Flowchart

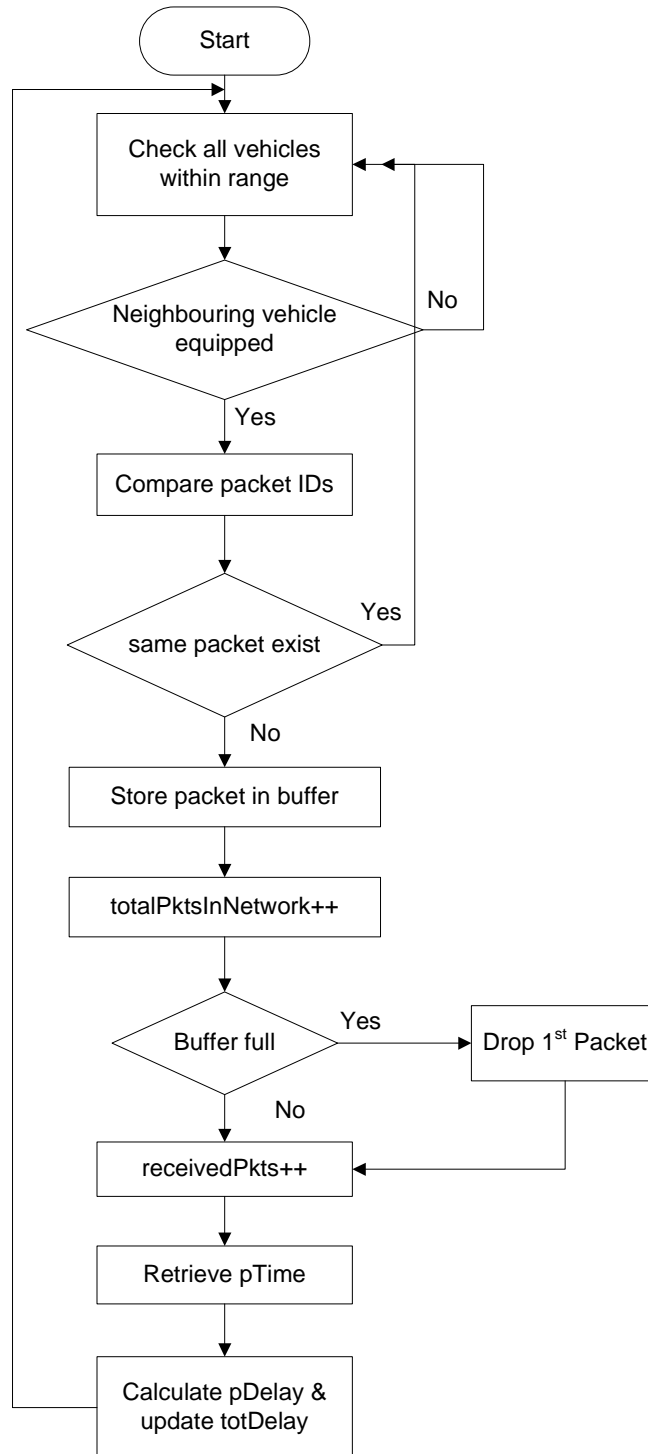


Figure B.3: Flowchart for MH routing

B.4 PRMFR and PRNFP Routing Flowchart

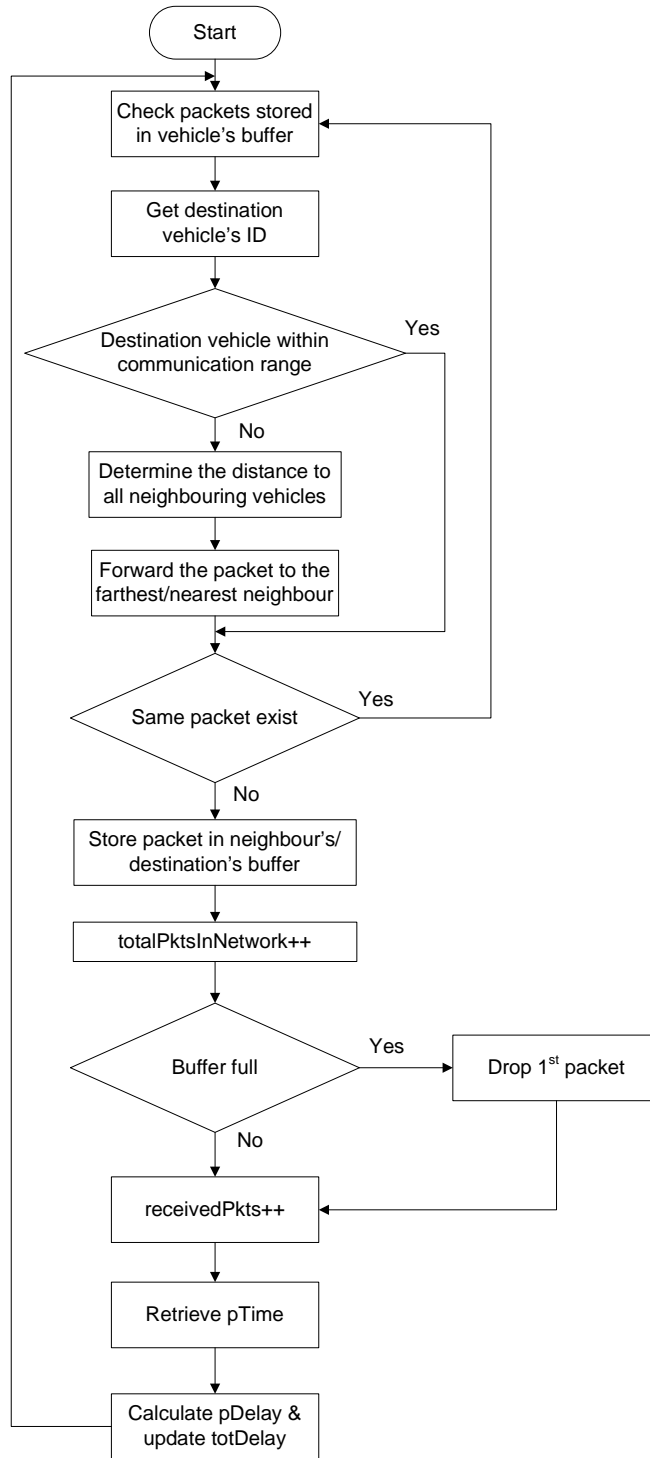


Figure B.4: Flowchart for PRMFR and PRNFP protocols

B.5 SCH Routing Flowchart

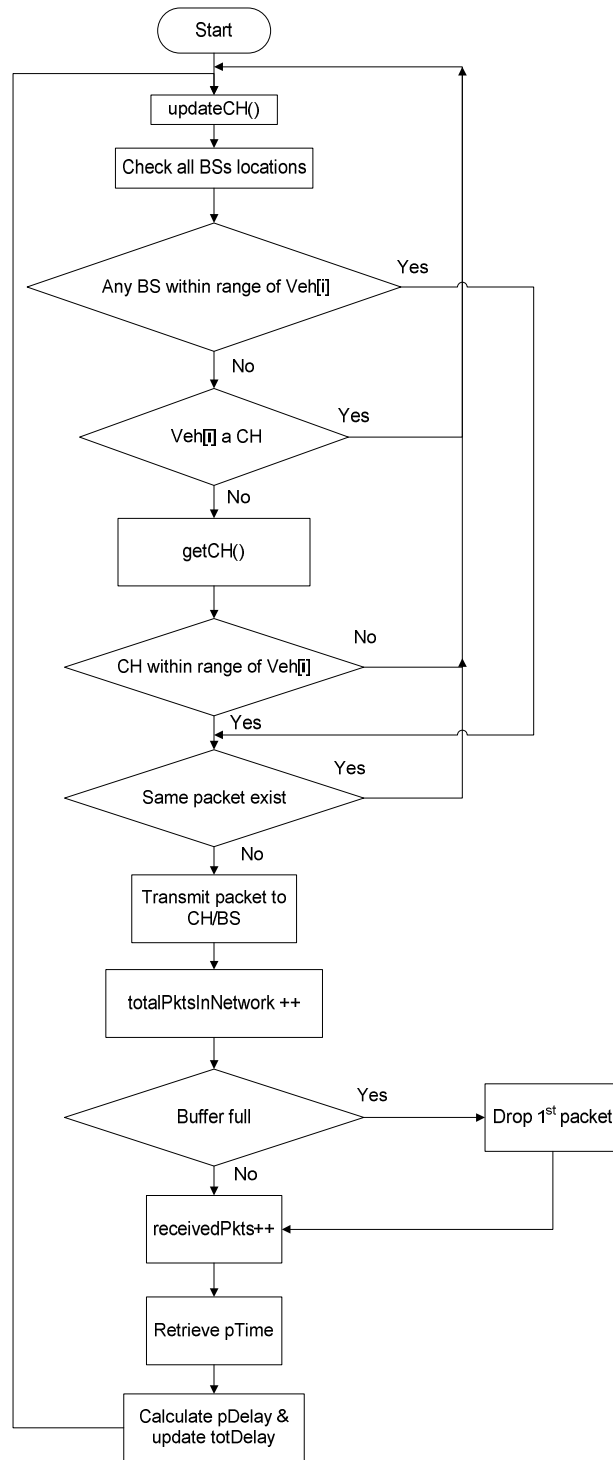


Figure B.5: SCH routing flowchart